The Tumour Microenvironment Interactions Of Small Cell Lung Cancer.

Philip Simon Hodkinson

PhD by Research.

The University of Edinburgh.

2008

DECLARATION:

This thesis is my own work. The work that has been performed by other members of the research group is clearly indicated in the text. The data presented in chapter 6 and 7 were obtained in collaboration with Dr Fiona McLaren. This work has not been submitted for any other degree or professional qualification.

Philip S Hodkinson (24/10/2008)

TABLE OF CONTENTS:

ABSTRACT		i
ABBREVIATIONS		iii
LIST OF FIGURES		viii
ACKNOWLEDGEMENTS		xii
CHAPTER 1: Current Problems And Novel Therapeutic Targets In Small Cell Lung Cancer.		
1.1	Introduction	1
1.2	Epidemiology – The Burden Of Small Cell Lung Cancer.	1
1.3	Clinical features, Diagnosis And Staging Of SCLC.	3
1.4	Treatment Of SCLC.	
1.4.1	Chemotherapy.	5
1.4.2	Radiotherapy.	7
1.5	Pathogenesis Of SCLC.	
1.5.1	Understanding The Carcinogenesis Of SCLC.	8
1.5.2	Mechanisms of SCLC Escape From Normal Control Of Cellular Proliferation.	9
1.5.3	Anti-Apoptotic Mechanisms In SCLC.	11
1.5.4	Mechanisms Of Angiogenesis In SCLC.	12
1.5.5	Mechanisms Of Migration And Invasion In SCLC.	13
1.6	Novel Targeted Therapies In SCLC.	
1.6.1	Neuropeptide Antagonists.	14
1.6.2	Receptor Tyrosine Kinase Inhibitors.	15
1.6.3	Inhibitors Of Cell Survival Pathways.	15
1.6.4	Inhibitors of Angiogenesis.	16
1.7	The Role Of The Tumour Microenvironment in SCLC.	
1.7.1	Extracellular Matrix.	18
1.7.2	Fibroblasts.	18
1.7.3	Immune Cells.	19
1.8	Concluding Remarks.	21

AIMS 22

CHAPTER 2: Materials And Methods.

2.1 Cell Lines And Maintenance Cultures. 23

2.2 DNA Constructs. 23

2.3 Antibodies.

2.3.1 Antibodies Used In Western Blot Analysis. 25

2.3.2 Antibodies Used For Flow Cytometry. 25

2.3.3 Antibodies Used For Immunohistochemistry. 26

2.3.4 Antibodies Used In Cell Culture. 26

2.4 Transfection Of Cell Lines. 26

2.5 Western Immunoblots. 28

2.6 Assessment Of Apoptosis In SCLC Cells By Acridine Orange/Ethidium Bromide Staining. 28

2.7 Assessment Of Apoptosis In SCLC Cells By Cell Death ELISA Kit. 30

2.8 Assessment Of Apoptosis In SCLC Cells By Annexin-V. 31

2.9 PI3-kinase Activity Assay. 32

2.10 PKB Activity. 33

2.11 Caspase-3 Activity. 33

2.12 Cell Cycle Analysis. 34

2.13 Visualisation Of DNA Double Strand Breaks. 35

2.14 Assessment Of Integrin Affinity In CHO(αβ-py) Cells. 35

2.15 Preparation Of FN 9-11 Fragment For Integrin Affinity Experiments. 36

2.16 Assessment Of Integrin Affinity In CHO-K1 Cells. 37

2.17 Assessment Of Cell Adhesion. 38

2.18 Knockdown Of PLCε Expression In CHO Cell Lines. 40

2.19 Measurement Of HES-1 Expression By RT-PCR. 42

2.20 CSL-Luciferase Activity. 42

2.21 R-Ras Activation Assay. 43

2.22 Immunohistochemistry. 44

2.23 RT-PCR Of Notch Signalling Components In SCLC Cell Lines. 44

2.24 Preparation Of Human Peripheral Blood Mononuclear Cells. 45

2.25 Co-Culture Of SCLC Cells And Mixed Leukocyte Reactions. 46
2.26 Preparation Of Human CD4+ T-Cells. 46
2.27 Co-Culture Of SCLC Cells And Human CD4+ T-Cells 48
2.28 Measurement Of TGF-β1 Concentration In SCLC Supernatants. 50
2.29 Measurement Of Cytokine Production By Human CD4+ T-Cells. 51
2.30 Expression Of Activation Markers (CD25, CD69) On Human CD4+ T-Cells. 52
2.31 Expression Of Human Macrophage Surface Markers. 52
2.32 Statistical Analysis. 53

CHAPTER 3: Extracellular Matrix Protects SCLC Cells From DNA Damage-Induced Cell Cycle Arrest And Apoptosis.

3.1 Introduction. 55
3.2 Results.
3.2.1 ECM Proteins Protect SCLC Cells From Chemotherapy- And Radiation-Induced Apoptosis. 57
3.2.2 β1 Integrin Activation Mediates ECM Protection From Apoptosis In SCLC Cells. 59
3.2.3 Adhesion To Laminin Stimulates PI3-Kinase Activity, PKB Phosphorylation And Activity And Increases GSK-3β Phosphorylation In SCLC Cells. 61
3.2.4 ECM-Mediated Protection Against Etoposide-Induced Apoptosis Is Dependent On PI3-Kinase Activation. 64
3.2.5 ECM Proteins Override Etoposide- And Radiation-Induced G2/M Cell Cycle Arrest Via PI3-Kinase Modulation Of Cell Cycle Regulators. 67
3.2.6 Expression Of A Dominant Negative PKB Mutant Prevents, And A Constitutively Active PKB Mutant Mimics, ECM-Mediated Protection From Apoptosis And Cell Cycle Arrest. 73
3.2.7 Adhesion To ECM Proteins Does Not Modulate Ongoing Etoposide- And Radiotherapy-Induced DNA Damage Or Repair. 77
3.3 Discussion. 79

CHAPTER 4: H-Ras Suppresses Integrin Activation Through A Phospholipase C-epsilon-Dependent Pathway.

4.1 Introduction. 83

4.2 Results.

4.2.1 PLCε Mediates Integrin Suppression. 85

4.2.2 H-Ras Suppresses Integrin Affinity Via Independent Raf And PLCe Signalling Pathways. 91

4.2.3 Modulating Rap1A Activity Does Not Affect Integrin Suppression. 93

4.2.4 PLCε Contributes To H-Ras Mediated Reduction In Cellular Adhesion. 93

4.3 Discussion. 98

CHAPTER 5: Notch Signalling Activates β1 Integrins Via The Small GTPase R-Ras and Protects SCLC Cells From Chemotherapy-Induced Apoptosis.

5.1 Introduction. 102

5.2 Results.

5.2.1 Notch-1 Activates Integrins And Reverses H-Ras/Raf-Mediated Integrin Suppression. 104

5.2.2 Activation Of β1 Integrins By Notch-1 Requires Intramembrane Cleavage (S3) To Release The Intracellular Domain. 109

5.2.3 Activation Of β1 Integrins By Notch-1 Is Not Dependent On CSL-Mediated Transcription. 112

5.2.4 Activation Of β1 Integrins By Notch-1 Requires The Ankyrin Repeat Domain 114

5.2.5 Activation Of β1 Integrins By Notch-1 Is Mediated By R-Ras. 116

5.2.6 Notch-1 Activates Native α5 β1 Integrins In An R-Ras Dependent Manner To Increase Cellular Adhesion To Fibronectin. 121

5.2.7 Notch Signalling Protects SCLC Cells From Chemotherapy-Induced Apoptosis. 124

5.2.8 Activation of Notch-2 does not modulate integrin affinity. 127

5.3 Discussion. 129

CHAPTER 6: The Presence Of Mononuclear Immune Cells In SCLC Tumour Sections Predicts Patient Survival.

6.1 Introduction. 134

6.2 Results.

6.2.1 A Mononuclear Cell Infiltrate Consisting Of Lymphocytes And Macrophages Is Present In SCLC Tumour Sections. 136

6.2.2 The Presence Of A CD45-Positive Mononuclear Immune Cell Infiltrate Is Associated With Improved Survival In SCLC. 145

6.3 Discussion. 149

CHAPTER 7: Small Cell Lung Cancer Cells Suppress Cell-Mediated Immune Responses *In Vitro*.

7.1 Introduction. 154

7.2 Results.

7.2.1 H69 And H345 SCLC Cells Suppress Proliferation Of A Mixed Leukocyte Reaction. 157

7.2.2 H69 and H345 SCLC Cell Lines Suppress Proliferation of Human CD4+ T-Cells. 159

7.2.3 H69 SCLC Cell Lines Increase IL-10 Secretion By Activated CD4+ T-Cells. 164

7.2.4 H69 SCLC Cells Do Not Alter CD4+ T-cell Surface Expression of Activation Markers CD25 or CD69. 166

7.2.5 A Soluble Factor Secreted By SCLC Cells Mediates Suppression Of CD4+ T-cell Proliferation. 168

7.2.6 Suppression of Human CD4+ T-Cells Proliferation By H69 SCLC Cells Is Not Reversed By A TGF-β Neutralising Antibody. 172

7.2.7 SCLC Cells Suppress Macrophage Surface Expression Of CD86 and CD16. 174

7.2.8 Suppression Of MLR Proliferation By H69 SCLC Cells Is Reversed By The Bombesin Antagonist RC-3095. 177

7.3 Discussion. 180

CHAPTER 8: Conclusions and Future Directions.

8.1 ECM-mediated chemo-resistance in SCLC cells. 186

8.2 Integrin affinity modulators. 190

8.3 Integrin-mediated survival mechanisms in SCLC. 193

8.4 The interaction of SCLC with immune cells. 195

8.4.1 Why do CD45+ infiltrating leucocytes predict patient prognosis in SCLC? 196

8.4.2 Do tumour-infiltrating CD4+ T-cells predict patient prognosis? 197

8.4.3 Why do patients have differences in leukocyte infiltration? 198

REFERENCES 200

APPENDIX: Published Papers. 244

ABSTRACT:

Small cell lung cancer (SCLC) is characterised by rapid growth, early metastatic spread and poor long-term survival. The tumour is initially sensitive to chemotherapy and thus objective response rates are high. Unfortunately, this response is often short-lived and SCLC recurs with acquired drug resistance, resulting in early patient death. Despite intensive chemo- and radiotherapy regimes survival has not improved significantly in 20 years. Prior research suggests a critical role for the tumour microenvironment in the pathogenesis of other cancers. Therefore, investigating interactions between SCLC cells and components of the tumour stroma may identify novel therapeutic targets.

This thesis demonstrates that extracellular matrix (ECM) proteins present in the tumour microenvironment protect SCLC cells *in vitro* from chemo- and radiotherapy induced cell cycle arrest and apoptosis via cell surface β1 integrins. Pharmacological and genetic inhibition of phosphoinositol-3 kinase signalling abrogates this effect, defining a central role for this pathway in SCLC *de novo* drug resistance. Furthermore, the protective effect of ECM occurs without alteration in chemotherapy-induced DNA damage allowing SCLC cells to survive with new genetic defects. Integrin-mediated drug resistance has been shown to be important in other tumours and thus development of strategies to inhibit this pathway may yield new anti-cancer treatments.

The design of targeted agents to down-regulate integrin-ECM interaction requires an in depth understanding of the intracellular signals that modulate integrin affinity. Two such pathways are investigated in this thesis. 1) H-Ras, a dominant suppressor of integrin affinity, acts in part through phosphorylation of Erk. Data presented here demonstrate that H-Ras also suppresses integrins through a phospholipase-C epsilon (PLCε)-dependent pathway, thus explaining discrepancies in prior data and confirming a physiological role for this recently identified phospholipase. 2) The Notch signalling pathway has been shown to have important roles in both development and cancer. It is shown here that activation of Notch signalling increases β1 integrin affinity and can protect SCLC cells from chemotherapy-induced apoptosis. However the mechanisms appear to be different; Notch-1

modulates integrin activation through the small GTPase R-Ras and Notch-2 promotes SCLC cell survival. These results define a new Notch pathway, a novel integrin modulator and a potential therapeutic target in SCLC cells.

In addition to ECM proteins, the tumour microenvironment contains immune cells that may contribute to cancer growth. The cellular composition of the SCLC stroma is poorly understood. The data presented here indicate that the microenvironment of SCLC is infiltrated by lymphocytes and macrophages, the degree of which independently predicts patient survival. This suggests that the host immune system may be able to suppress SCLC growth. It is well recognised that patients with SCLC have defects in cellular immunity which correlate with survival. An *in vitro* co-culture model was used to investigate the underpinning mechanisms, showing SCLC cells can suppress CD4+ T-cell proliferation and macrophage CD86 expression. Furthermore, preliminary data suggest a role for a soluble factor released by SCLC cells that up-regulates CD4+ T-cell production of IL-10.

The work in this thesis implies a complex interaction between SCLC cells, ECM and immune cells in the tumour microenvironment. Manipulation of these pathways may have important therapeutic implications. Further investigation is required to understand the mechanisms of this interplay, which may in part be aided by prospective analysis of patient tumour samples and an *in vivo* model of SCLC.

ABBREVIATIONS:

ANK	Ankyrin repeat domain of intracellular Notch.
AP-1	Activator Protein-1
APC	Antigen Presenting Cell or Allophycocyanin.
αSMA	Alpha Smooth Muscle Actin.
ATCC	American Type Culture Collection.
AVP	Arginine Vasopressin
Bad	Bcl-xL/Bcl-2-Associated Death Promoter.
bFGF	Basic Fibroblast Growth Factor.
BSA	Bovine Serum Albumin.
CA	Constitutively Active.
CAM	Cell Adhesion Molecule.
CD(45)	Cluster of Differentiation.
CDC	Cell Cycle Division.
CDK	Cyclin-Dependent Kinase.
CHO	Chinese Hamster Ovary.
Ci	Curie (as in dose of radiation).
c-MET	Mesenchymal-Epithelial Transition factor.
ConA	Concanavalin A
CRR	Complete Response Rate.
CSL	Core Binding Factor/Suppressor of Hairless/Lag-1.
CT	Computer Tomography.
DAB	3, 3'-Diaminobenzidine.
DAG	Diacylglycerol.
dH_2O	Distilled Water.
DLL-4	Delta-Like Ligand-4.
DMEM	Dulbecco's Modified Eagle's Medium.
DN	Dominant Negative.
DNA	Deoxyribonucleic Acid.
DNAPKcs	DNA-dependent Protein Kinase Subunit.
DTT	Dithiothreitol.

ECM	Extracellular Matrix.
ED	Extensive Disease Stage.
EDTA	Ethylenediaminetetraacetic acid.
EGFR	Extracellular Growth Factor Receptor.
EGTA	Ethylene Glycol Tetraacetic Acid
ELISA	Enzyme Linked Immunosorbant Assay.
EP	Etoposide/Platinum.
ERK	Extracellular Signal-Regulated Kinase
FACS	Fluorescent Activated Cell Sorting.
FCS	Foetal Calf Serum.
FHIT	Fragile Histidine Triad.
FN	Fibronectin.
FN9-11	Fibronectin Fragments 9-11.
GAP	GTPase Activating Protein.
GEF	Guanosine Exchange Factor.
GFP	Green Fluorescent Protein.
GPCR	G-Protein Coupled Receptor.
GRP	Gastrin Releasing Peptide.
GSK-3	Glycogen Synthase Kinase 3.
GST	Glutathione-S-Transferase.
GTP	Guanosine Tri-Phosphate.
Gy	Gray (as in dose of radiation).
hASH	human Achete-Scute Homolog.
HCl	Hydrochloric Acid.
HEPES	4-(2-hydroxyethyl)-1-piperazineethanesulfonic acid
HES	Hairy Enhancer of Split.
HGF	Hepatocyte Growth Factor.
H-Ras	Harvey Rat Sarcoma viral oncogene.
ICAM	Inter-Cell Adhesion Molecule.
ICE-V	Vincristine, Ifosfamide, Carboplatin, Etoposide.
ICN	Intracellular Notch (human).
IFN	Interferon.

IGF-1	Insulin-like Growth Factor.
IgG	Immunoglobulin G
IgM	Immunoglobulin M
IL-2	Interleukin-2
IL-2R	IL-2 Receptor.
IMDM	Iscove's Modified Dulbecco's Medium.
IP3	Inositol Triphosphate.
JAG-1	Jagged-1.
LB	Lysogeny Broth.
LD	Limited Disease.
LDH	Lactate Dehydrogenase.
LEMS	Lambert-Eaton Myasthenic Syndrome.
LiCl	Lithium Chloride.
LN	Laminin.
LNG	LIN-12 /Notch/GLP repeats of Notch.
MACS	Magnetic Cell Sorter.
MAPK	Mitogen Activated Protein Kinase.
MDR	Multi-Drug Resistance.
MEK	Mitogen Activated Protein Kinase.
$MgCl_2$	Magnesium Chloride.
MHC	Major Histocompatibility Complex.
MINT	Msx-2 Interacting Nuclear Targeting.
MLR	Mixed Leukocyte Reaction.
MMP	Matrix Metalloproteinase.
mTOR	Mammalian Target of Rapamycin.
Myc	Myelocytomatosis viral oncogene.
Na3VO4	Sodium Orthovanadate.
NaCl	Sodium Chloride.
NCAM	Neural Cell Adhesion Molecule.
NF-kB	Nuclear Factor kappa-light-chain-enhancer of activated B cells.
NIC	Notch Intracellular (mouse).
NMB	Neuromedin B.

NSCLC	Non-Small Cell Lung Cancer.
ORR	Objective Response Rate.
p21	Cyclin-dependent kinase inhibitor 1A.
p27	Cyclin-dependent kinase inhibitor 1B.
PAGE	Polyacrylamide Gel Electrophoresis.
PBL	Peripheral Blood Lymphocytes.
PBMC	Peripheral Blood Mononuclear Cells.
PBS	Phosphate Buffered Saline.
PCR	Polymerase Chain Reaction.
PDGF	Platelet Derived Growth Factor.
PE	Phycoerythrin.
PerCP	Peridinin-Chlorophyll-Protein.
PEST	Proline, Glutamate, Serine, Threonine rich sequence.
PGP	P-Glycoprotein Pump.
PHA	Phytohaemagglutinin.
PI	Propidium Iodide.
PI3-kinase	Phosphoinositide 3-kinase.
PIP2	Phosphatidylinositol Bisphosphate.
PKB	Protein Kinase B (also known as Akt).
PLC	Phospholipase C.
PNEC	Pulmonary Neuroendocrine Cell.
PTEN	Phosphatase and Tensin homolog.
RA	Ras/Rap Associated
RA	Ras/Rap Associating.
RAM	RBP-j Associated Molecule.
Rb	Retinoblastoma.
RNA	Ribonucleic Acid.
RPMI	Roswell Park Memorial Institute.
RTK	Receptor Tyrosine Kinase.
RT-PCR	Reverse Transcription PCR.
SCLC	Small Cell Lung Cancer.
SDS	Sodium Dodecyl Sulphate.

SEER	Surveillance Epidemiology End Results.
siRNA	small interfering RNA.
SITA	Selenium Insulin Transferrin Albumin.
TAD	Trans-Activating Domain.
TBS	Tris Buffered Saline.
TCR	T-cell Receptor.
TGF	Transforming Growth factor.
TIL	Tumour Infiltrating Lymphocyte.
TNF	Tumour Necrosis Factor.
TNM	Tumour, Node, Metastasis.
VAC	Vincristine, Adriamycin, Cyclophosphamide.
VEGF	Vascular Endothelial Growth Factor.
VHL	von Hippel Lindau.
WT	Wild-Type.

LIST OF FIGURES:

2.1 Transfection Of H345 SCLC Cells With Lipofectamine 2000™. 27

2.2 SCLC Cells Stained With Acridine Orange/Ethidium Bromide. 30

2.3 The CHO DNA Sequence Straddling The Oligonucleotides siRNAPLCε#3 And siRNAPLCε#5. 41

2.4 Typical Dot Plots Of Unlabelled Fraction Of Cells (i.e. CD4+ T-cells) From Automacs Stained With Anti-CD3 (APC) And Anti-CD4 (PE) Antibodies. 48

2.5 Identification Of CD11b+ CD14+ Macrophages In 7 Day Adherent Monocyte Cultures. 54

3.1 ECM Protects SCLC Cells From Etoposide- And Radiation-Induced Apoptosis. 58

3.2 ECM-Mediated Protection From Etoposide-Induced Apoptosis Is β1 Integrin-Dependent. 60

3.3 Adhesion To ECM Stimulates PI3-Kinase Activity In SCLC Cells. 62

3.4 LY294002 Inhibits ECM- And Na_3VO_4- Stimulated PI3-Kinase Activity In SCLC Cells. 63

3.5 ECM-Mediated Protection From Chemotherapy-Induced Apoptosis Requires PI3-Kinase Signalling. 65

3.6 ECM-Mediated Protection From Chemotherapy-Induced Caspase-3 Activation Requires PI3-Kinase Signalling. 66

3.7 ECM Overrides Etoposide- And Radiation-Induced Cell Cycle Arrest Via β1 Integrin-Mediated PI3-Kinase Activation. 69

3.8 ECM Overrides Etoposide-Induced Changes In Expression Of Key Cell Cycle Regulators Via β1 Integrin And PI3-Kinase Activation. 72

3.9 The Effect Of Dominant Negative And Constitutively Active PKB Mutants On ECM-Mediated Protection From Etoposide-Induced Apoptosis. 74

3.10 The Effect Of Dominant Negative And Constitutively Active PKB Mutants On ECM-Mediated Protection From Etoposide-Induced Cell Cycle Arrest. 75

3.11 Adhesion To ECM Does Not Affect Etoposide-Induced DNA Double Strand Break Formation And Repair. 78

4.1	H-Ras(G12V/E37G) And H-Ras(G12V/D38N) Mutants Suppress Integrin Activation Without Phosphorylating ERK.	86
4.2	PLCε(H1433L) Blocks Integrin Suppression Mediated By H-Ras (G12V/D38N).	88
4.3	Sequence Of The Region Of CHO Cell DNA Surrounding A Previously Described siRNAOligonucleotide For Rat PLCε (siRNAPLCε#3).	89
4.4	Knockdown Of Endogenous PLCε Blocks H-Ras(G12V/D38N)-Mediated Integrin Suppression.	90
4.5	H-Ras Suppresses Integrin Affinity Via Independent Raf And PLCε Signalling Pathways.	92
4.6	Rap1A Does Not Mediate H-Ras(G12V/D38N)-Induced Integrin Suppression.	94
4.7	PLCε Modulates H-Ras(G12V/D38N) Suppression Of CHO(αβ-py) Cell Adhesion To Von Willebrand Factor.	95
4.8	PLCε Modulates H-Ras(G12V/D38N)-Mediated Reduction In Cellular Adhesion.	97
4.9	Schematic Of Raf-Dependent And Raf-Independent Signalling Pathways Of Integrin Suppression.	98
5.1	Notch-1 Activates Integrins And Reverses H-Ras-Mediated Suppression Of Integrin Affinity.	105
5.2	Notch does not alter β3 integrin expression.	107
5.3	Notch Reverses Raf-Mediated Suppression Of Integrin Affinity.	108
5.4	Description Of Notch Constructs.	110
5.5	Notch-1 Activation Of Integrins Requires Intramembranous (S3) Cleavage.	111
5.6	Notch Activation Of Integrins Is Not Blocked By Msx2-Interacting Nuclear Target (MINT) Protein.	113
5.7	Expression Of Msx2-Interacting Nuclear Target (MINT) Protein And Notch-1 Intracellular Domain In CHO Cells.	114
5.8	Notch-1 Activation Of Integrins Requires The Ankyrin Repeats But Not The Transactivation Domains.	115
5.9	Wild Type R-Ras Potentiates Notch-1-Mediated Integrin Activation.	118

5.10 Dominant Negative R-Ras (R-Ras(T43N)) Reverses Notch-1 Activation Of Integrins. 119
5.11 The Intracellular Domain Of Notch-1 Activates R-Ras. 120
5.12 Notch-1 Intracellular Domain Increases K562 Cell Adhesion In A _1 Integrin/R-Ras-Dependent Manner. 122
5.13 Notch Signalling Initiated By Delta-Like Ligand 4 Increases K562 Cell Adhesion. 123
5.14 Notch Signalling Components Expressed By SCLC Cell Lines (RT-PCR) 125
5.15 Notch Ligand Jagged-1 Protects SCLC Cell Lines From Etoposide-Induced Apoptosis. 126
5.16 Activation Of Notch-2 Does Not Modulate Integrin Affinity. 128
6.1 SCLC Sections Are Variably Infiltrated By CD45+ Mononuclear Cells. 137
6.2 SCLC Sections Are Infiltrated By CD3+ T-Lymphocytes. 140
6.3 SCLC Sections Are Infiltrated By CD4+ T-Lymphocytes. 141
6.4 SCLC Sections Are Infiltrated By CD8+ T-Lymphocytes. 142
6.5 SCLC Sections Are Infiltrated By CD68+ Macrophages. 143
6.6 SCLC Sections Are Sparsely Infiltrated By CD20+ B-Lymphocytes. 144
6.7 X-Y Scatter Plot Showing Correlation Between Average Number Of CD45+ Cells/High Power Tumour Field And Survival In SCLC. 147
6.8 Kaplan-Meier Survival Curves For 40 SCLC Cases Separated Into Equal CD45 ‘High’ And CD45 ‘Low’ Groups. 148
7.1 H69 And H345 SCLC Cell Lines Suppress ^{3}H-Thymidine Uptake By A Mixed Leukocyte Reaction. 158
7.2 H69 SCLC Cell Lines Suppress CD4+ T-cell Proliferation. 162
7.3 Increasing The Ratio Of SCLC Cells To CD4+ T-cells In Co-culture Increases Suppression Of T-cell Proliferation. 163
7.4 SCLC Cells Increase IL-10 Release By Activated CD4+ T-cells. 165
7.5 SCLC Cells Do Not Suppress Surface Expression Of CD25/CD69 On Activated CD4+ T-cells. 167
7.6 SCLC Produce A Soluble Factor Which Suppresses CD4+ T-cell Proliferation. 170

7.7	The Soluble Factor Produced by H69 SCLC Cells That Suppresses CD4+ T-cell Proliferation Is < 30kDa and Thermostable.	171
7.8	Suppression of Human CD4+ T-Cells Proliferation By SCLC Cells Is Not Mediated By TGF-beta.	173
7.9	Macrophages Matured From Monocytes With H69 SCLC Cells Show Reduced Surface Expression Of CD86 and CD16.	176
7.10	The Bombesin Receptor Antagonist RC-3095 Reverses MLR Suppression By H69 SCLC Cell Line.	179
8.1	ECM protects SCLC cells via β1 integrins.	187
8.2	The multiple cellular functions of β1 integrins.	190
8.3	Integrin affinity modulation by PLCε and Notch.	191
8.4	The mechanisms of β1 integrin-mediated chemo-protection in SCLC.	194
8.5	The interaction of SCLC cells with CD4+ T-cells and macrophages.	197

ACKNOWLEDGEMENTS:

I would like to give thanks to my supervisors, Professors Tariq Sethi and Sarah Howie, for their guidance and support during this period of laboratory research; to the other members of the laboratory team (Dr Alison MacKinnon, Dr Brian McHugh and Dr Fiona McLaren) for their assistance and direction on many occasions; to the Medical Research Council for their generous funding; and to my wife for her patience and support.

CHAPTER 1: Current Problems And Novel Therapeutic Targets In Small Cell Lung Cancer.

1.1 Introduction.

Lung cancer is the most common cause of cancer related mortality, accounting for 6% of all UK deaths (~33,000 per year) (1,2). It is categorised into two histological groups that have distinct clinical behaviours (3). Non-small cell lung cancer (NSCLC) accounts for approximately 80% of all lung cancer cases in the UK and includes squamous cell carcinoma (30-40%), adenocarcinoma (25-35%) and large cell carcinoma (10%) (4,5). These tumours normally present with locally confined disease and therefore curative surgery or radiotherapy, possibly in combination with chemotherapy are the treatments of choice (6,7). Consequently NSCLC has the best outcome of the two broad types of lung cancer; depending on the stage the survival rates for NSCLC following surgery vary from 25% to 65% at 5-years (stage IIIa compared with stage Ia respectively) (8,9).

Small cell lung cancer (SCLC) accounts for 15-20% of all lung cancers and is characterised by rapid growth and early metastatic spread (6). It has the most aggressive clinical course of any lung tumour and as a result surgical resection is rarely possible (10). Therefore overall prognosis is very poor with a 2-year survival rate despite treatment of 20% and a 5-year survival rate of less than 5% (11). These figures have unfortunately not improved significantly in the past two decades despite advances in diagnosis and treatment (12). This has led many clinicians to call for an urgent research focus on SCLC to develop new and effective therapeutic strategies for this especially lethal cancer. This chapter will provide an introduction to the clinical features, current treatment and biology of SCLC, which will act as a background for the discussion of potential new therapeutic targets.

1.2 Epidemiology – The Burden Of Small Cell Lung Cancer.

More than 38,000 new cases of lung cancer are diagnosed each year in the UK, accounting for 1 in 7 cancer cases. This equates to 13% of all male cancers and 11% of all female cancers (1,13). Unfortunately, Scotland has a particularly high incidence, with an age-standardised rate of 67.5 per 100, 000 population (4,5).

Furthermore, lung cancer causes more deaths per year than the sum of breast, colon or prostate cancer (2,14). SCLC accounts for disproportionately greater numbers of lung cancer deaths (~25%) due to its poor survival rate. Despite these alarming statistics it would appear that the incidence rates for lung cancer in the UK have declined steadily over the last twenty years (4,5). In addition the proportion of cases attributable to SCLC appears to be decreasing. Cancer registries in Europe and the United States indicate that in the past decade only 12-13% of lung tumours are of small cell type (5,15). The reasons for the decline in SCLC are not entirely clear and may relate to changes in pathological classification and exposure to causative factors.

Lung cancer is rare in patients under 40 years; the incidence rises with age and peaks in the eighth decade (70-79 years) (16). More cases of lung cancer are diagnosed in men than women. However this difference has become smaller; in the UK the male/female ratio has declined over the past fifty years from 6:1 to approximately 7:5 (22,495 male cases and 15,818 female case in 2004) due to increased lung cancer incidence in women (5,16). Lung cancer incidence rates are strongly associated with deprivation. The incidence of lung cancer is 2.5-3 times greater in the most deprived groups and is therefore more commonly diagnosed in individuals of lower socio-economic status (17). Specific demographic data for each histological type of lung cancer is limited. However a study from Poland indicates that SCLC is frequently diagnosed in the sixth and seventh decade (mean age at diagnosis 58.2 years for women and 60.2 years for men) and is more common in men than women (18). The SEER registry indicates that SCLC is most commonly diagnosed between the ages 60-70 and that in 2003 the incidence was slightly greater for men than women (8.5/100,000 c.f. 7.2/100,000 respectively) (19).

The most significant risk factor for lung cancer is cigarette smoking. The causal link between lung cancer and tobacco smoke was established more than 50 years ago (20). Subsequently, it has been estimated that the risk of lung cancer in cigarette smokers is 8-20 times that in life-long non-smokers (21,22). SCLC has the clearest association with tobacco consumption; it is now accepted that greater than 95% of SCLC cases are attributable to tobacco smoking (23,24). Other risk factors have been defined and include atmospheric pollution, industrial exposure to carcinogens and chronic lung disease (25). The clear association between smoking and lung cancer

indicates that trends in lung cancer cases closely follow changes in tobacco consumption with a lag time of 25-30 years (26). Therefore, the future trends in lung cancer, and particularly SCLC, will be shaped by the increase in female smokers and the higher prevalence of tobacco use in lower socio-economic groups (27). Unfortunately, it is clear that SCLC will continue to be a significant health burden for the foreseeable future.

1.3 Clinical features, Diagnosis And Staging Of SCLC.

SCLC produces no symptoms for the majority of its growth and thus presents late, often with widespread disease (28). The duration of symptoms reported is short, typically 2-3 months prior to diagnosis (29). Symptoms can result from local tumour growth (cough, haemoptysis and chest pain), spread of tumour to the mediastinum (superior vena cava obstruction syndrome, hoarseness and dysphagia) and metastatic spread to distant organs (28,29). The presentation of distant metastases is dependent on the structures involved, typically brain, bone, liver and adrenal glands (30). SCLC can also cause significant non-specific systemic upset, including cachexia, weakness, and poor appetite (31). Due to the aggressive nature of the tumour, mediastinal and metastatic complications are more frequent than in other lung tumours (28).

In addition to the direct effects of tumour growth and/or spread, SCLC is associated with a variety of paraneoplastic manifestations, which can be broadly categorised into endocrine and neurological syndromes (32). The endocrine syndromes result from ectopic production of peptide hormones by SCLC cells and include hyponatraemia (10-15% of patients, secondary to anti-diuretic hormone or atrial natriuretic peptide secretion) and Cushing's syndrome (<5% of patients, caused by ectopic production of corticotropin) (33-35). The neurological paraneoplastic syndromes associated with SCLC are much less frequent (<3%) (36). The best described is the Lambert-Eaton myasthenic syndrome (LEMs), which presents with proximal muscle weakness and autonomic dysfunction often prior to the detection of SCLC (37). Patients with LEMs frequently have detectable serum levels of antibodies directed against P/Q-type voltage gated calcium channels (38).

The radiographic appearance of SCLC is typically a central tumour mass with hilar and mediastinal lymphadenopathy (39). There may be a peripheral tumour nodule

that is smaller than the central lymph node involvement (40). Diagnosis is most commonly made by histological analysis of a tumour biopsy sample taken either at bronchoscopy or by percutaneous needle aspiration (41). Typically tumour sections of SCLC reveal malignant cells that are oval or spindle shaped, have scant cytoplasm and minimal or absent nucleoli (42). There is a high mitotic count, the borders between cells are often poorly defined and frequently areas of necrosis are observed (42). Unfortunately, SCLC biopsy samples can be subject to sampling damage and thus differentiation from NSCLC can be difficult based on morphology alone (43). Therefore immunohistochemical analysis is used in more difficult cases to demonstrate the presence of neuroendocrine markers (e.g. chromogranin, CD56 and synaptophysin) on SCLC cells (43).

The TNM (Tumour, Node, Metastasis) staging system used for many tumours has previously been considered inappropriate for SCLC and therefore the Veterans Administration Lung Study Group described a separate system (44). Limited-stage disease (LD) was defined as SCLC confined to one hemi-thorax (including ipsilateral supraclavicular lymph nodes) and able to be encompassed within a single, tolerable radiation field (44,45). Extensive-stage disease (ED) was described as any case of SCLC with tumour spread beyond these boundaries and included patients with malignant pericardial or pleural effusions (44,45). These definitions have subsequently been debated and there is now growing interest in the application of the TMN system, particularly for research on LD SCLC (45,46). Treatment and prognosis varies significantly between these groups and therefore the main aim of staging investigations is to identify those patients with extensive disease (44,45). Computer tomography (CT) scanning is used to determine the intra-thoracic and liver/adrenal gland involvement by tumour (41). Further imaging, guided by the patients symptoms, includes CT or magnetic resonance imaging (MRI) scan of the brain and radionuclide bone scan to assess the presence of metastatic deposits (41). Occasionally patients require biopsy samples to be taken from liver or adrenal lesions and bone marrow aspirates to be analysed as indicated by peripheral blood counts (41).

1.4 Treatment Of SCLC.

60-70% of SCLC patients have ED at the time of diagnosis. Therefore curative surgical resection is not a viable treatment option (47). Fortunately, SCLC cells are highly sensitive to cytotoxic therapies and thus systemic administration of chemotherapeutic drugs is the primary treatment modality (48). However, despite excellent initial objective response rates (ORR), tumour relapse is common and most patients eventually succumb to disseminated disease. Recent studies have attempted to intensify chemotherapy dose, use new combinations of drugs, trial new drugs and combine chemotherapy with radiotherapy to prolong patient survival.

1.4.1 Chemotherapy.

In the late 1960's it was demonstrated that treatment with cyclophosphamide could produce a survival advantage in SCLC patients when compared to placebo (4 months c.f. 1.4 months median survival respectively) (49). Subsequently, other cytotoxic drugs have been shown to be active in SCLC including platinum-based agents, vinca alkaloids and anthracyclines (50). However, single agent treatment results in only a short-lived tumour response (3-4 months). Thus, combination regimes were tested, improving median survival up to 5-fold compared with no anti-cancer treatment (51,52). In 1992, the results of a phase III trial comparing vincristine, adriamycin and cyclophosphamide (VAC) with etoposide and cisplatin (EP) were published, concluding that both regimes produced similar rates of tumour response and survival, although VAC was associated with greater toxicity (53). Importantly, a meta-analysis published in 2000 concluded that randomisation to a cisplatin-containing chemotherapy regime improved objective tumour response and overall survival without adversely affecting toxicity (54). Thus, standard chemotherapy for the first-line treatment of SCLC is comprised of etoposide plus a platinum-based agent (e.g. cisplatin or carboplatin) given for 4-6 cycles. In LD SCLC EP has been shown to achieve up to an 85% ORR with a complete response (CR) in up to 60% of patients (55,56). In ED an ORR of 60% and a CR of 10% is observed (53). Unfortunately, the response duration is often short (approximately 9 months) and relapsed or refractory disease resistant to further first-line chemotherapy ensues (56). Trials of second-line chemotherapy have been disappointing showing poor ORR (24% at best) even with

alternate drug regimes to the first line therapy (e.g. EP first-line, VAC second-line) (57). Ultimately, this results in early patient death with overall survival less than 5% at 5 years (25).

Various strategies have been explored to improve survival in SCLC aimed at preventing drug resistance and eradicating clinically silent residual disease. Research has focused on dose intensification through increased drug dose or shortened interval between chemotherapy cycles (58,59). Frequently these strategies are accompanied by severe bone marrow suppression and therefore trials have attempted to support the bone marrow through the use of granulocyte/macrophage colony stimulating factor or stem cell transplant (58,59). Unfortunately, there is no convincing evidence that the increase in ORR with these regimes is converted into long-term patient survival and thus they are not currently recommended (58,59). Similarly, no role has been demonstrated for alternation of chemotherapy regimes (e.g. VAC and EP) (53). A recent meta-analysis has indicated that maintenance chemotherapy can improve 1- and 2-year survival in SCLC, although a randomised controlled trial is required to confirm this (60). Other groups have investigated whether the addition of third and fourth agents to standard chemotherapy regimes can improve survival. Evidence for the efficacy of these toxic treatments is limited. However, the combination of vincristine, ifosfamide, carboplatin and etoposide (ICE-V) has been shown to improve ORR and survival compared with EP alone (61). The generally poor results have prompted trials of newer chemotherapeutic drugs in SCLC.

Paclitaxel is a newer chemotherapeutic drug derived from tree bark that binds to microtubules promoting arrest of the cell cycle (62). A phase II trial indicated that paclitaxel as a single-agent, was active in ED SCLC (ORR 53%) (63). However a subsequent phase III trial concluded that paclitaxel in combination with EP produced limited survival benefit and increased toxicity (64). Gemcitabine is an antimetbolite of pyrimidine that has been shown to have anticancer activity *in vitro* (65). However, the results of a phase II trial indicate that gemcitabine plus cisplatin whilst active in ED SCLC offers no benefit over other regimes and is more expensive (66). Irinotecan is a camptothecin derivative that inhibits topoisomerase I causing irreversible DNA double-strand breaks (67). A phase III trial conducted in Japan compared irinotecan plus cisplatin with EP in patients with ED SCLC (68). A

significant survival advantage was demonstrated with the irinotecan/cisplatin regime (12.8 months versus 9.4 months median survival). Unfortunately, a further phase III trial in America has failed to confirm this result (69). Topotecan is a similar agent to irinotecan and has been shown to have activity equivalent to VAC as a second-line agent for treatment of recurrent SCLC (70). Despite some success, it is clear from clinical trial data that a new, effective, low-toxicity chemotherapeutic agent is not yet available for SCLC.

1.4.2 Radiotherapy.

SCLC cells are more sensitive to radiotherapy than NSCLC (71). Meta-analyses have demonstrated that the addition of thoracic irradiation to chemotherapy in patients with LD SCLC improves 3-year survival (approximately 5% absolute increase) (72,73). Thus combined chemo- and radiotherapy is considered the standard treatment for patients with LD SCLC (74). The issue of radiotherapy timing is contentious and has been addressed in several randomised trials. A recent (2007) meta-analysis of 7 studies concluded that when radiotherapy was combined with platinum-based chemotherapy, earlier irradiation improved 2- and 5-year survival (75). The optimal dose of radiation has also been investigated in phase I and II trials and results favour dose intensification (76,77). Until these trials are confirmed in phase III studies, it is currently accepted that concurrent treatment to a dose of 45 Gray (Gy) should be considered standard therapy in LD SCLC (78).

The central nervous system (CNS) is a common site for tumour metastasis in SCLC. Standard chemotherapy regimes produce poor ORR in SCLC cases involving the CNS (79). Therefore prophylactic cranial irradiation has been studied as a method to reduce CNS disease. A meta-analysis of 987 SCLC patients who achieved complete response after chemotherapy concluded an approximate 5% improvement in 3-year survival with the addition of prophylactic cranial irradiation (80). The optimum dose is uncertain but the most commonly used in studies are 24-30 Gy given over 8-10 fractions.

It is clear that the discovery of chemotherapy as a treatment for SCLC has dramatically improved patient survival. Furthermore important advances have been made particularly with respect to combination chemotherapy regimes and dual

modality treatment. Unfortunately, despite excellent initial tumour response rates, long-term survival is limited and SCLC remains a lethal disease for many patients. Crucially 5-year survival has not improved dramatically in the past 20 years, despite considerable investment of time and money into new chemotherapy drugs and more toxic regimes. The main predictors of survival remain age, gender, performance status at diagnosis and stage of SCLC (81). It has been proposed that cytotoxic therapy has reached a plateau and further research in this particular area is futile. It is clear that a further understanding of the pathobiology of SCLC is needed to allow the development of rational targeted therapies and new prognostic indicators. It is predicted such strategies will act as important adjuncts to chemo- and radiotherapy in the future.

1.5 Pathogenesis Of SCLC.

The biology of SCLC, like all tumours, is complex and involves many of the processes common to malignant transformation. These include, escape from the normal control of cellular proliferation, avoidance of cell death, maintenance of an adequate blood supply and invasion of distant tissues (82). Accumulation of abnormalities in the important cellular pathways that control these processes underpins the pathogenesis of SCLC.

1.5.1 Understanding The Carcinogenesis Of SCLC.

Studying the development of cancer cells (carcinogenesis) from precursor lesions to malignant tumours, including the step-wise acquisition of genetic defects, is crucial to understanding the biology of a particular cancer. The primary distinguishing feature between the two broad histological types of lung cancer is that SCLC cells possess a neuroendocrine phenotype (i.e. express a variety of neuropeptide markers) (29). They are not unique in this and SCLC belongs to a broader category of pulmonary neuroendocrine tumours that includes carcinoid (typical and atypical) and large cell neuroendocrine carcinoma (29). It has previously been suggested that these tumours arise from a specialised group of cells within the lung airway epithelium called pulmonary neuroendocrine cells (PNEC) and that the range of changes observed from carcinoid to SCLC tumours may represent definite steps in malignant transformation (29,83). However, more recently it has been proposed that SCLC

cells have an endodermal origin with acquisition of neuropeptide expression as a feature of malignant transformation rather than a feature of the precursor cell (84). This is further supported by data from cDNA array analysis indicating that SCLC cells are more closely related to epithelial cells than carcinoid (85). Despite this data the precursor cell for SCLC remains to be clearly defined.

The specific sequence of genetic alterations leading to the development of SCLC is still unclear. A significant reason for this is lack of genetic data from pre-cancerous or small-size SCLC lesions due to the late presentation of the disease. Furthermore, absence of an animal model for SCLC prevents comparative genetic studies. However, over the last 30 years a host of chromosomal and molecular abnormalities have been identified in SCLC specimens and cell lines leading to the proposal of a genetic multi-step model of carcinogenesis. In SCLC the most frequently observed chromosomal abnormality is the deletion of the short arm of chromosome 3 (3p(14-25)), which is seen in more than 90% of SCLC cases (86,87). This region contains genes such as fragile histidine triad (FHIT) and von Hippel Lindau (VHL), which are important tumour suppressors and may therefore contribute to the pathogenesis of SCLC (87,88). Other common chromosomal alterations include loss of 5q, 17p and 13q (89). The latter two chromosome regions encode tumour suppressor genes *p53* and *Rb* respectively. In addition, inactivating mutations of *p53* and *Rb* are frequently observed in SCLC tumours and cell lines (90,91). However, the exact role of each genetic alteration in SCLC development and progression remains to be elucidated.

1.5.2 Mechanisms of SCLC Escape From Normal Control Of Cellular Proliferation.

A key event in malignant transformation is uncontrolled cellular proliferation. SCLC cells express receptors for and secrete a variety of peptide growth factors (92). These peptides can act in autocrine (secreted by and acting on the same cell) or paracrine (secreted by one cell and acting on another) growth loops to drive the uncontrolled proliferation of SCLC cells (93).

SCLC cell lines produce several neuropeptides including gastrin-releasing peptide (GRP, the human homologue of amphibian peptide bombesin), neuromedin B, bradykinin, cholecystokinin, gastrin and vasopressin (92). These diverse peptides

exert their cellular effects by binding to specific G-protein coupled receptors (GPCR) on the surface of SCLC cells (94). In addition to driving unrestrained proliferation, the development of resistance to conventional chemotherapy that is inevitable in SCLC, is accompanied by an increase in expression of neuropeptide growth factor receptors (95). Importantly, a monoclonal antibody (clone 2A11) directed against GRP that prevents GRP-receptor binding, inhibits SCLC cell proliferation *in vitro* and in a nude mouse model of tumour growth (96).

Not all autocrine growth loops in SCLC are regulated by GPCRs and recent work has focused on the role of receptor tyrosine kinases (RTK). The proto-oncogene *c-kit*, which encodes an RTK, is highly expressed in SCLC being found in up to 70% of SCLC cell lines and tumours (97). Furthermore, the frequent co-expression of its ligand, stem cell factor (SCF), suggests that this receptor/ligand system may have an autocrine function in SCLC (98). In support of this, pre-clinical studies have demonstrated that Imatinib^{TM}, a small molecule inhibitor of c-kit tyrosine kinase, suppresses SCLC proliferation *in vitro* (99). Another prominent autocrine loop in SCLC involves the expression of insulin-like growth factor-1 (IGF-1) and its RTK (IGF-1R). It has been shown that increased levels of IGF-1 correlate with an increased risk of lung cancer and IGF-1 can promote proliferation of SCLC cells *in vitro* (100,101).

In addition to autocrine growth factor loops, SCLC cells also display abnormalities in other crucial cell proliferation regulators. The *Myc* family of proto-oncogenes encode nuclear proteins that interact with other transcription factors to regulate expression of target genes and cell cycle progression (102). Amplification of the *Myc* family of genes has been observed in approximately 20% of SCLC tumour samples and 50% of SCLC cell lines (103). In addition increased N-Myc expression has been correlated with poor survival and chemotherapy response in SCLC (104). Furthermore, treatment of a SCLC cell line (NCI-H209) with L-*Myc* anti-sense DNA has been shown to down-regulate L-Myc expression with resultant reduction in cell proliferation (105). Genetic abnormalities in the tumour suppressor genes *p53* and *Rb* also contribute to abnormal cell proliferation as these molecules regulate cell cycle progression (106). Furthermore, aberrations in these pathways can contribute to cytotoxic therapy resistance by modulating the response to DNA damage (107). As

further studies are carried out using microarray techniques the patterns of gene expression that correlate with SCLC progression will be determined.

1.5.4 Anti-Apoptotic Mechanisms In SCLC.

Apoptosis is tightly controlled in normal cells, but these processes are altered in cancers allowing cell survival when cell death would normally occur. Thus the acquisition of defects in the normal control of apoptosis is a crucial step in malignant transformation and is also important in resistance to chemotherapy and radiation. The *bcl-2* proto-oncogene was one of the first members of a group of highly conserved genes to be identified that encode proteins central to the regulation of apoptosis (108). The Bcl-2/Bax system regulates apoptotic cell death through mitochondrial release of cytochrome c (108). Bcl-2 is anti-apoptotic and is frequently over-expressed in SCLC cases (up to 90%) and cell lines (109,110). Studies *in vitro* have demonstrated that Bcl-2 has a central role in SCLC apoptosis and drug resistance; over-expression of Bcl-2 protects SCLC cells against apoptosis whereas reducing Bcl-2 expression with antisense nucleotides promotes apoptosis in response to chemotherapeutic drugs (111). In addition to defects in Bcl-2, SCLC cells also frequently display mutations in *p53*, which in normal cells promotes cell cycle arrest and apoptosis in response to DNA damage (112). Studies have demonstrated that restoration of wild type *p53* in SCLC cells promotes apoptosis but not G1 cell cycle arrest (106).

Prior research has identified an important role for the phosphatidyl inositol-3 kinase (PI3-kinase) signalling pathway in SCLC cell survival. The PI3-kinase family of enzymes phosphorylate inositol-containing phospholipids, which initiates downstream signalling cascades involving phosphorylation of Akt (113). It has been shown that PI3-kinase is a central component of the anti-apoptotic pathway in fibroblasts and is activated by the SCLC autocrine growth factors IGF-1 and SCF (114-116). Furthermore, elevated levels of PI3-kinase activity have been demonstrated in SCLC cell lines and inhibition of PI3-kinase has been shown to prevent SCLC cells from growing in an anchorage independent fashion, promoting apoptosis (117). Thus PI3-kinase may act as a central mediator of multiple survival signals in SCLC cells making it an attractive therapeutic target.

Several other mechanisms of resistance to apoptosis induced by chemotherapy agents have been described in SCLC cells. Although these are not steps in malignant transformation, the development of chemotherapy resistance is central to the biology of SCLC and thus they warrant further discussion. Cellular resistance to chemotherapeutic agents can be mediated by active efflux of drugs thereby reducing intracellular concentration. The MDR-1 gene encodes P-glycoprotein (PGP), which acts as a drug efflux pump at the cell membrane, and its role in acquired drug resistance has been extensively studied in haematological malignancies (118). In a small study of SCLC biopsy specimens (n=50), PGP expression was significantly correlated with a poor response to chemotherapy (119). Furthermore, polymorphisms in the MDR-1 gene have been shown to predict chemotherapy (EP) response in SCLC (120). However, SCLC response to chemotherapy has not been consistently shown to correlate with PGP expression and thus its role remains unclear (121). SCLC cells may also acquire chemo-resistance through alteration in drug targets. Several important chemotherapeutic agents, including etoposide, cause cancer cell apoptosis through inhibition of the topoisomerase family of enzymes, resulting in DNA double-strand breaks (122). It has been shown that an etoposide-resistant SCLC cell line established from a recurrent drug resistant tumour displayed lower levels of topoisomerase II expression and activity (123). However, the role of alteration in topoisomerase II as a predictor of chemotherapy response remains uncertain. It is likely that these mechanisms may contribute to SCLC drug resistance in recurrent or refractory tumours but that other mechanisms are important in cell survival from the initial chemotherapy insult. Thus, research has continued to define new mechanisms of SCLC resistance to apoptosis.

1.5.5 Mechanisms Of Angiogenesis In SCLC.

Angiogenesis, the formation of new blood vessels that is central to normal tissue growth and repair, is a crucial process in tumorigenesis (124). Tumour growth beyond a microscopic size is dependent on the formation of new blood vessels to provide a supply of oxygen and nutrients (124). Furthermore, new blood vessels provide a means for the tumour to spread to distant sites (124). Vascular endothelial growth factor (VEGF) is a central regulator of angiogenesis (125). Increased VEGF

levels are observed in the serum of SCLC patients compared to healthy controls and in a Japanese population it has been shown that a low concentration of serum VEGF correlates with improved survival (126). Study of angiogenesis within the local tumour environment is difficult in SCLC due to the paucity of surgical resection specimens. However, one group have shown that in 87 resected SCLC tumours VEGF expression and degree of angiogenesis (assessed by microvessel count) predicted patient survival and metastatic potential (127). In addition, inhibition of VEGF receptor restricts SCLC growth *in vivo* (128). Basic fibroblast growth factor (bFGF) is also a key mediator of angiogenesis (129). Increased levels have been observed in serum from patients with SCLC and have been shown to correlate with survival, suggesting an important role for this factor in SCLC pathogenesis (129). These data indicate that SCLC is a vascular tumour and that targeting angiogenesis factors may restrict cancer growth and spread.

1.5.6 Mechanisms Of Migration And Invasion In SCLC.

As previously indicated, SCLC has a highly metastatic potential and although the specific mechanisms of migration and tissue invasion are not yet clear, several candidates been implicated. c-Met is an RTK, which is expressed in SCLC cell lines and established xenografts (130). Stimulation of SCLC cell lines with the ligand for c-Met, hepatocyte growth factor (HGF), has been shown to result in increased cellular migration and formation of filopodia, mediated by PI3-kinase signalling (131,132). Fibroblasts and smooth muscle cells are the major source of HGF (133). Therefore, it is plausible that HGF production by non-cancer cells within the tumour microenvironment may act in a paracrine fashion to promote SCLC migration. Another RTK, epidermal growth factor receptor (EGFR), has also been implicated in SCLC invasive phenotype (134). However, the expression of EGFR in SCLC cases has been reported to be low or undetectable and thus the significance of these findings is uncertain (135). Other growth factors may also contribute to SCLC migration; e.g. GRP has been shown to have a positive chemotactic effect on SCLC cell lines (136).

Matrix metalloproteinases (MMP) are a family of proteolytic enzymes that may facilitate tumour invasion, metastasis and angiogenesis (137). Expression of MMPs

has been confirmed in SCLC tumour sections and correlates independently with poor patient survival (138). Furthermore, inhibition of MMPs in pre-clinical models has been shown to reduce tumour growth and dissemination suggesting a role for these enzymes (139). SCLC has a propensity for metastasis to the bone marrow. Interestingly, the chemokine receptor, CXCR4, which has a central role in haematopoietic cell migration to the bone marrow, is highly expressed on SCLC cells and tumour samples (140). Stimulation of SCLC cells with the chemokine CXCL12 has been shown to promote SCLC cell invasion through extracellular matrix (140). This may prove to be an important mechanism for distant tissue invasion by SCLC cells.

1.6 Novel Targeted Therapies In SCLC.

The greater understanding of the biology of SCLC has prompted the clinical trial of a variety of targeted therapies. Primarily, these have focused on growth factor pathways, anti-apoptotic mechanisms and modulators of angiogenesis. In addition new agents targeting chromosomal instability or SCLC-specific tumour markers have been developed which are undergoing pre-clinical evaluation.

1.6.1 Neuropeptide Antagonists.

Although the anti-GRP monoclonal antibody, 2A11, has shown pre-clinical efficacy in SCLC it has not demonstrated significant efficacy in a small (n=13) clinical trial (96,141,142). This may be explained by the presence of multiple neuropeptide growth pathways in SCLC. Thus, research has focused on the design of 'broad-spectrum' neuropeptide antagonists. Initially, synthetic peptide analogues were produced (e.g. SP-G - [Arg^{6},D-$Trp^{7,9}$,$N^{me}Phe^{8}$]-substance-P(6-11)) to antagonise the cellular effects of substance-P (143). Subsequently, these compounds have been shown to inhibit calcium mobilisation stimulated by GRP and AVP in SCLC cells (144). Furthermore, broad-spectrum neuropeptide antagonists have been shown to inhibit SCLC proliferation *in vitro* and inhibit the growth of SCLC tumours in nude mice xenograft models (145). SP-G has completed a phase I clinical trial where it showed minimal toxicity at therapeutic plasma concentrations (146). In addition, a study of SCLC cell lines (GLC-14, -16, -19) derived from a single patient before and after the development of drug resistance has shown an increase in SP-G response in

more chemo-resistant cells (95). These data suggest that the development of neuropeptide antagonists may be an important new therapeutic strategy for SCLC, particularly in recurrent and/or drug resistant tumours. Phase II and III clinical trials are urgently needed.

1.6.2 Receptor Tyrosine Kinase Inhibitors.

SCLC cells utilise a variety of RTKs in growth, angiogenesis and migration. Recently, several small molecule inhibitors of tyrosine kinase activity have been developed and shown to have efficacy in NSCLC and other solid tumours (92). Some of these have a broad spectrum of action and can inhibit the tyrosine kinase activity of several important receptors implicated in SCLC pathogenesis. Imatinib™ (STI 571), a known small molecule inhibitor of platelet derived growth factor (PDGF) receptor and ABL tyrosine kinase activity, has also been shown to have activity against c-Kit (147). Although Imatinib™ inhibits the growth of SCLC lines *in vitro* and in xenograft models it has not shown efficacy as single agent or in combination with standard chemotherapy in phase II trials (99,148,149). Vandetanib™ (ZD6474) is a small molecule inhibitor of VEGF receptor 2 that also has activity against EGFR (150). Pre-clinical studies have shown that Vandetanib™ induces apoptosis in SCLC cells and reduces the frequency of large metastastic deposits in a xenograft model (151). Unfortunately a phase II trial failed to show any benefit with Vandetanib™ as maintenance therapy in SCLC (152). Other RTK inhibitors have been developed and will soon see clinical trial. Unfortunately, it seems increasing likely that these agents are unlikely to be successful. The use of small molecule inhibitors of RTK in NSCLC has indicated that the efficacy of such agents relies heavily on receptor activation through mutation rather than high levels of expression (92). Further research is needed to define signalling pathways in SCLC that are constitutively activated, perhaps through gene array experiments, rather than simply demonstrating the presence of receptors and ligands.

1.6.3 Inhibitors Of Cell Survival Pathways.

It has been demonstrated that SCLC cells possess a variety of mechanisms for survival of external pro-apoptotic stimuli including cytotoxic therapy. Thus, these cell survival pathways could be useful clinical targets to treat SCLC and overcome

treatment failure due to chemoresistance. SCLC expression of Bcl-2 has been targeted with anti-sense oligonucleotides but unfortunately a phase II clinical trial has failed to show any anti-cancer efficacy (153). As alternatives to anti-sense molecules, which suffer from delivery problems, selective non-peptide Bcl-2 inhibitors have been developed, which mimic BH domains in Bcl-2 that normally allow interaction with pro-apoptotic proteins such as Bid (e.g. ABT-737) (154). These agents have considerable cytotoxic efficacy against SCLC lines in pre-clinical studies and the results of phase II trials are keenly awaited (155).

Despite the central role of PI3-kinase in SCLC survival and as a downstream target for growth factor pathways, little clinical research has addressed the role of PI3-kinase inhibitors in SCLC. Temsirolimus is an inhibitor of mammalian target of rapamycin (mTOR) a downstream signalling moiety in a variety of cell signalling pathways including PI3-kinase (156). Unfortunately in a phase II trial this agent has not been shown to improve median survival in extensive disease SCLC (157). The failure of this compound to produce a clinical effect may reflect activity of mTOR-independent survival pathways in SCLC. The role of PI3-kinase inhibition requires further study.

1.6.4 Inhibitors of Angiogenesis.

Bezacizumab is a monoclonal antibody that binds to VEGF and prevents ligand interaction with the VEGF receptor (158). It has been shown in clinical trials to be effective in NSCLC, breast and colon cancer (92). Bezacizumab is currently in a phase II clinical trial as maintenance for limited disease SCLC after standard chemotherapy. Thalidomide has been shown to have potent anti-angiogenic effects (159). In a phase II trail of ED SCLC, thalidomide treatment for responders to standard chemotherapy was well tolerated and gave a median survival of 12.8 months (160). This prompted a phase III trial completed in 2007 (n=119) that demonstrated a small but significant survival advantage with thalidomide for chemotherapy responders of good performance status (161). Thalidomide exerts its effects in part through decreased VEGF and bFGF activity and therefore tyrosine kinase inhibitors that target the receptors for these growth factors may be more effective and less toxic (162). However, the VEGFR inhibitor Vandetanib^{TM} has

failed to show any efficacy in SCLC and thus further evaluation of these pathways are required in SCLC (152). Another anti-angiogenic strategy studied in solid malignancies has been the use of matrix metalloproteinase (MMP) inhibitors. MMP expression is associated with a poor prognosis in SCLC (163). Unfortunately marimastat, which inhibits MMP-2 and –9, has shown no clinical efficacy and is associated with significant musculoskeletal toxicity in SCLC (163).

It is clear that there has been a considerable investment both in time and money into the development of new treatment strategies for SCLC. The targeted therapies have been rationally designed with respect to the current understanding of SCLC biology. Furthermore, efficacy has frequently been observed in pre-clinical studies. However, not a single effective new treatment has arisen. The reasons for these failures are multitude and include inadequate information about the development of SCLC cancer, the paucity of ample clinical samples for genetic/proteomic analysis and the lack of an animal model to allow comparative studies. In addition, it is clear that SCLC has been viewed in isolation from its microenvironment and therefore pre-clinical studies inhibiting SCLC intrinsic pathways may produce misleading information. Understanding the interactions between SCLC cells and the tumour microenvironment may explain key features of SCLC biology.

1.7 The Role Of The Tumour Microenvironment in SCLC.

The role of the inflammatory tumour microenvironment in cancer cell development, growth and spread has been recognised for more than a century. In 1863, Virchow described inflammatory cells within neoplastic tissue and proposed a functional connection (164). Furthermore, Paget, in 1898, recognised that breast cancer cells (designated the seed) required a permissive environment (soil) to develop their full potential (165). Studies in epithelial skin tumours have significantly contributed to our understanding of the tumour microenvironment and clearly implicate inflammatory cells in the initiation and progression of cancer (166). It is now widely accepted that tumours are complex ‘tissues’ similar to a wound, containing stromal cells and a supporting matrix of extracellular proteins (166). Interaction between the neoplastic cells, matrix and stromal cells promote tumour growth, survival and

spread (166). Understanding this interplay is critical to the development of new and rational anti-cancer therapies.

1.7.1 Extracellular Matrix.

In 1999, Sethi *et al* published seminal work investigating the role of extracellular matrix (ECM) within the tumour microenvironment in SCLC growth and survival (167). These data demonstrate that an extensive network of ECM proteins infiltrates SCLC, including fibronectin, laminin and collagen IV. In addition, the extent of ECM surrounding tumour cells correlates with survival; patients with extensive fibronectin matrix had a significantly ($p< 0.05$) shorter survival time (8.4 months) than those who had little or no fibronectin matrix (15 months) (167). Previous work has indicated that ECM proteins support SCLC cell growth *in vivo* (168). Sethi *et al* confirmed this, showing that ECM proteins stimulate clonogenic growth of SCLC cells *in vitro* (167). Furthermore, they demonstrated that SCLC cells adhere to ECM *in vitro*, adopting a flattened morphology, which protects against the pro-apoptotic effects of chemotherapeutic agents (cisplatinum, etoposide and cyclophosphamide), a process mediated by β1 integrins (α2 β1, α3 β1, α6 β1 and αv β1) (167).

These results strongly suggest that SCLC-ECM interaction in the local microenvironment mediated by β1 integrins promote SCLC growth and protect against the cytotoxic effects of chemotherapeutic agents. Subsequently, this would allow tumour recurrence at the primary site after the initial cycles of treatment. Therefore, disrupting this interaction could have important therapeutic implications and improve survival in SCLC. Understanding the mechanisms of ECM/integrin-mediated chemo-resistance and integrin activation is central to the development of novel targeted therapies.

1.7.2 Fibroblasts.

Extensive work has demonstrated the role of the fibroblast in carcinogenesis (169). The presence of proliferating, activated fibroblasts (known as myofibroblasts) has been demonstrated in a variety of solid tumours (169). Myofibroblasts are large spindle shaped cells that express vimentin (a mesenchymal marker) and α-smooth muscle actin (α-SMA) (170). They have been observed at the tumour-stroma border

and correlate with the invasive potential of malignancy (171). Importantly, *in vivo* models have demonstrated the importance of myofibroblasts in tumour initiation, growth and spread (172-174). Tumour-myofibroblast interactions can result in the release of ECM proteins, MMPs and angiogenic factors (171). The signals mediating tumour-fibroblast interactions have been studied and include transforming growth factor-beta (TGF-β) and platelet derived growth factor (PDGF) (171). SCLC cell lines secrete a variety of bioactive molecules including GRP and transforming growth factor-β (TGF-β) (93,175,176). TGF-β has been shown to increase ECM production by primary lung fibroblasts and GRP has been shown to promote fibroblast proliferation (177,178). This data is of interest, as the source of the ECM in the SCLC stroma remains unclear. Positive staining for fibronectin and laminin is observed within the cytoplasm of SCLC cells in a proportion (>15%) of tumour sections suggesting autocrine production of ECM (167,179). However, SCLC cell lines infrequently secrete ECM proteins *in vitro* (179). Thus, paracrine interactions between SCLC cells and stromal fibroblasts could create a matrix rich microenvironment promoting tumour growth. Further research is required to define the role of the fibroblast in the SCLC stroma, which may reveal novel targets for modulating ECM production and thus chemo-resistance.

1.7.3 Immune Cells.

In addition to fibroblasts, the tumour stroma is also comprised of immune cells. The role of the immune response in cancer has long been debated. It is clear that certain cancers are more common in the immunocompromised host (180). In addition the presence of certain immune cells (e.g. tumour infiltrating lymphocytes (TIL)) within solid malignancies is associated with a better cancer stage and overall prognosis (181). Furthermore, cancer patients can develop immune responses against specific tumour antigens supporting the concept of tumour immunosurveillance (182). However, it is widely accepted that tumours can develop within sites of chronic inflammation and the presence of immune cells (e.g. macrophages) within the tumour stroma can support cancer growth and spread (183). Two main processes have been proposed to explain how cancer cells may evade immunosurveillance, chiefly immunoselection and immunosubversion. Immunoselection involves the host

immune system, early in carcinogenesis, eradicating tumour cells that display immunogenic antigens thus positively selecting for the growth of tumour cells that are not recognised (184). The concept of immunnosubversion proposes that tumour cells can suppress or alter immune cell function throughout tumour development and these tumour-associated immune cells may support cancer growth and spread (180). Thus, whilst utilising anti-tumour immune responses to specifically target cancer cells is a highly attractive therapeutic option, the mechanisms involved in immunosubversion need to be understood first. It is likely that this will result from research into cancer-immune cell interaction in the tumour microenvironment.

There is a paucity of data regarding immune responses in SCLC. It is clear from studies of neurological paraneoplastic complications in SCLC that the immune system can recognise tumour antigens (185). SCLC cells express a variety of proteins (HuD, HuC and Hel-N1) also shared by neurons, which are recognised by anti-Hu antibodies found in the serum of patients with paraneoplastic neuropathy (185). Interestingly, some case reports suggest that these patients have a better prognosis and may display spontaneous tumour regression (185,186). However an effective anti-tumour immune response is rarely observed, which has prompted the search for immune defects in SCLC.

Early studies have indicated that peripheral immune responses are blunted in patients with SCLC. It has been shown that peripheral blood lymphocytes from SCLC cases showed reduced proliferative responses and IL-2 production when stimulated with phytohemagglutinin compared to healthy volunteers or NSCLC patients (187). Another group demonstrated that IL-2 production from peripheral lymphocytes predicted patient survival and that decreased production was corrected when the tumour load was reduced, raising the possibility of local tumour factors in immunomodulation (188,189). A more recent study (2000) demonstrated that the presence of infiltrating CD8+ lymphocytes predicted small tumour size and increased survival in SCLC cases removed surgically (190). Thus, it appears from these data that the host immune response may contribute to local control of SCLC growth but that SCLC cells can subvert aspects of cellular immunity. Vaccine and monoclonal antibody strategies are under evaluation as new therapies for SCLC (191). The

mechanisms of SCLC-immune cell interaction will need to be investigated prior to the further design of effective anti-cancer vaccines.

1.8 Concluding Remarks.

It is clear that SCLC will continue to be a significant health burden at least for the next two decades. Despite advances in chemotherapy and radiotherapy there has been little impact on the long-term survival in this frequently lethal cancer. Our understanding of SCLC biology has increased dramatically and we now are in the process of designing novel therapy to target growth factors, cell survival pathways and angiogenesis. Unfortunately clinical trials of these agents have produced unremarkable results. One important explanation for this is that historically we have viewed cancer cell biology in isolation from its inflammatory stroma, focusing instead on the step-wise acquisition of genetic defects. This is particularly apparent in SCLC research and is well demonstrated by the paucity of information regarding the tumour microenvironment and mechanisms of SCLC-stroma interaction. Addressing this balance will prove essential in the development of future treatments.

AIMS:

With the background described in the introduction the aims of this PhD were to investigate the mechanisms of SCLC interaction with two main components of the tumour microenvironment; ECM and immune cells. The following specific aims were:

(1) Define the mechanisms of ECM-mediated chemo-resistance in SCLC cells.

(2) Define new integrin affinity modulation pathways:

- **(a) Determine the role of phospholipase C epsilon in H-Ras-mediated integrin suppression.**
- **(b) Determine the signalling pathways involved in Notch-mediated integrin activation.**
- **(c) Investigate the role of Notch signalling in SCLC cells.**

(3) Investigate the local immune cell infiltrate in SCLC and correlate this with patient survival.

(4) Investigate mechanisms of immunosuppression by SCLC cells.

CHAPTER 2: Materials And Methods.

2.1 Cell Lines And Maintenance Cultures.

Small cell lung cancer cell lines, NCI-H69, NCI-H345 and NCI-H510 were obtained from ATCC (Rockville, Maryland, USA) and maintained in HEPES buffered RPMI 1640 medium (Invitrogen) supplemented with 10% (v/v) heat-inactivated foetal calf serum (FCS) (Labtec), 5μg/ml L-glutamine, 50U/ml penicillin and 50μg/ml streptomycin (Invitrogen Ltd, UK). SCLC cells were maintained in suspension at 2-5 x 10^5 cells/ml and passaged up to 10 times prior to use. It was confirmed that all SCLC cell lines expressed typical human neuroendocrine markers (CD56, CAM 5.2 and synaptophysin).

CHO-K1 cells were obtained from ATCC (Rockville, Maryland, USA). The CHO(αβ-py) cell line, which stably expresses a chimeric integrin comprised of αIIb α6 β3 β1 has been described previously and was a kind gift from M. Ginsberg (Scripps Research Institute, La Jolla, California, USA) (192). All CHO cell lines were maintained in Dulbecco's Modified Eagles Media (DMEM) (Sigma) supplemented with 10% (v/v) FCS, 5μg/ml L-glutamine, 50U/ml penicillin and 50μg/ml streptomycin and 1% non-essential amino acids. G418 (Invitrogen) was added at a final concentration of 400μg/ml to CHO(αβ-py) cell cultures. Adherent cultures of CHO cell lines were maintained at 10-80% confluence and passaged by treatment with trypsin (0.1%) (Sigma) up to 10 times prior to use.

The human myeloid leukaemia cell line, K562 was obtained from ATCC. K562 cells were maintained in HEPES buffered RPMI medium (Invitrogen) supplemented with 10% (v/v) heat-inactivated FCS (Labtec), 5μg/ml L-glutamine, 50U/ml penicillin and 50μg/ml streptomycin (Invitrogen Ltd, UK). K562 cells were maintained in suspension culture at less than 1 x10^6 cell/ml and passaged up to 10 times prior to use.

2.2 DNA Constructs.

All DNA constructs were prepared using Maxiprep™ kits (Qiagen) according to the manufacturers instructions, sequenced prior to use (MWG Biotechnology) and checked by restriction enzyme digestion.

Mouse Notch-1 constructs, NIC, NΔE, NΔE(V1774K) and NLNG in pCS2 (C-terminal Myc-tag) were a kind gift from R. Kopan (Washington University School of Medicine, St Louis, USA) (193). Human Notch-1 constructs, ICN1, ΔTADP, ΔEN1 and ΔANK in pcDNA3.1 were a kind gift from J. C. Aster (Department of Pathology, Harvard Medical School, USA) (194). The human Notch-1 constructs were subcloned into pCMV Tag 4A (Stratagene) to incorporate a C-terminal Flag-tag. The intracellular domain of human Notch-2 (ICN2) in the vector IRES/GFP was a kind gift from C. Klug (University of Alabama, Birmingham, USA) and was subcloned into pCMV Tag 4A to incorporate a C-terminal Flag-tag. MINT in pEF-Bos-Neo (N-terminal Myc-tag) was a kind gift from T. Honjo (Kyoto University, Japan) (195).

Wild type (WT) and kinase dead (H1433L) PLCε in pCMV were provided by G. G. Kelley (SUNY Upstate Medical University, Syracuse, USA). Tac-α5 was a kind gift from S. E. LaFlamme (Centre for Cell Biology and Cancer research, NY, USA). H-Ras-G12V and effector mutants in pDCR (Myc-tag) were a kind gift from M. H. Wigler (Cold Spring Harbour Laboratory, NY, USA). Y. Lad produced the D38N mutation of pDCR-H-Ras (G12V) by site directed mutagenesis. R-Ras(WT), R-Ras(T43N) and R-Ras(G38V) (Myc-tag) in pSG5 were a kind gift from M. Ginsberg (Scripps Research Institute, La Jolla, California). pCDNA3-Raf-CAAX (Flag-tag) was a gift from C. K. Weber (University of Ulm, Germany). Plasmids encoding myc-tagged constitutively active PKB-pUSEamp myr-Akt1/PKBα and myc-tagged dominant-negative PKB-pUSEamp Akt1/PKBα (K179M) were obtained from Upstate Biotechnology.

pGEX-4T2 containing the 9-11 type III repeats of fibronectin was a kind gift from M. Ginsberg. J. de Gunzburg (INSERM U-528, Paris, France) provided pRK-Rap1A(S17N). A. Wittinghofer (Max Planck Institut, Dortmund, Germany) donated pGEX-RAP1-GAP (75-415). RAP1-GAP (75-415) was subcloned into pCMV Tag 3B (Stratagene) to incorporate an N-terminal Myc-tag. pGL2 4xCSL was a gift from A. Israel (Institute Pasteur, France) (193). pEGFP-C3 was purchased from Clontech (Basingstoke, UK). pcDNA3.1 LacZ was purchased from Invitrogen.

2.3 Antibodies.

2.3.1 Antibodies Used In Western Blot Analysis.

Anti-HA (Y-11), anti-Myc (9E10), anti-ERK2 (C-14), anti-β3-integrin (N-20) and anti-PLCε antibody (V-20) were from Santa Cruz Biotechnology (Santa Cruz, CA, USA). Anti-phospho-ERK1/2 (ERK-PT115), anti-phospho-PKB (pThr308) (P3862), mouse anti-$p21^{Cip1/WAF1}$ (clone CP74), mouse anti-$p27^{Kip1}$ (clone DCS-72), anti-β-actin (AC-40) and anti-FLAG (M2) were from Sigma (Dorset, UK). Anti-RalA antibody was from Transduction Laboratories (Lexington, USA). Anti-GSK-3α/β, anti-phospho-GSK-3β (pS9), anti-caspase-3 (Asp175) (5A1) and anti-caspase-9 (CCSA 315/316) were obtained from Biosource International (Nivelles, Belgium). Anti-phospho-CDK2 (Thr160), anti-phospho-CDK1 (Tyr15), anti-phospho-Bad (Ser136) and anti-Bad (9292) were obtained from Cell Signalling Technology (Hitchin, Hertfordshire, UK). Anti-cyclin A was obtained from Oncogene Research Products (San Diego, CA). Anti-cyclin B was from BD Transduction Labs (San Jose, CA, USA). Mouse anti-cyclin D1 (clone AM29) was obtained from Zymed (Invitrogen, Paisley, UK). Anti-cyclin E (clone HE12) and anti-γH2Ax were obtained from Upstate Biotechnology (Lake Placid, NY, USA). Mouse anti-DNA-PKcs (p350 clone 6) was from BD Biosciences (Oxford, UK). All anti-species specific horseradish peroxidase-conjugated antibodies were from DAKO (Cambridgeshire, UK).

2.3.2 Antibodies Used For Flow Cytometry.

Anti-CD4, anti-CD80, anti-CD86, anti-HLA-DR, anti-CD16 (all phycoerythrin (PE)-conjugated), anti-CD3, anti-CD25, anti-CD69, anti-CD11b (all allophycocyanin (APC)-conjugated), anti-CD14 (peridinin chlorophyll protein (PerCP)-conjugated), activation specific anti αIIb β3 (PAC1) (unlabelled) and appropriately conjugated isotype controls were obtained from BD Biosciences (Oxford, UK). The PE conjugated anti-Tac-α5 antibody (ACT-1) was from Dako (Cambridgeshire, UK). Anti-mouse IgM-FITC was from Biosource (Nivelles, Belgium).

2.3.3 Antibodies Used For Immunohistochemistry.

Anti-CD3 (clone 565), anti-CD4 (clone 368) and anti-CD8 (clone 4B11) were obtained from Novocastra Reagents (Leica Microsystems, Wetzlar, Germany). Anti-CD20 (clone L26), anti-CD45 (clone 2B11 and PD7/26) and anti-CD68 (clone PGM1) were obtained from Dako (Cambridgeshire, UK). Anti-species specific horseradish peroxidase-conjugated antibodies were from DAKO (Cambridgeshire, UK).

2.3.4 Antibodies Used In Cell Culture.

Anti-CD3 (clone UCHT1), anti-CD28 (clone AEG04) and pan-isotype specific anti-TGF-β (clone AB-100-NA) were obtained from R&D systems (MN, USA). The β1 integrin-stimulating antibody, TS2/16 (sc-53711), was obtained from Santa Cruz Biotechnology (California, USA). Anti-β1 integrin antibody, 4B4, was obtained from Beckman Coulter (California, USA). All antibodies used in cell culture were obtained free of azide and maintained sterile.

2.4 Transfection Of Cell Lines.

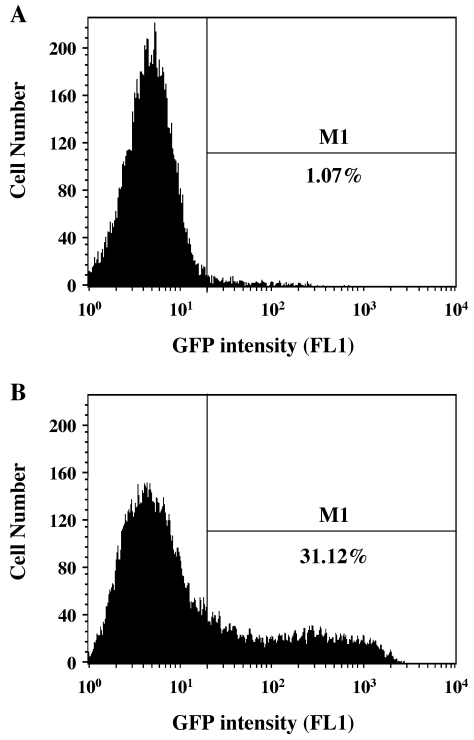
SCLC cell lines were washed twice in phosphate buffered saline (PBS), re-suspended in RPMI (w/o serum or antibiotics) (0.5 x 10^6 cells /ml) and transfected with 1μg of DNA/10^6 cells using Lipofectamine 2000 (1:5 ratio) according to the manufacturers instructions. Subsequently, cells were cultured in HEPES buffered RPMI 1640 medium (Invitrogen) supplemented with 10% (v/v) FCS (Labtec), 5μg/ml L-glutamine, 50U/ml penicillin and 50μg/ml streptomycin (Invitrogen Ltd, UK) prior to experiments. Using this method, transfection of pEGFP as a marker routinely gave transfection efficiencies of 30-40% at 24 hours. Thus to enrich for a transfected population, GFP positive cells were separated prior to experimentation using a flow-sorting technique (Fig. 2.1)

Transient transfections of CHO cell lines were performed with Lipofectamine™ and Plus reagent (Life Technologies) as per manufacturers instructions. Twenty-four hours after transfection, media containing DNA-Lipofectamine complexes were removed and replaced with fresh complete media. Transfected cells were cultured in DMEM (Sigma) supplemented with 10% (v/v) FCS, 1% L-Glutamine, 5μg/ml L-

glutamine, 50U/ml penicillin and 50μg/ml streptomycin for 48 hours prior to experiments.

K562 cells were transfected with test DNA as indicated by Nucleofector electroporation (Amaxa, Germany) according to the manufacturers instructions. Programme T-16 and solution V was used. Immediately following electroporation, cells were transferred to RPMI (with 10% FCS, no antibiotics) media kept at 37^{o}C and cultured for 48 – 72 hours prior to experiments. Using pEGFP this produced transfection efficiencies of 60-80% at 48-72 hours.

Figure 2.1: Transfection Of H345 SCLC Cells With Lipofectamine 2000^{TM}.



H345 cells were transfected with (A) empty vector (pcDNA3.1) or (B) pEGFP (both 1μg of DNA/10^6 cells) as indicated above. The percentage of GFP positive cells was determined by flow cytometry after 24 hours (marker M1). It was observed that the transfection efficiency with pEGFP was between 30 and 40%. Thus, pEGFP was co-transfected with test plasmid DNA to identify transfected cells. To enrich the transfected cell population, GFP positive cells were selected by sterile flow sorting and retained for further experiments.

2.5 Western Immunoblots.

Cells were washed twice in PBS, re-suspended in lysis buffer (0.3M NaCl, 1.5mM $MgCl_2$, 0.2mM EDTA, 25mM HEPES pH 7.4, 0.25% Triton X-100, 1x protease inhibitor (Boheringer), 20mM β-glycerophosphate, 0.5mM dithiothreitol and 1mM orthovanadate) and agitated on ice for 15 minutes. Whole cell lysates were balanced for protein concentration using a BCA protein assay according to the manufacturers instructions (Pierce, USA). Balanced whole cell lysates were re-suspended in 4x Laemmli sample buffer (0.25M Tris, pH 6.86, 6% SDS, 40% glycerol, 0.04% bromophenol blue, 20% 2-mercaptoethanol) and denatured by heating to 95°C for 5 minutes. Samples were resolved on 8-12% SDS-PAGE gels (10μg protein per lane) and transferred onto Hybond C nitrocellulose (Amersham Pharmacia Biotech). Blots were blocked in either 5% milk or 3% BSA in TBS Tween and probed with the specified antibodies overnight at 4°C in blocking buffer, followed by incubation in appropriate horseradish peroxidase labelled secondary antibodies (Dako) diltuted in blocking buffer (1:5000). Bands were visualised with Enhanced Chemiluminescence reagent (Amersham).

2.6 Assessment Of Apoptosis In SCLC Cells By Acridine Orange/Ethidium Bromide Staining.

Prior to experiments, SCLC cells were cultured overnight in quiescent media (RPMI supplemented with 0.25% (w/v) BSA, 50U/ml penicillin and 50μg/ml streptomycin), washed twice in PBS and then re-suspended in SITA media (RPMI supplemented with 30nM selenium, 5μg/ml insulin, 10μg/ml transferrin, 0.25% (w/v) BSA, 50U/ml penicillin and 50μg/ml streptomycin). Exclusion of FCS from media for experiments was necessary to prevent contact of cells with the ECM protein fibronectin, which is a significant active component of FCS.

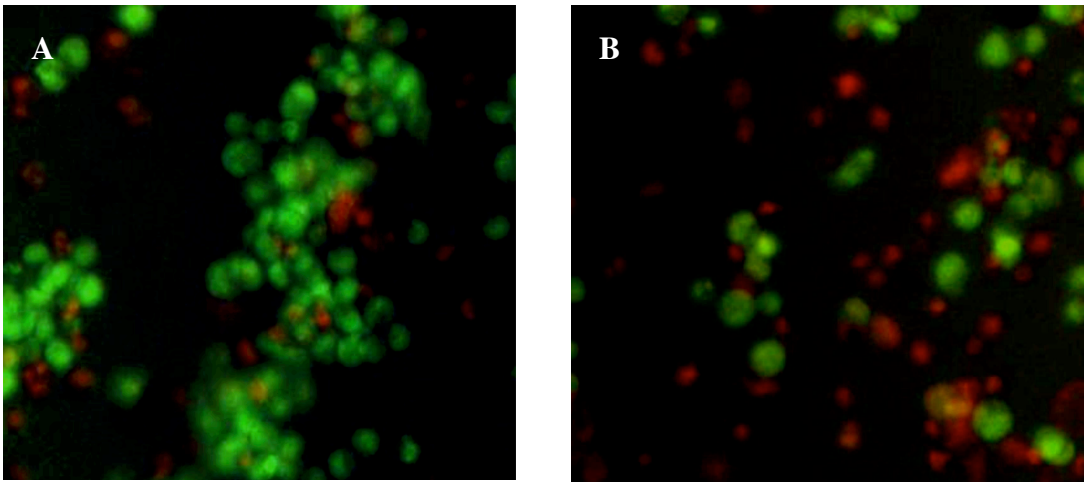
For experiments assessing the role of ECM, 96 well plates were pre-coated, by incubation at 37°C for 1 hour, with 100μl/well of poly-l-lysine (10μg/ml) (Sigma), laminin (10μg/ml) (Sigma), fibronectin (20μg/ml) (Sigma) or TS2/16 (10μg/ml) (Santa Cruz Biotechnology) solution in PBS as indicated. Wells were washed twice in PBS prior to use. SCLC cells were added (4×10^4 cells/well) and allowed to settle

for 1 hour at 37ºC to promote cell adhesion. Subsequently, cells were treated with ionizing radiation (1-4 Gray) using a 6MV linear accelerator or the chemotherapy agent etoposide (25μg/ml) (Sigma) as specified. In experiments using 4B4 to block β1 integrin function, cells were incubated with 4B4 (10μg/ml) (Beckman Coulter) at 37ºC for 30 minutes prior to seeding onto ECM. In some experiments sodium orthovanadate (Na_3VO_4) (200μM) (Sigma), LY294002 (30μM) (Calbiochem) or tyrphostin-25 (25 μM) (Calbiochem) was added immediately prior to irradiation or etoposide. In experiments investigating the genetic manipulation of PI3-kinase signalling, H345 SCLC cells were transfected with test DNA or vector as described above and cultured for 24 hours prior to use in these experiments.

In experiments investigating the effect of Notch signalling on apoptosis, 96-well plates were pre-coated with human recombinant Notch ligands. Delta-like ligand-4 (DLL-4), polyhistidine peptide (control for DLL-4), Jagged-1 or IgG1 (control for Jagged-1) (all R&D systems) were diluted to 0-10μg/ml in PBS and 100μl of solution was added to each well of a 96-well plate. Plates were incubated for 1 hour at 37°C and washed twice with PBS prior to use. Subsequently, H69 SCLC cells (4 x 10^4/ml in SITA media) were cultured with immobilised Notch ligands for 12 hours at 37ºC prior to treatment with etoposide (25μg/ml) as described above.

Apoptosis was assessed at time points specified (0-72 hours) by the addition of 1μl of ethidium bromide (1mg/ml) (Sigma) and 1μl acridine orange (1mg/ml) (Sigma) to each well of the 96-well plate to be assessed. After 2 minutes the percentage of apoptotic cells were determined by fluorescent microscopy (Olympus BH2 fluorescence microscope). This assay relies upon alterations in cell membrane permeability during cell death. The cell membrane is always permeable to the cationic dye; acridine orange, which when intercalated with DNA can be excited to emit green fluorescence. Conversely, ethidium bromide is not able to penetrate the cell membrane of viable cells but on binding DNA can be excited to emit orange fluorescence. Cell death increases membrane permeability and therefore apoptotic cells can be identified as small green (early apoptosis) or small orange cells (late apoptosis) allowing the percentage of apoptotic cells to be counted for each experimental condition (Fig. 2.2).

Figure 2.2: SCLC cells stained with acridine orange/ethidium bromide.



(A) SCLC cells cultured in RPMI (SITA) for 72 hours. (B) SCLC cells cultured in RPMI (SITA) plus etoposide 25μg/ml for 72 hours. 1μl of ethidium bromide (1mg/ml) and 1μl acridine orange (1mg/ml) was added to the wells, and the cells were viewed by fluorescent microscopy (400x). Apoptotic cells are small and either green (early apoptosis) or orange (late apoptosis).

2.7 Assessment Of Apoptosis In SCLC Cells By Cell Death ELISA Kit.

SCLC cells were cultured overnight in quiescent media, washed twice in PBS and then re-suspended in SITA media. 2 x 10^5 SCLC cells/well were seeded into 24-well plates pre-coated with poly-l-lysine (10μg/ml) (Sigma), laminin (10μg/ml) (Sigma), fibronectin (20μg/ml) (Sigma) or TS2/16 (10μg/ml) (Santa Cruz Biotechnology) as indicated. Cell were allowed to settle for 1 hour at 37ºC and then treated with ionizing radiation (1-4 Gray) using a 6MV linear accelerator or the chemotherapy agent etoposide (25μg/ml) (Sigma) as specified. In experiments using 4B4 to block β1 integrin function, cells were incubated with 4B4 (10μg/ml) (Beckman Coulter) at 37ºC for 30 minutes prior to seeding onto ECM. In some experiments sodium orthovanadate (Na_3VO_4) (200μM) (Sigma) or LY294002 (30μM) (Calbiochem) was added immediately prior to irradiation or etoposide. In experiments investigating the genetic manipulation of PI3-kinase signalling, H345 SCLC cells were transfected with test DNA or vector as described above and cultured for 24 hours prior to use in these experiments.

Apoptosis was assessed after 48 hours using the cell death detection ELISA^{TM} kit according to the manufacturer's instructions (Roche Diagnostics). This assay is based on the quantitative detection of histone-associated DNA fragments in mono- and oligonucleosomes. In brief, SCLC cells were re-suspended in lysis buffer (30 minutes), nuclei were removed by centrifugation and supernatants were transferred to a streptavidin-coated micro-plate. Biotin labelled anti-histone and peroxidase conjugated anti-DNA antibodies were added and the plate was incubated for 2 hours at room temperature. The wells of the microplate were washed three times with buffer and substrate solution was added for 15 minutes. Absorbance was measured at 405 nm using an MRX microplate reader (Dynatech, Chantilly, VA).

2.8 Assessment Of Apoptosis In SCLC Cells By Annexin-V.

SCLC cells were prepared as in 2.7. $5x10^5$ cells/well were seeded into 6-well plates pre-coated with poly-l-lysine (10μg/ml) (Sigma), laminin (10μg/ml) (Sigma), fibronectin (20μg/ml) (Sigma) or TS2/16 (10μg/ml) (Santa Cruz Biotechnology) as indicated. Cells were allowed to settle for 1 hour at 37ºC and then treated with ionizing radiation (1-4 Gray) using a 6MV linear accelerator or the chemotherapy agent etoposide (25μg/ml) (Sigma) as specified. In experiments using 4B4 to block β1 integrin function, cells were incubated with 4B4 (10μg/ml) (Beckman Coulter) at 37ºC for 30 minutes prior to seeding onto ECM. In some experiments sodium orthovanadate (Na_3VO_4) (200μM) (Sigma) or LY294002 (30μM) (Calbiochem) was added immediately prior to irradiation or etoposide. In experiments investigating the genetic manipulation of PI3-kinase signalling, H345 SCLC cells were transfected with test DNA or vector as described above and cultured for 24 hours prior to use in these experiments. Percentage apoptosis was assessed after 48 hours by flow cytometric analysis of Annexin V staining according to the manufacturers instructions (Annexin V-PE BD Bioscience). Briefly, SCLC cells (1×10^5) were incubated (5 minutes in the dark) with 1x binding buffer and 5μl Annexin V-PE. ToPro3 (Molecular Probes, Leiden, Netherlands) at a final concentration of 1μM (in PBS) was added to each sample. The percentage of apoptotic cells (Annexin V positive) was determined using a FACS Calibur flow cytometer (BD Biosciences).

2.9 PI3-kinase Activity Assay.

PI3-kinase activity was measured as previously described (117). Cells were spun onto 6-well plates pre-coated with poly-l-lysine (10μg/ml) (Sigma), laminin (10μg/ml) (Sigma), fibronectin (20μg/ml) (Sigma), or TS2/16 (10μg/ml) (BioLegend) as specified. Cells were lysed at the time points indicated by addition of ice-cold lysis buffer (50mM HEPES (pH 7.4), 15mM NaCl, 1.5mM MgCl2, 1mM EGTA, 10mM sodium pyrophosphate, 100mM sodium fluoride, 10% (v/v) glycerol, 1% (v/v) Triton X-100, 0.5mM dithiothreitol, 1mM sodium orthovanadate, 50mM 4-(2-aminoethyl-benzenesulfonyl fluoride, 5mg/ml leupeptin, 20mg/ml aprotinin, and 10μg/ml soybean trypsin inhibitor). After 30 minutes lysates were clarified by centrifugation at 13,000g for 10 minutes. For each assay point 0.5μg of total protein from the supernatant was incubated with 1.0μg of p85-SH3 PI 3-kinase antibody overnight at 4ºC. 30μg of goat anti-mouse IgG agarose beads in lysis buffer were added for an additional 2 hours.

The beads were pelleted and washed twice with lysis buffer, once with a high salt buffer containing 100mM Tris-HCl and 500mM LiCl (pH 7.6) and twice with a solution containing 200mM HEPES, 40mM $MgCl_2$ and 600mM NaCl (pH 7.4). PI3-kinase assays were performed using phosphatidylinositol as substrate in a final volume of 200μl containing: (final concentrations) 50mM HEPES (pH 7.4), 10mM MgCl2, 150mM NaCl, [γ32P] ATP (5μCi, 5000Ci/mmol), 50μM ATP, and 0.5mg/ml sonicated phosphatidylinositol: phosphatidylserine (3:1, w/w). Reactions were carried out for 20 minutes at 37ºC and terminated by the addition of chloroform: methanol: 0.1M HCl (40:80:1, v/v/v; 750μl). A phase-partition was achieved by the addition of chloroform (250μl) and 0.1M HCl (250μl). After centrifugation, the lower phase was washed twice with synthetic upper-phase (methanol: 1M HCl: chloroform, 48:47:3, v/v/v), dried and the lipids were separated by thin layer chromatography (TLC). 3'-phosphorylated lipids were identified by autoradiography using Kodak 'X-OMAT' film and radioactivity was quantified by liquid scintillation counting using 'Flo-Scint IV' (Packard, Biosciences; Groningen, Netherlands) and a Packard 1900 TR liquid scintillation analyser.

2.10 PKB Activity.

PKB activity was measured as previously described (117). SCLC cells were cultured overnight in quiescent media, gently disaggregated and then treated as specified. Cells were lysed using 250µl of ice-cold lysis buffer (50mM Tris/HCl (pH 7.5), 0.1% (v/v) Triton X-100, 1mM EDTA, 1mM EGTA, 0.27mM sucrose, 50mM sodium fluoride, 10mM sodium β-glycerophosphate, 5mM sodium pyrophosphate, 1mM sodium orthovanadate, 0.1% (v/v) 2-mercaptoethanol, 1µM microcystin, 5µg/ml leupeptin, 20µg/ml aprotinin and 10µg/ml soybean trypsin inhibitor). Lysates were clarified by centrifugation at 13,000g for 10 minutes, and PKB was immunoprecipitated by incubating the lysates (containing 150µg of protein) for 90 minutes at 4ºC with 1µg of anti-PKB antibody pre-conjugated to 5µl of protein G-sepharose in lysis buffer. Immunoprecipitates were washed twice with lysis buffer containing 0.5M NaCl and once with wash buffer (50mM Tris/HCl (pH 7.5), 0.03% (v/v) Brij-35, 0.1mM EGTA and 0.1% (v/v) 2-mercaptoethanol). PKB activity was assayed by incubating washed immunoprecipitates at 30ºC for 20 minutes in a thermomixer in 30µl of kinase assay buffer (50µM Crosstide, 50mM Tris/HCl, 0.1mM EGTA, 20µM adenosine 3', 5'-cyclic monophosphate-dependent protein kinase inhibitor, 20mM ATP, 1µM microcystin and [g-32P] ATP (1.0µCi 1000Ci/mmol). The assays were terminated by placing 40µl of the assay mixture onto P8l chromatography paper (Whatman; Maidstone, UK) and washing four times with 0.5% (v/v) phosphoric acid and once with acetone. Radioactive incorporation was quantified by liquid scintillation counting.

2.11 Caspase-3 Activity.

SCLC cells were cultured overnight in quiescent media. Cells were washed twice in PBS, re-suspended in SITA media and then allowed to adhere for 1 hour at 37ºC to poly-l-lysine (10µg/ml) (Sigma), laminin (10µg/ml) (Sigma), fibronectin (20µg/ml) (Sigma), or TS2/16 (10µg/ml) (BioLegend) as specified. In addition, cells were treated with sodium orthovanadate (Na_3VO_4) (200µM) (Sigma), LY294002 (30µM) (Calbiochem), tyrphostin-25 (25µM) (Calbiochem), etoposide (25µg/ml) (Sigma) or z-VAD (100 µM) (Promega) as indicated. Cells were lysed at 48 hours and caspase-3 activity was assayed using a caspase-3 cellular activity kit according to the

manufacturer's instructions (Cat no: 235419 Calbiochem). Specific caspase-3 activity (pmol/minute/μg protein) in each experiment was normalised to untreated cells.

2.12 Cell Cycle Analysis.

SCLC cells were cultured overnight in quiescent media (RPMI supplemented with 0.25% (w/v) BSA, 50U/ml penicillin and 50μg/ml streptomycin), washed twice in PBS and re-suspended in SITA media. For some experiments, H345 SCLC cells were transfected with DNA as described above and cultured for 24 hours prior to use in these experiments. Cells were seeded into 24-well ($2x10^5$/well) or 6-well ($5x\ 10^5$ /well) plates pre-coated with laminin (10μg/ml) (Sigma), fibronectin (20μg/ml) (Sigma), or TS2/16 (10μg/ml) (BioLegend) as specified and allowed to adhere for 1 hour at 37ºC. In experiments using 4B4 to block β1 integrin function, cells were incubated with 4B4 (10μg/ml) (Beckman Coulter) at 37ºC for 30 minutes prior to seeding onto ECM. Subsequently, cells were treated with ionizing radiation (1-4 Gray) using a 6MV linear accelerator or etoposide (25μg/ml) (Sigma) as specified. In some experiments sodium orthovanadate (Na_3VO_4) (200μM) (Sigma) or LY294002 (30μM) (Calbiochem) was added immediately prior to irradiation or etoposide.

Cells were fixed 24 hours later in 70% ice-cold ethanol (for at least two hours) and washed twice in PBS (300g for 5 minutes). Cell pellets were re-suspended in 1ml of propidium iodide (PI) staining solution (50μg/ml PI (Sigma), 0.1% (v/v) Triton X-100 (Sigma) in PBS plus 50μl of DNase-free RNase A (10ug/ml) (Sigma)) and incubated in the dark for 15 minutes at 37ºC. Cells were washed in a further 3 ml of PBS (300g for 5 minutes) and re-suspended in 500μl of PBS prior to analysis by flow cytometry (FACSCalibur (BD Biosciences)). Data were collected from 10,000 events using CELLQuest™ software. Aggregates were excluded by gating for single cells in FL2-W/FL2-A dot plots. The percentage of cells in each phase of the cell cycle was analysed with FlowJo™ using the Watson pragmatic model (196).

2.13 Visualisation Of DNA Double Strand Breaks.

8 well cover slides (Nalge NUNC) were pre-coated with 250µl/well of poly-l-lysine (10µg/ml) (Sigma), laminin (10µg/ml) (Sigma) or fibronectin (20µg/ml) (Sigma) as indicated by incubation at 37ºC for 1 hour. SCLC cells were cultured in quiescent media overnight, washed twice in PBS (200g for 5 minutes) and seeded into the 8-well cover slides at a density of $2.5x10^5$ cells/cm^2. Cells were allowed to adhere for 1 hour at 37ºC and then treated with etoposide (25µg/ml) for 2 hours. Cells were then washed and allowed to recover in RPMI with 10% FCS. Cells were fixed at 0-24 hours after etoposide treatment with 3% paraformaldehyde for 5 minutes, washed twice with PBS, permeabilised with 0.1% Triton and blocked with 0.2% fish skin gelatin. Cells were incubated with 1:500 dilution of anti-γH2Ax (Upstate) for 2 hours at room temperature and washed twice with PBS. Secondary antibody labelled with ALEXAflour 488 (1:500 dilution in PBS) was applied for 1 hour at room temperature in the dark. The slides were viewed using a Zeiss Axioskop 2 microscope. Image analysis was performed using Openlab software from Improvision.

2.14 Assessment Of Integrin Affinity In CHO(αβ-py) Cells.

Cells were transfected with test DNA (as stated) together with 0.75µg Tac-α5 transfection reporter construct (extracellular domain of the IL-2 receptor and the intracellular domain of the α5 integrin). As indicated, CHO(αβ-py) cells were treated with MW167 (50µM) at 36 and 12 hours prior to analysis. Integrin affinity in transfected CHO(αβ-py) cells was analysed by three-color flow cytometry forty-eight hours post transfection. Single cell suspensions of trypsinised cells were resuspended in a total volume of 50µl containing PAC1 (5µg/ml) for 30 minutes at room temperature in HEPES/NaCl buffer (20mM HEPES, 140mM NaCl, 1.8mM $CaCl_2$, 1mM $MgCl_2$ and 2mg/ml Glucose, pH 7.4). Internal controls for each sample were performed containing either 5mM EDTA or 100µM $MnCl_2$. Cells were washed with cold PBS and incubated on ice with 50µl DMEM containing 4% (v/v) anti-mouse IgM-FITC for 30 minutes in the dark. Cells were washed again and incubated on ice for a further 30 minutes with 50µl DMEM containing 2% anti-Tac-α5 antibody (ACT-1) conjugated to RPE (v/v). Cells were finally washed and

resuspended in cold PBS. Immediately prior to analysis on a FACS-Caliber (BD, Erembodegem, Belgium), ToPro3 (Molecular Probes, Leiden, Netherlands) at a final concentration of 1μM (in PBS) was added to each sample.

PAC1 binding was determined by gating for live and highly transfected cells (ToPro3 negative and high Tac-α5 binding respectively). To obtain numerical estimates of integrin activation, an integrin activation index (AI) was calculated, where AI = $((F_N-F_I)/(F_A-F_I))*100$ and Percent Inhibition = $(AI_0-AI)/(AI_0)*100$. F_N is Geometric mean (GM) fluorescence intensity (MFI) of PAC1 binding of the native integrin, F_I is MFI of PAC1 binding in the presence of 5mM EDTA and F_A is MFI of PAC1 binding in the presence of 100μM Mn^{2+}. AI_0 is the Activation index with the control vector and AI is the Activation index with DNA under test. AI was used to calculate percentage integrin suppression $((AI_0-AI)/(AI_0)*100)$. For analysis of β3 integrin surface expression (independent of integrin affinity), anti-CD61 (β3) antibody (Serotec) was used in the above conditions.

2.15 Preparation Of FN 9-11 Fragment For Integrin Affinity Experiments.

The soluble 9-11 type III repeats of fibronectin (FN 9-11), that contain the RGD domain responsible for integrin binding, were expressed as a GST fusion protein from pGEX-4T2 vector. LB media (10g tryptone, 5g yeast extract, 10g NaCl in 1l distilled H_20), LB agar (LB media with 15g agar) and SOB media (20g tryptone, 5g yeast extratct, 2ml 5M NaCl, 2.5ml 1M KCl, 10ml 1M $MgSO_4$ in 1l distilled H_2O) were prepared and autoclaved. 100μl of BL21 competent *E. Coli* (Sigma) were transformed with 10ng of pGEX-Fn(9-11) by heat shock (ice for 20 minutes, 42ºC for 45 seconds, ice for 2 minutes, addition of 700μl of SOB media and agitated for 1 hour 37ºC), plated onto LB agar plates with 50μg/ml ampicillin and incubated overnight at 37ºC. Single colonies were inoculated into 500ml of LB media (with 50μg/ml ampicillin) and incubated overnight at 37ºC. A further 500ml of LB media (with 50μg/ml ampicillin) was inoculated with 0.5ml of the overnight culture and incubated at 37ºC until the OD_{600} was 0.7-0.8. The culture was then induced with 1mM IPTG overnight at 37ºC.

E. Coli were subsequently pelleted (centrifuged 4500rpm for 20 minutes), washed in PBS (4500rpm for 20 minutes) and lysed in GST-lysis buffer (PBS, 1x protease inhibitor, 5mM DTT) (all components from Sigma) by sonication on ice (4x30 seconds). Sonicate was centrifuged at 13,000rpm for 30 minutes at 4ºC (JA-20 rotor in Beckman centrifuge). TritonX-100 (1% final concentration) was added to the cleared lysate and incubated at 4ºC for 20 minutes. 0.1g of GST-agarose beads were rehydrated in 10ml distilled H_2O, washed twice with PBS and resuspended as 1:1 slurry in PBS. The cleared lysate was incubated with the GST-beads at 4ºC overnight on a roller. The beads were washed twice in GST-lysis buffer, loaded into a column and the protein eluted at 4ºC using elution buffer (25mM glutathione. 50mM Tris pH 8.8, 200mM NaCl). The eluate was dialysed using Slide-A-Lyzer™ cassettes (cat. No. 66380 Pierce Protein Research) in 1l PBS overnight at 4˚C. The purified protein was subsequently biotinylated by incubation with 0.8mM biotin N-hydroxy succinimide ester (Sigma H1759) in 0.1M $NaHCO_3$ for 1 hour at room temperature plus 2 hours at 4ºC. The biotinylated protein was dialysed using Slide-A-Lyzer™ cassettes in 1l HEPES/NaCl buffer overnight at 4˚C and stored at 4ºC prior to use.

2.16 Assessment Of Integrin Affinity In CHO-K1 Cells.

CHO-K1 cells were transfected with test DNA together with 0.75µg Tac-α5 transfection reporter construct (extracellular domain of the IL-2 receptor and the intracellular domain of the α_5 integrin) as indicated. Cells were cultured for 48 hours prior to analysis. Single cell suspensions of trypsinised cells were resuspended in 50µl biotinylated FN 9-11 solution (prepared as indicated above) for 30 minutes at room temperature in HEPES/NaCl buffer (20mM HEPES, 140mM NaCl, 1.8mM $CaCl_2$, 1mM $MgCl_2$ and 2mg/ml Glucose, pH 7.4). Internal controls for each sample were performed containing either 5mM EDTA or 100µM $MnCl_2$. Cells were washed with cold PBS and incubated on ice with 50µl DMEM containing streptavidin-FITC for 30 minutes in the dark. Cells were washed again and incubated on ice for a further 30 minutes with 50µl DMEM containing 1:50 anti-Tac-α5 antibody (ACT-1) conjugated to RPE (v/v). Cells were finally washed and resuspended in cold PBS. Immediately prior to analysis on a FACS-Caliber (BD, Erembodegem, Belgium),

ToPro3 (Molecular Probes, Leiden, Netherlands) at a final concentration of 1μM (in PBS) was added to each sample.

FN 9-11 binding was determined by gating for live and highly transfected cells (ToPro3 negative and high Tac-α5 binding respectively). To obtain numerical estimates of integrin activation, an integrin activation index (AI) was calculated as described in 2.12, where AI = $((F_N-F_I)/(F_A-F_I))*100$ and Percent Inhibition = $(AI_0-AI)/(AI_0)*100$. F_N is Geometric mean (GM) fluorescence intensity (MFI) of FN 9-11 binding of the native integrin, F_I is MFI of FN 9-11 binding in the presence of 5mM EDTA and F_A is MFI of FN 9-11 binding in the presence of 100μM Mn^{2+}. AI_0 is the Activation index with the control vector and AI is the Activation index with DNA under test.

2.17 Assessment Of Cell Adhesion.

CHO(αβ-py) cells were co-transfected with test DNA together with 2μg pEGFP in 100mm plates as described above and cultured in quiescent media (DMEM with no FCS) 24 hours post-transfection. Cells were harvested 48 hours following transfection and re-suspended at 1 x 10^6 cells/ml in DMEM. 96-well cell culture cluster plates were coated with 5μg/ml von Willebrand factor (vWF) in PBS for 60 minutes at 37°C. Plates were then washed and blocked with 2% (w/v) bovine serum albumin in PBS for 60 minutes at room temperature. Cell suspension (200μl) was added to each well and allowed to adhere for 15 minutes at 37°C. Non-attached cells were removed by gentle shaking at 500rpm for 3 x 10s and washed with PBS. Total cell adhesion was assessed by centrifugation of the plate at 1000 rpm for 5 minutes. Cell adhesion was quantified on a fluorescence plate reader and expressed as % adhesion compared to total cell adhesion. Background cell adhesion to plastic subtracted from all values.

CHO-K1 cells were transfected with test DNA as described above and cultured in quiescent media (DMEM with no FCS) 24 hours post-transfection. 96-well cell culture cluster plates were coated with 10μg/ml fibronectin in PBS for 60 minutes at 37°C and blocked with 2% (w/v) bovine serum albumin in PBS for 60 minutes at room temperature. Single cell suspensions of trypsinised cells were resuspended at 1

x 10^6 cells/ml in DMEM. 200µl of cell suspension was added to each well and allowed to adhere for 15 minutes at 37°C. Non-attached cells were removed by gentle shaking at 500rpm for 3 x 10 seconds. Total cell adhesion was assessed by centrifugation of the plate at 1000 rpm for 5 minutes. CHO-K1 cells adhesion was quantified by staining adhered cells with methylene blue (0.4%) for 5 minutes, washed x3 in PBS and stain eluted with 100µl of 0.1N HCl. The absorbance (at 640nM) of each sample was read on an optical plate reader. Adhesion was expressed as a percentage compared to total cell adhesion with background cell adhesion to plastic subtracted against all values.

K562 cells (1 x 10^6/ml in RPMI) were seeded into 12-well plates pre-coated with human recombinant Delta-like ligand-4 (DLL-4) (R+D) or polyhistidine peptide (control) (both 10µg/ml in PBS for 60 minutes at 37°C) and cultured for 12 hours at 37°C with or without MW167 (50 µM) or DMSO (Vehicle) (Calbiochem) as indicated. 2x10^5 K562 cells were resuspended in HEPES/NaCl buffer and incubated with 4B4 (Beckman Coulter) (10µg/ml 45 minutes 37°C), EDTA (5mM final concentration) or Mn^{2+} (100µM final concentration) as indicated. Cells were seeded into plates coated with fibronectin or poly-l-lysine (10µg/ml in PBS for 60 minutes 37°C) and incubated for 30 minutes at 37°C. Non-adherent cells were removed by gentle washing with PBS x 2. Remaining cells were fixed with 3% paraformaldehyde (5 minutes) and stained with 0.4% methylene blue (5 minutes). Intracellular methylene blue was eluted with 0.1N HCl and the absorbance (at 630nM) of each sample was determined using an automated plate reader. Cell adhesion for each experimental condition was expressed as a percentage of total cellular adhesion to poly-l-lysine, with background cell adhesion to plastic subtracted against all values.

SCLC cells (1 x10^6/ml in RPMI) were cultured in 12-well plates pre-coated with human recombinant Delta-like ligand-4 (DLL-4) (R+D), polyhistidine peptide (control for DLL-4), Jagged-1 (R+D) or IgG1 (R+D) (all 10µg/ml in PBS for 60 minutes at 37°C) for 12 hours at 37°C. SCLC cells were resuspended in HEPES/NaCl buffer, seeded into 96-well plates (1x10^5 cells/well) pre-coated with laminin or poly-l-lysine and incubated for 30 minutes at 37°C. Non-adherent cells were removed by gentle washing with PBS x 2. Remaining cells were fixed with 3%

paraformaldehyde (5 minutes) and stained with 0.4% methylene blue (5 minutes). Intracellular methylene blue was eluted with 0.1N HCl and the absorbance (at 630nM) of each sample was determined using an automated plate reader. Cell adhesion for each experimental condition was expressed as a percentage of total cellular adhesion to poly-l-lysine, with background cell adhesion to plastic subtracted against all values.

2.18 Knockdown Of PLCε Expression In CHO Cell Lines.

Kelley *et al* previously described siRNA oligonucleotides specific to rat PLCε and scrambled non-targeting controls (197). The targeting oligonucleotides have been shown to effectively knockdown PLCε expression in rat cell lines and have considerable cross-species sequence homology (197). To assess the whether these siRNA oligonucleotides could be used in CHO cells, the DNA regions surrounding two siRNA sequences reported in Kelley *et al* (designated siRNAPLCε#3 and siRNAPLCε#5) were amplified from CHO cell cDNA by RT-PCR using primers designed to consensus rat/mouse PLCε sequence (197). Forward primer for siRNAPLCε#3: TTCCGCACAAAACCCATCC; Reverse primer for siRNAPLCε#3: GCTTTAAGACAATCCTGCCTACG; Forward primer for siRNAPLCε#5: GGCTACGTAGGCAGGATTGTCTTA; Reverse primer for siRNAPLCe#5: TTTCCCTGCACCCTTCCACTTGC.

Total RNA was extracted from 1 x 10^6 CHO-K1 cells using an RNeasy kit (Qiagen) according to the manufacturers instructions. Contaminating DNA was removed by treatment with RQ1 DNase (Promega), the RNA was quantified using a spectrophotometer and then stored at -80 °C. cDNAs were generated by reverse transcription of 400ng of RNA using TaqMan reverse transcription reagents (Applied Biosystems) according to the manufacturers instructions and stored at -20°C. All reagents for PCR were obtained from Promega. Reaction: 2.5μl 10x buffer, 0.25μl Taq polymerase, 1μl dNTP (10mM), 0.5μM forward and reverse primers, 17.25μl nuclease-free water and 2μl cDNA. PCR programme: 95˚C 2 minutes, 35 cycles 95˚C 45s, 56˚C 45s and 72˚C 45s, final extension 72˚C 5 minutes. The respective 616bp (siRNAPLCε#3) and 380bp (siRNAPLCε#3) products were resolved on a 2% agarose gel, purified using a QIAquick gel extraction kit (QIAGEN Cat no. 28704)

according to the manufacturers instructions and sequenced on both strands commercially (MWG biotechnology). The CHO DNA sequence data for the region surrounding siRNAPLCε#3 and siRNAPLCε#5 is demonstrated below (Fig. 2.3) with the siRNA oligonucleotide target sequence underlined.

This confirmed that the region targeted by the siRNAPLCε#3 and siRNAPLCε#5 was 100% conserved in CHO cells. Thus, these siRNA oligonucleotides were used to knockdown PLCε expression in CHO cells. Transient transfection of cells with siRNA was performed with Oligofectamine (Invitrogen) as per the manufacturers instructions. Twenty-four hours after transfection, media containing siRNA-Oligofectamine complexes were removed and replaced with fresh complete media. Cells were then transfected with plasmid constructs using Lipofectamine, as indicated. Seventy-two hours post-siRNA transfection, cells were used for integrin affinity determination as described above (2.14). In all experiments cells were also lysed for immunoblot or RT-PCR analysis (using above protocols) of PLCε expression to confirm knockdown of message and protein.

Figure 2.3: The CHO DNA Sequence Straddling The Oligonucleotides siRNAPLCε#3 And siRNAPLCε#5.

Sequence Data For The DNA Surrounding siRNAPLCε#3:

ATCGAAACACTCTAAACCCCATGTGGAATGAGCAGTTTCTCTTCCGGGTTCACTTTGAAG
ATCTTGTATTTCTTCGTTTTGCAGTCGTGGAAAACAACAGTTCGGCGATAACGGCTCAGA
GAATCATTCCACTCAGAGCTTTGAAACGAGGATATCGACATCTTCAGCTGCGGAACCTCC
ACAATGAAATCTTGGAAATCTCTAGCTTATTCATAAACAGCAGAAGGATGGAAGAAAAC
CCCTCTGGCAGTTCCATGCCAGCCTCGTTGATGTTTAATACTGAAGAGAGGAAATGTTCT
CAGACTCACAAAGTCACAGTGCATGGTGTCCCAGGTCCAGAGCCCTTTGCTGTTTTCACT
ATAAACGAA**GGCACCAAGGCAAAGCAGC**TTCTCCAACAGGTTTTGGCAGTTGACCAAG
ACACCAAATGTACTGCCACAGACTATTTTTTGATGGAAGAGAAGCATTTTATATCTAAGG
AAAAGAATGAATGCAGGAAACAACCATTCCAGAGAGCTGTGGGTCCAGAAGAAGATATT
GTGCAGATTTTAAACAGYTGGTTCCCAGAAGAAGGCTACGTAGGCAGGATTGTCTTAAA
GC

Sequence Data For The DNA Surrounding siRNAPLCε#5:

AAGCCCCAACAAGAAACCCTAGAAGAGAAAAACATTGTCCACGATGACAGAGAGGTGA
TCTTGAGCTCAGAAGAGGAGAGTTTCTTTGTCCAAGTGCACGATGTCTCTCCAGAGCAGC
CTCGAACTGTCATCAAAGCCCCACGTGTCAGCACTGCACAGGATGTGATTCAGCAGACCT
TGTGCGAA**GCCAAATATTCCTACAGCA**TCCTGAACAACCCCAATCCGTGTGACTATGTG
CTTTTGGAAGAGGTAATGAAAGATGCACCCAATAAGAAGTCTTCTACCCCGAAGTCCTCA
CAGAGGATCCTCTTGGACCAAGAATGTGTGTTTCAAGCCCAAAGCAAGTGGAAGGGTGC
AGGGAAA

2.19 Measurement Of HES-1 Expression By RT-PCR.

K562 cells (1 x 10^6/ml in RPMI) were seeded into 12-well plates pre-coated with human recombinant Delta-like ligand-4 (DLL-4) (R+D) or polyhistidine peptide (control) (both 10μg/ml in PBS for 60 minutes at 37°C) and cultured for 12 hours at 37°C with or without MW167 (50 μM) or DMSO (Vehicle) (Calbiochem) as indicated. SCLC cells (1 x10^6/ml in RPMI) were cultured in 12-well plates pre-coated with human recombinant Delta-like ligand-4 (DLL-4) (R+D), polyhistidine peptide (control for DLL-4), Jagged-1 (R+D) or IgG1 (R+D) (all 10μg/ml in PBS for 60 minutes at 37°C) for 12 hours at 37°C as indicated.

After 12 hours total RNA was extracted from 1x10^6 cells/experimental condition using an RNeasy kit (Qiagen) according to the manufacturers instructions. Contaminating DNA was removed by incubation with RQ1 DNase (Promega) (15 minutes 37°C) as per the manufacturers instructions. cDNA was generated by reverse transcription of 400ng RNA using TaqMan reverse transcription reagents as per manufacturer's instructions (Applied Biosystems). cDNA quality was verified by PCR amplification of β-actin. Real time quantitative RT-PCR analysis was performed with TaqMan reagents and an ABI 7900HT machine as per manufacturer instructions (Applied Biosystems).

HES-1 for: CATTCTGGAAATGACAGTGAAGCA;

HES-1 rev: CAGCGCAGCCGTCATCT;

HES-1 probe: CTCCGGAACCTGCAGCGGGC fam labelled.

Triplicate measurements were performed and analyzed with ABI sequence detector software (version 2.1) using the $2^{-\Delta\Delta Ct}$ method. HES-1 expression for each condition was normalised for 18S expression and represented as a fold change from control cells.

2.20 CSL-Luciferase Activity.

Notch activity was assayed as previously described using a reporter plasmid containing 4 CSL binding sites upstream of a gene encoding the enzyme luciferase (pGl2 4xCSL-luc) (193). Co-expression of intracellular Notch with this plasmid

promotes transcription of luciferase, the activity of which can be detected using luciferin as a substrate. CHO(αβ-py) cells were transfected with test DNA plus pGl2 4xCSL-luc (0.2μg) and pcDNA3.1 LacZ (0.1μg). After 48 hours cell were lysed and luciferase activity was determined using Steady-Glo (Promega) according to the manufacturers instructions. In parallel samples, galactosidase activity was determined using Galacto-Plus (Tropix). Luciferase activity for each transfection condition was normalised for galactosidase activity and expressed as a fold change from that observed with empty vector.

2.21 R-Ras Activation Assay.

R-Ras activity was determined using the Ras binding domain (RBD) of Raf as previously described (198). In brief, Raf-RBD was expressed as a GST fusion protein from pGEX 2T vector as described in 2.13. Transformed *E. Coli* were pelleted (centrifuged 4500rpm for 20 minutes), washed in PBS (4500rpm for 20 minutes) and lysed in GST-lysis buffer (PBS, 1x protease inhibitor, 5mM DTT) (all components from Sigma) by sonication on ice (4x30 seconds). Sonicate was centrifuged at 13,000rpm for 30 minutes at 4ºC (JA-20 rotor in Beckman centrifuge). TritonX-100 (1% final concentration) was added to the cleared lysate and incubated at 4ºC for 20 minutes. 0.1g of GST-agarose beads were rehydrated in 10ml dH_2O, washed twice with PBS and resuspended as 1:1 slurry in PBS. The cleared lysate was incubated with the GST-beads at 4ºC overnight on a roller. The beads were washed twice in RIPA buffer (200mM NaCl, 2.5mM $MgCl_2$, 50mM Tris-HCl pH 7.4, 15% glycerol, 1% NP40 and Complete protease inhibitor (Boehringer Mannheim, Sussex, UK)) prior to use. CHO(αβ-py) cells were transfected with either R-Ras(WT) or R-Ras(G38V) (0.25μg) (both myc-tagged) and test DNA. Cells were quiesced in serum free media and lysed at 48 hours in RIPA buffer at 4°C for 20 minutes. The clarified lysate was incubated with GST-Raf-RBD coupled to glutathione agarose beads for 2 hours at 4°C. Beads were isolated by centrifugation, washed twice in RIPA buffer and resuspended in Laemmli sample buffer. Protein samples were separated by SDS-PAGE. Bound R-Ras was detected by western immunoblotting with anti-Myc (9E10) antibodies.

2.22 Immunohistochemistry.

Immunohistochemistry was performed in collaboration with the pathology department at the New Royal Infirmary using a Dako Envision kit according to the manufacturers instructions. In brief, formalin-fixed, paraffin-embedded sections were de-waxed in xylene for 10 minutes. Tissue was rehydrated through graded ethanol (100% → 90% → 70%, 1 minute each). Antigen retrieval was performed by heating rehydrated tissue in 740ml distilled water plus 7.5ml Vector Antigen Retrieval solution using a 750W microwave oven for 15 minutes at maximum power. Sections were cooled in running tap water for 15 minutes, immersed in 3% hydrogen peroxide (v/v in distilled water) for 15 minutes, rinsed once with TBS and then loaded into a Sequenza® (Shandon) slide rack. Appropriate primary antibodies were diluted to 1:100 in DAKO diluent and 100 µl was added to each slide for 1 hour at room temperature. Slides were rinsed twice with TBS and 3 drops of labelled polymer-HRP (species specific) was added to each slide for 30 minutes at room temperature. Slides were rinsed twice with TBS and 100 µl DAB solution was applied for 5 minutes at room temperature. Slides were rinsed once in TBS, counterstained with Mayers haematoxylin, immersed in Scotts tap water (3 minutes), dehydrated through graded ethanol (70% → 90% → 100%), cleared in xylene and mounted with DPX. Stained slides were viewed with a Leica DM1000 microscope at 100-400x magnifications and photographed with a Leica DFC400 digital camera (both from Leica Microsystems, UK).

2.23 RT-PCR Of Notch Signalling Components In SCLC Cell Lines.

Total RNA was extracted from $1x10^6$ SCLC cells using an RNeasy kit (Qiagen) according to the manufacturers instructions. RNA extracted from $1x10^6$ MLR cells and $1x10^6$ K562 cells was used as a positive control. RNase free water (Promega) was used as a negative control. Contaminating DNA was removed by incubation with RQ1 DNase (Promega) (15 minutes 37°C) as per the manufacturers instructions and RNA concentration determined by light absorbance at 260nm. RT-PCR was performed on 500ng of RNA using an Access RT-PCR kit (Promega) according to the manufacturers instructions. Reverse transcription was carried out at 45˚C for 45 minutes. PCR reactions were performed using previously published primers for

human Notch signalling components (described in Table 2.1) at a final concentration of 0.5 μM. PCR programme: 95˚C 2 minutes, 35 cycles 95˚C 45s, [annealing temperature indicated for primer pairs – see table 2.1] 45s and 72˚C 45s, final extension 72˚C 5 minutes. The PCR products were resolved on 2% agarose gels and photographed under UV illumination.

Table 2.1: The Forward (Fw.) And Reverse (Rv.) Primer Sequences, Product Size In Base Pairs (Bp) And Annealing Temperature Are Indicated For Each Gene.

Primer:	Sequence:	Product (bp):	AT:
Notch-1	Fw. 5'-GCACTGCGAGGTCAACAC-3' Rv. 5'-AGGCACTTGGCACCATTC-3'	177	57
Notch-2	Fw. 5'-TGGTTCAGAGAAAACATACA-3' Rv. 5'-TCCACTTCATACCAGTTGA-3'	425	57
Notch-3	Fw. 5'-GGAGGGAGAAGCCAAGTC-3' Rv. 5'-GGGAAAAAGGCAATAGGC-3'	164	56
Notch-4	Fw. 5'-TTCGGGACTTCTGGTCAG-3' Rv. 5'-GGAGGGAGAAGCCAAGTC 3'	176	56
Jagged-1	Fw. 5'-AGTCACTGGCACGGTTGTAG-3' Rv. 5'-TCGCTGTATCTGTCCACCTG-3'	227	56
Jagged-2	Fw. 5'-GATTGGCGGCTATTACTGTG-3' Rv. 5'-AGGCAGTCGTCAATGTTCTC-3'	600	56
Delta-1	Fw. 5'-AGACGGAGACCATGAACAAC-3' Rv. 5'-TCCTCGGATATGACGTACAC-3'	382	55
Delta-3	Fw. 5'-GTGAATGCCGATGCCTAGAG-3' Rv. 5'-GGTCCATCTGCACATGTCAC-3'	256	57
Delta-4	Fw. 5'-TGACCACTTCGGCCACTATG-3' Rv. 5'-AGTTGGAGCCGGTGAAGTTG-3'	620	55
Hes-1	Fw. 5'-TGGATGCGGAGTCTACGATG-3' Rv. 5'-TAAGGCCACTTGCCACCTTC-3'	468	57
Deltex	Fw. 5'-TGATGCCTGTGAATGGTCTG-3' Rv. 5'-TCTGCGACATGCTGTTGAAG-3'	450	57
hASH-1	Fw. 5'-TCCCCCAACTACTCCAACGAC-3' Rv. 5'-CCCTCCCAACGCCACTG-3'	280	58
β-actin	Fw. 5'-CATCACCATTGGCAATGAGC-3' Rv. 5'-CGATCCACACGGAGTACTTG-3'	284	58

2.24 Preparation Of Human Peripheral Blood Mononuclear Cells.

Peripheral blood mononuclear cells (PBMCs) were separated from single donor buffy coats prepared within 24 hours of donation by the local blood transfusion

service (41 Lauriston Place, Edinburgh). The buffy coat was diluted 1:2.5 with sterile PBS (Ca^{2+} and Mg^{2+} free). 8 x 50 ml Falcon™ tubes were prepared by the addition of 15mls of room temperature Lymphoprep™. 25mls of the diluted Buffy coat was carefully layered onto the Lymphoprep™ in each tube using a sterile pastette and then centrifuged at 800g (room temperature) for 30 minutes with the brake off. The white cell layers were carefully removed with a pastette to a separate 50 ml Falcon tube, diluted with PBS (total volume 50 ml), and centrifuged at 300g for 7 minutes with brake on. The cell pellet was resuspended in Iscove's Modified Dulbecco's Medium (IMDM) prior to use in further experiments.

2.25 Co-Culture Of SCLC Cells And Mixed Leukocyte Reactions.

H69, H345 and H510 SCLC cells from maintenance cultures were washed (PBS 200g 5 minutes), re-suspended in PBS (1 $x10^6$ cells/ml) and incubated with mitomycin C (50μg/ml) for 3 hours at 37°C. The cells were washed 3x in PBS (50ml 200g 5 minutes) prior to use. It was confirmed in initial experiments that this produced the maximum suppression in SCLC proliferation with the least loss in cell viability. The PBMCs of two separate unrelated donors were prepared as described above and resuspended in IMDM (Sigma) with 10% FCS, 5μg/ml L-glutamine, 50U/ml penicillin and 50μg/ml streptomycin (Invitrogen Ltd, UK). In a round-bottom 96 well plate, 5 x 10^4 PBMCs/donor/well were combined with Con A (5μg/ml) and co-cultured with mitomycin C treated SCLC cells at a 1:1 ratio (i.e. 1 x 10^5 SCLC cells and 1 x 10^5 mixed leukocytes/well) for 72 hours at 37°C. After 48 hours 1 μCi ^{3}H-thymidine was added to each well. 24 hours later cells were harvested and cellular incorporation of ^{3}H-thymidine was assessed by liquid scintillation counting using a beta plate reader (Wallac, Finland). In experiments investigating the role of bombesin-like peptides, the specific bombesin antagonist, RC-3095 (Sigma), was dissolved in DMSO and used at a final concentration of 1μM.

2.26 Preparation Of Human CD4+ T-Cells.

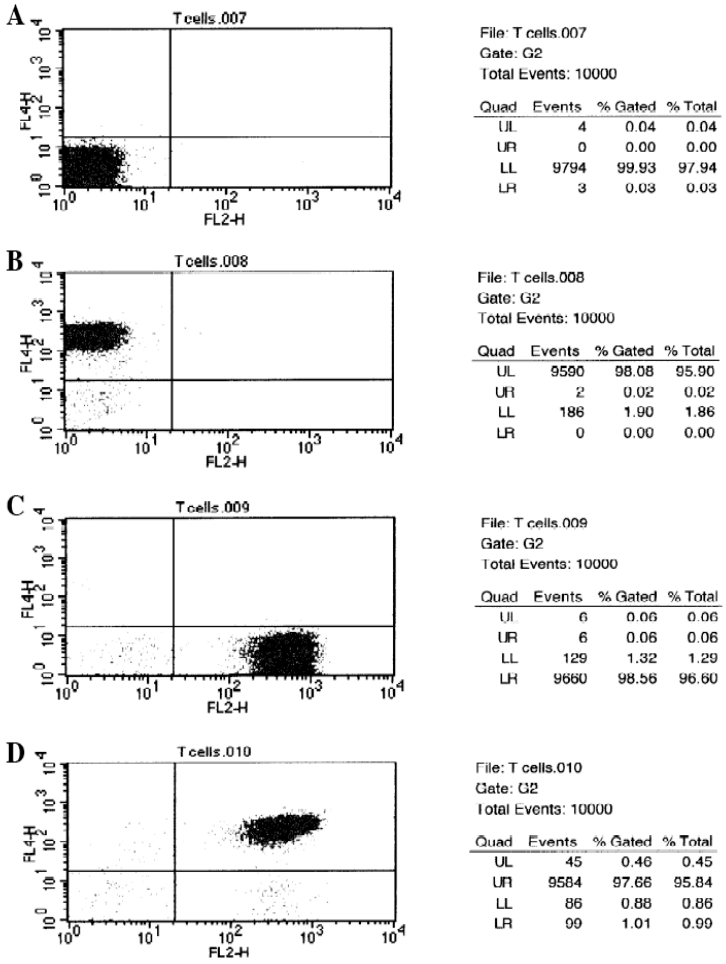
PBMCs were separated from single donor human buffy coats as indicated above and resuspended in IMDM (Sigma) with 5μg/ml L-glutamine, 50U/ml penicillin and 50μg/ml streptomycin (Invitrogen Ltd, UK) at a final concentration of $5x10^6$ cells per

ml. PBMCs were incubated for 1 hour at 37ºc in tissue culture flasks (Costar) (40ml into 162cm^2 flask, 20ml into 75cm^2 flask). The supernatants containing non-adherent cells were removed, counted and washed in PBS (300g for 10 minutes) prior to CD4+ T-cell separation using magnetic microbeads and an autoMACS^{TM} magnetic cell sorter (Miltenyi Biotec) according to the manufacturers instructions.

In brief, cells were re-suspended in 40µl MACS buffer per 10^7 cells (PBS Ca2+ and Mg2+ free, with 0.5% bovine serum albumin (BSA) and 2mM EDTA, pH 7.2, sterile filtered) and incubated with 10µl of biotin-antibody cocktail per 10^7 cells (CD4+ T-cell isolation kit II, 130-091-155 Miltenyi Biotec) for 10 minutes at 4ºC. A further 10µl of MACS buffer, 20µl of CD15 microbeads (130-046-601, Miltenyi Biotec) and 20µl of anti-biotin microbeads (CD4+ T-cell isolation kit II, 130-091-155 Miltenyi Biotec) were added per 10^7 cells and the mixture was incubated 10 minutes at 4ºC. The cells were washed with 10-20ml of MACS buffer (300g for 10 minutes), re-suspended in 500µl of MACS buffer per 10^8 cells and separated into labeled and unlabelled fractions using an autoMACS^{TM} magnetic cell sorter (deplete program). CD4+ cells were re-suspended in IMDM (Sigma) with 10% FCS, 5µg/ml L-glutamine, 50U/ml penicillin and 50µg/ml streptomycin (Invitrogen Ltd, UK) prior to use.

To ensure the purity of CD4+ T-cell separations using this method, an aliquot of each unlabelled fraction from the autoMACS was analysed for percentage of CD3+CD4+ cells using flow cytometry. 1 x 10^5 cells were incubated with a 1:10 dilution of PE-conjugated anti-CD4, APC-conjugated anti-CD3 or appropriately labelled isotype controls (BD Biosciences) in FACS wash (PBS with 2% FCS and 0.1% sodium azide) for 30 minutes at 4ºC in the dark. The cells were washed twice and re-suspended in a 1:1 mixture of FACS wash and FACS fix (1% formaldehyde in PBS) before analysis. See figure 2.4 for a representative dot blot of CD4+ T-cell purity.

Figure 2.4: Typical Dot Plots Of Unlabelled Fraction Of Cells (i.e. CD4+ T-Cells) From Automacs[tm] Stained With Anti-CD3 (APC) And Anti-CD4 (PE) Antibodies.



The unlabelled fraction from the autoMACS™ (i.e. CD4+ T-cells) was stained as described above and the percentage CD3+CD4+ cells determined by flow cytometry. (A) Cell stained with isotype control antibodies. (B) Cells stained with anti-CD3 (APC) and isotype. (C) Cells stained with anti-CD4 (PE) and isotype. (D) Cells stained with anti-CD3 (APC) and anti-CD4 (PE). The percentage CD3+CD4+ cells were calculated from quadrant statistics and in this example is 95.84%.

2.27 Co-Culture Of SCLC Cells And Human CD4+ T-Cells.

CD4+ T-cells were isolated from single donor buffy coats as described above. H69, H345 and H510 SCLC cells from maintenance cultures were washed (PBS 300g 5 minutes), re-suspended in PBS (1 x10^6 cells/ml) and incubated with mitomycin C (50µg/ml) for 3 hours at 37^{o}C. The cells were washed 3x in PBS (50ml 200g 5 minutes) prior to use. Round-bottom 96-well plates were coated with 50µl of anti-

CD3 antibody (5μg/ml in PBS) (R&D systems) for 1 hour at 37ºC. CD4+ T-cells were re-suspended at a concentration of $1x10^6$ cells/ml in IMDM with 10% FCS, 5μg/ml L-glutamine, 50U/ml penicillin and 50μg/ml streptomycin (Invitrogen Ltd, UK). 1 or 2 x 10^5 CD4+ T-cells were added to each well of the pre-coated 96 well plate and soluble anti-CD28 (R&D systems) at a final concentration of 1μg/ml was added. Mitomycin C treated SCLC cells were added to co-culture wells (1-4 x 10^5 cells/well) and plates were incubated for 72 hours at 37°C. After 48 hours 1 μCi ^{3}H-thymidine was added to each well. 24 hours later cells were harvested and cellular incorporation of ^{3}H-thymidine was assessed by liquid scintillation counting using a beta plate reader (Wallac, Finland).

For experiments using non-mitomycin treated SCLC cells, CD4+ T-cells were re-suspended in IMDM (with 10% FCS, 5μg/ml L-glutamine, 50U/ml penicillin and 50μg/ml streptomycin) and activated in 24-well plates (5 x 10^5 cells/well) with immobilised anti-CD3 (5μg/ml) and soluble anti-CD28 (1μg/ml). Live SCLC cells (2 x 10^6 cells/well) in transwells (0.4 μm pore size - Costar) were added and the plates were incubated for 72 hours prior to harvesting for liquid scintillation counting.

For experiments using SCLC media, SCLC cells were cultured in IMDM (with 10% FCS, 5μg/ml L-glutamine, 50U/ml penicillin and 50μg/ml streptomycin) at a concentration of 0.5 x 10^6 cells/ml in 24 well plates. After 72 hours supernatants were removed from the SCLC cells by centrifugation at 200g for 5 minutes. In some experiments, supernatants were separated into fractions containing soluble factors < 30kDa or > 30kDa using centrifugal filtration columns according to the manufacturers instructions (Centricon-30, Millipore). The retanate (i.e. fraction > 30kDa) was reconstituted to the original volume following separation. In addition, for some experiments, supernatants were also heated to 56°C for 10 minutes. SCLC supernatants were then diluted to 20% or 40% in IMDM (with 10% FCS, 5μg/ml L-glutamine, 50U/ml penicillin and 50μg/ml streptomycin). Round-bottom 96-well plates were coated with 50μl of anti-CD3 antibody (5μg/ml in PBS) (R&D systems) for 1 hour at 37ºC. CD4+ T-cells were re-suspended ($1x10^6$ cells/ml) in IMDM (10% FCS, 5μg/ml L-glutamine, 50U/ml penicillin and 50μg/ml streptomycin), IMDM (10% FCS, 5μg/ml L-glutamine, 50U/ml penicillin and 50μg/ml streptomycin) with

40% PBS, or media containing SCLC factors as indicated. 2 x 10^5 CD4+ T-cells were added to each well of the pre-coated 96 well plate and soluble anti-CD28 (R&D systems) at a final concentration of 1μg/ml was added. Plates were incubated for 72 hours at 37°C prior to harvesting for liquid scintillation counting.

For experiments investigating the role of TGF-β in SCLC-mediated suppression of CD4+ T-cell proliferation, an anti-TGF-β antibody was used (clone AB-100-NA from R&D systems) that has been shown to bind and neutralise all isotypes of TGF-β. To determine the optimum dose of anti-TGF-β antibody, CD4+ T-cells were cultured in 96-well plates pre-coated with anti-CD3 (5μg/ml). Proliferation was determined after 72 hours by incorporation of ^{3}H-thymidine. CD4+ T-cell proliferation was inhibited by the addition of recombinant human TGF-β1 (100-B-001 R+D systems) (1ng/ml final concentration). The bioactivity of rTGF-β1 was neutralised by pre-incubation (2 hours at 37°C in IMDM with 10% FCS, 1% L-Glutamine and 1% Penicillin/Streptomycin) with increasing concentrations (1.25-20μg/ml) of anti-TGF-β antibody. The optimal neutralising concentration of anti-TGF-β was found to be 10μg/ml and thus this dose was used in subsequent experiments.

2.28 Measurement Of TGF-β1 Concentration In SCLC Supernatants.

The concentration of TGF-β1 in SCLC supernatants was determined using a DuoSet™ ELISA kit (DY240 R&D Systems) according to the manufacturers instructions. In brief, H69 SCLC cells were cultured in IMDM (with 10% FCS, 1% L-Glutamine and 1% Penicillin/Streptomycin) at a concentration of 0.5 x 10^6 cells/ml in 24 well plates. After 72 hours supernatants were removed from the SCLC cells (centrifuged at 200g for 5 minutes) and activated with 1N HCl for 10 minutes at room temperature followed by 1.2N NaOH/0.5M HEPES. Capture antibody was added to the 96 well microplate and incubated overnight at room temperature. Plates were washed twice and blocked for 1 hour at room temperature. Plates were washed twice, 100μl of activated sample or standard was added to each well and incubated for 2 hours at room temperature. Plates were washed twice, 100μl of detection antibody was added to each well and incubated for 2 hours at room temperature.

Plates were washed twice, 100µl of streptavidin-HRP was added to each well and incubated for 20 minutes at room temperature. 100µl of substrate solution was added to each well for 20 minutes in the dark, followed by 50µl of stop solution. Absorbance (at 450nM) was determined for each well using an automated plate reader (MRX microplate reader).

2.29 Measurement Of Cytokine Production By Human CD4+ T-Cells.

CD4+ T-cells were isolated from single donor buffy coats as described above. H69 SCLC cells from maintenance cultures were washed (PBS, 300g, 5 minutes), re-suspended in PBS (1 x10^6 cells/ml) and incubated with mitomycin C (50µg/ml) for 3 hours at 37°C. The H69 cells were washed 3 x in PBS (50ml 200g 5 minutes) prior to use. 24-well plates were pre-coated with 250µl of anti-CD3 (5µg/ml in PBS) by incubation for 1 hour at 37°C. 5 x 10^5 CD4+ T-cells in IMDM (with 10% FCS, 1% L-Glutamine and 1% Penicillin/Streptomycin) were added to each well and supplemented with soluble anti-CD28 (final concentration 1µg/ml). 2 x 10^6 mitomycin treated H69 SCLC cells were added to the appropriate wells and the plates were incubated for 72 hours at 37°C. Cell supernatants were removed from the 24-well plates and stored in aliquots at – 80°C prior to use. The concentrations of cytokines IL-2, IL-4, IL-6, IL-10 IFN-γ and TNF-α were measured using a human TH1/TH2 cytokine cytometric bead array (BD Bioscience) according to the manufacturers instructions. In brief, a mixture of beads (50µL/sample) pre-coated with antibodies specific to the cytokines to be detected was added to each cell supernatant sample. PE detection reagent (PE-labelled antibodies specific to the cytokines to be detected) (50µl/sample) was added and supernatants were incubated for 2 hours at room temperature in the dark. The beads were washed, re-suspended in 200µl of Wash buffer (provided in the kit) and FL-2 intensity was measured for each cytokine specific bead (detected by FL-3 intensity) using a FACSArray flow cytometer (BD Bioscience) dedicated to CBA acquisition. The FL-2 intensity was compared to standard curves (20-5000 pg/ml) for each cytokine to give a concentration for each supernatant.

2.30 Expression Of Activation Markers (CD25, CD69) On Human CD4+ T-Cells.

CD4+ T-cells were isolated from single donor buffy coats as described above. H69 SCLC cells from maintenance cultures were washed (PBS, 300g, 5 minutes), re-suspended in PBS (1 x10^6 cells/ml) and incubated with mitomycin C (50μg/ml) for 3 hours at 37°C. The H69 cells were washed 3x in PBS (50ml 200g 5 minutes) prior to use. 24-well plates were pre-coated with 250μl of anti-CD3 (5μg/ml in PBS) by incubation for 1 hour at 37°C. 5 x 10^5 CD4+ T-cells in IMDM (with 10% FCS, 1% L-Glutamine and 1% Penicillin/Streptomycin) were added to each well and supplemented with soluble anti-CD28 (final concentration 1μg/ml). 2 x 10^6 mitomycin treated H69 SCLC cells were added to the appropriate wells and the plates were incubated for 72 hours at 37°C. Subsequently, cells were washed twice in PBS and incubated with a 1:10 dilution of PE-conjugated anti-CD4, APC-conjugated anti-CD25, APC-conjugated anti-CD69 or appropriately labelled isotype controls (BD Biosciences) in FACS wash (PBS with 2% FCS and 0.1% sodium azide) for 30 minutes at 4°C in the dark. The cells were washed twice and re-suspended in a 1:1 mixture of FACS wash and FACS fix (1% formaldehyde in PBS) before analysis. Mean fluorescence intensity of CD25 or CD69 binding to CD4+ cells (thus excluding SCLC cells) was determined using a FACSCalibur flow cytometer (BD Biosciences). Data were collected from 10,000 events using CELLQuest™ software.

2.31 Expression Of Human Macrophage Surface Markers.

Monocytes were isolated from PBMCs by adhesion purification. PBMCs were prepared from single donor human buffy coats as described above and re-suspended at 2x10^6 cells/ml in serum-free IMDM (1% L-Glutamine and 1% Penicillin/Streptomycin). 4ml of cell suspension was added to each well of a 6-well plate and incubated for 1 hour at 37°C. Monocytes adhered to the tissue culture plastic. Non-adherent cells were removed by gently washing the monocyte-monolayer with IMDM. 4ml of IMDM (10% FCS, 1% L-Glutamine and 1% Penicillin/Streptomycin) was added to each well with 0.25 x 10^6 cells/ml H69 SCLC cells in the co-culture wells. For experiments with SCLC media, SCLC cells were cultured in IMDM (with 10% FCS, 1% L-Glutamine and 1%

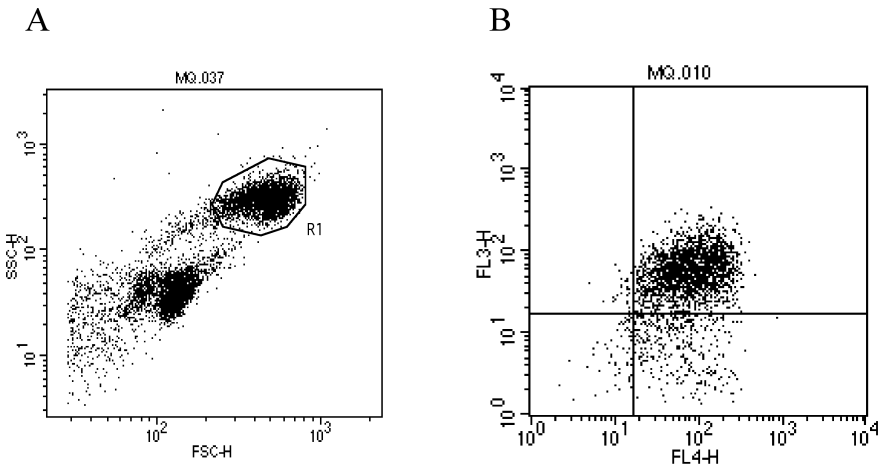
Penicillin/Streptomycin) at a concentration of 0.5 x 10^6 cells/ml in 24 well plates. After 72 hours supernatants were removed from the SCLC cells (centrifuged at 200g for 5 minutes). SCLC supernatants were then diluted to 40% in IMDM (with 10% FCS, 1% L-Glutamine and 1% Penicillin/Streptomycin).

Cell cultures were incubated for 7 days at 37ºC in 5%CO_2, following which adherent macrophages were removed from the wells by mechanical detachment. Monolayers were covered with ice-cold PBS (w/o Ca^{2+} or Mg^{2+}), incubated on ice for 10 minutes, gently scraped and the resulting cell suspension collected. Cell suspensions were centrifuged at 200g for 5 minutes, re-suspended in FACS-wash and incubated on ice, in the dark for 30 minutes with a 1:10 dilution of the appropriate antibodies. Cells were washed and re-suspended in FACS-wash prior to analysis using a FACS-Calibur flow-cytometer (BD Biosciences). Macrophages were identified by immunostaining with allophycocyanin (APC)-conjugated anti-CD11b and peridinin chlorophyll protein (PerCP)-conjugated anti-CD14 (Fig. 2.5). Surface marker expression on CD11b+CD14+ cells was determined by counter-staining with phycoerythrin (PE)-conjugated anti-CD80, anti-CD86, anti-HLA-DR, anti-CD16 or appropriately labelled IgG_1 isotype controls (BD Biosciences). At least 10,000 events were collected per sample and data processed using Cell Quest software (BD Biosciences).

2.32 Statistical Analysis.

Unless otherwise specified in the text, data were analysed using InStat™ by one-way analysis of variance (ANOVA) and the appropriate post-test analyses were applied. p values < 0.05 were considered to be significant.

Figure 2.5: Identification Of CD11b+CD14+ Macrophages In 7-Day Adherent Monocyte Cultures.



Monocytes were incubated for 7-days in IMDM (with 10% FCS) media. Adherent cells were lifted in ice cold PBS and immunostained with flurochrome conjugated anti-CD14 (PerCP - FL3) and anti-CD11b (APC - FL4). (A) Forward and side-scatter dot blot of cells with a gate surrounding cells with the characteristics of macrophages. (B) FL3 (CD14) and FL4 (CD11b) dot blots of the cells contained with the gate in (A) showing that these cells are predominantly CD11b+CD14+. The surface expression of CD16, CD80, CD86 and HLA-DR on this population of cells was then determined with PE conjugated antibodies.

CHAPTER 3: Extracellular Matrix Protects SCLC Cells From DNA Damage-Induced Cell Cycle Arrest And Apoptosis; A Process Mediated By β1 Integrin-Dependent Activation Of PI3-Kinase.

3.1 Introduction.

It has been shown previously that SCLC is surrounded by an extensive stroma of ECM and that high levels of expression correlate with poor patient prognosis (167). Cells interact with ECM components via heterodimeric cell surface proteins called integrins (199). ECM-integrin interaction stimulates signal transduction pathways that regulate a number of cellular processes important in cancer including cell cycle transition and protection from apoptosis (200). This is termed "outside-in" signalling. It has been demonstrated that adhesion of SCLC cells via β1 integrins to ECM components promotes cell survival and confers resistance to chemotherapeutic agents (167). Subsequently, this has been shown to be a general mechanism for acquired drug resistance in a number of malignancies including breast, glioma and colon cancer (201-203). However the intracellular signals activated by ECM in cancer cells, which influence response to chemotherapy and radiotherapy, have not been fully elucidated. A clear understanding of these mechanisms is essential to the development of rational strategies to overcome acquired multi-drug resistance and enhance the effects of chemotherapy and radiotherapy.

Central to the cellular response to chemotherapy and radiation-induced DNA damage is cell cycle arrest, predominantly at the G1/S and G2/M checkpoints (204). Alterations in expression of genes that control progression through the cell cycle have been demonstrated to affect chemosensitivity. These include altered expression of p53 and the retinoblastoma protein (Rb). Mutated forms of p53 and/or Rb have been shown to be associated with increased resistance of tumour cells to various anti-cancer drugs and irradiation, mainly because of disruption of cell cycle checkpoints (205). Alterations in other cell cycle regulators such as the cyclins, cyclin dependent kinases (CDKs) and their inhibitors, $p21^{Cip1/WAF1}$ and $p27^{Kip1}$ may also play a key role in the regulation of chemo-sensitivity (206).

Anchorage to ECM is required for survival of all un-transformed cells and the development of anchorage independence is an important stage in transformation

(207). Regulation of the cell cycle by cell adhesion in un-transformed cells is typically restricted to the G1/S transition (208,209). Progression through the G1 phase of the cell cycle is mediated by CDK 2, 4 and 6, whose activities are controlled by their associated cyclins and CDK inhibitors, $p21^{Cip1/WAF1}$ and $p27^{Kip1}$ (210). Accumulation of cyclin D, which associates with and activates CDK 4 and 6, initiates progression through G1 (211). The cyclin D-CDK 4 and 6 complex also prevents transcriptional repression of cyclin E and the de-repression of cyclin A promoting onset of S phase (212). Cells in suspension have higher levels of CDK 2 inhibitors than do attached cells leading to impaired cyclin E-CDK 2 activity with resultant cell cycle arrest in late G1 (210, 213). This suggests that the regulation of cyclin E-CDK 2 activity is an important mechanism by which anchorage to ECM controls progression through the G1/S transition in untransformed cells. Regulation of cyclin E-CDK2 activity may also represent how ECM protects cancer cells from chemotherapy-induced cell cycle arrest and subsequent apoptosis.

The PI3-kinase signalling pathway has been demonstrated to be an essential survival signal in SCLC cells and is a key regulator of cell cycle progression (214,215). Integrin activation by ECM couples integrin cytoplasmic tails to focal adhesion kinase and activates PI3-kinase, which phosphorylates inositol lipids, leading to activation of protein kinase B (PKB) and phosphorylation of glycogen synthase kinase 3β (GSK3β) (215,216). PKB phosphorylates and inactivates pro-apoptotic factors such as caspase 9 and Bad preventing apoptosis (215). Phosphorylation of GSK3β stabilizes cyclin D1 promoting progression through G1 phase of the cell cycle and prevents apoptosis by altering gene expression through NF-κB and AP-1 (217-219).

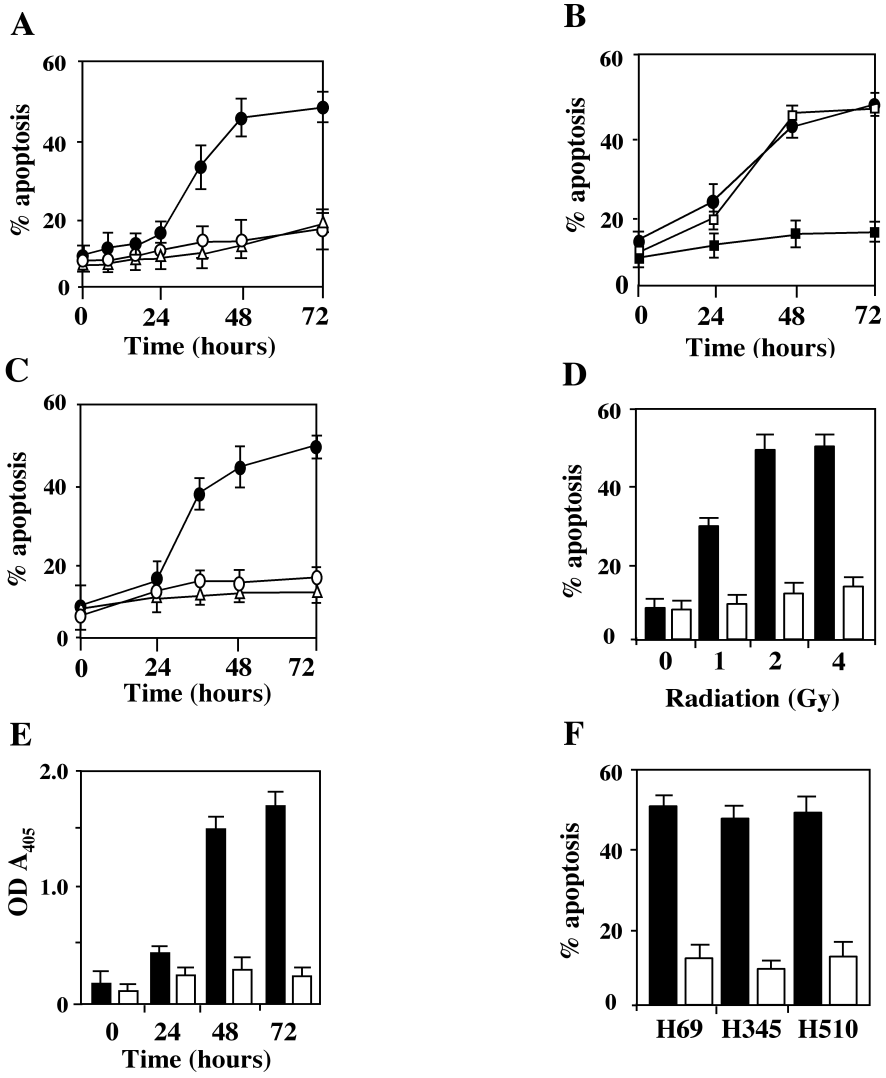
This background led to the hypothesis that prevention of cell cycle arrest and subsequent apoptosis through integrin-mediated activation of PI3-kinase may represent an important mechanism by which ECM proteins protect SCLC cells from chemotherapy and radiation.

3.2 Results.

3.2.1 ECM Proteins Protect SCLC Cells From Chemotherapy- And Radiation-Induced Apoptosis.

Robert Rintoul and Tony Elliot previously investigated the anti-apoptotic effects of ECM proteins on SCLC cells *in vitro*, using acridine orange/ethidium bromide staining, cell death ELISA and Annexin V expression. This data is summarised in figure 3.1. Increase in apoptosis induced by etoposide in H345 SCLC cells plated onto tissue culture plastic or adhered to poly-l-lysine was first observed at 24 hours reaching a maximum at 48-72 hours (percentage apoptosis (72 hours): 50.4 +/- 5.3% (poly-l-lysine) and 51.2 +/- 4.6% (plastic); mean of n=5 independent experiment +/- SEM, $p = 0.912$) (Fig. 3.1 a). However, adhesion to both laminin and fibronectin significantly protected H345 SCLC cells from apoptosis at all time points (percentage apoptosis (72 hours): 50.4 +/- 5.3% (poly-l-lysine), 18.2 +/- 9.7% (laminin) and 19.5 +/- 3.6% (fibronectin); mean of n=5 independent experiment +/- SEM, $p < 0.05$) (Fig. 3.1 a). This effect was not due to a physical interaction between etoposide and ECM as medium that had been treated with etoposide and incubated with laminin-coated plastic for 72 hours was still able to induce apoptosis when added to SCLC cells adhered to poly-l-lysine (Fig. 3.1 b). In addition, adhesion of H345 SCLC cells to ECM proteins significantly protected SCLC cells from the pro-apoptotic effect of ionizing radiation (Fig. 3.1 c, d), further confirming that ECM-mediated protection is not caused by a physical effect on chemotherapeutic agents. These results were confirmed using a cell death detection ELISA kit based on the quantitative detection of histone-associated DNA fragments (Fig. 3.1 e). Similar results were seen with H69 and H510 cells (Fig. 3.1 f). In addition, Robert Rintoul previously confirmed that this effect was due to a survival benefit and not an increase in the growth rate of cells on ECM (167).

Figure 3.1: ECM Protects SCLC Cells From Etoposide- And Radiation-Induced Apoptosis.



(A) H345 SCLC cells were adhered to poly-l-lysine (10 μg/ml) (●), laminin (10 μg/ml) (O) or fibronectin (20 μg/ml) (Δ) and treated with etoposide (25 μg/ml). The percentage of apoptotic cells was determined at the times indicated by acridine orange/ethidium bromide staining (mean of n=5 independent experiments +/- SEM). (B) H345 cells were adhered to poly-l-lysine (10 μg/ml) and treated with etoposide (25 μg/ml) (●) or medium, incubated for 72 hours in 6 well laminin-coated plates (10 μg/ml) with (□) or without (■) etoposide (25 μg/ml). Percentage of apoptotic cells was determined as above (mean of n=3 independent experiments +/- SEM). (C) H345 cells were adhered to poly-l-lysine (10 μg/ml) (●), laminin (10 μg/ml) (O) or fibronectin (20 μg/ml) (Δ) and treated with ionizing radiation (2 Gy). Percentage of apoptotic cells was determined as above (mean of n=3 independent experiments ± SEM). (D) H345 cells were adhered to poly-l-lysine (10 μg/ml) (black bar) or laminin (10 μg/ml) (white bar) and treated with ionizing radiation (0-4Gy) as indicated. Percentage of apoptotic cells was determined at 48 hours (mean of n=3 independent experiments in quadruplicate ± SEM). (E) H345 cells were adhered to poly-l-lysine (black bar) or laminin (white bar) and treated with etoposide (25μg/ml). Apoptosis was assessed at time indicated using a cell death ELISA kit. Mean absorbance at 405nm from n=3 experiments ± SEM. (F) H69, H345 and H510 SCLC cells were adhered to poly-l-lysine (10 μg/ml) (black bar) or laminin (10 μg/ml) (white bar) and treated with etoposide (25μg/ml). Percentage of apoptotic cells was determined at 48 hours (mean of n=3 independent experiments in quadruplicate ± SEM).

3.2.2 β1 Integrin Activation Mediates ECM Protection From Apoptosis In SCLC Cells.

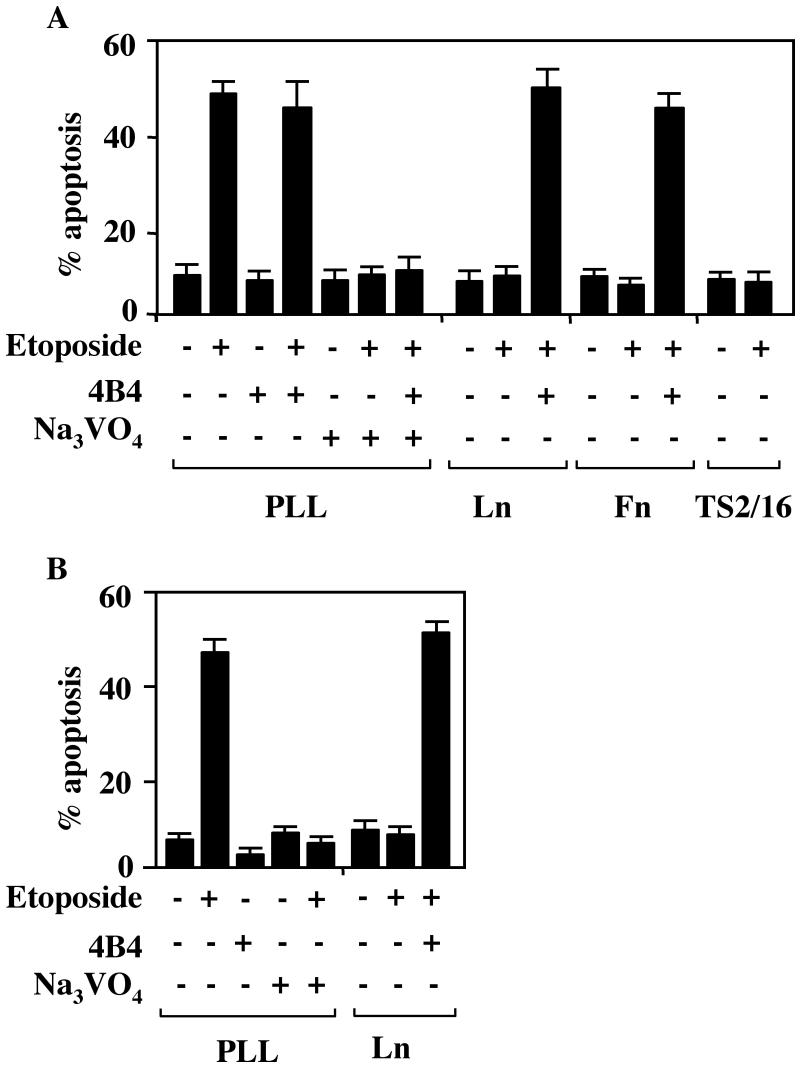
This data suggests that ECM proteins can specifically protect SCLC cells from apoptotic cell death induced by chemotherapy or radiotherapy. Cells interact with ECM via cell surface integrins. Integrin expression on SCLC cells has been previously characterised and the β1 integrin subunit is highly expressed (167). To investigate whether the anti-apoptotic effect of ECM proteins was mediated by the activation of β1 integrins on SCLC cells, specific β1 integrin function blocking and stimulating antibodies were used and the effect on ECM-mediated chemoprotection was assessed.

H345 SCLC cells were adhered to poly-l-lysine (control) or laminin, treated with etoposide (25 μg/ml) and apoptosis was assessed at 48 hours. The basal levels of apoptosis in H345 SCLC cells on poly-l-lysine was 8 ± 2% and this was increased to 55 ± 4% in the presence of etoposide (n=3 independent experiments in quadruplicate ± S.E.M.) (Fig. 3.2 a, b). Adhesion of H345 SCLC cells to the ECM proteins laminin or fibronectin significantly reduced apoptosis caused by etoposide at 48 hours from 55 +/- 4% to 7 +/- 1.7% and 8 +/- 1.4% respectively (n=3 independent experiments in quadruplicate +/- SEM) (Fig. 3.2 a, b). ECM-mediated protection from etoposide-induced apoptosis was completely abolished by pre-incubation of H345 SCLC cells with the β1 integrin function-blocking antibody 4B4 (10μg/ml). Furthermore the β1-stimulating antibody TS2/16 (10μg/ml) reproduced the effects of ECM proteins (Fig. 3.2 a, b). This data suggests that β1 integrins mediate the protection of SCLC cells from chemotherapy by ECM.

Binding to ECM promotes integrin clustering which results in the association of integrin intracellular domains with cytoskeletal proteins and recruitment of tyrosine kinases (220). Subsequently, integrin activation triggers an increase in tyrosine phosphorylation, an important step in downstream signalling pathways (220). To simulate integrin activation sodium orthovanadate (Na_3VO_4), a broad-spectrum phosphatase inhibitor that increases protein phosphorylation, was used (221). It was observed that treatment of H345 SCLC cells adhered to poly-l-lysine with Na_3VO_4 (200μM) prevented etoposide from inducing apoptosis in a similar manner to

adhesion to ECM proteins (Fig. 3.2 a, b). Taken together these results indicate that ECM proteins prevent apoptosis in SCLC cells through activation of β1 integrins and tyrosine kinase signalling pathways.

Figure 3.2: ECM-Mediated Protection From Etoposide-Induced Apoptosis Is β1 Integrin-Dependent.



(A) H345 cells were incubated with (+) or without (-) the function blocking anti-β1 integrin antibody 4B4 (10μg/ml) for 30 minutes at 37ºC as indicated and then seeded into 96 well plates pre-coated with poly-l-lysine (PLL) (10 μg/ml), laminin (Ln) (10 μg/ml), fibronectin (Fn) (20 μg/ml) or the integrin-activating antibody TS2/16 (10 μg/ml). Cells were treated with (+) or without (-) etoposide (25 μg/ml) or sodium orthovanadate (Na_3VO_4) (200 μm) as indicated. The percentage of apoptotic cells was determined at 48 hours as above (mean of n=3 independent experiments in quadruplicate ± SEM). (B) H345 cell were treated as above and apoptosis was assessed by surface expression of Annexin V using flow cytometry (mean of n=3 experiments ± SEM).

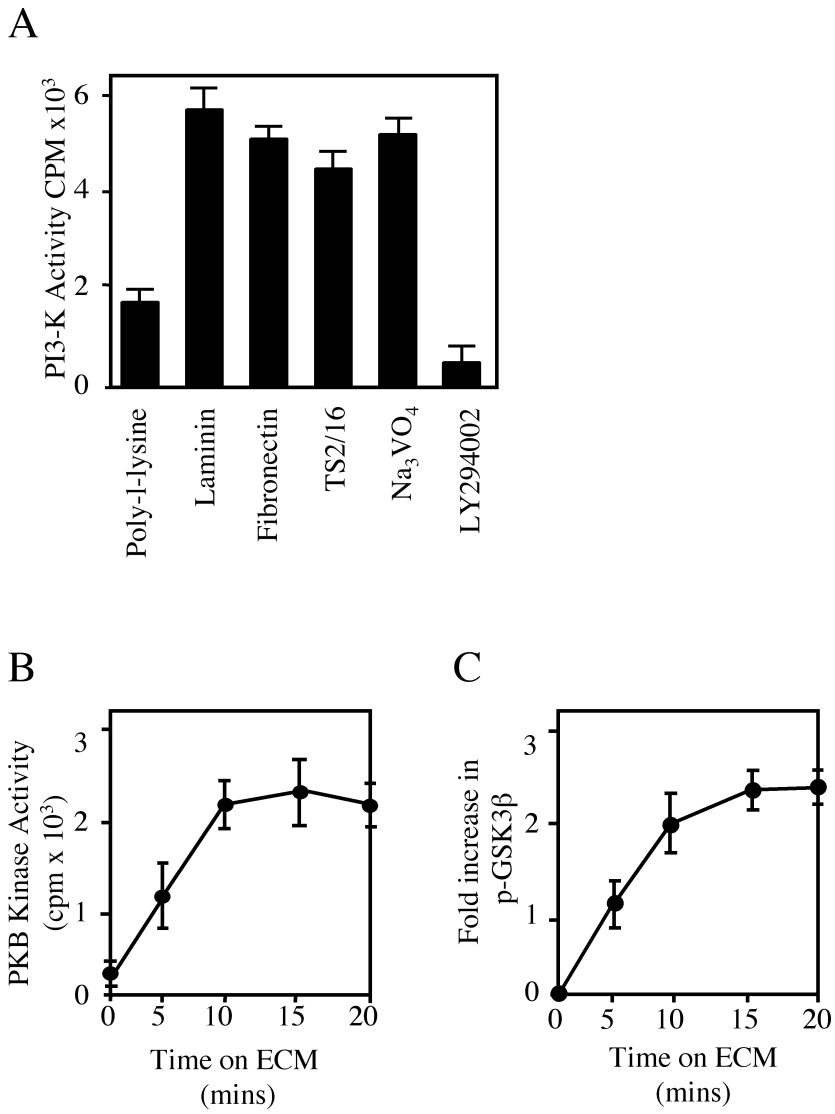
3.2.3 Adhesion To Laminin Stimulates PI3-Kinase Activity, PKB Phosphorylation And Activity And Increases GSK3β Phosphorylation In SCLC Cells.

Integrin dependent cell adhesion triggers an increase in PI3-kinase activation (215). PI3-kinase has been shown to mediate matrix-induced survival in normal epithelial cells (221). Robert Rintoul previously demonstrated that adhesion of H345 cells to ECM proteins laminin and fibronectin stimulated a marked increase in PI3-kinase activation (average 3.1x and 2.9x increase in PI3-kinase activity respectively n=3 independent experiments in quadruplicate) (Fig. 3.3 a). Furthermore, he observed that the β1 integrin-stimulating antibody TS2/16 (10 μg/ml) and Na_3VO_4 (200 μM) increased PI3-kinase activity to a similar extent (average 2.5x and 2.8x increase respectively n=3 independent experiments in quadruplicate). As predicted the PI3-kinase inhibitor, LY294002, reduced basal levels of PI3-kinase activity (Fig. 3.3 a).

PKB and GSK3β, which are down-stream effectors of PI3-kinase and regulate cell survival, may also participate in overriding chemotherapy- and radiation-induced apoptosis in SCLC cells (214,222). Weng Sie Wong previously showed that adhesion of H345 SCLC cells to laminin caused a time-dependent increase in PKB activity and GSK3β phosphorylation (Fig. 3.3 b, c). Furthermore, she showed that Na_3VO_4 (200 μM) stimulated PKB and GSK3β phosphorylation in H345 cells adhered to poly-l-lysine (Fig. 3.4 a, b) and that the ECM-mediated increase in phosphorylation of PKB and GSK3β was sensitive to PI3-kinase inhibition with LY294002 (10μM) but was not affected by etoposide treatment (25μg/ml) (Fig. 3.4 a, b).

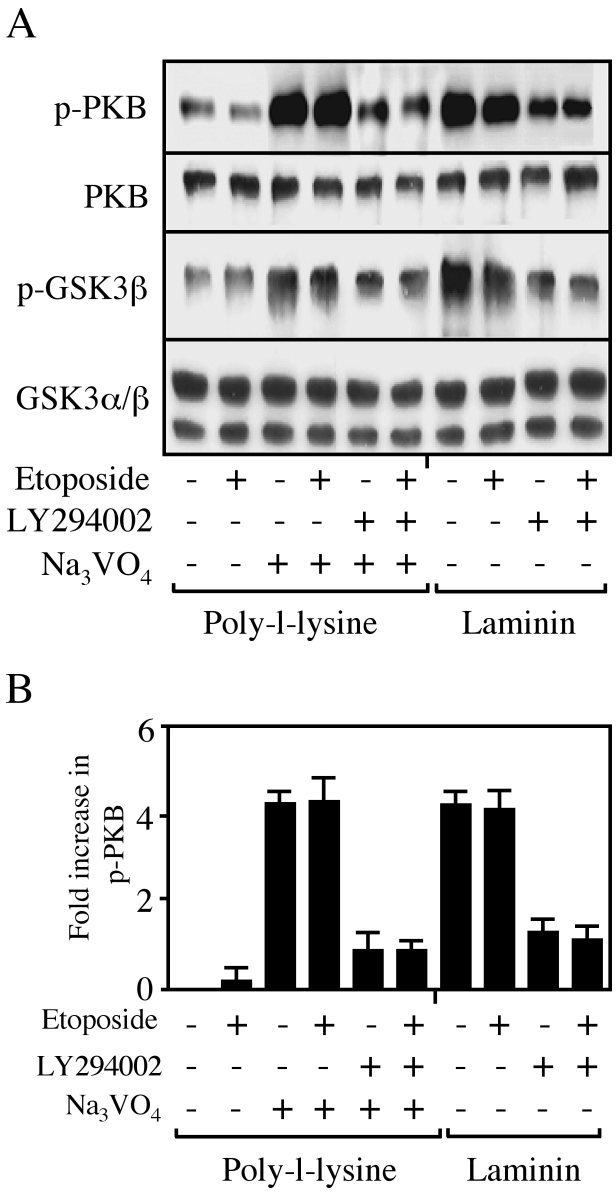
These experiments by Robert Rintoul and Weng Sie Wong suggest that ECM proteins stimulate PI3-kinase activity in SCLC cells and that PI3-kinase signalling can be inhibited pharmacologically with LY294002 (10μM) (Fig. 3.3 and 3.4). Therefore this inhibitor was used to specifically investigate the role of PI3-kinase in ECM-mediated chemo-protection.

Figure 3.3: Adhesion To ECM Stimulates PI3-Kinase Activity In SCLC Cells.



(A) H345 cells were adhered to 6 well plates pre-coated with poly-l-lysine (10 μg/ml), laminin (10 μg/ml), fibronectin (20 μg/ml) or TS2/16 (10 μg/ml). In addition cells on poly-l-lysine were treated with sodium orthovanadate (Na_3VO_4) (200 μm) or LY294002 (30 μM) as indicated. PI3-kinase activity was assayed after 10 minutes as described in the materials and methods. (B) H345 cells were adhered to laminin for the times indicated and PKB activity was determined as described in materials and methods. (C) H345 cells were adhered to laminin for the times indicated and expression of phosphorylated GSK3β was determined by Western blot analysis. Relative protein expression was quantified using Image J software (mean of n=3 experiments +/- SEM).

Figure 3.4: LY294002 Inhibits ECM- And Na_3VO_4- Stimulated PI3-Kinase Activity In SCLC Cells.



(A) H345 cells were adhered to 6 well plates pre-coated with poly-lysine (PLL) (10 μg/ml) or laminin (10 μg/ml) and treated with (+) or without (-) etoposide (25 μg/ml), sodium orthovanadate (Na_3VO_4) (200 μM) or LY294002 (30 μM) as indicated. Cells were lysed after 10 minutes and expression of phosphorylated protein kinase B (p-PKB), total protein kinase B (PKB), phosphorylated glycogen synthase kinase 3β (p-GSK3β) and glycogen synthase kinase 3α/β (GSK3α/β) was determined by Western blot analysis. Representative blots from n=3 experiments. (B) Relative expression of phosphorylated PKB (p-PKB) from cells treated as above. Mean fold increase in p-PKB relative to untreated from n=3 experiments ± SEM.

3.2.4 ECM-Mediated Protection Against Etoposide-Induced Apoptosis Is Dependent On PI3-Kinase Activation.

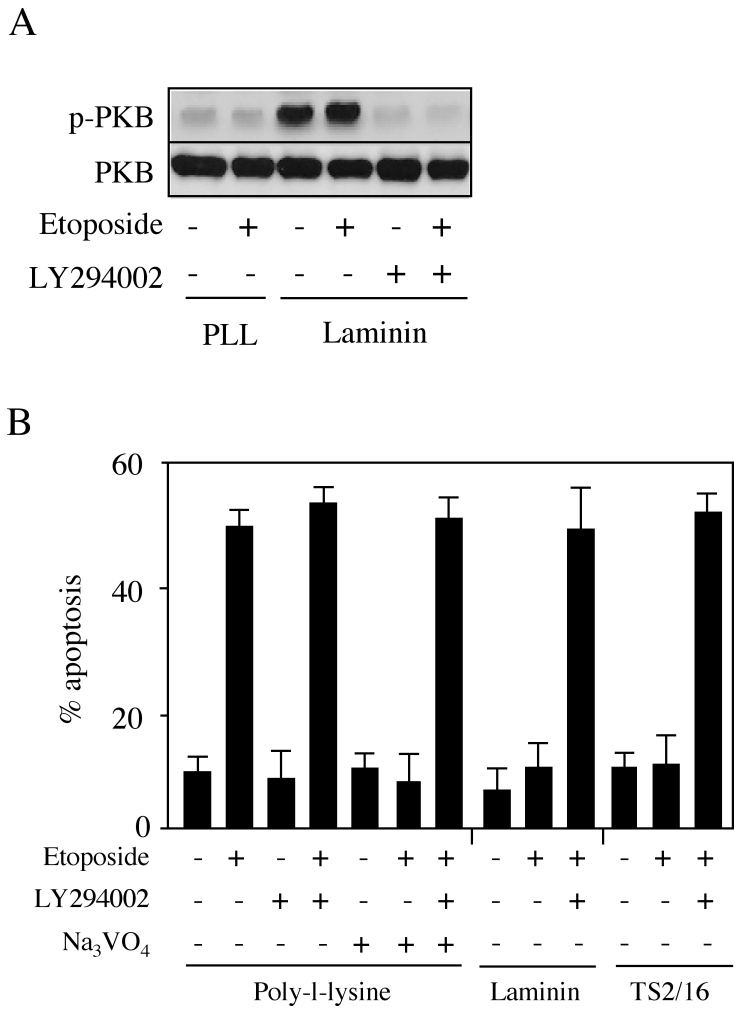
Using Western blot analysis of phospho-PKB (p-PKB), it was confirmed that LY294002 could inhibit ECM-mediated PI3-kinase activity up to 48 hours after treatment (Fig. 3.5 a). Furthermore, it was confirmed that inhibition of PI3-kinase in H345 SCLC cells with LY294002 (10μM) did not affect basal levels of apoptosis (Fig. 3.5 b). A moderate, non-significant increase in the degree of apoptosis induced by etoposide in cells adhered to poly-l-lysine and treated with LY294002 was observed (Fig. 3.5 b). However, the ECM-mediated protection of H345 SCLC cells against etoposide-induced apoptosis was completely reversed by the addition of LY294002 (Fig. 3.5 b). Furthermore chemo-protection resulting from specific β1 integrin stimulation with TS2/16 or stimulation of the tyrosine kinase pathway with Na_3VO_4 was abrogated by LY294002. This data suggests a central role for PI3-kinase in ECM/integrin-mediated chemoprotection.

PI3-kinase activates downstream PKB, which phosphorylates pro-apoptotic factors such as caspase-9 and Bad preventing cell death (216-218). Thus, the effect of ECM proteins on Bad phosphorylation and etoposide-induced caspase-9 activation in H345 SCLC cells was investigated. It was found that adhesion of H345 SCLC cells to ECM stimulated phosphorylation of Bad and prevented cleavage of caspase-9 induced by etoposide after 24 hours (Fig. 3.6 a). These effects were prevented by treatment with LY294002. Activation of caspase-9 initiates cleavage of the effector caspase-3, which ultimately results in apoptosis. It was found that etoposide could induce caspase-3 cleavage in H345 cells adhered to poly-l-lysine but not in cells adhered to laminin. However, treatment with LY294002 prevented laminin from blocking casapse-3 cleavage without affecting caspase-3 activation in cells adhered to poly-l-lysine (Fig. 3.6 a).

In parallel experiments, Alison MacKinnon measured caspase-3 activity (Fig. 3.6 b). It was confirmed that etoposide induced an increase in caspase-3 activity in H345 SCLC cells, which, as expected, was blocked by z-VAD. Adhesion to laminin and stimulation of the tyrosine kinase pathway with Na_3VO_4 overcame etoposide-induced caspase-3 activation preventing cells undergoing apoptosis. Furthermore,

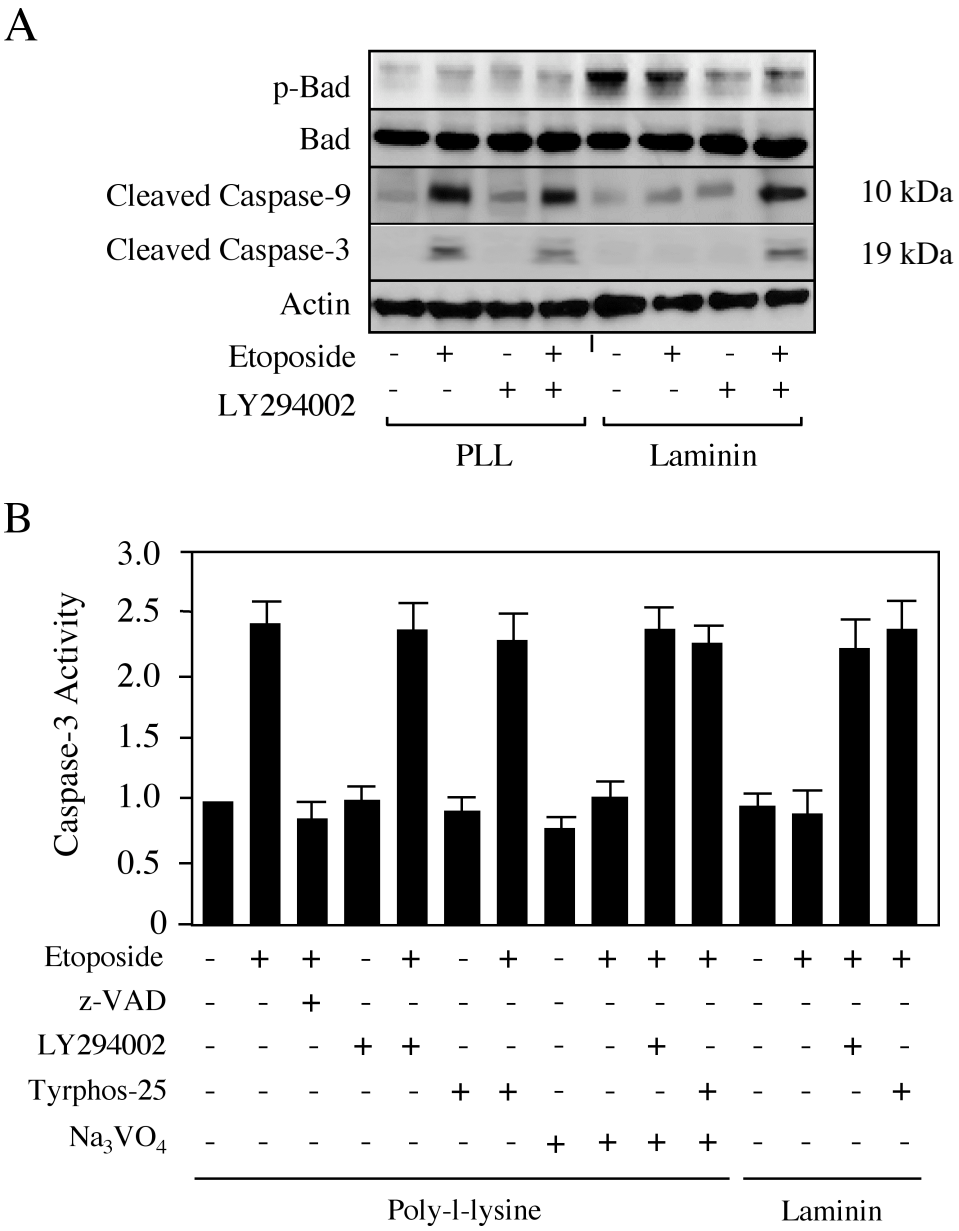
the ECM- and Na_3VO_4- mediated inhibition of etoposide-induced caspase-3 activation was prevented by the tyrosine kinase inhibitor tyrophostin-25 and the PI3-kinase inhibitor LY294002 (Fig. 3.6 b). Taken together, these results indicate that PI3-kinase signalling, can modulate phosphorylation of Bad and caspase activity, suggesting a central mechanism for ECM-mediated resistance to etoposide-induced apoptosis in SCLC cells.

Figure 3.5: ECM-Mediated Protection From Chemotherapy-Induced Apoptosis Requires PI3-Kinase Signalling.



(A) H345 cells were plated on to laminin or poly-l-lysine and treated as indicated. Cells were lysed after 48 hours and phospho-PKB (p-PKB) and total PKB expression was determined by Western blot. Representative blot from n=3 experiments. (B) H345 cells were seeded into 96 well plates pre-coated with poly-l-lysine (PLL) (10 μg/ml), laminin (10 μg/ml) or TS2/16 (10 μg/ml), allowed to adhere for 1 hour and then treated with (+) or without (-) etoposide (25 μg/ml), Na_3VO_4 (200 μM) or LY294002 (30 μM) as indicated. The percentage of apoptotic cells was assessed at 48 hours by flow cytometric analysis of surface Annexin V staining (mean of n=3 independent experiments ± SEM).

Figure 3.6: ECM-Mediated Protection From Chemotherapy-Induced Caspase-3 Activation Requires PI3-Kinase Signalling.



(A) H345 cells were seeded into 6-well plates pre-coated with poly-l-lysine (10 μg/ml) or laminin (10 μg/ml) and treated with (+) or without (-) etoposide (25 μg/ml) or LY294002 (30 μM) as indicated. After 24 hours the cells were lysed and the expression of phospho-Bad (p-Bad), Bad, cleaved-caspase-9 and cleaved-caspase-3 was determined by Western blot. Representative blots from n=3 experiments are shown. Actin is shown as a loading control. The molecular weights of the caspase-3 and caspase-9 fragments are shown. (B) H345 cells were seeded into 6-well plates pre-coated with poly-l-lysine (10 μg/ml) or laminin (10 μg/ml) and treated with (+) or without (-) etoposide (25 μg/ml), z-VAD (100 μM), LY294002 (30 μM), tyrphostin-25 (tyrpho-25) (25 μM) or Na_3VO_4 (200 μM) as indicated. Caspase-3 activity was measured after 48 hours as described in materials and methods and normalized to untreated cells on poly-l-lysine (mean of n=3 experiments ± SEM).

3.2.5 ECM Proteins Override Etoposide- And Radiation-Induced G2/M Cell Cycle Arrest Via PI3-Kinase Modulation Of Cell Cycle Regulators.

DNA damage is central to the cellular response to chemotherapy and radiation and results in cell cycle arrest predominantly at the G1/S and G2/M checkpoints (204). Subsequent activation of checkpoint signalling cascades can result in apoptotic cell death preventing accumulation of genetic damage. Modulation of cell cycle checkpoints may play an important role in sensitivity to radiation and chemotherapy. Therefore it was hypothesised that ECM proteins could override cell cycle arrest induced in SCLC cells by etoposide and radiation.

To investigate this, H345 SCLC cells were adhered to poly-l-lysine or laminin, treated with etoposide (25 μg/ml) or ionizing radiation (2 Gy) and nuclear DNA content was assessed after 24 hours by flow cytometric analysis of propidium iodide staining. H345 SCLC cells showed similar cell cycle profiles whether grown in suspension or adhered to poly-l-lysine or laminin (Fig. 3.7 a). 24 hours after treatment with etoposide (25 μg/ml) or ionizing radiation (2Gy) H345 SCLC cells adhered to poly-l-lysine showed a significant increase in the percentage of cells in the S and G2/M phases of the cell cycle with a reciprocal reduction in the percentage of cells in G1 (Fig. 3.7 a, Table 3.1).

In contrast H345 cells adhered to laminin and treated with etoposide or ionizing radiation showed only a small increase in the percentage of cells in S and G2/M phase with a minimal reciprocal reduction in the percentage of cells in G1. There was no significant difference in sub-G0 peaks at 24 hours between cells treated with etoposide on laminin or poly-l-lysine, which is also reflected by the data in figure 3.1. However, the percentage of apoptotic cells observed at 24 hours is higher when measured by acridine orange and Annexin V than when measured by PI staining and flow cytometry. This difference probably reflects a difference in preparation of cells for an assay, which aims to investigate cell cycle, changes rather than apoptosis and is not indicative of an altered cellular response to etoposide.

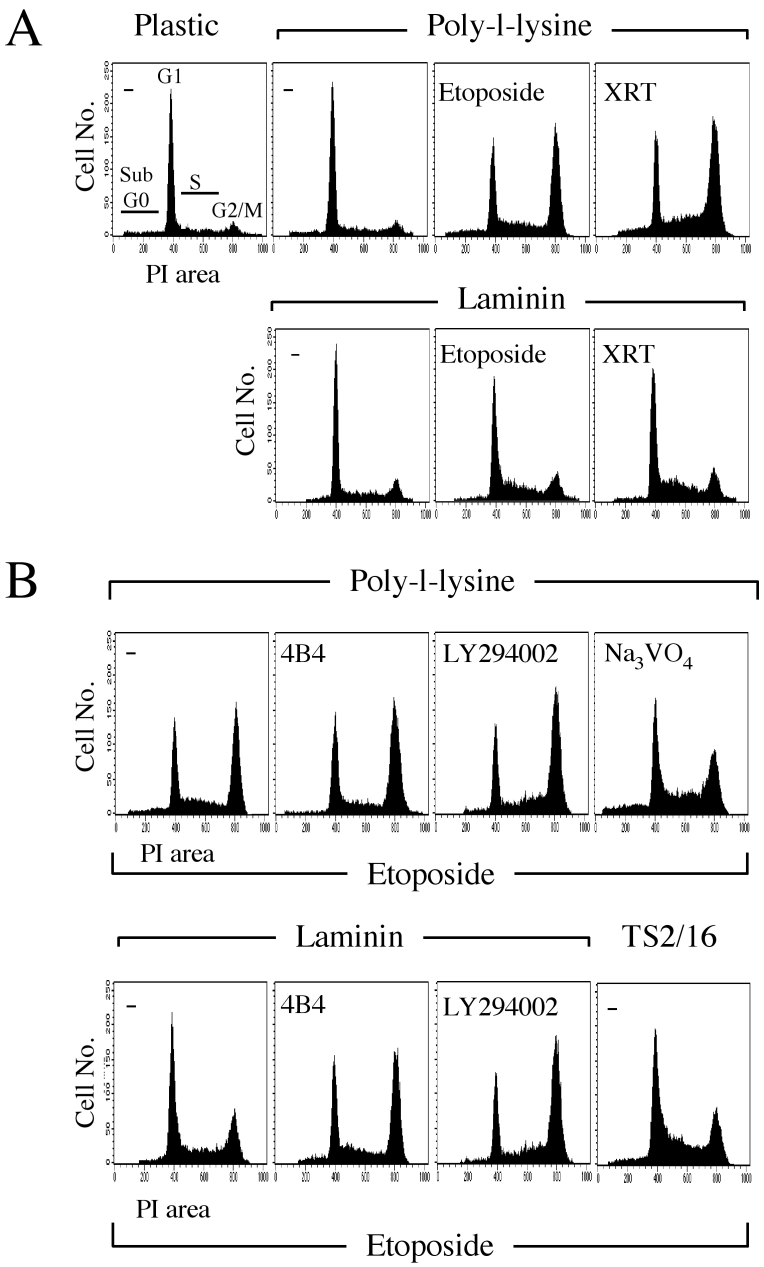
To investigate whether ECM protects against cell cycle arrest via activation of β1 integrin/PI3-kinase signalling, H345 SCLC cells were adhered to poly-l-lysine or laminin and treated with etoposide for 24 hours in the presence of the β1 integrin

function-blocking antibody 4B4, the β1 integrin-stimulating antibody TS2/16, Na_3VO_4 or LY294002. After 24 hours progression through the cell cycle was assessed (Fig. 3.7 b, Table 3.2). Blockade of β1 integrins on H345 SCLC cells with 4B4 completely abrogated laminin-mediated protection from G2/M cell cycle arrest induced by etoposide without affecting cell cycle progression in cells adhered to poly-l-lysine. Furthermore laminin-mediated protection from etoposide-induced G2/M cell cycle arrest was blocked by inhibition of PI3-kinase with LY294002. In addition stimulation of β1 integrins on H345 SCLC cells with TS2/16 or activation of tyrosine kinase with Na_3VO_4 reduced etoposide-induced G2/M cell cycle arrest simulating the effects of ECM. These results indicate that protection of SCLC cells from etoposide-induced cell cycle arrest by ECM proteins is mediated via β1 integrin activation of PI3-kinase signalling.

DNA damage can activate $p21^{Cip1/WAF1}$ and $p27^{Kip1}$ and inhibit Cdc25s (activator of CDK1) to cause G1/S and G2/M arrest (204). PI3K-kinase has been shown to induce expression of D-type cyclins and to increase stability of cyclin-D1 through PKB dependent phosphorylation of GSK3β (217). Therefore it was investigated whether ECM proteins could modulate expression of key cell cycle regulators through PI3-kinase. After 24 hours of etoposide treatment H345 SCLC cells showed an increase in expression of the CDK inhibitors $p21^{Cip1/WAF1}$ and $p27^{Kip1}$ and phosphorylated CDK1 (inactive form) with decreased expression of phosphorylated CDK2 (active form) and cyclins E, A and B (Fig. 3.8). Adhesion of H345 SCLC cells to laminin increased cyclin D expression and blocked the etoposide-induced changes in $p21^{Cip1/WAF1}$, $p27^{Kip1}$, phosphorylated CDK1 and 2 and cyclins E, A and B. Furthermore, the effects of ECM were reproduced by TS2/16 antibodies. The effects were less pronounced probably due to the bivalent nature of antibody binding inducing less integrin clustering and 3-dimensional changes than laminin. The ability of laminin or TS2/16 to overcome etoposide-induced changes in cell cycle regulators was blocked by the PI3-kinase inhibitor LY294002.

These results suggest that ECM proteins via β1 integrins can override etoposide-induced G2/M cell arrest by modulating expression of cyclins/CDK inhibitors and phopsphorylation of CDKs in a PI3-kinase dependent manner.

Figure 3.7: ECM Overrides Etoposide- And Radiation-Induced Cell Cycle Arrest Via β1 Integrin-Mediated PI3-Kinase Activation.



H345 cells were seeded into 6-well tissue culture plates either uncoated (plastic) or pre-coated with poly-l-lysine (10 μg/ml) or laminin (10 μg/ml). Progression through the cell cycle was assessed 24 hours later by flow cytometric analysis of DNA content. (A) Representative histograms (cell number/PI area) are shown from n=5 independent experiments of H345 cells treated as indicated: nil (-), etoposide (25 μg/ml) or ionizing radiation (2 Gy) (XRT) as indicated. (B) Representative histograms are shown from n=5 independent experiments of H345 cells treated as indicated: blockade of β1 integrin function with 4B4 (10 μg/ml), stimulation of β1 integrins with TS2/16 (10 μg/ml), inhibition of PI3-kinase with LY294002 (30 μM) or activation of tyrosine kinase with sodium orthovanadate (Na_3VO_4) (200μM).

Table 3.1: ECM Protects SCLC Cells From Etoposide- And Radiation-Induced Cell Cycle Arrest.

Cell Cycle Phase	Plastic -
Sub G0	5.6 +/-1.6
G1	64.8 +/-2.5
S	17.3 +/-2.0
G2/M	8.8 +/-1.0

Cell Cycle Phase	Poly-l-lysine -	Etoposide	XRT
Sub G0	6.1 +/-1.3	4.9 +/-2.4	5.4 +/-1.4
G1	65.3 +/-2.8	23.2 +/-2.3	22.1 +/-1.8
S	18.2 +/-1.7	25.4 +/-1.6	24.5 +/-2.1
G2/M	9.1 +/-0.6	46.2 +/-1.5	47.8 +/-2.1

Cell Cycle Phase	Laminin -	Etoposide	XRT
Sub G0	6.3 +/-1.7	5.1 +/-1.1	3.5 +/-1.7
G1	67.1 +/-3.1	53.2 +/-1.9	60.1 +/-2.6
S	16.7 +/-2.3	22.2 +/-1.7	20.1 +/-1.8
G2/M	8.4 +/-2.1	16.8 +/-2.0	16.1 +/-1.9

Table 3.1 shows the mean percentage of H345 SCLC cells treated as indicated for 24 hours in each phase of the cell cycle (n=5 independent experiments +/- SEM). Corresponds to the histograms in Fig. 3.7a.

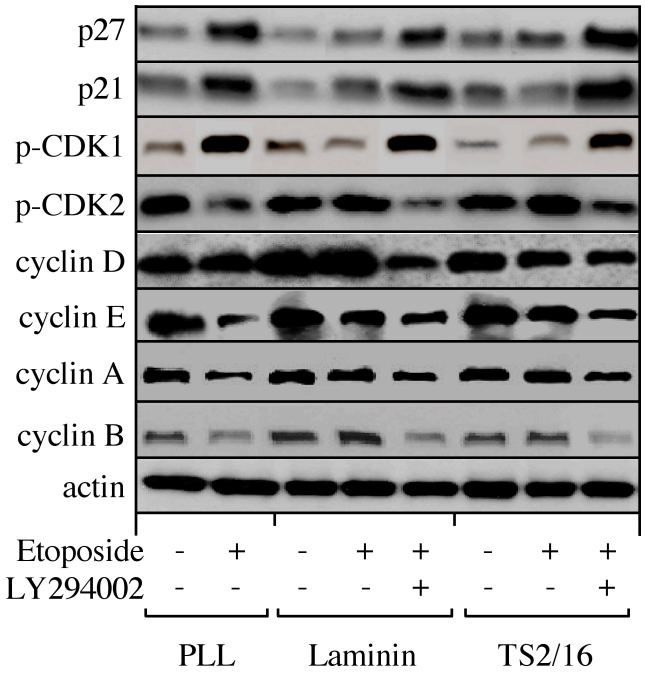
Table 3.2: ECM Protects SCLC Cells From Etoposide- And Radiation-Induced Cell Cycle Arrest Via β1 Integrin-Mediated PI3-Kinase Activation.

Cell Cycle	Poly-l-lysine			
Phase	-	4B4	LY294002	Na3VO4
Sub G0	3.6 +/-1.7	4.9 +/-1.1	4.3 +/-0.9	4.5 +/-0.7
G1	24.2 +/-3.9	23.2 +/-2.2	22.1 +/-2.5	39.8 +/-1.8
S	22.6 +/-2.1	20.8 +/-2.8	19.3 +/-1.3	24.5 +/-2.1
G2/M	48.2 +/-3.1	46.9 +/-2.8	52.5 +/-3.0	28.6 +/-2.0

Cell Cycle	Laminin			TS2/16
Phase	-	4B4	LY294002	-
Sub G0	4.2 +/-2.1	4.3 +/-1.1	3.2 +/-0.9	4.1 +/-2.1
G1	52.3 +/-3.1	22.8 +/-2.0	20.9 +/-1.7	44.2 +/-1.8
S	20.2 +/-1.9	19.7 +/-3.0	16.1 +/-2.4	28.7 +/-2.2
G2/M	18.4 +/-2.5	51.2 +/-2.2	58.8 +/-3.1	21.7 +/-2.6

Table 3.2 shows the mean percentage of H345 SCLC cells treated as indicated for 24 hours in each phase of the cell cycle (n=5 independent experiments +/- SEM). Corresponds to the histograms in Fig. 3.7b.

Figure 3.8: ECM Overrides Etoposide-Induced Changes In Expression Of Key Cell Cycle Regulators Via β1 Integrin And PI3-Kinase Activation.



H345 SCLC cells were seeded into 6 well plates pre-coated with poly-l-lysine (10 μg/ml) (PLL), laminin (10 μg/ml) or TS2/16 (10 μg/ml). Cells were treated with (+) or without (-) etoposide (25 μg/ml), LY294002 (30 μM) or sodium orthovanadate (Na_3VO_4) (200 μM) as indicated. Cells were lysed after 24 hours and the expression of $p21^{Cip1/WAF1}$, $p27^{Kip1}$, phosphorylated CDK1 (p-CDK1 - inactive), phosphorylated CDK2 (p-CDK2 - active) and cyclins D, E, A and B were determined by Western blot analysis. Representative blot from n=3 experiments. Actin is shown as a loading control.

3.2.6 Expression Of A Dominant Negative PKB Mutant Prevents, And A Constitutively Active PKB Mutant Mimics, ECM-Mediated Protection From Apoptosis And Cell Cycle Arrest.

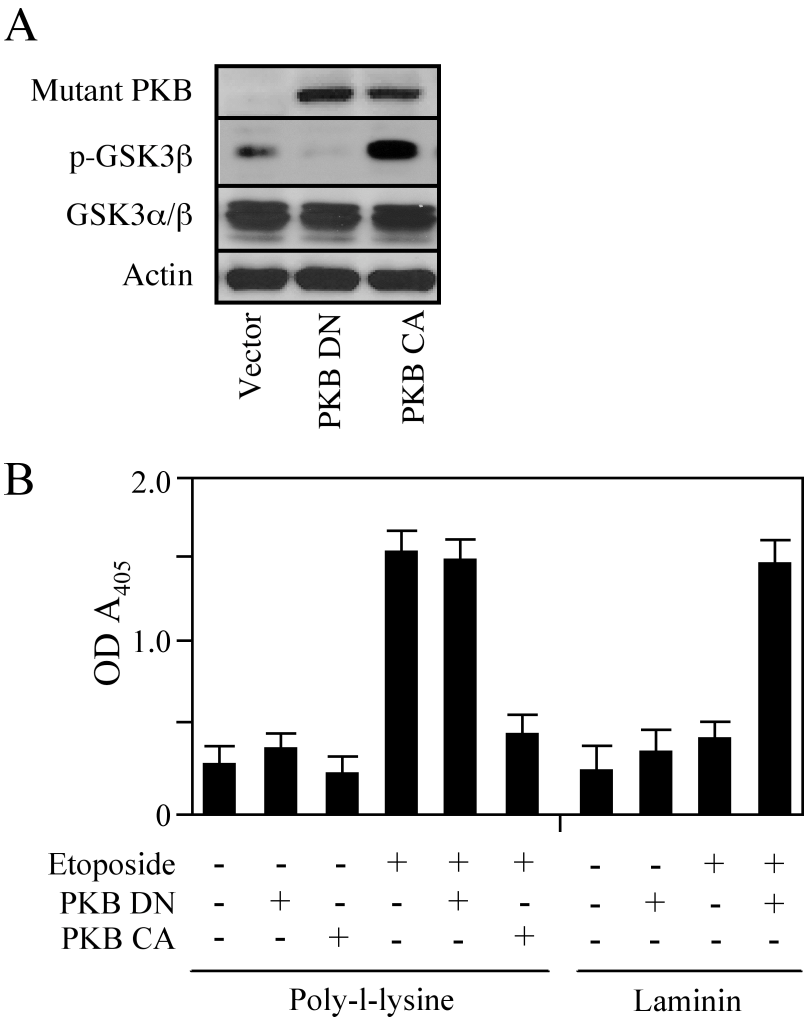
Although LY294002 is accepted as a specific inhibitor of PI3-kinase/PKB signalling at the doses used, it can inhibit other pathways that may affect cell survival (223). Therefore, PI3-kinase signalling was genetically inhibited in SCLC cells to confirm the effects of LY294002 on ECM-mediated chemoprotection. The data presented above clearly demonstrates that binding of SCLC cells to ECM leads to activation of PI3-kinase, which activates protein kinase B (PKB). Thus, to specifically examine downstream PKB signalling, the activity of PKB was manipulated through the expression of either constitutively active (PKB CA) or dominant negative (PKB DN) PKB mutants.

It was observed that transient expression of PKB DN in H345 SCLC cells markedly inhibited phosphorylation of downstream GSK3β whereas expression of PKB CA increased phospho-GSK3β levels, in accordance with the expected activity of these mutants on PKB signalling (Fig. 3.9 a). Importantly, expression of PKB CA protected H345 cells adhered to poly-l-lysine from etoposide-induced apoptosis (measured with cell death ELISA kit as described in chapter2) (Fig. 3.9 b). Expression of PKB DN produced a small but non-significant increase in apoptosis in cells adhered to poly-l-lysine. However, PKB DN markedly increased etoposide-induced apoptosis in cells adhered to laminin (Fig. 3.9 b). Tony Elliott confirmed these results using flow cytometric analysis of Annexin V staining (data not shown).

To confirm the results obtained with LY294002 on ECM-mediated protection from G2/M arrest, either PKB DN or PKB CA were transiently expressed in H345 cells. Transfected cells were then adhered to poly-l-lysine or laminin and progression through the cell cycle was analysed as previously described. It was observed that transient expression of PKB CA reversed etoposide-induced G2/M arrest (Fig. 3.10). Furthermore expression of PKB DN produced a modest increase in the G2/M population with and without etoposide treatment. Crucially, expression of PKB DN in cells adhered to laminin, reversed protection from etoposide-induced G2/M arrest and caused a small increase in G2/M arrest without etoposide treatment (Fig. 3.10,

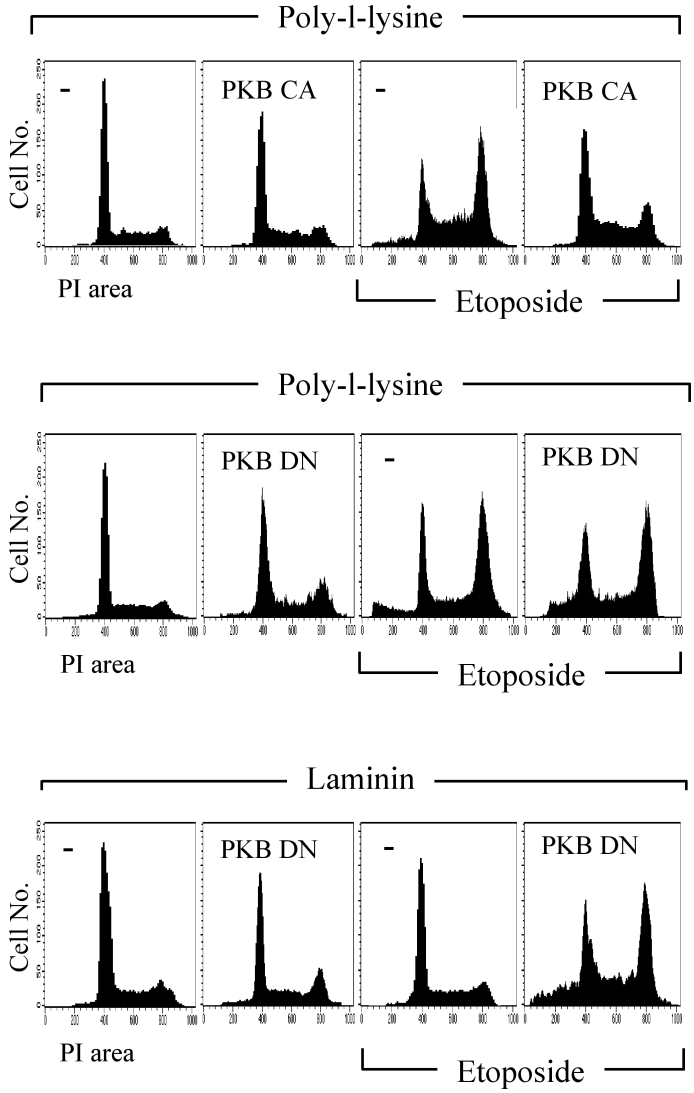
Table 3.3). Taken together these results indicate a central role for PI3-kinase and PKB signalling in ECM-mediated chemoprotection in SCLC cells.

Figure 3.9: The Effect Of Dominant Negative And Constitutively Active PKB Mutants On ECM-Mediated Protection From Etoposide-Induced Apoptosis.



H345 SCLC cells were transfected with equal amounts of empty vector (pUSEamp), dominant negative PKB (PKB DN) or constitutively active PKB (PKB CA) as indicated plus pEGFP as a reporter of transfection. After 24 hours flow sorting was used to enrich transfected cells. (A) Cells were lysed and expression of the Myc-tagged PKB mutants, GSK3 α/β and phospho-GSK3α (p-GSK3α) was determined by Western blot. A representative blot is shown from n=3 experiments. (B) Cells were resuspended in SITA, plated onto poly-l-lysine or laminin and treated with etoposide as indicated. After 48 hours apoptosis was assessed using a cell death ELISA kit. Mean absorbance at 405nm from n=4 independent experiments ± SEM.

Figure 3.10: The Effect Of Dominant Negative And Constitutively Active PKB Mutants On ECM-Mediated Protection From Etoposide-Induced Cell Cycle Arrest.



H345 cells were transfected with equal amounts of dominant negative PKB (PKB DN) (+), constitutively active PKB (PKB CA) (+) or pUSEamp (-) plus pEGFP as a reporter of transfection. After 24 hours flow sorting was used to enrich transfected cells. Cells were quiesced, seeded into 6 well plates pre-coated with poly-l-lysine or laminin and treated with etoposide as indicated. Progression through the cell cycle was assessed 24 hours later by flow cytometric analysis of DNA content using CELL Quest software. Representative histograms are shown from n=5 independent experiments.

Table 3.3: The Effect Of Dominant Negative And Constitutively Active PKB Mutants On ECM-Mediated Protection From Etoposide-Induced Cell Cycle Arrest.

Poly-l-lysine				
Cell Cycle Phase			Etoposide Treatment	
	-	PKB CA	-	PKB CA
Sub G0	4.3 +/-0.7	4.1 +/-0.8	8.3 +/-1.3	3.6 +/-0.9
G1	63.2 +/-2.9	60.1 +/-3.3	19.6 +/-2.1	49.8 +/-1.8
S	15.6 +/-1.8	17.3 +/-1.6	27.3 +/-1.4	21.5 +/-3.1
G2/M	12.2 +/-1.1	14.2 +/-1.1	53.5 +/-3.0	22.6 +/-2.3

Poly-l-lysine				
Cell Cycle Phase			Etoposide Treatment	
	-	PKB DN	-	PKB DN
Sub G0	3.2 +/-0.7	4.1 +/-0.8	7.5 +/-2.3	8.9 +/-1.7
G1	61.3 +/-3.9	51.6 +/-3.3	24.6 +/-1.9	27.6 +/-1.9
S	17.3 +/-2.1	20.4 +/-1.9	26.8 +/-2.4	26.8 +/-2.7
G2/M	14.2 +/-2.1	23.2 +/-3.1	47.5 +/-3.1	43.6 +/- 3.8

Laminin				
Cell Cycle Phase			Etoposide Treatment	
	-	PKB DN	-	PKB DN
Sub G0	4.0 +/-1.8	4.2 +/-1.9	3.1 +/-0.7	8.1 +/-1.1
G1	64.5 +/-3.0	47.6 +/-1.5	55.3 +/-2.2	20.8 +/-2.2
S	16.2 +/-1.7	24.5 +/-2.9	20.6 +/-1.1	27.7 +/-1.7
G2/M	11.6 +/-2.1	21.2 +/-2.0	15.2 +/-1.0	49.2 +/-2.1

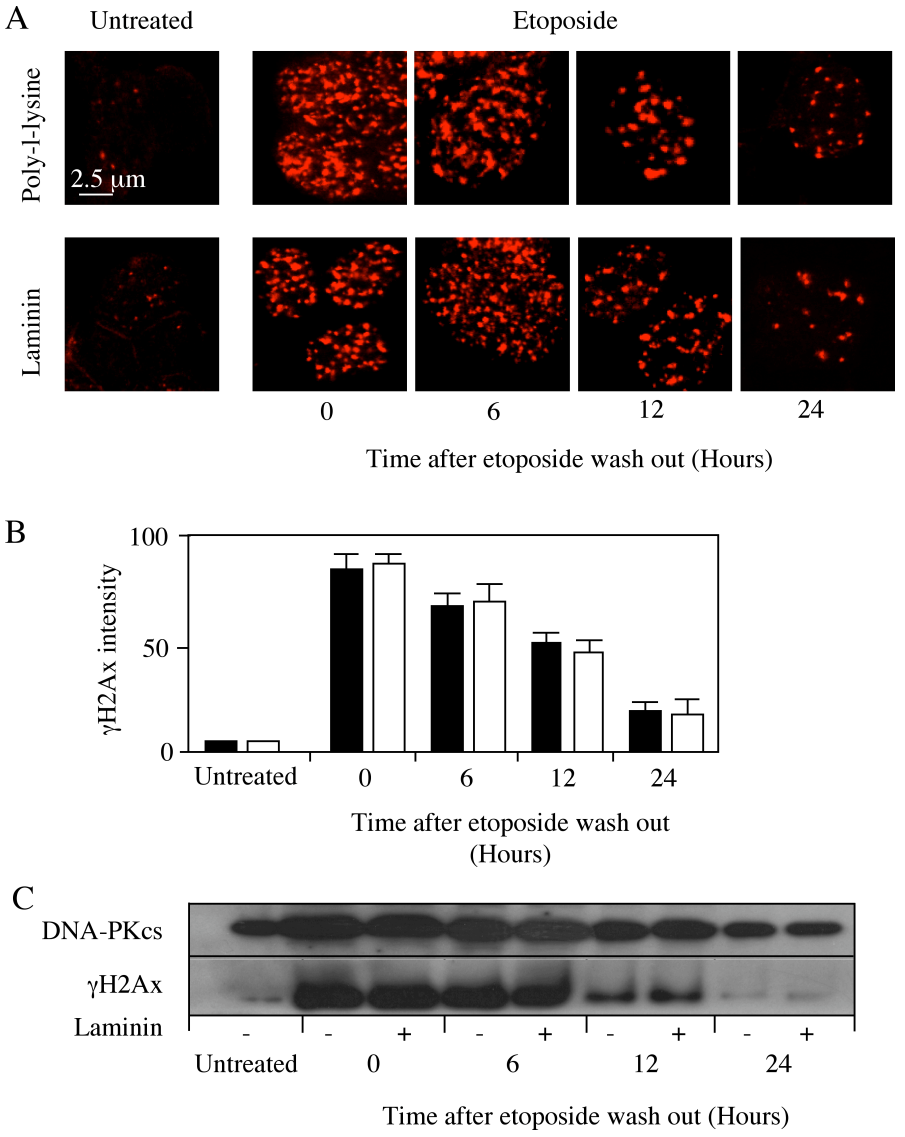
Table 3.3 shows the mean percentage of H345 SCLC cells treated as indicated for 24 hours in each phase of the cell cycle (n=5 independent experiments +/- SEM). Corresponds to the histograms in Fig. 3.10.

3.2.7 Adhesion To ECM Proteins Does Not Modulate Ongoing Etoposide- And Radiotherapy-Induced DNA Damage Or Repair.

The enzyme topoisomerase II resolves sister chromatid entanglement by binding to DNA, cleaving both strands and passing a second duplex through the first before reannealing the cleavage site (224). Etoposide inhibits the activity of topoisomerase II resulting in DNA double strand break formation, cell cycle arrest and apoptosis (225). It has previously been demonstrated that ECM proteins do not affect the inhibition of topoisomerase II activity by etoposide (167). However, ECM could protect SCLC cells from cell cycle arrest and subsequent apoptosis by promoting repair of etoposide-induced DNA damage. To test this hypothesis, H345 cells were treated with etoposide and the amount of DNA double strand breaks were measured over time.

H345 cells were seeded onto plastic pre-coated with poly-l-lysine or laminin and then treated as specified. The cells were washed, allowed to recover and the amount of DNA double strand breaks in cell nuclei were determined by immunofluorescence staining of phosphorylated H2AX (γH2AX). Foci of γH2AX represent actual DNA double strand breaks and correlate closely with cell death in response to DNA damage (226) (Fig. 3.11 a). DNA double strand breaks were also confirmed by Western immunoblotting for γH2Ax and DNA-PKcs (Fig. 3.11c). A very marked and equal increase in γH2Ax foci was seen 2 hours after etoposide treatment. Over the following 24-hour period there was a decrease in the number of double strand breaks as DNA damage was repaired (Fig. 3.11). Crucially there was no difference in the amount of DNA damage in response to etoposide or the rate of repair between cells plated on laminin or non-specifically adhered to plastic by poly-l-lysine. Interestingly, whilst nearly all of the DNA damage was repaired there were still a significant number of γH2Ax foci present at 24 hours, suggesting persistence of DNA damage.

Figure 3.11: Adhesion To ECM Does Not Affect Etoposide-Induced DNA Double Strand Break Formation And Repair.



(A) H345 SCLC cells were adhered to poly-l-lysine (10 µg/ml) or laminin (10 µg/ml) and treated with etoposide (25 µg/ml) for 2 hours. Cells were washed twice and allowed to recover in RPMI (10% FCS). Cells were subsequently fixed at 0-24 hours after removal of etoposide, stained with anti-γH2Ax antibody and foci viewed by fluorescence microscopy. Representative images of γH2Ax foci at each time point are shown with H345 cells without etoposide (untreated) for comparison. (B) The mean intensity of γH2Ax staining from 10 random high power fields was quantified with Openlab image analysis software and normalized to untreated cells. Mean relative γH2Ax intensity +/- SEM from n=4 independent experiments. Closed bars – cells plated on poly-l-lysine; open bars – cells plated on laminin. (C) H345 cells were adhered to poly-l-lysine (-) or laminin (+) in 6-well plates, treated with etoposide (25 µg/ml) and lysed at the times indicated. Expression of DNA-PKcs and γH2Ax was determined by Western blot analysis. Representative blots from n=3 independent experiments.

3.3 Discussion.

The results described in this chapter show that ECM proteins activate β1 integrins to protect SCLC cells against the pro-apoptotic effects of etoposide and ionizing radiation through PI3-kinase activation. Etoposide, which inhibits the re-annealing activity of topoisomerase II causing DNA damage, upregulates CDK inhibitors $p21^{Cip1/WAF1}$ and $p27^{Kip1}$, increases CDK 1 phosphorylation and down regulates cyclins D, E, A and B and CDK 2 phosphorylation. This causes G2/M cell cycle arrest, activation of the caspase cascade and subsequent apoptosis. In SCLC cells β1 integrin-mediated PI3-kinase activation via phosphorylation of PKB and GSK3β leads to maintenance of cyclins D, E, A and B, increases expression of phosphorylated CDK2 and down regulates CDK inhibitors, $p21^{Cip1/WAF1}$ and $p27^{Kip1}$ despite the presence of etoposide. This leads to continued progression through the cell cycle, overriding etoposide-induced G2/M arrest and results in phosphorylation of Bad preventing caspase-9 and -3 activation. As a consequence, SCLC cells in the presence of ECM are resistant to chemotherapeutic agents and continue to cycle despite damaged DNA, which may ultimately lead to the emergence of drug resistant clones. Because the DNA damage is random, genetic drug resistance can be achieved as a result of a wide variety of insults, explaining why no unifying mechanism for the emergence of multi-drug resistance (MDR) in SCLC has been defined.

The development of MDR is a major cause of treatment failure in cancer (227). Central to the cellular response to DNA damage is cell cycle arrest at regulated checkpoints with subsequent activation of cell death by apoptosis (228). MDR is a multi-factorial phenomenon. Therefore, it may be more effective to target the processes that enhance survival and prevent apoptosis in cancer cells thus preventing the emergence of acquired drug resistance (229). Resistance mechanisms *in vitro* differ from those *in vivo*, suggesting that the local cellular environment plays a significant role in selection for *in vivo* drug resistance. Prior results in SCLC suggest that *in vivo* interactions between tumour cells and ECM proteins in the microenvironment are involved in the early stages of drug selection providing a

survival advantage to ECM adherent SCLC cells and promote the acquisition of the classical forms of drug resistance.

Detachment of anchorage-dependent cells results in apoptotic cell death (230). This can be prevented by constitutive activation of integrin-dependent signalling pathways such as PI3-kinase and PKB (117). While anchorage-independent growth is a major step in cellular transformation leading to cancer and metastases, cancer cells may still use integrin survival signals. The data shown here and that of other groups indicates that a number of cancers including, SCLC, breast, prostate, colon cancer and haematological malignancies all use ECM adhesion for survival to evade the cytotoxic effects of chemotherapy or radiotherapy (201-203). While this appears to be a general and important phenomenon, the actual intracellular mechanisms coupling integrin activation to protection from chemotherapy and radiotherapy - induced apoptosis may be cancer cell type specific. Previous studies in haematopoetic tumour cells have demonstrated that adhesion to fibronectin protected against chemotherapeutic agents through increased expression of $p27^{Kip1}$ and G1 cell cycle arrest (231). Furthermore, integrin-mediated adhesion in haematopoetic cancer cells reduced DNA double-strand breaks and apoptosis caused by chemotherapeutic agents such as mitoxantrone and etoposide (232,233). This $\alpha5$ $\beta1$-mediated reduction in DNA damage correlated with decreased topoisomerase-II enzymatic activity. However the $\alpha5$ $\beta1$ integrin is not found in SCLC cells and is reduced in other carcinomas (167,234). Furthermore, prior data indicate that in SCLC cells grown in suspension or adhered to ECM proteins such as laminin and fibronectin the enzymatic activity of topoisomerase-II remains unchanged (167). In addition, Robert Rintoul showed that the rate of proliferation of SCLC cells is also unaffected by adhesion to ECM proteins. These results indicate that decreased proliferation and changes in topoisomerase II activity are not the mechanisms of integrin-mediated drug resistance in SCLC cells.

The PI3-kinase/PKB pathway contributes to the pathogenesis of cancer and confers resistance to apoptosis (215,235). Activated PI3-kinase phosphorylates inositol lipids resulting in the activation of the serine/threonine kinase PKB that phosphorylates caspase-9 and Bad, promoting cell survival (215). Activated PKB can also regulate cellular proliferation by interaction in the nucleus with cell cycle regulators

governing G1/S and G2/M checkpoints (236). The data shown in this chapter indicates that inhibition of PI3-kinase prevents β1 integrins from overriding etoposide-induced G2/M cell cycle arrest and apoptosis indicating that PI3-kinase is crucial for ECM-mediated chemoprotection in SCLC cells.

Integrins and growth factors in untransformed cells regulate cell cycle progression at the G1/S checkpoint (207). Current evidence suggests a central role for PI3-kinase signalling pathway in regulating cell cycle progression. PI3-kinase activation can be sufficient to induce G1 transit in fibroblasts. Thus, downstream targets of PI3-kinase/PKB dependent pathways that regulate normal cell cycle progression may also participate in overriding etoposide and radiation induced cell cycle checkpoints (236). PI3-kinase activity has been shown to induce expression of D-type cyclins and to increase cyclin D1 stability through PKB-dependent phosphorylation of GSK3β (217,237). G1 progression depends on the sustained expression of D type cyclins. The cyclin D-CDK 4 and 6 complex sequesters the CDK inhibitors $p21^{Cip1/WAF1}$ and $p27^{Kip1}$. This allows cyclin E-CDK 2 to drive the cell cycle through late G1 thus promoting the derepression of cyclin A at the onset of S phase (212). Deletion of the $p27^{Kip1}$ gene restores the growth phenotype of cyclin D1 null mice (238). Furthermore cells, which over-express cyclin E, still depend on cyclin D1 accumulation to sequester the enhanced $p21^{Cip1/WAF1}$ levels, suggesting that a major function of cyclin D1 in cell cycle control is the redistribution of CDK inhibitors (239). PI3-kinase effects on G1 phase progression may also be mediated through the downregulation of expression and function of $p27^{Kip1}$ (240). Thus adhesion to ECM via integrin-mediated activation of PI3-kinase may reduce levels of $p21^{Cip1/WAF1}$ and $p27^{Kip1}$ allowing cells to progress through the G1/S phase of the cell cycle.

The results in this chapter confirm prior reports that etoposide and ionizing radiation lead to G2/M cell cycle arrest. The data clearly demonstrates that β1 integrin/PI3-kinase signalling in SCLC cells regulates progression through the G2/M checkpoint. Furthermore PI3-kinase activation via β1 integrins in SCLC cells down regulates $p21^{Cip1/WAF1}$ and $p27^{Kip1}$, reduces phosphorylation of CDK1, maintains expression of cyclin D, E, A and B and phosphorylates CDK2, despite the presence of etoposide-induced DNA damage. The ability of integrins to regulate G2/M phase of the cell

cycle in SCLC highlights differences in key cell cycle regulators between transformed and untransformed cells. SCLC cells have previously been shown to have a defective G1/S checkpoint, which correlates with mutant inactive p53 (241). Prolonged cell cycle arrest as a result of unrepaired DNA damage eventually leads to caspase-3 activation and apoptosis, this is overridden by adhesion to ECM and β1 integrins in SCLC, which drives the cell cycle despite continued DNA damage and prevents caspase-3 activation and apoptosis. The mechanisms described here for SCLC, differ from those reported previously, particularly myeloma cells. This may reflect cell type specificity potentially relating to differing integrin behaviour between haematological malignancies and solid tumours.

β1–integrin mediated adhesion between tumour cells and the ECM in their environment confers a survival advantage to SCLC cells. This may provide initial or *de novo* mechanisms of resistance to DNA damaging therapy facilitating further transforming mutations and the acquisition of multi drug resistance. Once cells evade the initial cytotoxic effects of chemotherapy or radiation, multi-drug resistance may be inevitable. Thus, the environmental context and specificity of cancer cells may have important consequences on the acquisition of multi drug resistance. Strategies designed to disrupt specific interactions between cells and their environment may be important in the circumvention of multi drug resistance. However, since integrins play a key role particularly in the immune system and protection against infection, targeting β1 integrins may have deleterious side effects. A better understanding of the β1 specific mechanisms mediating integrin protection against the pro-apoptotic effect of DNA damaging drugs may lead to the development of novel therapeutic targets in the circumvention of multi drug resistance.

CHAPTER 4: H-Ras Suppresses Integrin Activation Through A Phospholipase C-epsilon-Dependent Pathway.

4.1 Introduction.

The data presented in chapter 3 indicate that β1 integrins play a key role in SCLC survival and resistance to chemotherapy. An essential feature of integrins is their ability to regulate the strength of extracellular matrix (ECM) protein binding, a process termed affinity modulation (199). Various intracellular signals can induce a conformational change in the integrin heterodimer, activating or suppressing ECM binding (199). Understanding the signalling pathways that regulate integrin affinity has the potential to reveal novel targets for anti-cancer drug development.

H-Ras, a member of the Ras family of small GTP binding proteins, has a crucial role in the pathogenesis of cancer and expression of a constitutively active mutant of H-Ras, H-Ras(G12V), has been shown to suppress integrin activation (242). Thus, H-Ras signalling may be an important anti-cancer target. H-Ras activates the downstream effector Raf, which leads to the phosphorylation and activation of extracellular signal-regulated kinase (ERK1/2). Constitutively active Raf has also been shown to suppress integrin activation (242,243). H-Ras mediated suppression of integrin affinity can be reversed by expression of MAP Kinase Phosphatase-1 (MKP-1) which can dephosphorylate and inactivate ERK1/2 (242). However, studies using H-Ras chimeras have revealed that integrin affinity modulation does not precisely correlate with ERK1/2 activation (244,245). Remarkably, although targeting of ERK1 to the plasma membrane has been shown to be sufficient to suppress integrins (246), inhibition of ERK1/2 activation with either MAP Kinase Phosphatase-3 (MKP-3) or the chemical inhibitor UO126, fails to affect integrin suppression by H-Ras (244). This discrepancy suggests an alternative pathway for H-Ras-mediated integrin suppression that does not rely on ERK1/2 activation.

Several other effector pathways are activated by H-Ras in addition to Raf, including PI3-kinase and Ral Guanine Exchange Factors (Ral-GEFs). Amino acid substitution mutants of H-Ras have been extensively utilized in dissecting its downstream effector pathways. The effector mutant T35S retains its ability to activate Raf, whereas the mutants E37G and Y40C are Raf-independent and activate Ral-GEFs

and PI3-kinase respectively (247,248). These H-Ras mutants also display differential action upon other H-Ras effectors including Rin-1, AF-6, PKCε, p120 GAP (249-252) and recently phospholipase C-epsilon (PLCε) (253-255).

Phosphoinositide-specific phospholipase C (PI-PLC) catalyses the hydrolysis of phosphatidylinositol 4,5-bisphosphate (PIP_2) into diacylglycerol (DAG) and inositol 1,4,5-trisphosphate (IP_3). DAG stimulates protein kinase C activation and IP_3 mobilizes intracellular Ca^{2+} (256). Three major classes of PI-PLC have been described previously: PLCβ, PLCγ, and PLCδ (257). They all contain an N terminus pleckstrin homology (PH) domain, an EF-hand domain, catalytic X and Y domains, and a regulatory C2 domain. These PLC classes are activated by distinct signalling mechanisms (258). PLCβ is activated by the α subunit (Gα) or βγ subunits (Gβγ) of heterotrimeric G proteins. PLCγ is activated by tyrosine phosphorylation following binding to tyrosine kinase of receptor or non-receptor types through its SH2 domain. PLCδ is activated by the high-molecular-weight G-protein, Gh and/or by an increase in the concentration of intracellular Ca^{2+}.

Recently, a fourth class of PI-PLC has been identified, PLCε (253-255). PLCε shares the typical X, Y and C2 domains with the other classes of PI-PLC, contains putative PH and EF-hand domains and is activated by Gβγ subunits (259). Furthermore, PLCε is unique in that it possesses two functional domains not seen in other classes. At its N terminus, PLCε possesses a CDC25 homology domain - a guanine nucleotide exchange factor (GEF) domain for the Ras family of small G proteins, which exhibits GEF activity toward Rap1 and H-Ras (255,260). PLCε also possesses, at its C terminus, two H-Ras/Rap1-associating (RA) domains, RA1 and RA2 domains (253-255). However, despite the characterization of these domains within PLCε, its physiological function has remained unclear.

Prior data has indicated that H-Ras can bind to PLCε in a GTP-dependent manner through its RA2 domain to stimulate the hydrolysis of PIP_2 into the secondary messengers IP_3 and DAG (253-255). This suggests that PLCε may be a downstream effector of H-Ras. Other PI-PLC classes have been shown to have an important role in integrin affinity modulation (261,262). Therefore, it was hypothesized that PLCε could act as a downstream effector of H-Ras in integrin suppression.

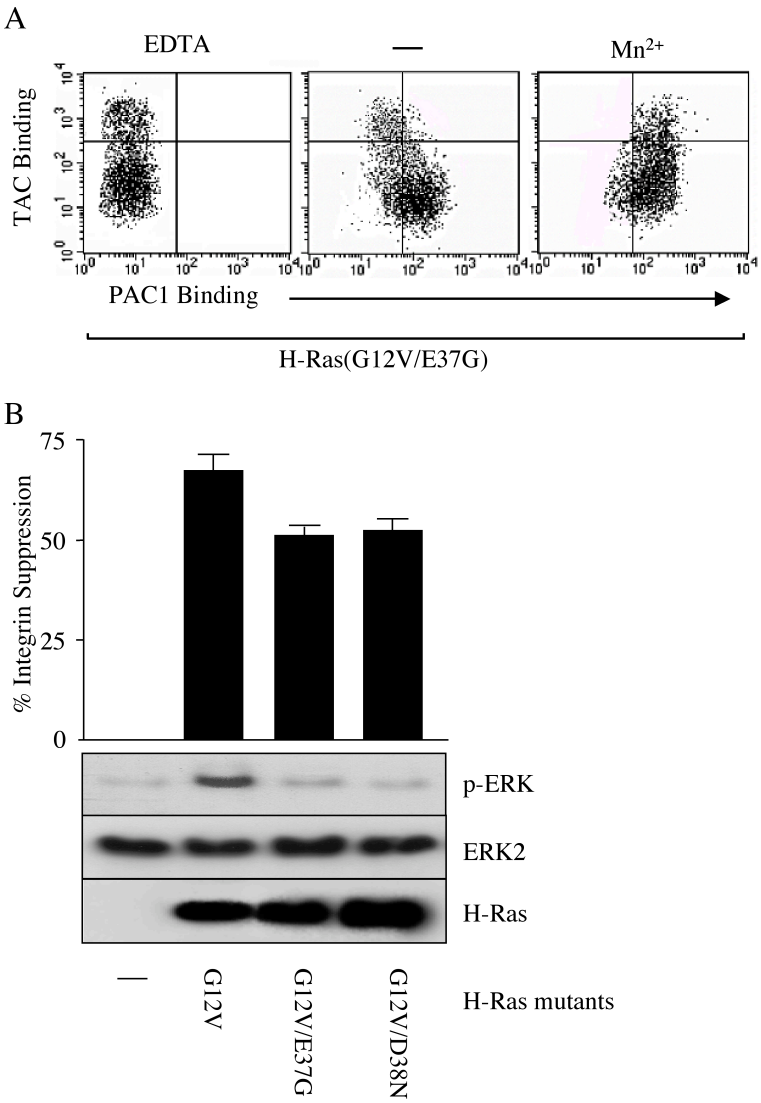
4.2 Results.

4.2.1 PLCε Mediates Integrin Suppression.

To examine the role of downstream effectors of H-Ras in integrin suppression, a Chinese hamster ovary cell line (CHO(αβ-py)) was used that stably expresses a chimeric integrin containing the extracellular and transmembrane domains of αIIb β3 fused to the cytoplasmic domains of α6 β1 (242,243). H-Ras effector mutants were transiently expressed in CHO(αβ-py) cells and an integrin suppression index was quantified from changes in the binding levels of the αIIb β3 ligand mimetic monoclonal antibody, PAC1, detected by flow cytometry as described in material and methods.

Yatish Lad previously demonstrated that H-Ras(G12V) effector mutants, E37G and D38N, which were unable to phosphorylate ERK1/2, could suppress integrin affinity in CHO(αβ-py) cells (Summarised in Fig. 4.1). Both H-Ras(G12V/E37G) and H-Ras(G12V/D38N) have been shown by other groups to stimulate PLCε activity (15-17). However, H-Ras(G12V/D38N) does not stimulate the Ral GEFs or bind to Raf. Therefore this mutant was used to examine the role of PLCε in H-Ras-mediated integrin suppression. Yatish Lad also confirmed that wild type PLCε could potentiate the effect of H-Ras(G12V/D38N) on integrin suppression in CHO(αβ-py) cells (263). Furthermore he demonstrated that wild type PLCε could potentiate IP3 production in CHO(αβ-py) cells stimulated by H-Ras(G12V/D38N) and that this could be blocked by co-transfection of a kinase dead mutant of PLCε (PLCε(H1433L)) (263). Using Western blot analysis he confirmed that transient expression of PLCε did not affect H-Ras-mediated phosphorylation of ERK1/2 (263). This preliminary data suggested a central role for PLCε in integrin affinity modulation by H-Ras.

Figure 4.1: H-Ras(G12V/E37G) And H-Ras(G12V/D38N) Mutants Suppress Integrin Activation Without Phosphorylating ERK.



(A) CHO(αβ-py) cells were transiently transfected with H-Ras(G12V/E37G) and the reporter construct Tac-α5. The dot blots show PAC1 binding (integrin affinity) in the presence of EDTA or Mn^{2+} as indicated and TAC binding (transfection efficiency). The quadrant markers separate high and low PAC1 binding cells (x-axis) and high and low transfected cells (y-axis). (B) CHO(αβ-py) cells were transfected with H-Ras(G12V) effector mutants E37G and D38N (1μg) and the reporter construct Tac-α5. Forty-eight hours post transfection cells were harvested and assessed for integrin affinity by flow cytometry. Percentage inhibition was calculated in reference to empty vector. The results shown are the mean ± SEM of five independent experiments. Lower panel: Transfected cell lysates were probed to determine H-Ras expression and ERK1/2 phosphorylation.

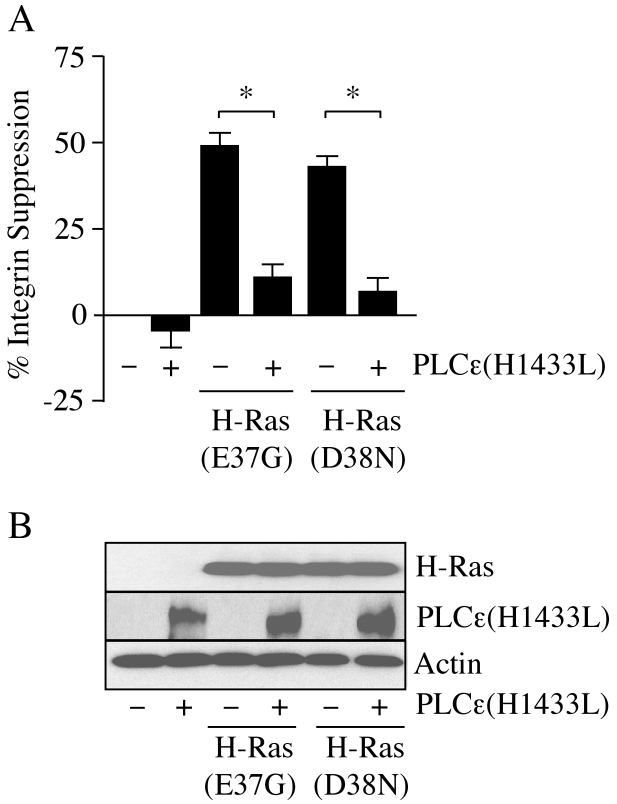
To further investigate the role of PLCε in integrin suppression, the kinase dead mutant of PLCε (PLCε(H1433L)) was co-transfected into CHO(αβ-py) cells with either H-Ras(G12V/E37G) or H-Ras(G12V/D38N) and the effect on integrin affinity determined. It was observed that that expression of PLCε(H1433L) alone in CHO(αβ-py) cells had no significant effect on integrin activation (Fig. 4.2a). However, co-transfection of H-Ras(G12V/E37G) or H-Ras(G12V/D38N) with PLCε(H1433L) significantly blocked integrin suppression mediated by these H-Ras mutants (49.3 ± 3.0% to 10.1 ± 2.3%, $p<0.01$ and 47.2 ± 2.9% to 7.2 ± 2.5%, $p<0.001$ respectively) (Fig. 4.2a). Western blot analysis confirmed equal Flag-tagged expression of PLCε mutants in transfected cells and expression of PLCε(H1433L) did not alter H-Ras expression.

To confirm the data obtained with PLCε(H1433L), endogenous PLCε expression in CHO(αβ-py) cells was knocked-down and the effect on H-Ras(G12V/D38N)-mediated integrin suppression was determined. siRNA oligonucleotides targeting conserved sequences from rat, human and mouse PLCε have previously been described, and shown to reduce PLCε expression by up to 97% (197). Analysis from the surrounding regions of siRNAPLCε#3 and siRNAPLCε#5 showed that CHO PLCε is nearly identical between rat and hamster, and the two siRNA target sites of siRNAPLCε#3 and siRNAPLCε#5 are both completely conserved (Fig. 4.3). Therefore, CHO(αβ-py) cells were transfected with either the PLCε targeting siRNA or a scrambled non-targeting oligonucleotide and the effect on integrin suppression mediated by transient expression of H-Ras(G12V/D38N) was assessed.

It was found that transfection of the non-targeting siRNA oligonucleotide had no significant effect on H-Ras(G12V/D38N)-mediated integrin suppression (49.3 ± 3.1% and 48.6 ± 2.9% respectively) (Fig. 4.4 a). In contrast, transfection of the PLCε targeting siRNA (siRNAPLCε#5) significantly blocked H-Ras(G12V/D38N) mediated integrin suppression (11.6 ± 2.9%, $p<0.05$). As expected, transfection with siRNAPLCε#5 markedly reduced levels of PLCε mRNA as assessed by RT-PCR (Fig. 4.4 b). Comparable levels of PLCε mRNA were observed in untransfected cells and cells transfected with non-targeting siRNA. Furthermore knockdown of endogenous PLCε protein in CHO(αβ-py) cells was confirmed by Western blot

analysis (Fig. 4.4 b). Brian McHugh validated these results by transfecting CHO(αβ-py) cells with siRNAPLCε#3 and observed similar knockdown of PLCε and reversal of H-Ras(G12V/D38N) mediated integrin suppression. Importantly, transfection of cells with siRNA oligonucleotides did not affect expression of H-Ras(G12V/D38N) or actin (Fig. 4.4 b). Taken together, these results indicate that endogenous PLCε can modulate integrin suppression mediated by H-Ras.

Figure 4.2: PLCε(H1433L) Blocks Integrin Suppression Mediated By H-Ras(G12V/D38N)



(A) CHO(αβ-py) cells were co-transfected with H-Ras(G12V/E37G), H-Ras(G12V/D38N) (1μg) and PLCε(H1433L) (15μg), together with the reporter construct Tac-α5. Forty-eight hours post transfection cells were harvested and assessed for integrin affinity by flow cytometry. Percentage inhibition was calculated in reference to empty vector. The results shown are the mean ± SEM of 5 independent experiments. * indicates $p<0.05$. (B) Transfected cell lysates from (A) were analyzed by western blot to determine HA-H-Ras and Flag-PLCε expression.

Figure 4.3: Sequence Of The Region Of CHO Cell DNA Surrounding A Previously Described siRNA Oligonucleotide For Rat PLCε (siRNAPLCε#3).

```
1   - G A A T G A G C A G T T T C T C T T C C G G G T T C A C T T T G A A G A T C T  mouse 03 region
1   T G G A T G A G C A G T T T C T C T T C C G G G T T C A C T T T G A A G A T C T  PCR1

40  T G T A T T T C T T C G T T T T G C A G T C G T G G A A A A C A A C A G T T C G  mouse 03 region
41  T G T A T T T C T T C G T T T T G C A G T T G T G G A G A A C A A C A G T T C G  PCR1

80  G C G A T A A C G G C T C A G A G A A T C A T T C C A C T C A G A G C T T T G A  mouse 03 region
81  G C G A T A A C G G C T C A G A G A A T C A T T C C A C T C A A A G C T T T A A  PCR1

120 A A C G A G G A T A T C G A C A T C T T C A G C T G C G G A A C C T C C A C A A  mouse 03 region
121 A G A G A G G A T A T C G G C A T C T T C A G C T G C G G A A C C T C C A C A A  PCR1

160 T G A A A T C T T G G A A A T C T C T A G C T T A T T C A T A A A C A G C A G A  mouse 03 region
161 C G A G A T C T T G G A A A T C T C T A G C T T A T T C A T A A A C A G C A G G  PCR1

200 A G G A T G G A A G A A A A C C C C T C T G G C A G T T C C A T G C C A G C C T  mouse 03 region
201 A G G A T G G A A G A T A A T C C C T C T G G C A G T A C C C G G C C A G C C T  PCR1

240 C G T T G A T G T T T A A T A C T G A A G A G A G G A A A T G T T C T C A G A C  mouse 03 region
241 C T T T G A T G T T C A A T A C T G A A G A G A G G A A A T G T T C T C A G A C  PCR1

280 T C A C A A A G T C A C A G T G C A T G G T G T C C C A G G T C C A G A G C C C  mouse 03 region
281 T C A C A A A G T C A C A G T G C A T G G T G T C C C A G G T C C A G A G C C C  PCR1

320 T T T G C T G T T T T C A C T A T A A A C G A A G G C A C C A A G G C A A A G C  mouse 03 region
321 T T T G C T G T T T T C A C A A T A A A C G A A G G C A C C A A G G C A A A G C  PCR1

360 A G C T T C T C C A A C A G G T T T T G G C A G T T G A C C A A G A C A C C A A  mouse 03 region
361 A G C T T C T C C A A C A G A T T T T G G C A G T T G A C C A G G A C A C C A A  PCR1

400 A T G T A C T G C C A C A G A C T A T T T T T T G A T G G A A G A G A A G C A T  mouse 03 region
401 A C T T A C A G C C G C A G A C T A T T T T C T G A T G G A A G A G A A G C A T  PCR1

440 T T T A T A T C T A A G G A A A A G A A T G A A T G C A G G A A A C A A C C A T  mouse 03 region
441 T T T A T A T C T A A G G A A A A G A A T G A A T G C A G G A A A C A A C C A T  PCR1

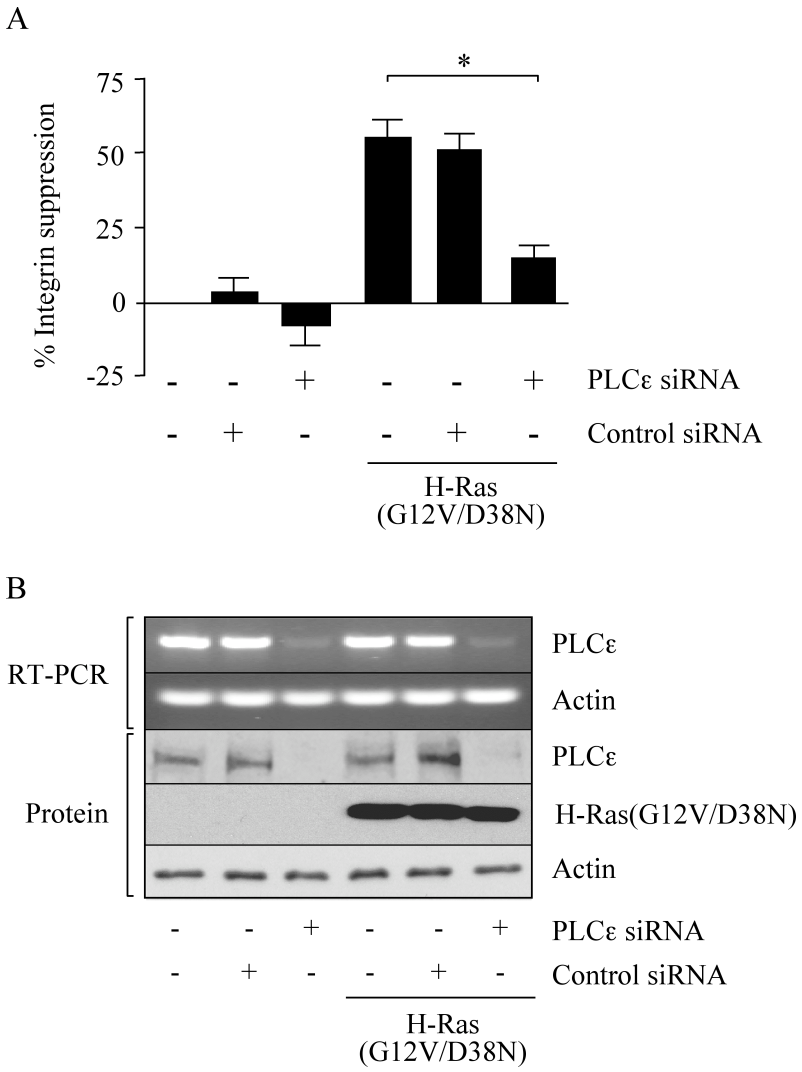
480 T C C A G A G A G C T G T G G G T C C A G A A G A A G A T A T T G T G C A G A T  mouse 03 region
481 T C C A G A G A G C T G T G G G C C C A G A G G A A G A T A T T G T G C A G A T  PCR1

520 T T T A A A C A G Y T G G T T C C C A G A A G A A G G C T A C G T A G G C A G G  mouse 03 region
521 T T T A A A C A G C T G G T T C C C A G A A G A A G G C T A C G T A G G C A G G  PCR1

560 A T T G T C T T A A A G C C C                                                 mouse 03 region
561 A T T G T C T T A A                                                         PCR1
```

Kelley *et al* previously described siRNA oligonucleotide sequences for rat PLCε (designated siRNAPLCε#3 and siRNAPLCε#5) that show considerable cross-species homology (197). The DNA sequence of CHO cell PLCε straddling these siRNA oligonucleotides, was determined using forward and reverse primers designed to consensus rat/mouse PLCε sequence as described in the materials and methods chapter. The DNA sequence data above for CHO PLCε (designated PCR1) surrounding siRNAPLCε#3 is aligned to mouse PLCε sequence (designated mouse 03 region). The shaded nucleotides differ from mouse PLCε. The siRNAPLCε#3 target site is shown as underlined. It is clear from this data that the siRNAPLCε#3 target site is 100% conserved between mouse and CHO cell DNA. This was also confirmed for siRNAPLCε#5 – see chapter 2.

Figure 4.4: Knockdown Of Endogenous PLCε Blocks H-Ras(G12V/D38N)-Mediated Integrin Suppression.



(A) CHO(αβ-py) cells were transiently transfected with either PLCε targeting siRNA or scrambled non-targeting siRNA. 24 hours later the media was replaced and cells were transfected with H-Ras(G12V/D38N) DNA or control vector (1μg), together with the reporter construct Tac-α5. Integrin affinity was assessed by flow cytometry forty-eight hours post transfection. Percentage inhibition was calculated in reference to empty vector. The results shown are the mean ± SEM of 4 independent experiments. * indicates $p<0.05$. (B) Total RNA or protein was extracted from transfected cells and expression of PLCε and actin was determined by RT-PCR and Western blot analysis respectively.

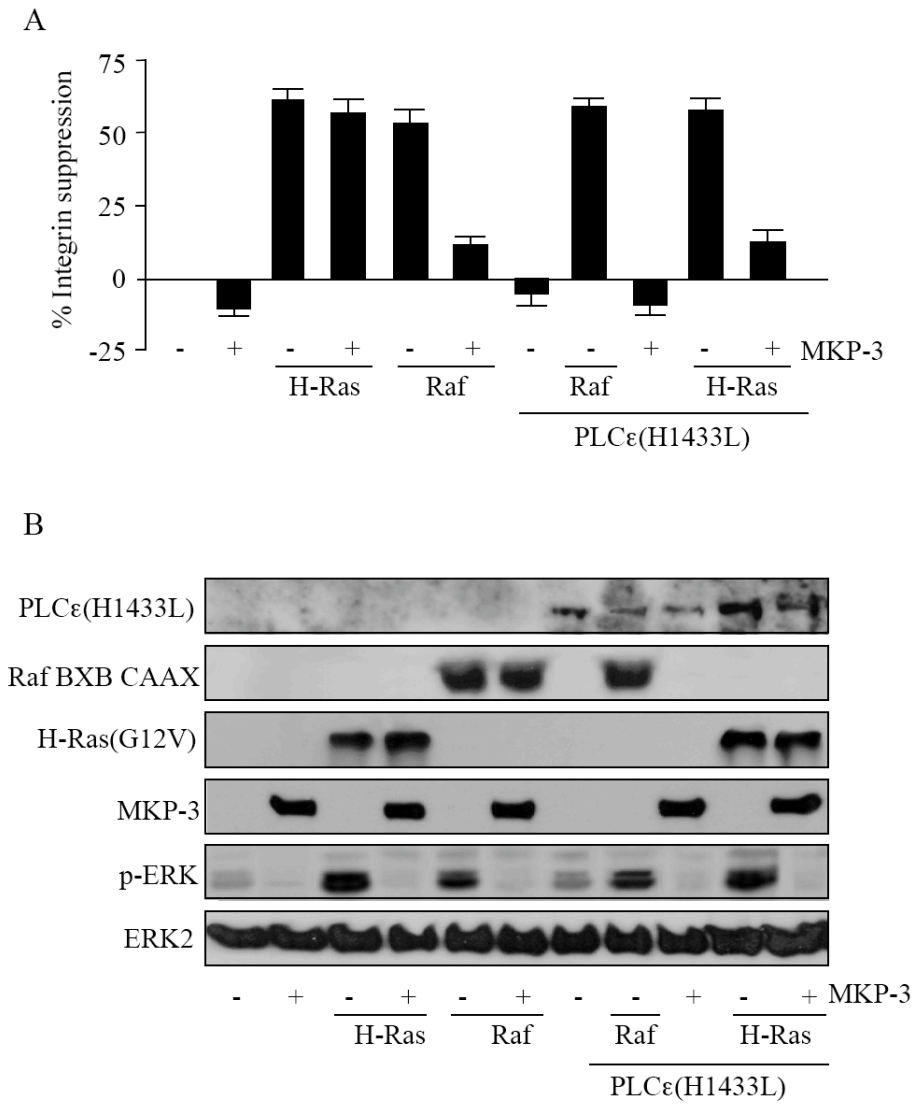
4.2.2 H-Ras Suppresses Integrin Affinity Via Independent Raf And PLCε Signalling Pathways.

Hughes *et al* (1997) previously reported that a constitutively active mutant of H-Ras (H-Ras(G12V)) suppresses integrin function via Raf (242). Raf phosphorylates and activates downstream kinases ERK1/2, which are negatively regulated by MAP kinase phosphatases (MKPs). Prior data has indicated that, although H-Ras can suppress integrin activation through Raf, MAP kinase phosphatase-3 (MKP-3) does not reverse H-Ras-mediated integrin suppression (246). Furthermore pharmacological inhibition of ERK does not reverse integrin suppression by H-Ras. This suggests a MAP kinase independent integrin suppression pathway.

To investigate this CHO(αβ-py) cells were transfected with constitutively active H-Ras (H-Ras(G12V)) or a constitutively active form of Raf (Raf BXB CAAX) and the effect of co-expression of MKP-3 on integrin affinity was determined. As expected, it was observed that MKP-3 reversed integrin suppression mediated by Raf BXB CAAX (53.2 +/- 6.0% to 11.7 +/- 3.1% $p<0.05$) (Fig. 4.5 a). However, co-transfection of MKP-3 had no significant effect on H-Ras(G12V) mediated integrin suppression (61.7 +/- 4.3% and 57.5 +/- 5.6% respectively) (Fig. 4.5 a). Importantly, co-transfection of MKP-3 blocked both Raf BXB CAAX and H-Ras(G12V) induced ERK-2 phosphorylation (Fig. 4.5 b). This data confirms the presence of a Raf independent integrin suppression pathway by H-Ras.

To determine whether PLCε activation could mediate MAP kinase-independent integrin suppression by H-Ras the effect of kinase dead PLCε (PLCε(H1433L)) on Raf BXB CAAX- and H-Ras(G12V)-mediated integrin suppression was observed. It was found that PLCε(H1433L) expression did not affect integrin suppression by either Raf BXB CAAX or H-Ras(G12V) (53.2 +/- 6.0% to 57.9 +/- 2.8% and 61.7 +/- 4.3% to 56.8 +/- 5.7% respectively) (Fig. 4.5 a). Furthermore PLCε(H1433L) had no effect on ERK1/2 phosphorylation (Fig. 4.5 b). However, co-transfection of PLCε(H1433L) with MKP-3 blocked H-Ras(G12V) mediated integrin suppression (61.7 +/- 4.3% to 12.6 +/- 4.9% $p<0.05$) (Fig. 4.5 a). These results indicate that H-Ras suppresses integrin activation via independent Raf and PLCε pathways, and that either pathway is sufficient to modulate H-Ras mediated integrin suppression.

Figure 4.5: H-Ras Suppresses Integrin Affinity Via Independent Raf And PLCε Signalling Pathways.



(A) CHO(αβ-py) cells were transiently transfected with either control vector, H-Ras(G12V), Raf BXB CAAX, PLCε(H1433L), or MKP-3 as indicated together with the reporter construct Tac-α5. Forty-eight hours post transfection; cells were harvested and assessed for integrin affinity by flow cytometry. Integrin suppression was determined as described in materials and methods. The results shown are the mean ± SEM of three independent experiments. * indicates $p<0.05$. (B) In parallel, lysates of transfected cells were probed to determine H-Ras, Raf, PLCε, MKP-3 and ERK2 expression, and ERK1/2 phosphorylation. Representative Western blots are shown.

4.2.3 Modulating Rap1A Activity Does Not Affect Integrin Suppression.

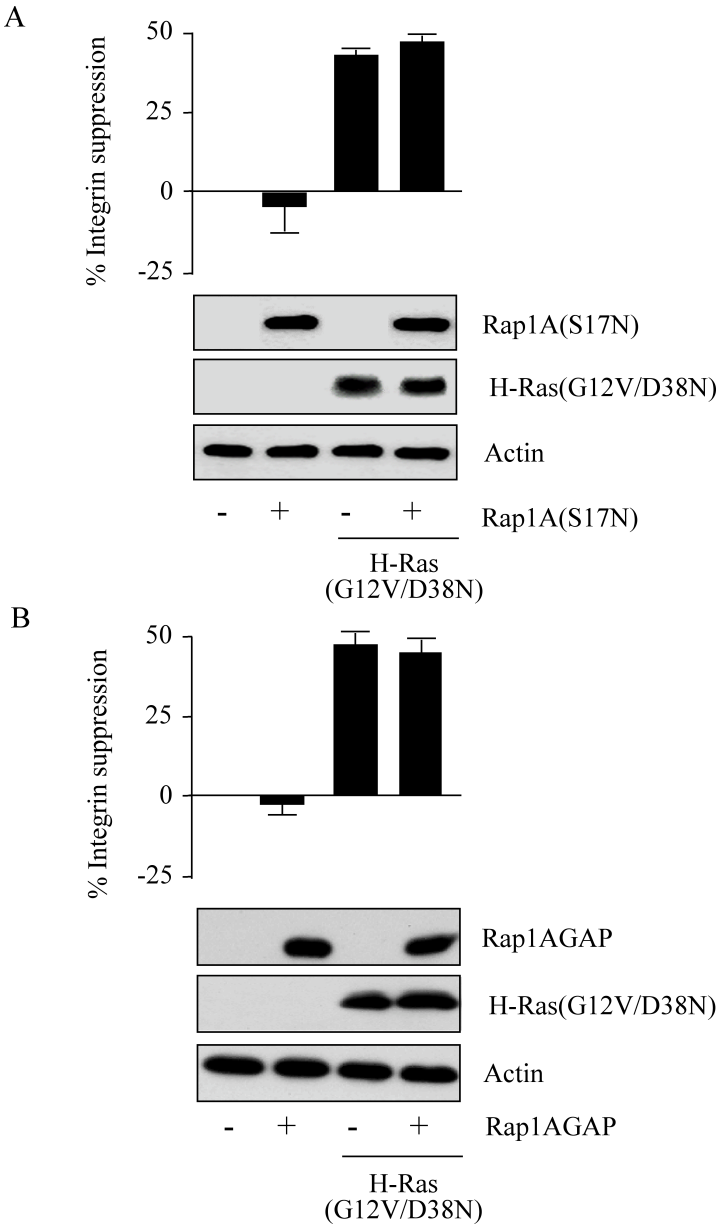
PLCε contains a CDC25 homology domain that has been shown to display guanine-nucleotide exchange activity towards Rap1 (264). Prior studies have indicated a role for Rap1 in integrin mediated cell adhesion (265) and therefore the role of Rap1 in integrin suppression by H-Ras(G12V/D38N) was examined. Initially, a dominant negative mutant of Rap1A, which has the amino acid substitution S17N and restricts the protein to the GDP-bound state, was used (266). As previously demonstrated, it was observed that H-Ras(G12V/D38N) suppressed integrin activation in CHO(αβ-py) cells (Fig. 4.6 a). However, expression of dominant negative Rap1A(S17N) did not modulate integrin affinity in CHO(αβ-py) cells (Fig. 4.6 a). Furthermore, co-transfection of Rap1(S17N) did not affect the ability of H-Ras(G12V/D38N) to suppress integrins (42.9 ± 1.6% and 47.0 ± 0.3% respectively) (Fig. 4.6 a). This data suggests that H-Ras(G12V/D38N)-mediated suppression of integrins does not occur through Rap1A dependent pathways. To confirm this, a truncated Rap1GAP construct (residues 75-415) was used. This has previously been shown to down-regulate Rap1 activity by catalyzing GTP hydrolysis (267). In support of the previous data it was observed that transient expression of Rap1GAP had no significant effect on integrin affinity (Fig. 4.6 b). In addition, co-transfection with H-Ras(G12V/D38N) did not affect integrin suppression in CHO(αβ-py) cells (Fig. 4.6 b). These results strongly suggest that Rap1 signalling is not required for H-Ras mediated integrin suppression through PLCε.

4.2.4 PLCε Contributes To H-Ras Mediated Reduction In Cellular Adhesion.

Modulation of integrin affinity is a central process in the control of cellular adhesion to ECM (268). To investigate whether PLCε participates in H-Ras-mediated reduction in cellular adhesion, Yatish Lad assessed adhesion of CHO(αβ-py) cells to von Willebrand Factor (vWF), a ligand for the chimeric αIIb α6 β3 β1 integrin present in this stable cell line. Transient transfection of H-Ras(G12V/D38N) produced a significant reduction in cell adhesion (46 ± 10% $p<0.01$) (Fig. 4.7). Co-expression of H-Ras(G12V/D38N) with PLCε(H1433L) significantly blocked this reduction in adhesion to vWF back to control cell levels of adhesion (120 ± 20% $p< 0.05$). This effect was not due to a reduction in expression of H-Ras(G12V/D38N)

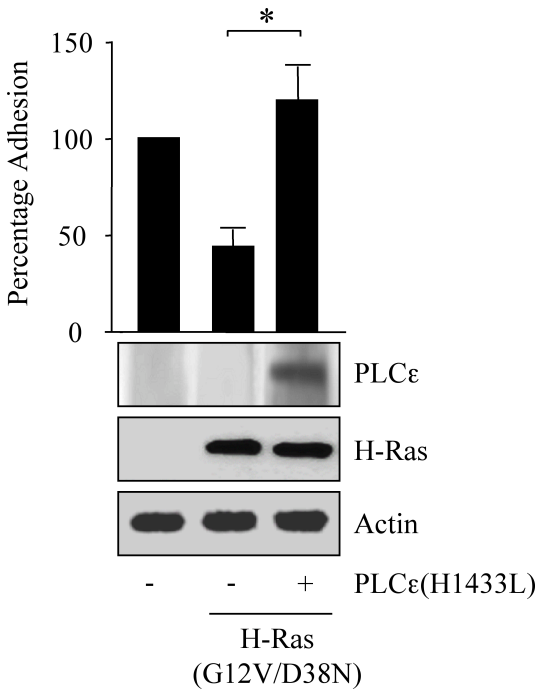
(Fig. 4.7). Reversing H-Ras(G12V/D38N) mediated integrin suppression by co-expression of PLCε(H1433L) therefore restores the cells' ability to adhere to vWF.

Figure 4.6: Rap1A Does Not Mediate H-Ras(G12V/D38N)-Induced Integrin Suppression.



(A) CHO(αβ-py) cells were co-transfected with H-Ras(G12V/D38N) (1μg) and dominant negative (S17N) Rap1A (1μg). 48 hours later integrin affinity was assessed by flow cytometry. Percentage inhibition was calculated in reference to empty vector (mean ± SEM of three independent experiments). Expression of Rap1A, H-Ras(G12V/D38N) and actin in parallel samples is shown by Western blot. (B) CHO(αβ-py) cells were co-transfected with H-Ras(G12V/D38N) (1μg) and Rap1GAP (1μg). 48 hours post later integrin affinity was assessed. Percentage inhibition was calculated in reference to empty vector (mean ± SEM of three independent experiments). Expression of Rap1GAP, H-Ras(G12V/D38N) and actin in parallel samples is shown by Western blot.

Figure 4.7: PLCε Modulates H-Ras(G12V/D38N) Suppression Of CHO(αβ-py) Cell Adhesion To Von Willebrand Factor.



CHO(αβ-py) cells were transfected with GFP (2μg) and H-Ras(G12V/D38N) ± PLCε(H1433L) (1μg ± 15μg). 48 hours later cells were allowed to adhere to vWF. Cell adhesion was quantified on a fluorescence plate reader. Adhesion was represented as percentage change in adhesion (mean ± SEM of 4 independent experiments). *indicates $p<0.05$. Expression of PLCε(H1433L), H-Ras(G12V/D38N) and actin in parallel samples is shown by Western blot.

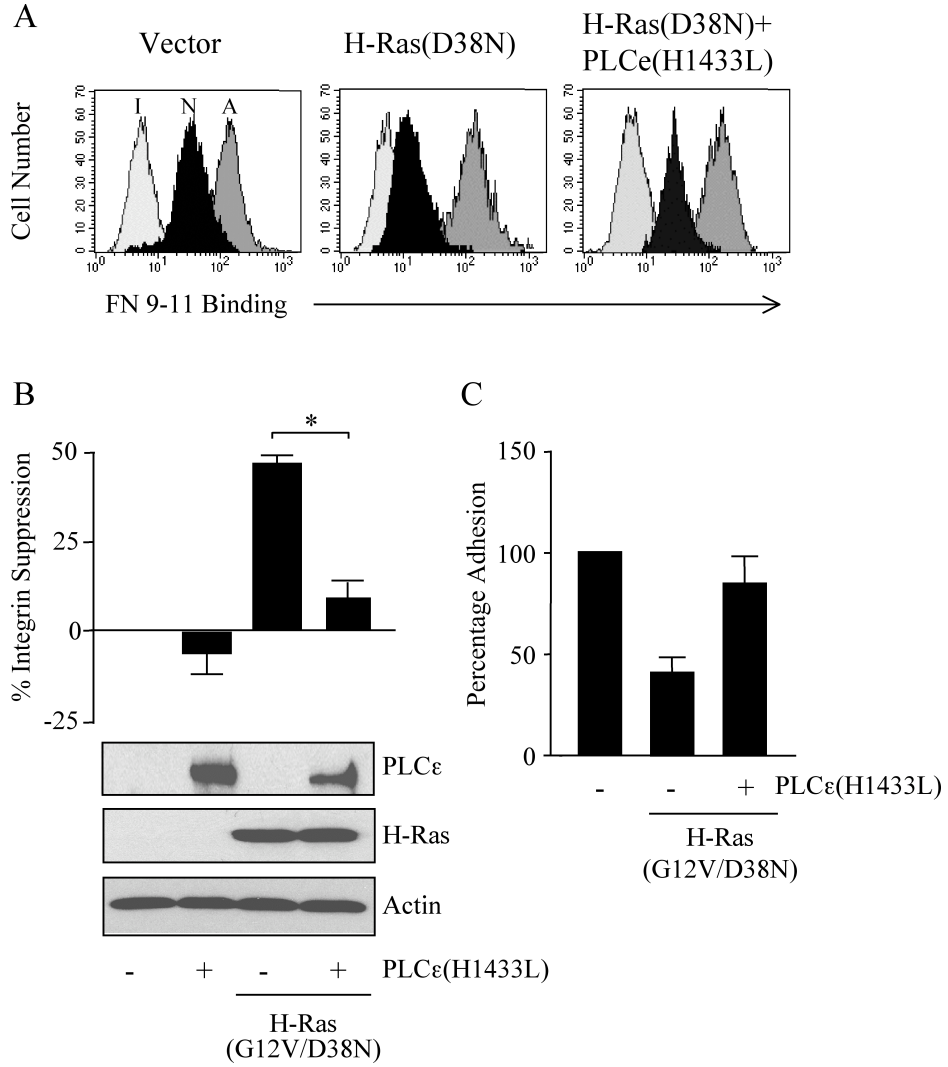
This data indicates that PLCε can contribute to H-Ras-mediated suppression of cellular adhesion. However the chimeric integrin expressed in CHO(αβ-py) cells is relatively active in the resting state and its affinity is modulated by a different (β1 integrin) intracellular domain than ligand binding domain (242). Thus the CHO(αβ-py) cell is not truly indicative of native integrins. Therefore, to confirm Yatish Lad's data the role of PLCε in the suppression of endogenous integrins was investigated.

It has been shown previously that a soluble fragment of fibronectin, composed of the 9, 10 and 11 type III repeats (designated FN9-11), can bind to endogenous α5 β1 integrins (245). Furthermore, cell surface fibronectin binding can be suppressed by activated Raf-1 signalling in CHO-K1 cells (242). Thus FN9-11 binding, determined by flow cytometry as described in chapter 2, was used to investigate the effect of transfection of H-Ras(G12V/D38N) with or without PLCε(H1433L) on endogenous

β1 integrins affinity in CHO KI cells. It was found that transfection of H-Ras(G12V/D38N) significantly suppressed FN9-11 binding and that this was blocked by co-transfection of dominant negative PLCε(H1433L) (46.2 ± 1.9% to 13.5 ± 2.1 % respectively) (Fig. 4.8 a and b). Importantly, Mn^{2+} activated and EDTA suppressed FN9-11 binding similarly in CHO-K1 cells regardless of the DNA transfected, indicating that changes in FN9-11 binding were not due to changes in integrin expression.

Fibronectin acts as a natural ligand for α5 β1 integrins and can be coated to tissue culture plastic. To confirm the data with FN9-11 fragment CHO-K1 cells transfected with H-Ras(G12V/D38N) with or without PLCε(H1433L) were allowed to adhere to fibronectin-coated plastic. The percentage of adherent cells was determined as described in materials and methods. It was observed that H-Ras(G12V/D38N) reduced CHO-K1 cell adhesion. Furthermore H-Ras(G12V/D38N) suppression of adhesion to fibronectin was blocked by co-transfection of PLCε(H1433L) (Fig. 4.8 c). Taken together this data indicates that PLCε modulates H-Ras suppression of endogenous α5 β1 integrin binding to fibronectin.

Figure 4.8. PLCε Modulates H-Ras(G12V/D38N)-Mediated Reduction In Cellular Adhesion.



(A) CHO-K1 cells were transfected with H-Ras(G12V/D38N) ± PLCε(H1433L) (1μg ± 15μg), together with the reporter construct Tac-α5. 48 hours later cells binding of soluble fibronectin fragment (FN9-11) was assessed by flow cytometry. Representative histogram overlays are shown of FN9-11 binding to highly transfected cells with internal controls of EDTA (I) and Mn^{2+} (A). (B) CHO-K1 cells were transfected with H-Ras(G12V/D38N) ± PLCε(H1433L) (1μg ± 15μg), together with the reporter construct Tac-α5 and FN 9-11 binding was assessed by flow cytometry as described. Mean percentage integrin suppression ± SEM from 3 independent experiments. * indicates $p<0.05$. Expression of PLCε(H1433L), H-Ras(G12V/D38N) and actin in parallel samples is shown by Western blot. (C) CHO-K1 cells were transfected with H-Ras(G12V/D38N) ± PLCε(H1433L) (1μg ± 15μg) and allowed to adhere to fibronectin coated plastic. Cell adhesion was quantified as described. Adhesion was normalized against control cells and represented as percentage change in adhesion. The results shown are the mean ± SEM of 3 independent experiments. * indicates $p<0.05$.

4.3 Discussion.

The data presented in this chapter demonstrates, for the first time, that PLCε, a novel H-Ras effector, suppresses integrin affinity. The constitutively active mutant of H-Ras suppresses integrins via two separate effector pathways, a Raf-dependent pathway and a Raf-independent pathway activated by H-Ras(G12V/E37G) and H-Ras(G12V/D38N) (Fig. 4.9). The data shown here indicates that the Raf-independent mechanism of integrin suppression utilizes PLCε. The suppression of integrins via PLCε also reduces cell adhesion to a vWF-coated surface and to the extracellular matrix component fibronectin. These results thus identify a new physiological function for PLCε.

Figure 4.9: Schematic Of Raf-Dependent And Raf-Independent Signalling Pathways Of Integrin Suppression.

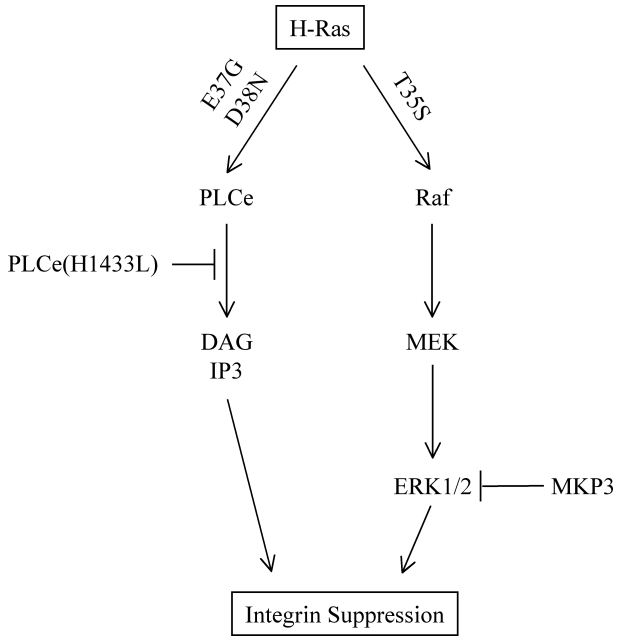


Diagram representing H-Ras signalling leading to integrin suppression. Prior data indicates that the H-Ras(T35S) effector mutant stimulates a Raf-dependent pathway. The results represented in this chapter show that the H-Ras(E37G) and H-Ras(D38N) mutants stimulate a Raf-independent pathway via PLCε.

Hughes *et al* (1997) have previously shown that both H-Ras(G12V) and activated Raf can suppress the binding of the αIIb β3 ligand mimetic antibody PAC1 to the stably expressed chimeric integrin αIIb α6A β3 β1 in CHO cells (242). FITC labeled fibronectin binding to endogenous α5 β1 on CHO cells was also suppressed by H-Ras(G12V) expression indicating that inside-out signalling can act upon a native integrin and be detected by a physiological integrin ligand (242). H-Ras(G12V/T35S) is a well-established activator of the Raf effector arm of H-Ras signalling and can mimic many of the putative effects of H-Ras, including integrin suppression through the activation of the ERK1/2 signalling cascade (247,269). However, the requirement of ERK1/2 activation for integrin affinity suppression is still unclear. Integrin suppression occurs in the absence of bulk ERK1/2 activation and is not reversed by co-expression of MKP-3 (Fig. 4.5). Targeting ERK1 to the plasma membrane with the CAAX box of H-Ras leads to integrin suppression, suggesting that localized ERK1/2 activity can allow integrin suppression in the absence of bulk ERK activation (246). The MEK inhibitor UO126 fails to inhibit both H-Ras(G12V) and activated Raf mediated integrin suppression; whether ERK1-CAAX activation at the plasma membrane is sensitive to MEK inhibition remains to be tested. The ability of H-Ras(G12V) to suppress integrins via PLCε in a Raf-independent manner provides a mechanism to resolve the conflicting data relating to the need for ERK1/2 activation. This alternative H-Ras pathway can compensate for and maintain integrin suppression in the presence of either MEK inhibitors or MKP-3 co-expression.

PLCε has previously been identified as an H-Ras effector (253-255). Kelley *et al*. (2001) showed that PLCε activity was stimulated by the constitutively active H-Ras(Q61L) mutant (253). PLCε activity was also stimulated by the effector mutant H-Ras(Q61L/E37G), implying that the H-Ras(E37G) mutant may not solely be an activator of Ral-GEFs. In contrast, the H-Ras effector mutants T35S or Y40C failed to significantly increase PLCε activity compared to control (253). However, the H-Ras(Q61L/D38N) mutant increased inositol production by 50-60%, implicating this mutant as an activator of PLCε along with E37G (253). The D38N mutation within the H-Ras effector domain is known to abrogate Raf binding and activation *in vitro* and displays minimal transformation potency in NIH/3T3 cells (270). Therefore the

ability of H-Ras(G12V/D38N) to selectively activate PLCε allowed specific examination of this pathway in isolation of other effectors, namely Raf, Ral-GEFs and PI3K.

The data represented in this chapter shows that H-Ras(G12V/D38N) induces a similar level of integrin suppression to that of H-Ras(G12V/E37G) (Fig. 4.2), indicating that the PLCε effector pathway can suppress integrin affinity. Unfortunately no constitutively active mutant of PLCε is available to test whether over expression of active PLCε could activate integrin affinity. Furthermore, whilst physiological agonists of PLCε have been described, others have previously demonstrated that detection of integrin suppression requires sustained, rather than transient, activation of H-Ras (197,243-245,271). However, the ability of kinase dead PLCε(H1433L) and knock-down of endogenous PLCε to block H-Ras(G12V/D38N) mediated integrin suppression (Fig. 4.2 and 4.4) provides good evidence that PLCε catalytic signalling modulates integrin affinity. The demonstration that PLCε(H1433L) does not affect H-Ras(G12V) ERK phosphorylation or integrin suppression (Fig. 4.5) even at high ratios (15:1) suggests that this dominant negative mutant is not acting through sequestration of H-Ras. Furthermore, the demonstration in Figure 4.5 that co-expression of both PLCε(H1433L) and MKP-3 are needed to reverse integrin suppression caused by H-Ras(G12V) is important. It shows that blocking either effector pathway individually is insufficient to fully prevent integrin suppression, and provides strong evidence for two independent pathways of H-Ras mediated integrin suppression.

Talin, a large actin-binding protein and a component of focal adhesions, links the cytoskeleton with integrin β tails (272). It plays a crucial role in focal adhesion assembly and in integrin-mediated signalling recruiting focal adhesion kinase (FAK) (273). Talin is a member of the FERM-containing domain protein family - this 30-kDa domain is a cysteine-rich basic charged motif, which has been reported to bind phosphoinositides and to target proteins to the plasma membrane (274,275). The talin head domain interacts with integrins through binding to the cytoplasmic β integrin tail (276). This interaction has been shown to be sufficient for integrin activation (277). Talin binding to integrins is regulated by phosphoinositides, which

may stabilize the activated conformational state (278,279). Thus, lipid metabolism by PLCε activity at the cell membrane may play a major role in the sequential assembly of focal adhesions and modulate integrin affinity by regulating talin binding to β integrin tails and other focal adhesion proteins.

The Ras family of small GTPases are the commonest mutated oncogene in human cancer, and these mutations will be particularly relevant in integrin suppression in cancer cells. Both H-Ras and Raf play an important role in cellular transformation and have been implicated in human tumorigenesis (280). H-Ras has been shown to be an up-stream effector of PLCε and binds to the RA domain leading to PLCε activation (253). PLCε has been demonstrated to play a role in tumorigenesis, though its precise function remains controversial. PLCε expression in PDGF stimulated BaF3 cells has been shown to enhance cell proliferation rates and inhibit apoptosis (264). However, colorectal cancer cells show a reduction in expression of PLCε, and restoring PLCε expression in these tumor lines inhibited tumor cell viability and proliferation (281). In a chemical induced skin tumor model, PLCε$^{-/-}$ mice displayed a reduction in the number of squamous tumors and conversion of papillomas into carcinomas failed to occur in these mice (282). PLCε may therefore provide the link between integrin activation state, which regulates proliferation and survival, and the conversion of papilloma to carcinoma associated with anchorage independence and down regulation of integrin function. The novel function of PLCε to modulate integrin affinity allows the H-Ras integrin suppression pathway to occur in a Raf/ERK-independent manner. Ras activation is a focal point for growth factor signalling and is associated with cell cycle control and proliferation (283). Activation of ERK1/2 via Raf is central to the control of cyclins and cyclin dependent kinases (284). H-Ras mediated integrin suppression via the PLCε pathway could therefore avoid inappropriate signalling to the cell cycle machinery.

In summary, this chapter demonstrates a novel and physiologically relevant function of PLCε in suppressing integrin affinity modulation and indicates a new, Raf-independent, H-Ras effector pathway with important implications for understanding H-Ras and integrin function particularly in cancer.

CHAPTER 5: Notch Signalling Activates β1 Integrins Via The Small GTPase R-Ras and Protects SCLC Cells From Chemotherapy-Induced Apoptosis.

5.1 Introduction.

The diverse biological processes intrinsic to the development of multi-cellular organisms are co-ordinated by communication between adjacent cells involving a small number of evolutionarily conserved signalling pathways. The Notch signalling pathway is an important mechanism for mediating these intercellular signalling events to direct cell fate decision (285). The components of the Notch pathway have been identified in a broad range of metazoans and have been extensively studied in insects, nematodes and mammals (286-288). Consequently, Notch has been shown to be a key regulator of many developmental processes including somitogenesis, vasculogenesis and neurogenesis (288-290). In addition, the Notch pathway plays a critical role in mammalian immune development and carcinogenesis (291,292).

The molecular components of the Notch pathway have been extensively studied and are highly conserved between species. Notch encodes a single-pass heterodimeric transmembrane receptor with an extracellular domain that contains epidermal growth factor (EGF)-like repeats (293). Four Notch receptors (Notch-1-4) and two groups of ligands (Delta-like (DLL -1, -3 and -4) and Serrate-like (Jagged 1, 2)) have been identified in mammals (294,295). Notch-ligand interaction triggers two distinct proteolytic cleavage events (S2 and S3) that release the intracellular portion of Notch (NIC) from the plasma membrane (193,296,297). NIC translocates to the nucleus where it binds to a transcriptional regulator CSL (CBF-1/Su(H)/LAG-1), displacing co-repressors and recruiting co-activators, thus inducing expression of Hairy-Enhancer of Split (HES) and HES-related (HERP) genes (298-301). Data from several groups suggest that Notch may also signal without cleavage at S3 or CSL-dependent transcription (302-304). The molecular components of this "non-classical" Notch signalling pathway are not yet fully understood.

Recent genetic studies have indicated important parallels between the developmental processes controlled by Notch and integrin-mediated adhesion. Integrins mediate cell-cell and cell-matrix interactions and have been identified in insects, nematodes and vertebrates (268). They are essential for embryogenesis and are involved in

neurogenesis, myogenesis and angiogenesis, processes also controlled by Notch (305-307). α6 β1 and α5 β1 integrins are highly expressed on stem cells and regulate survival, migration and differentiation (308,309). Notch has been shown to associate with β1 integrins in neural stem cells and expression of Notch 4 in endothelial cells increases adhesion to collagen, regulating angiogenesis (310,311). Additionally, data from Zebrafish somitogenesis suggests that mutations in the Notch pathway and integrin α5 subunit can produce a complementary disruption in somite formation (312). This suggests the possibility that Notch may affect integrin activation, modulating important developmental processes by altering cell-matrix interactions (313).

Data published over the past decade has indicated an important role for Notch signalling in pulmonary neuroendocrine differentiation. SCLC cells display a neuroendocrine phenotype, which is associated with expression of the basic helix-loop-helix transcription factor human achaete-scute homologue-1 (hASH-1) (314). Constitutive activation of Notch signalling in SCLC cells has been shown to reduce hASH-1 expression and increase cellular adherence (314). This phenotype is similar to NSCLC cell lines, which are inherently resistant to chemotherapy (314). The data presented in chapter 3 of this thesis indicates a key role for SCLC adhesion to ECM via β1 integrins in resistance to apoptosis induced by chemotherapy and radiotherapy. This prompted the hypothesis that Notch signalling could increase integrin affinity and promote chemo-resistance in SCLC cells therefore representing a potential anti-cancer target. This was investigated using the *in vitro* assays described in chapters 3 and 4.

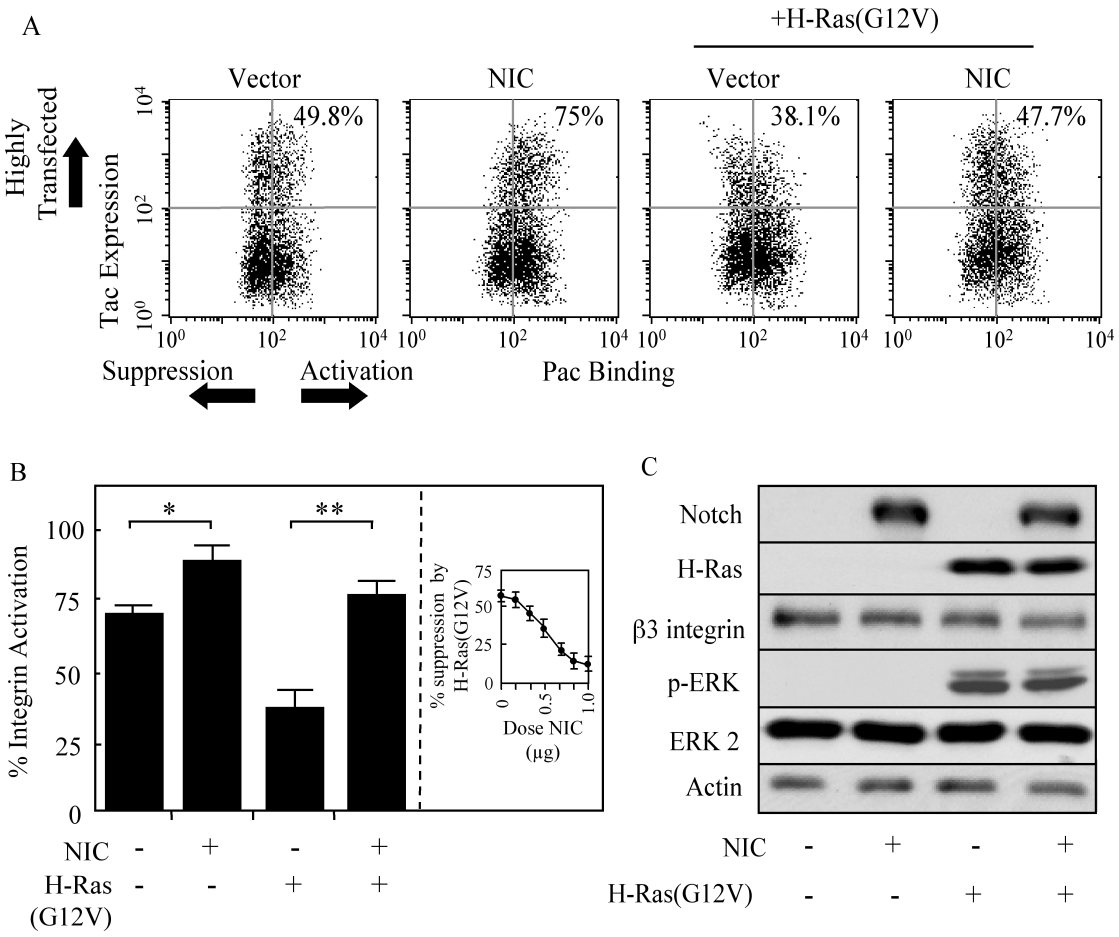
5.2 Results.

5.2.1 Notch-1 Activates Integrins And Reverses H-Ras/Raf-Mediated Integrin Suppression.

Initial experiments sought to investigate whether Notch signalling could modulate integrin activation. The well-established model of integrin affinity described in chapter 4 was used (242). In brief, test DNA was transfected into CHO(αβ-py) cells, which stably expresses a chimeric integrin (αIIb α6 β3 β1). This has the ligand binding properties of αIIb β3 but is activated through the α6 β1 cytoplasmic domains. A cell surface marker encoding the extracellular domain of the IL-2 receptor, termed Tac, and the intracellular domain of the α5 integrin (Tac-α5) was used as a marker for DNA transfection. The activation status of the chimeric integrin on highly transfected cells was assessed using flow cytometric analysis of cell surface binding of a monoclonal antibody specific for the active confirmation of αIIb β3 (PAC-1). For each DNA transfection PAC1 binding under 'native' conditions was compared to those in the presence of EDTA (maximally inhibited integrins) or manganese (maximally activated integrins) allowing calculation of an integrin activation or suppression index as described in chapter 2.

It has been shown previously that the intracellular domain of mouse Notch-1 (designated NIC hereafter) can constitutively activate the Notch signalling pathway (193). Therefore to investigate the effect of activated Notch signalling on integrin affinity, NIC was transfected into CHO(αβ-py) cells. It was found that after 48 hours, transfection of NIC increased integrin activation in CHO(αβ-py) cells compared to vector control. This was demonstrated by a rightward shift in PAC-1 binding in highly transfected cells (vector 49.8%, NIC 75% cells in right upper quadrant) (Fig. 5.1 a). There was no change in PAC-1 binding in the untransfected cells. Correspondingly, NIC expression increased integrin activation index (88.4 +/- 5.7%) compared to expression of vector alone (67.3 +/- 2.2%) (Fig. 5.1 b).

Figure 5.1: Notch-1 Activates Integrins And Reverses H-Ras-Mediated Suppression Of Integrin Affinity.



CHO(αβ-py) cells were transfected with Tac-α5 (0.75μg), intracellular Notch-1 (NIC) (1μg) and H-Ras(G12V) (0.375μg) as indicated. (A) Integrin affinity was analysed by flow cytometry. Representative dot blots (n=7 experiments) show PAC1-FITC binding (integrin activation status) on the x-axis and Tac-R-PE antibody binding (transfection efficiency) on the y-axis. The quadrant markers differentiate on the x-axis, cells with high and low integrin affinity status and on the y-axis, highly transfected cells (upper quadrants) and cells transfected to a lesser extent (lower quadrants). The number in the right upper quadrant of each dot blot represents the percentage of highly transfected cells present in that quadrant (i.e. cells with high integrin affinity). H-Ras(G12V) induced a left shift in PAC1 binding in transfected cells indicating integrin suppression. Co-transfection of NIC increased PAC1 binding and reversed the left shift, indicating integrin activation. (B) Mean percentage integrin activation +/- SEM is shown. Inset: Dose-dependent effect of NIC on H-Ras(G12V)-mediated integrin suppression. *($p<0.05$), **($p<0.01$). (C) Representative Western blot of Notch, H-Ras, β3 integrin, ERK2, phospho-ERK and β actin expression.

The chimeric integrin in CHO(αβ-py) cells is relatively activated in the resting state (242). Therefore, it was desirable to suppress integrin affinity and determine whether Notch signalling would reverse integrin suppression. Prior published data and that presented in chapter 4 indicates that the small GTP-binding protein H-Ras can suppress integrin activation (242). Therefore NIC was co-transfected with a constitutively active mutant of H-Ras (H-Ras(G12V)) into CHO(αβ-py) cells and the effect on integrin affinity determined. It was found that transfection of H-Ras(G12V) alone caused marked inhibition of PAC1 binding; however co-transfection with NIC completely reversed suppression of integrin activation (Fig. 5.1 a and b). This effect were not produced by alterations in H-Ras(G12V) or NIC expression when the constructs were co-transfected, nor was expression of the chimeric integrin in the CHO(αβ-py) cells affected (Fig. 5.1c).

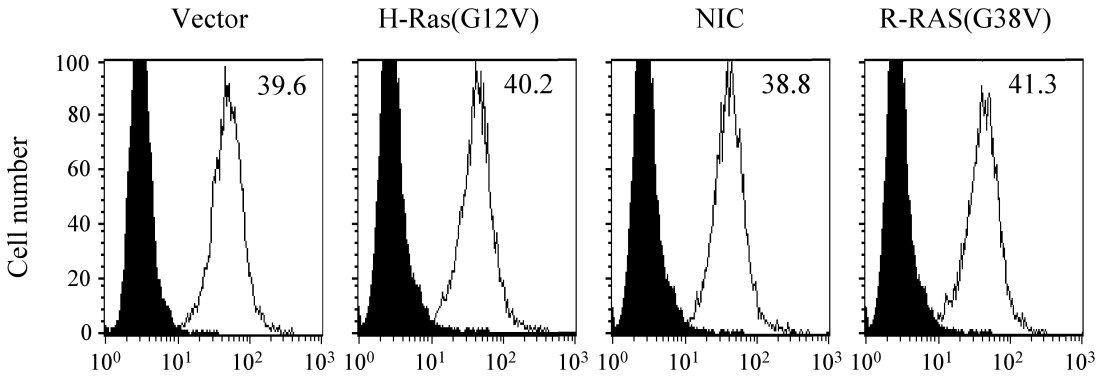
Hughes *et al* (1997) have previously shown that H-Ras-mediated suppression of the chimeric integrin in CHO(αβ-py) cells was not a consequence of a decrease in integrin expression levels (242). Notch activates transcription in the classical signalling pathway and therefore could alter integrin expression in CHO(αβ-py) cells. To confirm that Notch-1 expression did not alter surface integrin expression, flow cytometry was used to detect surface expression of β3 integrins. Using an anti-β3 integrin antibody whose binding was not dependent on integrin activation status it was found that neither H-Ras(G12V), NIC nor R-Ras(G38V) expression altered surface expression of β3 integrins in CHO(αβ-py) cells (Fig. 5.2). Thus changes in PAC1 binding are due to alterations in integrin activation not expression.

H-Ras suppresses integrin activation in part via its downstream effector kinase Raf-1 (242). Therefore the ability of active Notch-1 to reverse integrin suppression by an activated membrane-targeted variant of Raf, Raf-CAAX was tested. Similar results were observed to those found with H-Ras(G12V) (Fig. 5.3 a - c). Thus NIC reversed the suppressive effect of activated H-Ras or Raf-1 on integrin affinity, suggesting that Notch-1 signalling can over-ride integrin inactivation caused by the H-Ras-dependent suppression pathway.

Previous work has suggested that suppression of integrin activation by H-Ras and Raf-1 is dependent upon ERK1/2 function but does not correlate with bulk

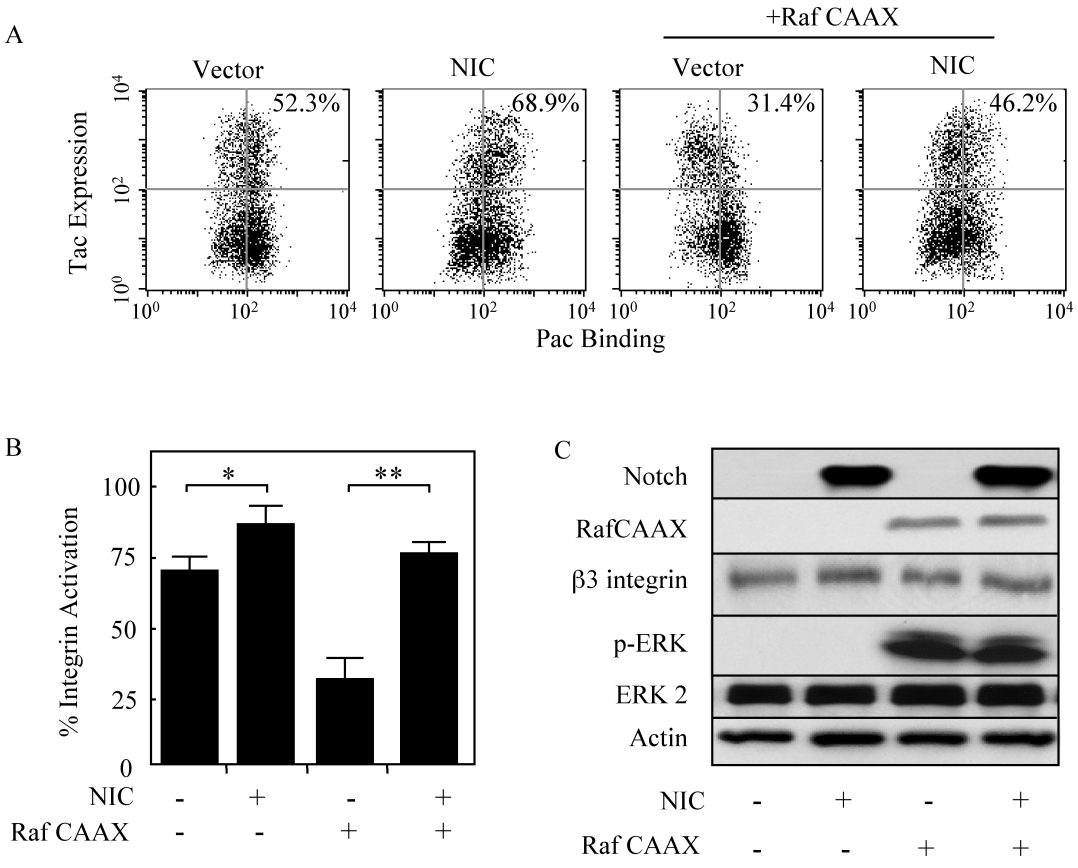
phosphorylation of ERK (244). However, reversal of integrin suppression by the small death effector domain-containing protein PEA-15 depends upon its capacity to bind ERK1/2 (246,315). Notch signalling has previously been shown to have differing effects on ERK phosphorylation depending upon cellular context (314,316). Therefore, it was investigated whether Notch signalling could reverse suppression of integrin activation by H-Ras through effects on ERK1/2. It was found that transfection with NIC alone did not affect ERK phosphorylation. Furthermore NIC did not affect phosphorylation of ERK induced by H-Ras(G12V) or Raf-CAAX (Fig. 5.1 c and 5.3c). This suggests that the mechanism of Notch-1 activation of integrins is distinct from effects on the Ras/Raf pathway.

Figure 5.2: Notch does not alter β3 integrin expression.



CHO(αβ-py) cells were transfected with Tac-a5 (0.75μg) and either vector, intracellular Notch-1 (NIC) (1μg) or H-Ras(G12V) (0.375μg) as indicated. As a positive control cells were transfected with R-Ras(G38V) (0.5μg), which has previously been shown to activate integrins in the CHO(αβ-py) assay. Surface expression of β3 integrins was determined by flow cytometry using an anti-β3 integrin antibody and a FITC labelled secondary. Representative overlay histograms of anti-β3 integrin (white) or isotype control (black) antibody binding to highly transfected cells are shown. The number in the right upper corner of each histogram represents the geometric mean fluorescence intensity for anti-β3 integrin antibody binding.

Figure 5.3: Notch Reverses Raf-Mediated Suppression Of Integrin Affinity.



CHO(αβ-py) cells were transfected with Tac-α5 (0.75μg), NIC (1 μg) and Raf-CAAX (0.5 μg) as indicated. (A) Representative dot blots (n=5 independent experiments) of Tac –RPE (y-axis) and PAC1-FITC (x-axis) binding are shown for each transfection condition. The numbers in the right upper quadrant represent the percentage of highly transfected cells with high integrin affinity. (B) Mean percentage integrin activation +/-SEM from n=5 experiments. (C) Representative Western blot analysis of NIC, Raf-CAAX, β3 integrin, ERK2, phospho-ERK and β-actin expression. Statistically significant differences between results are indicated by * ($p<0.05$) or ** ($p<0.01$).

5.2.2 Activation Of β1 Integrins By Notch-1 Requires Intramembrane Cleavage (S3) To Release The Intracellular Domain.

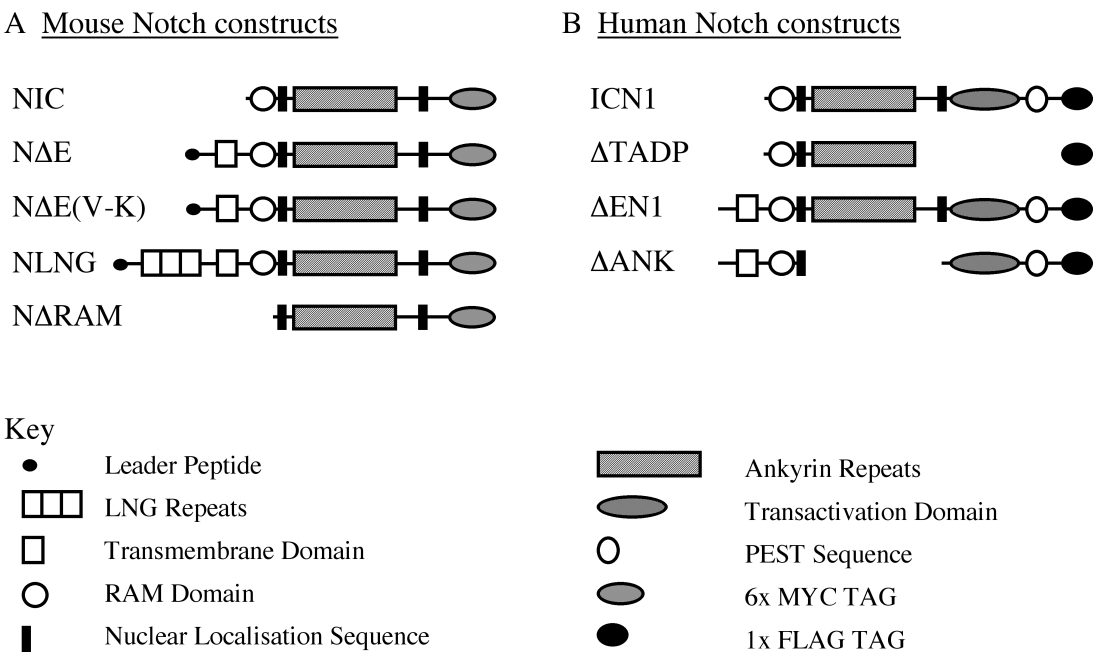
Classically, Notch activation requires ligand-induced cleavage of the Notch receptor approximately 12 amino acids N-terminal to the transmembrane domain (S2), which allows intramembrane cleavage (S3) by the protease complex termed γ-secretase (193,297,317). However, analysis of the role of Notch in patterning of the *Drosophila* embryo dorsal epidermis suggests that Notch may signal without membrane cleavage (318). It was therefore determined whether activation of β1 integrins by Notch was dependent on intra-membrane cleavage. Mutants of mouse Notch-1 that are membrane bound and show differing efficiencies of processing by γ-secretase were used (193). The structure of these mutants are summarised in Figure 5.4. These experiments sought to assess Notch-1 rescue of H-Ras(G12V)-induced integrin suppression and thus for simplicity, subsequent CHO(αβ-py) assays are represented as percentage integrin suppression.

The Notch-1 mutant NΔE consists of the transmembrane and intracellular domains of mouse Notch-1 with a short extracellular segment and is cleaved by the γ-secretase complex to yield active intracellular Notch (193). Transfection of CHO(αβ-py) cells with NΔE yielded a fragment of similar molecular weight to NIC and reversed H-Ras-mediated integrin suppression without affecting H-Ras expression or ERK1/2 activation (Fig. 5.5 a and b). The effect on integrin activity was less pronounced than observed with NIC, presumably as a result of a lower yield of intracellular Notch from NΔE (Fig. 5.5 a). To investigate this observation, two Notch mutants were used which are inefficiently processed by γ-secretase and do not yield detectable levels of intracellular Notch; an NΔE variant with a point mutation at amino acid 1774, NΔE(V1774K); and NLNG which has identical transmembrane/intracellular domains to NΔE but an extracellular domain containing LNG repeats. Transfection of CHO(αβ-py) cells with NΔE(V1774K) or NLNG did not yield detectable intracellular Notch and did not significantly reverse H-Ras suppression of integrins (Fig. 5.5 a). Furthermore, treatment of CHO(αβ-py) cells with the γ-secretase inhibitor MW167 blocked the processing of NΔE to intracellular Notch and

prevented integrin activation without altering H-Ras(G12V) expression or ERK1/2 phosphorylation (Fig. 5.5 b).

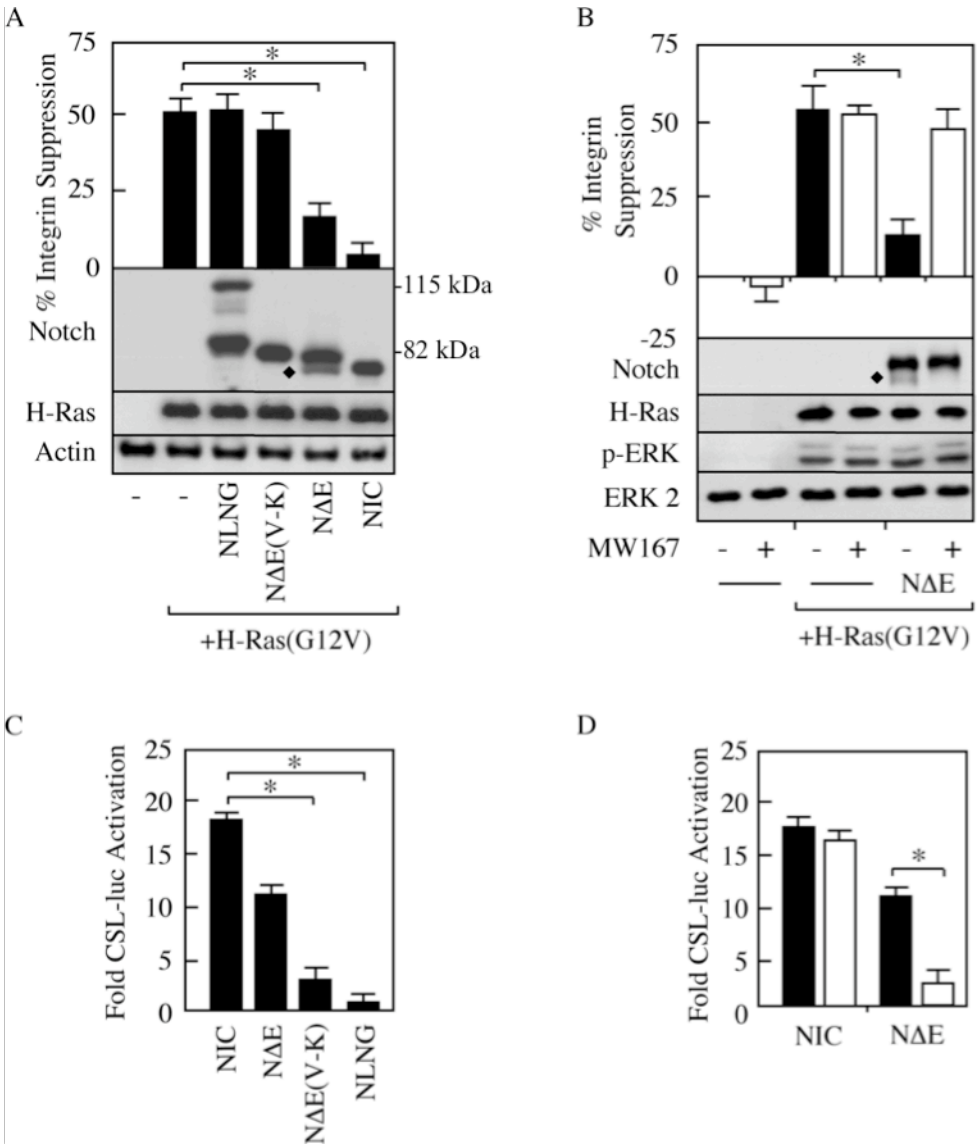
The transcriptional activity of the Notch mutants was confirmed by measuring CSL-dependent luciferase activity as previously described (193). As expected, CSL-luciferase activity was significantly stimulated by NIC and NΔE (Fig. 5.5 c). However, transfection of the Notch mutants NΔE(V1774K) or NLNG, which are inefficiently cleaved, stimulated CSL-luciferase activity significantly less than NIC (Fig. 5.5 c). Furthermore, inhibiting γ-secretase with MW167 significantly reduced the capacity of NΔE to activate CSL (Fig. 5.5 d). Taken together this data indicates that S3 cleavage is essential for both classical Notch activation and Notch-mediated integrin activation.

Figure 5.4: Description Of Notch Constructs.



Mouse (A) and Human (B) Notch-1 constructs used in this study. Key defines important structural components and mutations/deletions in the intracellular domain of each construct.

Figure 5.5: Notch-1 Activation Of Integrins Requires Intramembranous (S3) Cleavage.



(A) The effect of Notch mutants NIC, NΔE, NΔE(V1744K) and NLNG (1μg) on H-Ras(G12V) (0.375μg)-mediated integrin suppression (mean+/-SEM, n=4 independent experiments). Representative immunoblot of Notch, H-Ras(G12V) and β actin expression. (B) NΔE (1μg) reversal of H-Ras(G12V) (0.375μg)-mediated integrin suppression in the presence of MW167 (50μM) (□) or vehicle (■) (mean+/-SEM, n=4 independent experiments). Representative immunoblot of Notch, H-Ras(G12V), ERK2, phospho-ERK and β actin expression. (C) The effect of NIC, NΔE, NΔE(V1744K) or NLNG (1μg) on CSL-luciferase activity in CHO(αβ-py) cells (mean fold increase compared to empty vector +/-SEM, n=4 independent experiments). (D) The effect of NIC or NΔE (1μg) in the presence of MW167 (50μM) (□) or vehicle (■) on CSL-luciferase activity (mean fold increase compared to empty vector +/-SEM, n=3 experiments). Statistically significant differences between results are indicated by * ($p<0.05$). Molecular weight markers are shown to aid interpretation of cleavage fragments. The black triangle indicates the position of intracellular (active) Notch.

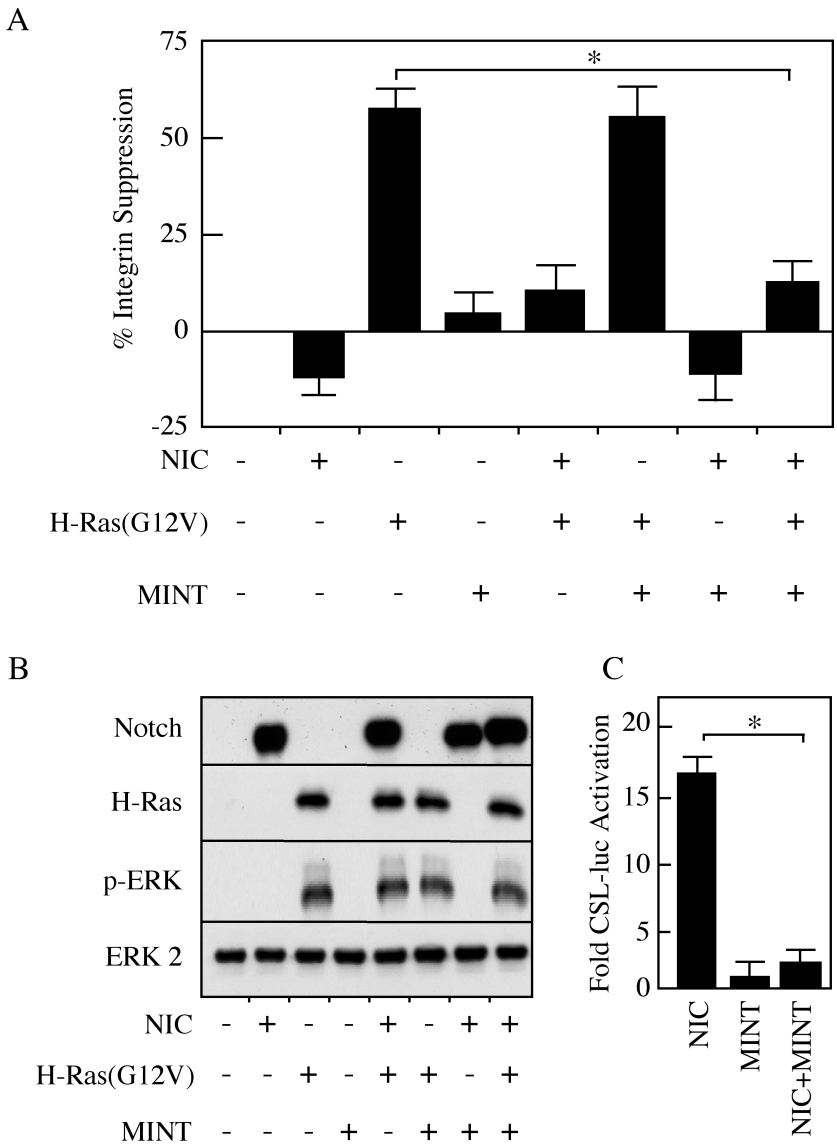
5.2.3 Activation Of β1 Integrins By Notch-1 Is Not Dependent On CSL-Mediated Transcription.

Intramembranous (S3) cleavage releases the intracellular portion of the Notch receptor, which associates with CSL (319). In the resting state CSL binds to DNA acting as a transcriptional repressor, but upon interaction with Notch, co-repressors are displaced and CSL activates transcription leading to up-regulation of downstream target genes (e.g. HES-1) (320,321). However, Notch may also signal independently from CSL-mediated transcription (322). Therefore the role of transcription in Notch-1 activation of integrins was determined using two approaches: inhibition of Notch-CSL interaction and deletion of the transactivation domain of Notch-1.

Msx2-interacting nuclear target (MINT) protein was used initially, which has been shown to compete with the intracellular region of Notch for binding to CSL, suppressing the transcriptional activity of Notch (195). Transfection of MINT into CHO(αβ-py) cells did not affect integrin affinity or the ability of H-Ras to suppress integrins/phosphorylate ERK1/2 (Fig. 5.6 a and b). Importantly, MINT expression did not block NIC activation of integrins despite significantly reducing CSL-luciferase activity (Fig. 5.6 a-c). Available MINT antibodies are ineffective for Western blot analysis, therefore expression of MINT was confirmed by immunofluorescence microscopy (Fig. 5.7 a-h) (195). This suggests that Notch activation of integrins is not dependent upon transcriptional activity.

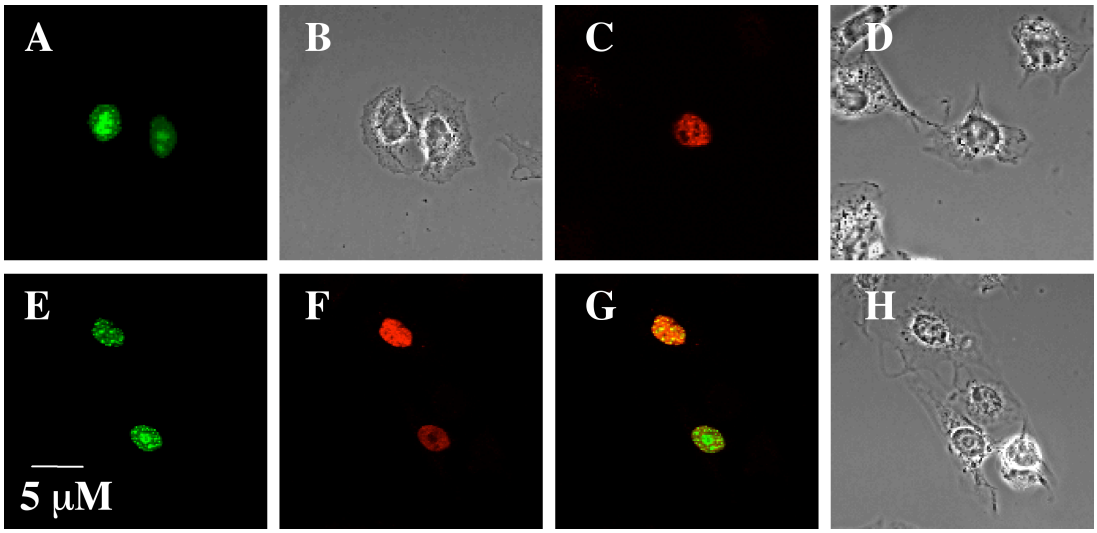
To confirm this data, intracellular Notch-1 truncation mutants were used (summarised in Fig. 5.4). The C-terminal transactivation/PEST (TADP) domain of Notch-1 is important for Notch transactivation and CSL-dependent transcription (194). Transfection of human intracellular Notch-1 (ICN1) into CHO(αβ-py) cells reversed H-Ras-mediated integrin suppression in a similar manner to mouse NIC (Fig. 5.8 b). Furthermore, transfection of an ICN1 truncation mutant, lacking the TADP domain (ΔTADP) also reversed H-Ras-mediated integrin suppression to a similar degree as ICN1 (Fig. 5.8 b). It was confirmed that removal of the TADP region from the intracellular domain of Notch-1 significantly reduced CSL-dependent transcription (Fig. 5.8 c). This data indicates that integrin activation by Notch is not dependent on CSL-dependent transcription.

Figure 5.6: Notch Activation Of Integrins Is Not Blocked By Msx2-Interacting Nuclear Target (MINT) Protein.



(A) The effect of NIC (1μg) and MINT (2μg) on H-Ras(G12V) (0.375μg)-mediated integrin suppression (mean+/-SEM, n=3 independent experiments). (B) Representative immunoblot of NIC, H-Ras(G12V), phospho-ERK and ERK2 expression. (C) The effect of NIC (1μg) and MINT (2μg) on CSL-luciferase activity (mean fold increase compared to empty vector +/-SEM, n=3 independent experiments). *($p<0.05$).

Figure 5.7: Expression Of Msx2-Interacting Nuclear Target (MINT) Protein And Notch-1 Intracellular Domain In CHO Cells.

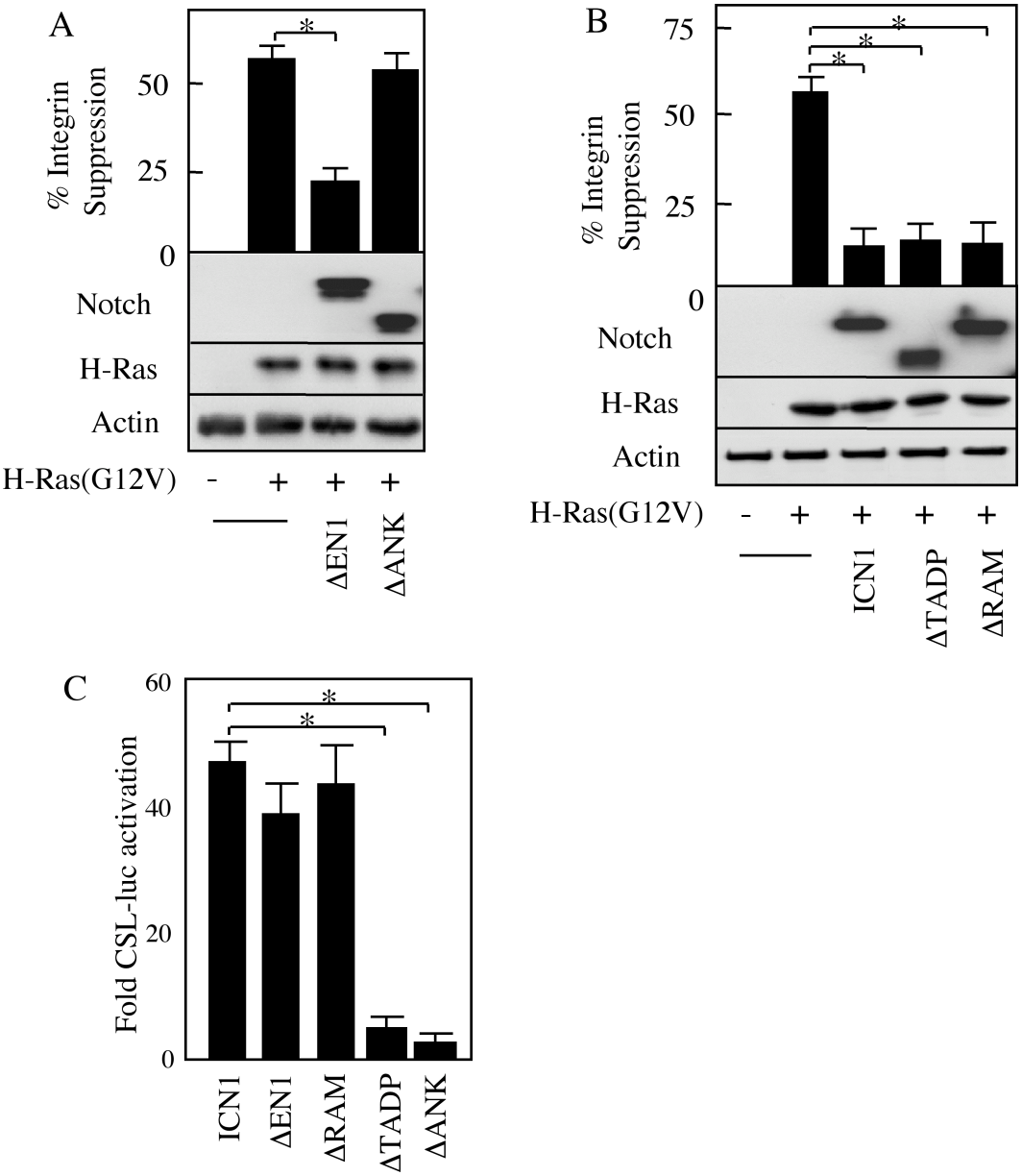


Expression of MINT (2μg) and NIC (1μg) in CHO(αβ-py) cells shown by immunofluoresence microscopy. (A-B) CHO(αβ-py) cells expressing NIC-GFP (green) and corresponding cells viewed with phase contrast. (C-D) CHO(αβ-py) cells expressing Myc-MINT (labelled with alexafluor 568) (red) and corresponding cells viewed with phase contrast. (E-F) CHO(αβ-py) cells expressing both NIC-GFP (green) and myc-MINT (alexafluor 568) (red). (G) Merge of green (NIC) and red (MINT) channels. (H) Phase contrast of cells shown in E-G.

5.2.4 Activation Of β1 Integrins By Notch-1 Requires The Ankyrin Repeat Domain.

The intracellular domain of the Notch receptor consists of the RAM domain, two nuclear localisation sequences, TAD, PEST and ankyrin repeat regions (322,323). It was therefore investigated whether the integrin activating function of Notch could be mapped to one of these regions using deletion mutants (Fig. 5.4) (193,194). A membrane bound Notch-1 mutant (ΔEN1) was used. This consists of a short extracellular segment, the transmembrane region and intracellular domain of human Notch-1 (Fig. 5.4), is processed by γ-secretase and is constitutively active.

Figure 5.8: Notch-1 Activation Of Integrins Requires The Ankyrin Repeats But Not The Transactivation Domains.



(A) The effect of Notch mutants ΔEN1 and ΔANK (1μg) on H-Ras(G12V) (0.375μg)-mediated integrin suppression (mean+/-SEM, n=4 independent experiments). Representative immunoblot of Notch, H-Ras(G12V) and β actin expression. (B) The effect of Notch mutants ICN1, ΔTADP and ΔRAM (1μg) on H-Ras(G12V) (0.375μg)-mediated integrin suppression (mean+/-SEM, n=5 independent experiments). Representative immunoblot of Notch, H-Ras(G12V) and β actin expression. (C) The effect of ICN1, ΔEN1, ΔRAM, ΔTADP and ΔANK (1μg) on CSL-luciferase activity (mean fold increase compared to empty vector +/-SEM, n=3 independent experiments). Statistically significant differences between results are indicated by * ($p<0.05$).

It was found that this mutant reversed H-Ras suppression of integrins in CHO(αβ-py) cells (Fig. 5.8 a). In addition a ΔEN1 mutant (ΔRAM) lacking the 23RAM domain and the ΔTADP mutant (lacking TAD, PEST or NLS domains) were able to activate integrins (Fig. 5.8 b). However a mutant of ΔEN1 (ΔANK), which was lacking the ankyrin repeats, was unable to reverse H-Ras suppression of integrins (Fig. 5.8 a). The previously described transcriptional activity of these mutants was confirmed in CHO(αβ-py) cells (Fig. 5.8 c) (193,194). This data specifically implicates the ankyrin repeats in Notch activation of integrins.

5.2.5 Activation Of β1 Integrins By Notch-1 Is Mediated By R-Ras.

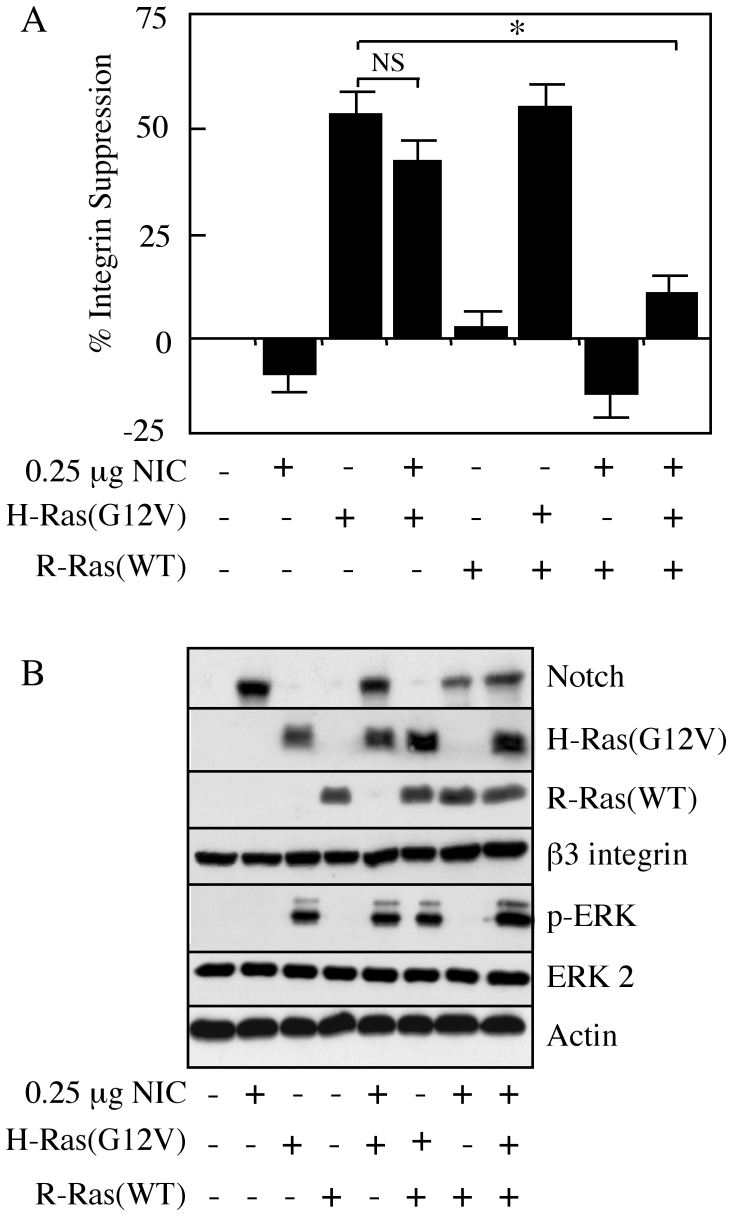
The CSL-independent effectors of Notch are not fully defined. However, the data presented in this chapter suggests that Notch may regulate integrin activity by activating effectors that antagonise H-Ras signalling to integrins. R-Ras is a small GTP-binding protein homologous to H-Ras that can activate integrins and reverse H-Ras/Raf-initiated integrin suppression without affecting bulk ERK phosphorylation (243,271). It was found that transfection of low doses of NIC (0.25μg) had a minimal effect on integrin suppression mediated by H-Ras(G12V) (Fig. 5.9 a). Importantly, whilst transfection of wild type R-Ras alone did not affect integrin affinity, co-transfection of wild type R-Ras with 0.25 μg of NIC reversed H-Ras-mediated integrin suppression, without affecting H-Ras expression or ERK1/2 phosphorylation (Fig. 5.9 a and b). This suggests that activation of integrins by Notch is potentiated by R-Ras.

To demonstrate a specific role for R-Ras in Notch-mediated integrin activation, a dominant-negative R-Ras mutant, R-Ras(T43N) was used (324). Transfection of R-Ras(T43N) alone had a minimal suppressive effect on integrin affinity; however co-transfection of R-Ras(T43N) with NIC blocked the ability of active Notch to increase integrin affinity (Fig. 5.10 a). Furthermore R-Ras(T43N) prevented NIC from reversing H-Ras(G12V)-mediated integrin suppression but did not affect integrin suppression when co-transfected with H-Ras(G12V) alone (Fig. 5.10 a). These effects occurred without alterations in expression of H-Ras, Notch or dominant-negative R-Ras (Fig. 5.10 b). In addition transfection of R-Ras(T43N) did not alter integrin expression in the CHO(αβ-py) cells or H-Ras stimulation of ERK1/2

phosphorylation (Fig. 5.10 b). Yatish Lad and Tony Elliot also demonstrated these data.

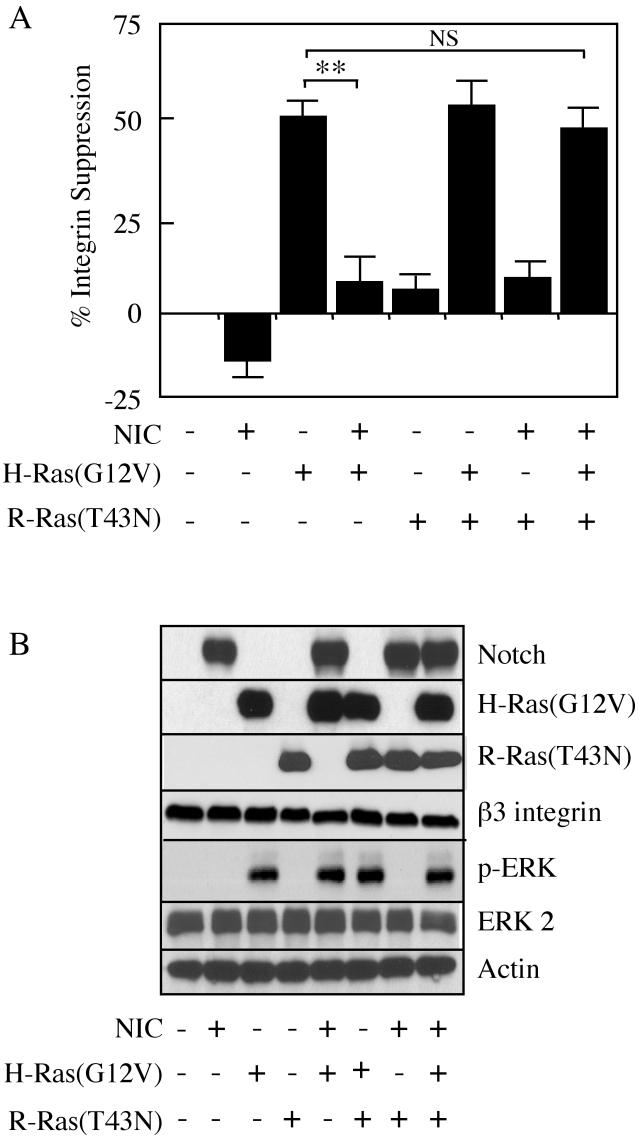
Finally experiments were conducted to determine whether Notch signalling could directly activate R-Ras. The Ras-binding domain (RBD) of Raf, linked to GST, was used to precipitate GTP-bound (active) R-Ras from CHO cell lysates (198). It was observed that transfection of NIC or NΔE stimulated an increase in active GTP-bound R-Ras in αβ-py cells, in comparison to wild type R-Ras alone, without affecting R-Ras expression levels (Fig. 5.11 a). Furthermore, ΔTADP, which did not activate transcription, was also able to activate R-Ras (Fig. 5.11 b). However, the Notch mutant NΔE(V1744K), which did not yield detectable intracellular Notch, or ΔANK, which lacked the ankyrin repeats, were not able to stimulate an increase in active R-Ras (Fig. 5.11 a and b). This suggests that the intracellular domain of Notch can specifically activate R-Ras in CHO cells, requiring the ankyrin repeats but not CSL-dependent transcription. Taken together these results demonstrate that the ability of Notch signalling to regulate integrin affinity is mediated through R-Ras.

Figure 5.9: Wild Type R-Ras Potentiates Notch-1-Mediated Integrin Activation.



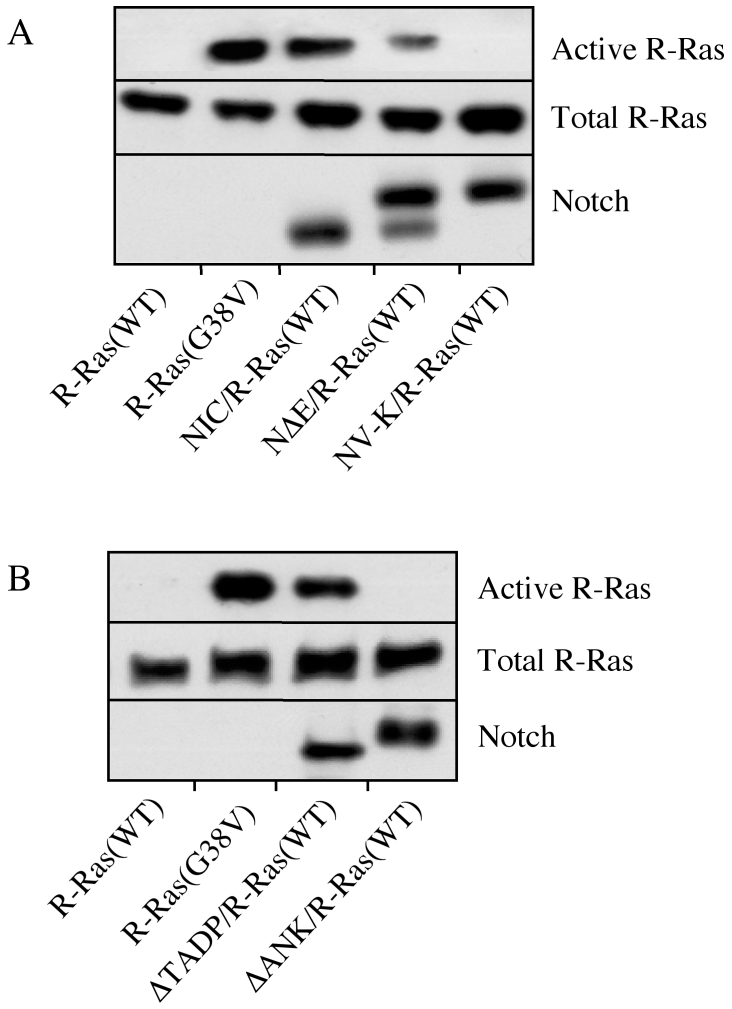
(A) CHO(αβ-py) cells were transfected with NIC (0.25μg), R-Ras(WT) (0.5μg) and H-Ras(G12V) (0.375μg) as indicated. Percentage integrin suppression was determined by flow cytometry. The bar graph represents mean +/-SEM of n=4 experiments. (B) Representative immunoblots of NIC, H-Ras(G12V), R-Ras(WT), β3 integrin, ERK2, phospho-ERK (p-ERK) and β actin expression in CHO(αβ-py) cells transfected as indicated. Statistically significant differences between results are indicated by * ($p<0.05$). NS indicates no significant difference.

Figure 5.10: Dominant Negative R-Ras (R-Ras(T43N)) Reverses Notch-1 Activation Of Integrins.



(A) CHO(αβ-py) cells were transfected with R-Ras(T43N) (1μg), NIC (1μg) and H-Ras(G12V) (0.375μg) as indicated. Percentage integrin suppression in αβ-py cells was determined by flow cytometry. The graph represents mean +/-SEM of n=4 experiments. (B) Representative immunoblots of NIC, H-Ras(G12V), R-Ras(T43N), β3 integrin, ERK2, phospho-ERK (p-ERK) and β actin expression. Statistically significant differences between results are indicated by * ($p<0.05$). NS indicates no significant difference.

Figure 5.11: The Intracellular Domain Of Notch-1 Activates R-Ras.



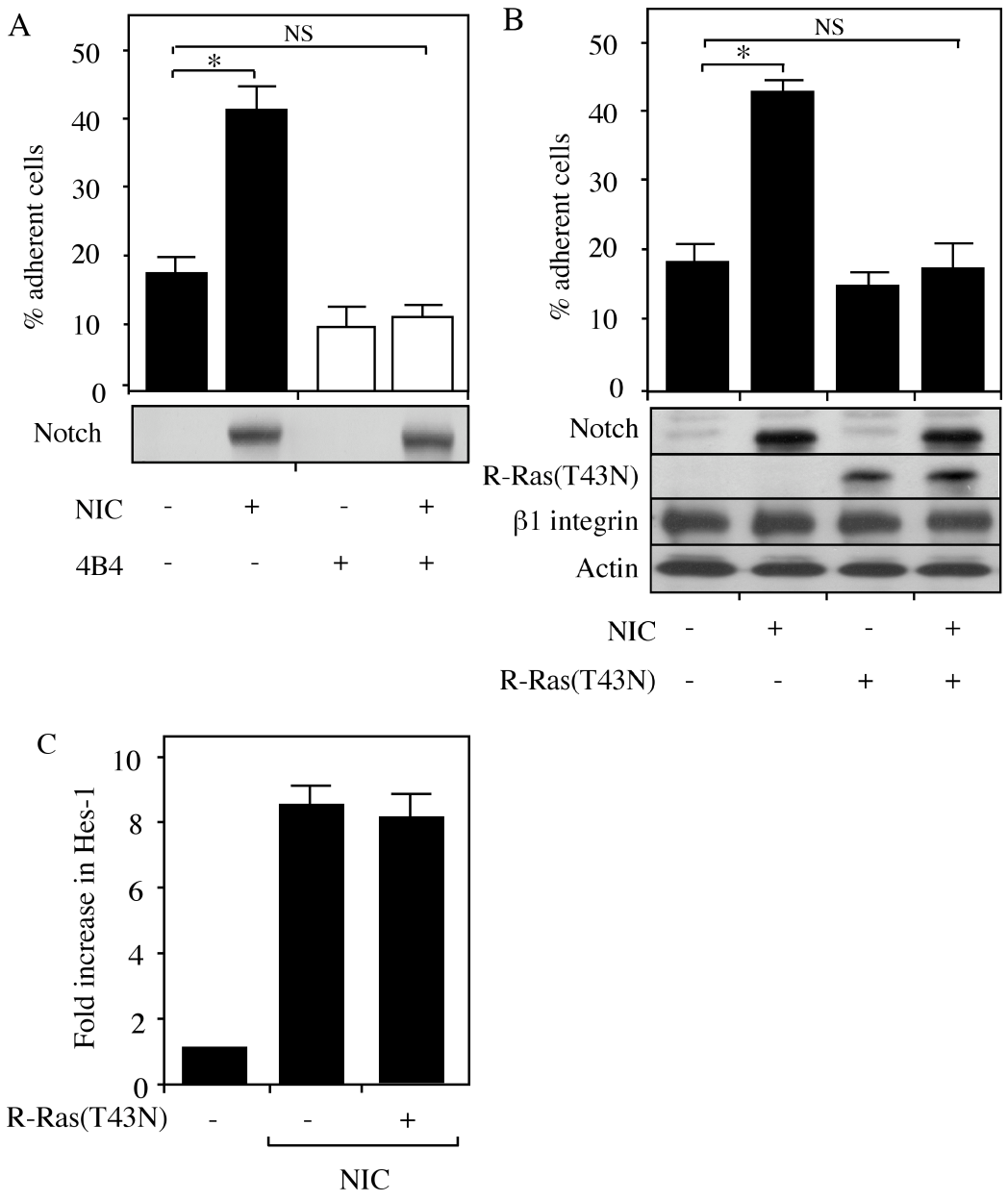
CHO(αβ-py) cells were transfected with wild type R-Ras (myc-tagged) (1μg) and the Notch mutants (1μg) as indicated. Constitutively active R-Ras and empty vector were used as controls. GTP-bound (active) R-Ras was precipitated from whole cell lysates using the Ras binding domain of Raf as described in the materials and methods chapter. Immunoblots using anti-myc antibody (clone 9E10) show active R-Ras and total R-Ras (whole cell lysates) expression. (A) The effect of Notch mutants, NIC, NΔE and NΔE(V1744K) (NV-K) (1μg), on R-Ras activation in αβ-py cells. (B) The effect of Notch mutants, ΔTADP and ΔANK (1μg), on R-Ras activation in αβ-py cells. Representative immunoblots from n=4 independent experiments.

5.2.6 Notch-1 Activates Native α5 β1 Integrins In An R-Ras Dependent Manner To Increase Cellular Adhesion To Fibronectin.

To investigate the physiological relevance of the above findings, the effect of Notch on the fibronectin receptor α5 β1 integrin, in the human myeloid cell line K562 was examined. K562 cells solely express α5 β1 integrins and therefore to test the effects of Notch signalling on the activation of this integrin, K562 cell adhesion to fibronectin (the natural ligand for α5 β1 integrins) was determined as described in chapter 2 (325). It was observed that transfection of K562 cells with NIC significantly increased adhesion to fibronectin in comparison to empty vector (Fig. 5.12 a). Adhesion of K562 cells transfected with either Notch or vector was significantly blocked by prior incubation with the β1 integrin-blocking antibody 4B4 (Fig. 5.12 a). Furthermore, co-expression of dominant-negative R-Ras blocked the effect of NIC on adhesion of K562 cells to fibronectin (Fig. 5.12 b). This occurred without alterations in Notch or β1 integrin expression. Importantly, NIC-mediated Notch signalling in K562 cells was unaffected by co-transfection of dominant-negative R-Ras as determined by real-time RT-PCR measurement of HES-1 expression (Fig. 5.12 c). These results indicate that Notch-1 signalling can regulate natively expressed integrin affinity through R-Ras activation.

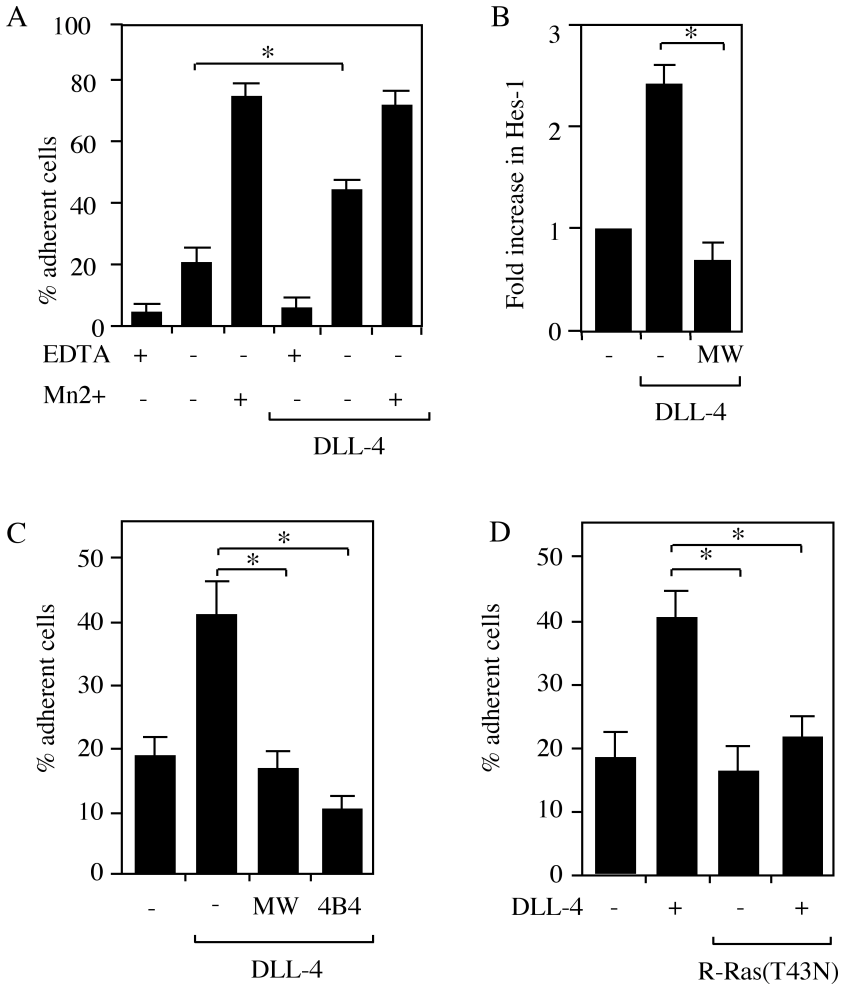
K562 cells express Notch-1 receptors in the undifferentiated state and previous data has shown that Notch signalling can be activated *in vitro* by recombinant Notch ligand coated to tissue culture plastic (326,327). It was found that 12-hour culture of K562 cells with immobilised human recombinant Delta-like ligand-4 (DLL-4) significantly increased adhesion of K562 cells to fibronectin (Fig. 5.13 a). This adhesion was blocked by EDTA and increased by Mn^{2+} (Fig. 5.13 a). DLL-4 increased HES-1 expression in K562 cells and this was prevented by MW167 (Fig. 5.13 b). Crucially, treatment of K562 cells with MW167, or pre-incubation with the β1 integrin blocking antibody 4B4, prevented DLL-4 from increasing adhesion to fibronectin (Fig. 5.13 c). Furthermore, DLL-4 induced activation of α5 β1 integrins was blocked by transfection of dominant-negative R-Ras (Fig. 5.13 d). These data indicate that ligation of Notch receptors by naturally occurring Notch ligands can activate β1 integrins increasing cellular adhesion to ECM through R-Ras.

Figure 5.12: Notch-1 Intracellular Domain Increases K562 Cell Adhesion In A β1 Integrin/R-Ras Dependent Manner.



(A) The effect of NIC (1μg) on K562 cell adhesion to fibronectin with (□) or without (■) 4B4 (mean percentage adhesion compared to poly-l-lysine +/-SEM, n=4 independent experiments). (B) The effect of NIC and R-Ras(T43N) on K562 cell adhesion to fibronectin (mean percentage adhesion compared to poly-l-lysine +/-SEM). Representative immunoblot of NIC, R-Ras(T43N), β1 integrin and β-actin expression (n=4 independent experiments). (C) The effect of NIC and R-Ras(T43N) (1μg) on HES-1 expression in K562 cells (mean fold increase in HES-1+/-SEM, normalised for 18S and compared to empty vector, n=3 independent experiments). Statistically significant differences between results are indicated by * ($p<0.05$). NS indicates no significant difference.

Figure 5.13: Notch Signalling Initiated By Delta-Like Ligand 4 (DLL-4) Increases K562 Cell Adhesion.



K562 cells were incubated for 12 hours with recombinant human Delta ligand 4 (Dll-4) with or without MW167 (50μM). (A) DLL-4 effect on K562 cell adhesion to fibronectin with or without EDTA (5mM) or Mn2+ (100μM) (mean percentage adhesion +/-SEM compared to poly-l-lysine, n=4 independent experiments). (B) The effect of Dll-4 +/- MW167 or 4B4 (10 μg/ml) on K562 cell adhesion to fibronectin (mean percentage adhesion +/-SEM compared to poly-l-lysine, n=3 independent experiments). (C) The effect of Dll-4 +/- MW167 on HES-1 expression in K562 cells (mean fold increase in HES-1+/-SEM, normalised for 18S and compared to empty vector, n=3 independent experiments). (D) The effect on K562 cell adhesion to fibronectin of cells transfected with R-Ras(T43N) or empty vector, and +/-Dll-4 (mean percentage adhesion +/-SEM compared to poly-l-lysine, n=3 independent experiments). Statistically significant differences between results are indicated by * ($p<0.05$).

5.2.7 Notch Signalling Protects SCLC Cells From Chemotherapy-Induced Apoptosis.

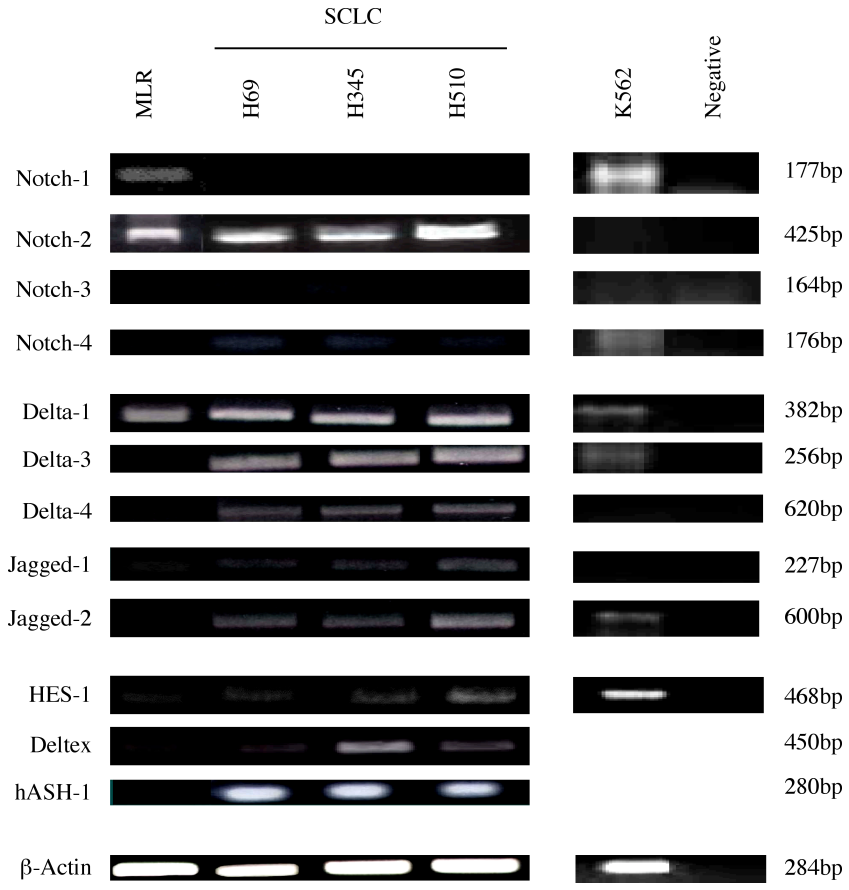
It is clear from the data presented thus far in this chapter that activation of Notch-1 signalling can activate β1 integrins. The results in chapter 3 indicate that adhesion of SCLC cells via β1 integrins to ECM proteins protects against cell cycle arrest and apoptosis induced by DNA-damaging agents. Published data has demonstrated that activation of Notch signalling in SCLC cells can promote an adherent cell phenotype, alter cell cycle progression and down-regulate hASH-1 which is highly expressed in neuroendocrine cells (314). Thus, it is possible that Notch may provide an important chemo-resistance signal to SCLC cells possibly through activation of β1 integrins.

Initial experiments sought to determine the expression of Notch signalling components in H69, H345 and H510 SCLC cell lines. The Notch pathway is highly conserved between species and therefore the commercially available antibodies available at the time of this research for immunoblot or flow cytometry detection of these proteins were of low affinity. Thus, prior published data has used RT-PCR techniques (328). mRNA was extracted from maintenance cell cultures of SCLC lines and RT-PCR was performed using an Access Kit (Promega) and published primers as described in chapter 2 (328). It was observed that SCLC cell lines preferentially expressed Notch-2 receptor with low or no expression (up to 35 cycles) of Notch- 1,3 or 4 receptor (Fig. 5.14). In contrast, SCLC cell lines expressed mRNA for all currently recognised Notch ligands. Expression of downstream target HES-1 was also observed. As previously described, mRNA for hASH-1 was detected confirming the neouroendocrine phenotype of the SCLC cell lines (314).

To investigate whether activation of Notch signalling could protect SCLC cells from chemotherapy-induced apoptosis immobilised Notch ligands Delta and Jagged were used. 96-well plates were coated with varying concentrations of recombinant Jagged-1, recombinant Delta-like ligand-4 (DLL-4) or a control peptide (IgG1) as indicated. H69 SCLC cells were incubated with the immobilised ligands for 12 hours and then treated for 48 hours with etoposide (25μg/ml). Staining cells with acridine orange/ethidium bromide was used to determine percentage apoptosis. It was

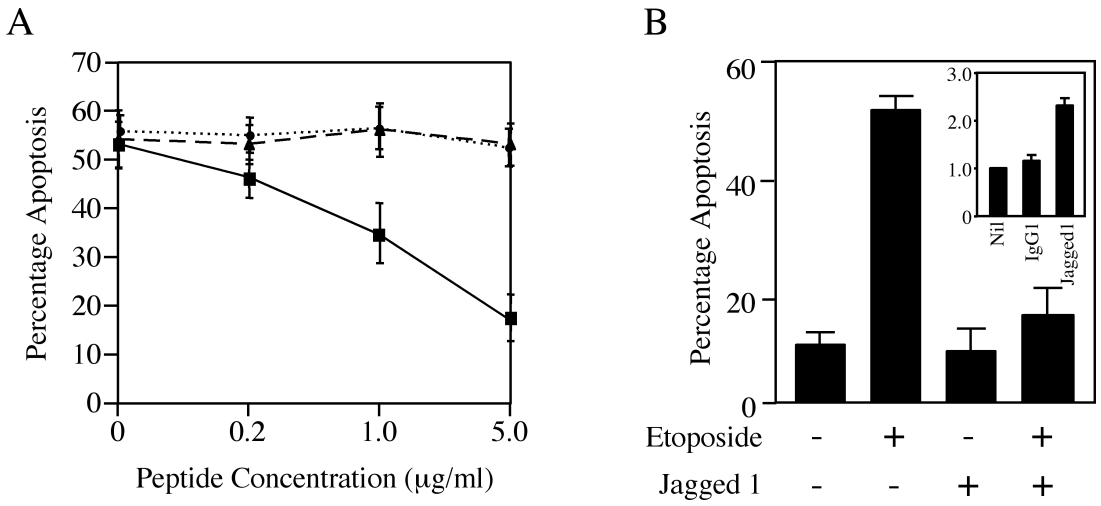
observed that Jagged-1 significantly reduced the percentage of apoptosis induced by etoposide, whilst IgG1 and DLL-4 had no significant effect (Fig. 5.15). Etoposide treatment of H69 cells incubated with IgG1 resulted in 52 +/- 2.7% apoptosis. However, incubation with Jagged-1 (5μg/ml) reduced the etoposide-induced apoptosis to 17 +/- 4.8% (mean +/- SEM, n=3 independent experiments, $p<0.01$). It was confirmed that incubation with immobilised Jagged-1 induced a Notch signal in H69 SCLC cells by real-time RT-PCR measurement of HES-1 expression (Fig. 5.15 b-insert). These data suggest that Notch signalling initiated by Jagged-1 can protect SCLC cells from etoposide-induced apoptosis.

Figure 5.14: Notch signalling components expressed by SCLC cell lines (RT-PCR).



RNA was extracted from SCLC cells and as positive controls from K562 and MLR cells. Using an Access™ RT-PCR kit (Promega) the expression pattern of Notch receptors, Notch ligands and downstream Notch signalling mediators were determined using published primers described in chapter 2 (328). β-actin RT-PCR is shown as a loading control. Negative controls were performed with nuclease free water (Promega) instead of template. The product sizes in base pairs (bp) are shown numerically next to each agarose gel picture

Figure 5.15: Notch ligand Jagged-1 protects SCLC cell lines from etoposide-induced apoptosis.



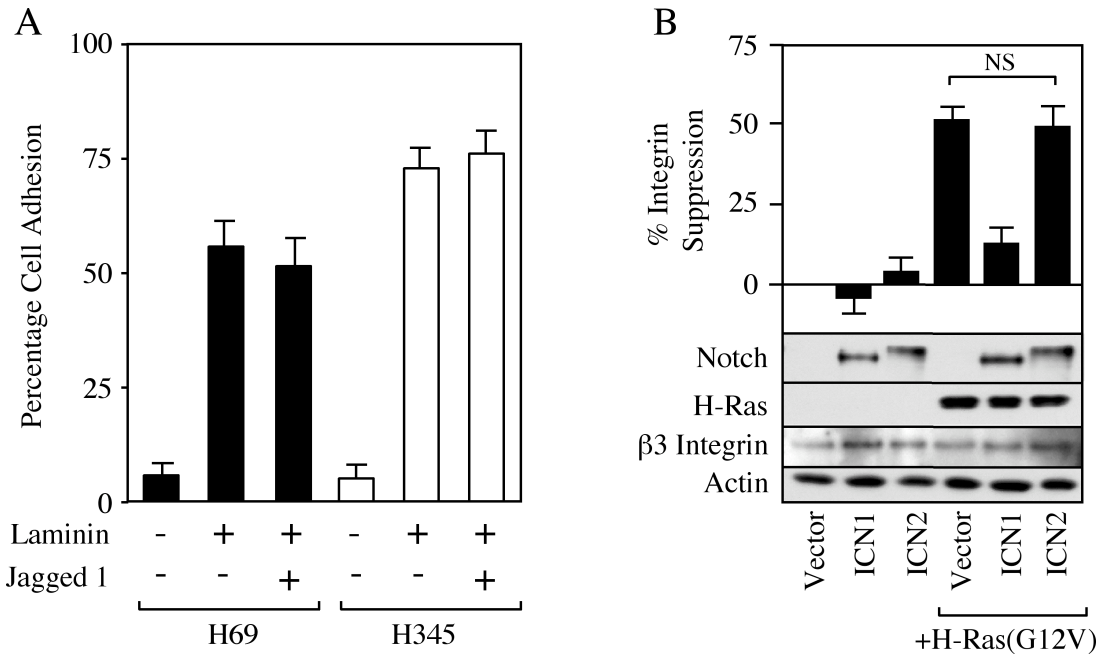
(A) 96-well plates were coated with Delta-like ligand-4 (broken line), Jagged-1 (solid line) or IgG1 (dotted line). Each peptide was dissolved in PBS (concentration 0-5μg/ml) and 100μl was added to each well. The plate was incubated at 37ºC for 1 hour. H69 SCLC cells were re-suspended in SITA medium and $4x10^4$ cells/well were added. Cells were incubated for 12 hours and then treated with etoposide (25μg/ml final concentration). The plate was incubated for a further 48 hours and percentage apoptosis determined by ethidium bromide/acridine orange staining. The graph shows the average percentage apoptosis induced by etoposide at each concentration of Notch ligand +/- SEM (n=3 independent experiments). (B) 96-well plates were coated with IgG1 or Jagged-1 (5μg/ml) as indicated. H69 SCLC cells ($4x10^4$ cells/well) were added, incubated for 12 hours and then treated with etoposide (25μg/ml final concentration) as indicated. After 48 hours percentage apoptosis was determined by acridine orange staining. The graph shows average percentage apoptosis +/- SEM (n=3 independent experiments). The insert graph shows Hes-1 expression in H69 SCLC cells incubated for 12 hours with immobilised IgG1or Jagged-1 measured by real-time RT-PCR (mean +/- SEM of n=3 experiments).

5.2.8 Activation of Notch-2 does not modulate integrin affinity.

These data suggest that Jagged-1 activation of Notch signalling in SCLC cells can protect against etoposide-induced apoptosis. It has also been demonstrated in this chapter that Notch-1 signalling can activate integrins. Increased cellular adhesion is associated with SCLC cell resistance to chemotherapy (chapter 3). Therefore it was investigated whether Notch activation could increase SCLC cell adhesion. H69 and H345 SCLC cells were incubated with immobilised Jagged-1 or control (IgG1) (both 5μg/ml) for 12 hours, gently disaggregated, washed and then allowed to adhere to laminin for 30 minutes. Non-adherent cells were removed by washing with PBS and cell adhesion was calculated as a percentage of total cellular adhesion to poly-l-lysine. It was observed that incubation with Jagged-1 did not increase adhesion of either SCLC cell line to laminin despite the ability of this ligand to induce a Notch signal (Fig. 5.16a and 5.15b-insert). The RT-PCR data shown above indicates that SCLC cells express Notch-2 receptor preferentially. Taken together, these results would suggest that activation of Notch-2 on SCLC cells by Jagged-1 does not alter cellular adhesion to ECM and thus by inference β1 integrin activation status. However, this system is not optimised for investigating integrin activation or Notch-2 activation in isolation.

To determine whether Notch-2 could activate β1 integrins, the CHO(αβ-py) system was employed. Cells were transfected with H-Ras(G12V) and the intracellular domains of human Notch-1 (ICN1) or human Notch-2 (ICN2) (both 1μg), which have been shown to constitutively activate Notch signalling (322). Subsequently, integrin affinity was assessed by flow cytometry as described in the materials and methods chapter and expressed as percentage integrin suppression. It was observed that whilst ICN1 was able to override suppression of integrins by H-Ras(G12V), ICN2 was unable to activate integrins (Fig. 5.16b). Western immunoblots confirmed that Notch and H-Ras were expressed and there was no alteration in integrin expression. Therefore these data indicate that activation of Notch-2 signalling does not modulate integrin affinity. Furthermore, it is suggested that Notch-protection of SCLC cells from chemotherapy must be occurring through a separate mechanism from integrin activation.

Figure 5.16: Activation Of Notch-2 Does Not Modulate Integrin Affinity.



(A) 12-well plates plates were coated with IgG1 (-) or Jagged-1 (+) (5μg/ml) as indicated. $1x10^6$ H69 and H345 SCLC cells in RPMI medium were added to each well. The cells were incubated (37ºC) for 12 hours, re-suspended in HEPES/NaCl buffer and seeded into 96-well plates ($1x10^5$ cells/well), uncoated (-) or pre-coated with laminin (+). The plate was incubated for 30 minutes at 37°C, adherent cells were fixed (3% paraformaldehyde, 5 minutes), stained with methylene blue (0.4%, 5 minutes) and eluted with 0.1N HCl. The absorbance (at 630nM) of each well was determined using an automated plate reader. Cell adhesion for each experimental condition was expressed as a percentage of total cellular adhesion to poly-l-lysine. The graph shows average percentage adhesion +/- SEM (n=4 experiments). (B) CHO(αβ-py) cells were transfected with ICN1, ICN2 (both 1μg) and/or H-Ras(G12V) (0.375μg) as indicated. Percentage integrin suppression was determined by flow cytometry. The graph represents mean +/-SEM of n=3 experiments. Representative immunoblots of Notch, H-Ras(G12V), β3 integrin, and β actin expression. NS indicates no significant difference.

5.3 Discussion.

The data presented in this chapter demonstrates that Notch-1 signalling in mammalian cells activates β1 integrins and increases cellular adhesion to fibronectin through α5 β1 integrins. In addition, Notch activation in SCLC cells provides significant protection against etoposide-induced apoptosis. However, this does not appear to be related to activation of β1 integrins and in contrast to Notch-1, Notch-2 signalling does not modulate integrin affinity. These results provide a potential mechanism for previous observations demonstrating key interactions between Notch and integrins, suggest crucial differences in downstream signalling from Notch receptors subtypes and raise questions about the role of Notch in SCLC.

Somitogenesis is the process whereby segmented precursors of the skeletal muscle and vertebral column are generated during vertebrate embryogenesis (313). Mutations in zebrafish integrin α5 disrupt anterior somite formation, giving a complementary phenotype to the posterior defects seen in Notch pathway mutants (312). Analysis of integrin:notch double mutants have revealed redundancy between integrin and Notch pathways in promoting somite border morphogenesis, suggesting a regulatory relationship between Notch and integrins (312). The data presented here demonstrates that Notch regulates integrin affinity and provides a mechanism for this interaction that is crucial to vertebrate development.

Genetic studies in mice have suggested that Notch signalling is important for formation of the vasculature. Mutations in Jagged-1, Notch-1 and Notch-1/Notch-4 in mice result in embryonic lethality with severe vascular defects (329). Genetic analyses also indicate a central role for integrins in vascular development - antagonists of β1 integrins inhibit angiogenesis in the chick chorioallantoic membrane, and Notch-4 increases endothelial cell adhesion preventing endothelial sprouting (311). Notch may therefore regulate vascular development through interaction with integrins. Interestingly, R-Ras knockout mice demonstrate defects in angiogenesis in response to vascular injury and tumour growth (330). The results in this chapter provide direct evidence of a link between Notch and β1 integrins involving R-Ras activation. This may represent a central mechanism for regulation of vascular development and angiogenesis. Notch-1 and DLL-4 expression on vascular

endothelial cells is regulated by VEGF and thus the observation of integrin activation by DLL-4 may be particularly relevant (289).

It has been shown here that Notch-1 overrides H-Ras-mediated integrin suppression via R-Ras activation. Studies of vulval development in *Caenorhabditis elegans* and the *Drosophila* eye have indicated important interactions between Notch and Ras (331,332). The Notch pathway can antagonise Ras signalling (333,334). Inhibitory cross-talk between Notch and H-Ras regulates *Drosophila* bristle patterning, *C. elegans* vulva formation and may be important in T-cell positive selection (335-337). These interactions occur in part because each pathway can affect the expression or activities of components of the other pathway (338). The data in this chapter provides a new mechanism for Notch antagonism of H-Ras through activation of R-Ras. This does not require CSL/transcription and may therefore allow for rapid changes in cellular signalling in response to interaction with Notch ligands expressed on adjacent cells. The importance of this signalling cascade in worms and insects remains to be demonstrated as these organisms have a simpler repertoire of small GTP-binding proteins and therefore may lack the essential signalling components (i.e. R-Ras) for this interaction (339).

The mechanisms by which R-Ras might antagonise H-Ras functions have not yet been defined. Previous work has demonstrated that reversal of H-Ras-mediated integrin suppression by R-Ras is not due to competition for downstream effectors or Raf-induced MAP kinase activation (243). Furthermore, specific mutations in the effector binding loop of R-Ras impaired the ability of R-Ras to reverse H-Ras-mediated integrin suppression but did not correlate with their ability to activate known R-Ras effectors (340). Prior data has indicated that targeting of R-Ras to focal adhesions at the cell surface is critical for its ability to regulate integrin activation (341). Interestingly, H-Ras has also been found to be associated with focal adhesions and data has suggested that Notch can interact with β1 integrins involving lipid rafts (310,342). Therefore, a better understanding of the interaction between Notch, the small GTPases and integrins at the cell surface may help to explain crucial processes in integrin activation and Notch antagonism of H-Ras.

The results presented here indicate that Notch-1-mediated integrin activation requires cleavage of the Notch receptor at S3 to release the intracellular domain but is independent of CSL-transcription. Importantly, it is shown that integrin activation by Notch is not inhibited by MINT, which prevents Notch binding to CSL (195). CSL-independent Notch signalling has been suggested by previous analysis of Notch mutant phenotypes in *Drosophila* - two gain of function classes of Notch alleles were defined which prevent development of sensory bristles, one of which is not rescued by removing Su(H) (302). *In vivo* evidence for CSL-independent signalling in vertebrates has been provided by experiments examining Delta-1 activated signals in the developing avian neural crest (343). *In vitro* studies have shown that Notch can prevent differentiation of C2C12 mouse myoblasts into myotubes. Myoblast differentiation is not blocked by a dominant negative CSL protein and can be mimicked by truncated forms of Notch, which cannot activate a CBF-1-dependent promoter (303). The mediators of these pathways are not well defined. In this chapter, direct evidence of CSL-independent Notch signalling is presented. Furthermore it is demonstrated that R-Ras is a key signalling moiety in this pathway. These data indicate that intracellular Notch specifically activates R-Ras and that dominant-negative R-Ras blocks Notch integrin activation. R-Ras has important cellular effects including survival, transcription and adhesion but the physiological activators are poorly understood (339). Thus, these observations define a novel Notch signalling pathway and describe a new R-Ras activator.

It is shown in this chapter that Notch activation of integrins requires the ankyrin repeat domain of intracellular Notch. Recent studies have indicated that this region is essential for all known Notch functions (323). Genetic analyses in *Drosophila* utilising Notch deletion mutants have indicated that deletion of the RAM-ANK region abolishes the ability of full length Notch to transduce a Su(H)-dependent signal (344). Point mutations within the ankyrin repeats of full length Notch produce strong dominant negative phenotypes, whereas mutations that eliminate RAM activity do not abolish Notch signalling (287,344). Studies of mouse Notch-1 have shown that the ankyrin repeats are responsible for binding to CSL and transactivation (321); Notch mutants consisting of the TAD/PEST region were unable to activate transcription but this could be rescued by co-expression of the ankyrin repeat

domain. The data presented here concurs with these genetic and *in vitro* studies. In addition it is shown that the ankyrin repeats have a previously undefined function not related to CSL binding. Therefore analysis of ankyrin repeat point mutations could enable dissection of Notch CSL-dependent and -independent signalling pathways.

Adenoviral expression of constitutively active Notch-1 and Notch-2 in SCLC cells has been previously shown to induce an adherent cell morphology associated with reduced hASH-1 expression, suggesting epithelial differentiation (314). In contrast, the data shown in this chapter indicates that Notch signalling induced in SCLC cells by Jagged-1 does not alter cell adhesion. The reasons for these discrepancies may be due to differences in cell lines used and the methods of Notch activation. Sriuranpong *et al* used SCLC cell lines that had no detectable expression of Notch-1 or Notch-2 (314). It is clear from RT-PCR data in this chapter that H69 and H345 SCLC cell lines express Notch-2 receptor mRNA. Furthermore, Sriuranpong *et al* transfected SCLC cell lines with the intracellular Notch to activate Notch signalling (314). In contrast, in this chapter, Jagged-1 was used to activate a Notch signal in SCLC cells. These two methods are likely to induce different strengths and durations of Notch activation, which may produce different cellular effects, a hypothesis that could be tested by comparing the changes in HES-1 and hASH-1 expression with intracellular Notch-1 and immobilised Jagged-1. However, another explanation is suggested by the data in this chapter showing that Notch-1 and Notch-2 have differential effects on integrin activation. Thus, ligation of Notch-2 receptor on SCLC cells by Jagged-1 would not activate integrins or increase cell adhesion. Interestingly, although Sriuranpong *et al* found that both Notch-1 and Notch-2 suppressed hASH-1 expression, Notch-2 produced much less marked cell morphology changes (314). Taken together these results suggest that some effects of Notch activation are common to all receptors, whilst some, e.g. integrin activation, are specific to receptor subtype. Comparison of Notch-1 and -2 signalling should therefore allow further investigation of the cellular mechanisms by which intracellular Notch interacts with and activates R-Ras, a crucial step in understanding in the upstream activators of small GTPases.

Activation of Notch-2 has also been shown here to protect SCLC cells from etoposide-induced apoptosis. Prior work has suggested that Notch signalling in

SCLC may in fact act as a tumour suppressor by restricting neuroendocrine phenotype (314). The data presented in this chapter suggests that this assumption may in fact be an over-simplification. In fact Notch signalling may restrict SCLC development in early tumorigenesis but in established neuroendocrine tumours may promote cell survival. An analysis of Notch expression in human SCLC tumour sections and appropriate correlation to treatment response would indicate the importance of this pathway *in vivo*. In addition, further investigation is needed to determine the downstream signalling pathways that are activated by Notch in SCLC cells that contribute to chemoresistance. Potential candidates include PI3-kinase and Jnk signalling, which can be chemically inhibited allowing the effect on Notch-induced chemoprotection to be studied (345,346).

In conclusion, the data presented in this chapter demonstrates clear evidence for a new Notch signalling pathway. Ligand-induced cleavage of the Notch-1 receptor at S3 releases the Notch intracellular domain, which activates R-Ras, in a CSL-independent manner involving the ankyrin repeats. Active R-Ras anatgonises H-Ras-mediated integrin suppression increasing integrin affinity allowing cells to interact with their microenvironment. This process is likely to be important in cancer growth, as tumour cells often express high levels of Notch-1, β1 integrins and are frequently found in an ECM rich niche environment (347,348). Thus, these results defining an interaction between Notch, the Ras family of GTPases and β1 integrins add a new level of complexity to the Notch signalling pathway and have important implications for the future understanding of development and disease.

CHAPTER 6: The Presence Of Mononuclear Immune Cells In SCLC Tumour Sections Predicts Patient Survival.

6.1 Introduction.

It is widely accepted that local host immune responses can control tumour growth and even eradicate malignant cells (349). Prior studies have demonstrated that tumour infiltrating T-lymphocytes (TIL) and dendritic cells (DC), which play a central role in the generation of tumour-specific effector T-cells, are commonly found in solid tumours, and have been associated with improved patient survival and reduced relapse rate in melanoma, breast and ovarian cancer (350-352). Therefore, a novel approach to the treatment of lethal residual disease in patients with SCLC could be the induction of a host-immune response to attack chemo-resistant tumour cells.

SCLC has a neuroendocrine phenotype and therefore expresses a number of specific antigens that could be used as immune targets. SCLC can present with paraneoplastic encephalomyelitis and peripheral neuropathy prior to clinical detection of the lung tumour (353). In these cases, antibodies are frequently detected in the patient's serum, which react to proteins expressed on both SCLC and neurons (HuD, HuC and Hel-N1) (354). The early presentation of SCLC in these patients and the more favourable outcome from SCLC associated with paraneoplastic encephalomyelitis has led to the suggestion that these patients have developed an effective anti-tumour immune response (185). Thus, the expression of HuD by SCLC triggers an immune response by the host that limits cancer growth but is also directed against proteins selectively expressed on neurons. These observations have led to the search for other SCLC-specific antigens that could be used in immunotherapy. Strategies that have been proposed include targeting tumour-specific gangliosides, neural cell adhesion molecule (NCAM) and aberrant expression of p53 (191). Unfortunately a phase III study using an anti-idiotypic antibody that mimics the ganglioside GD3 as a vaccine in chemo-responsive limited disease SCLC has showed no overall survival benefit (355). The failure of this trial to demonstrate a benefit, in part reflects the limited knowledge of the local immune response to SCLC and its role in tumour progression.

In addition to using the immune system as a therapy for cancer it may also be used as a prognostic marker. At present there are only a few indicators that can be used to stratify SCLC patients into prognostic groups. These include clinical markers such as performance status (PS) measured using the ECOG scale (0-4), disease stage (limited or extensive), age and sex (81). In addition, peripheral blood biochemical markers such as lactate dehydrogenase (LDH) have also been shown to predict survival (81). Definition of novel prognostic markers would assist medical and patient decision making, highlight potential new therapeutic strategies and improve future research design. Previous research has demonstrated several immune parameters that predict patient prognosis and disease stage in SCLC. These have included the degree of delayed-type hypersensitivity reaction and defects in peripheral blood lymphocyte (PBL) numbers, proliferative response and IL-2 secretion (187-189,356). However, these studies have focused on the role of systemic immune dysfunction and have relied on complicated tests of immune response, which relate to tumour burden and may not reflect the changes in the local tumour environment. In other solid malignancies, local tumour infiltration by immune cells has been shown to be associated with improved patient survival (181,350-352). Therefore studies of the local tumour inflammatory microenvironment in SCLC may reveal new and accurate prognostic indicators.

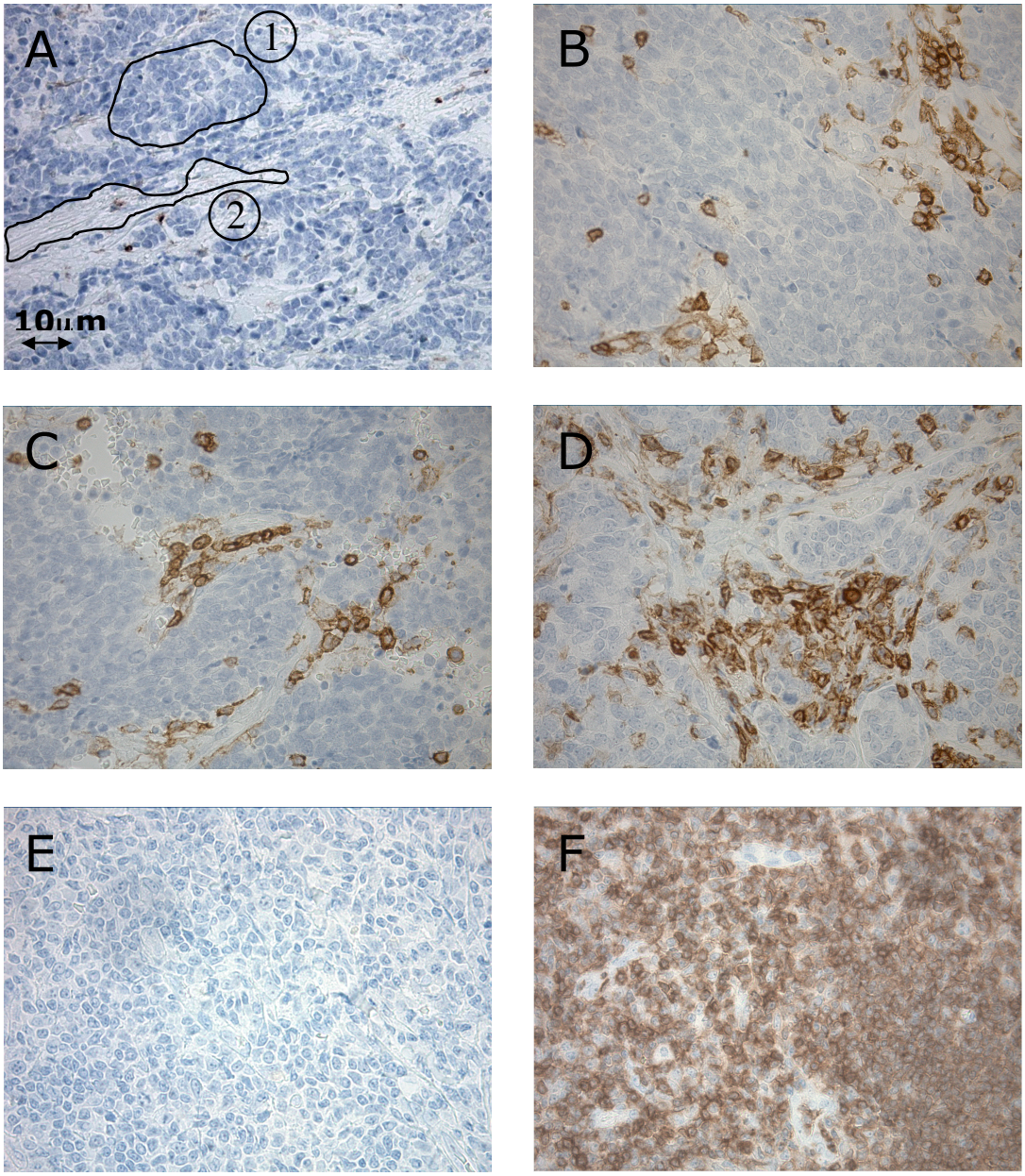
6.2 Results.

6.2.1 A Mononuclear Cell Infiltrate Consisting Of Lymphocytes And Macrophages Is Present In SCLC Tumour Sections.

Ten surgically resected SCLC tumour sections were identified from the pathology archive at the Royal Infirmary in Edinburgh between the years 2000 and 2001. Although SCLC patients do not usually undergo surgical treatment, infrequently SCLC is confirmed by histology when a solitary pulmonary nodule is excised for diagnosis (39). Surgical excision is usually followed by systemic chemotherapy and these patients have a marginally better prognosis than limited disease SCLC treated with chemotherapy alone (39). However, surgical specimens provide a greater quantity of tumour material for immunohistochemical analysis and were therefore used initially.

Using a mouse anti-human monoclonal antibody (Clone 565 Novacastra), which binds to CD45 on the surface of mononuclear immune cells but does not bind to SCLC cells, paraffin-embedded sections from surgically resected SCLC tumours were probed. Sections were immunohistochemically stained and viewed with light microscopy (Fig. 6.1). All 10 SCLC patients had CD45 positive (CD45+) cells within the majority of tumour areas viewed, indicating the presence of mononuclear immune cells within the tumour microenvironment. CD45+ cells were observed within the stroma surrounding the tumour (identified as fibrous tissue and blood vessels with no tumour cells) and also infiltrating the tumour cells in all of the sections analysed (areas defined in fig. 6.1 a). The number of CD45+ cells in 10 high power (400x) tumour fields for each SCLC patient was counted. The mean number of CD45+ cells/field varied from 6.4 to 127.4 with a median of 72.6 for the 10 SCLC tumours analysed. This suggested a significant variation in the amount of CD45+ cell infiltrate within the tumour microenvironment between SCLC patients. To confirm that this was not due to an artefact of sampling, further tumour sections sampled from a different part of the tumour block were probed and stained, giving similar results. Unfortunately the limited size of this preliminary study precluded any analysis of patient or tumour factors to explain this variation.

Figure 6.1: SCLC Sections Are Variably Infiltrated By CD45+ Mononuclear Cells.



(A) SCLC tumour section (400x) stained with haemotoxylin - areas indicated are (1) tumour and (2) stroma. (B-F) Formalin-fixed, paraffin-embedded tissue sections were probed with mouse anti-human CD45 antibody, followed by secondary rabbit anti-mouse HRP and DAB substrate. (B-D) Representative pictures (400x) of CD45 positive cells within tumour sections from 3 different SCLC patients. (E) CD45 negative control (formalin-fixed, paraffin-embedded glioblastoma section). (F) CD45 positive control (formalin-fixed, paraffin-embedded tonsil section).

To further characterise the cellular composition of the CD45+ infiltrate, mouse anti-human monoclonal antibodies that bind specifically to surface markers on T-lymphocytes (CD3, CD4 and CD8), macrophages (CD68) and B-lymphocytes (CD20) were used to probe tumour sections from the 10 SCLC cases. Sections were then immunohistochemically stained and viewed with light microscopy (Figs. 6.2 – 6.6). 10 randomly selected high power fields (400x) containing tumour cells and a blood vessel were viewed and positive staining for each immune cell marker was graded using a numerical system; 1: zero cells/section, 2: 1-10 cells/section, 3: 11-50 cells/section and 4: >50 cells/section. Both tumour infiltrating (contact with more than 1 tumour cell) and stromal (in fibrous tissue surrounding tumour islets) immune cells were graded in this way.

10/10 SCLC patients had CD3+ T-lymphocytes in the tumour sections and the amounts varied between patients in a similar fashion to CD45+ cells (Fig. 6.2). Interestingly the distribution of CD3+ cells was different from CD45+ cells being predominantly in the tumour stroma rather than infiltrating the tumour cells; 7/10 SCLC patients had more CD3+ cells within the stroma than infiltrating the tumour cells. In addition the CD3+ T-cells did not appear to be predominantly clustered in organised lymphoid tissue as would be seen in normal lung.

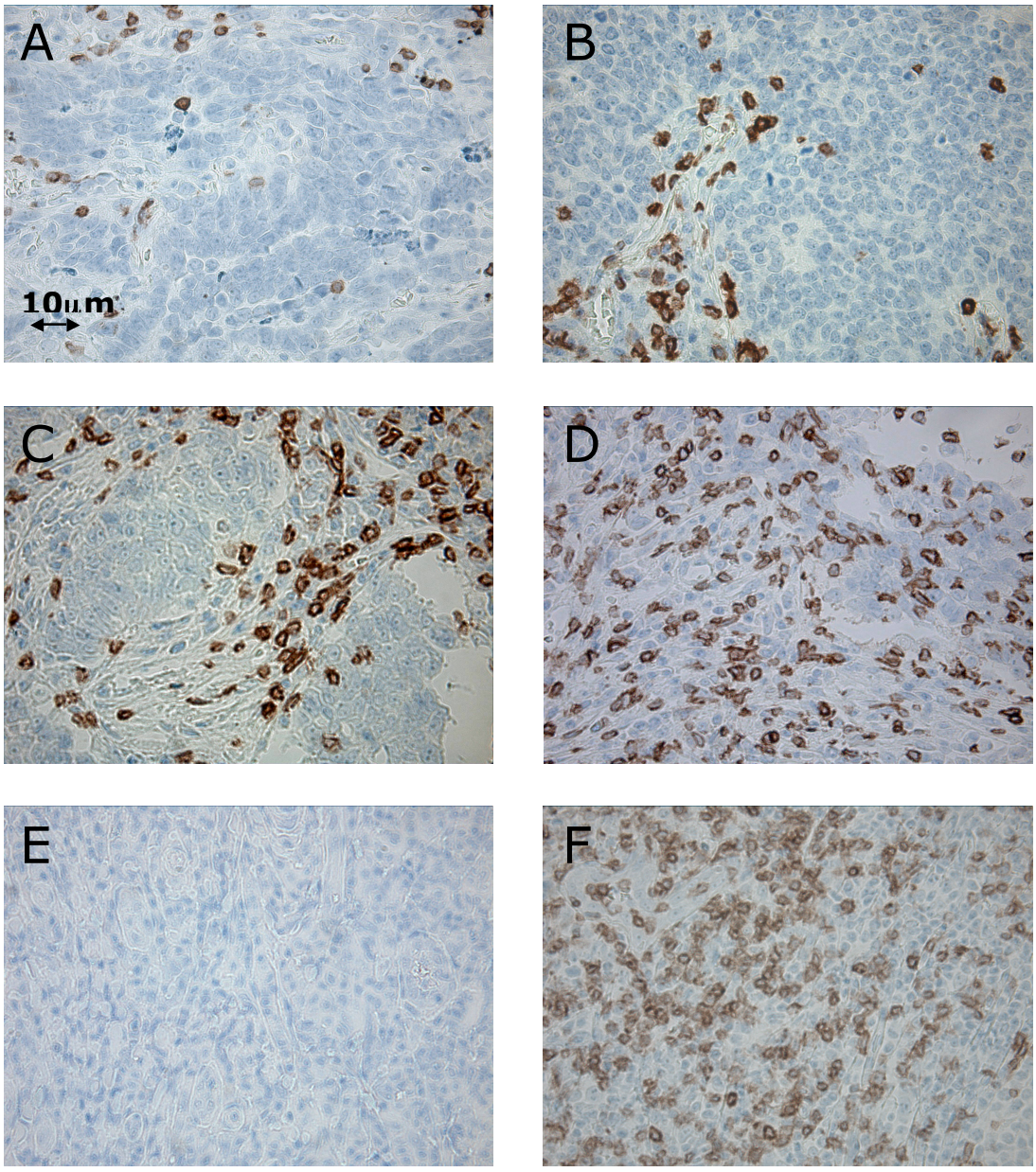
The CD3+ infiltrate was comprised of both CD4+ and CD8+ T-cells (Figs. 6.3 and 6.4). 6/10 patients had grade 2 or greater CD4+ T-cells in the SCLC sections analysed. CD4+ T-cells were observed both within the tumour stroma and infiltrating the tumour cells (Fig. 6.3). However a stromal distribution was observed more frequently (6/10 patients had greater CD4+ T-cell numbers in the stroma compared to within the tumour) suggesting a similar distribution to CD3+ cells. CD8+ T-cells were identified in 10/10 SCLC sections (grade 2 or greater) and were seen both in the tumour stroma and invading the mass of SCLC cells (Fig. 6.4). 8/10 patients had equal or greater numbers of CD8+ T-cells infiltrating the tumour mass compared to the peritumoural stroma. Interestingly 2/10 SCLC patients had intratumoral CD8+ T-cells but no identifiable CD4+ T-cells in the fields analysed suggesting that the types of T-cells that comprise the CD3+ intratumoral lymphocytes in SCLC can vary between patients. The significance of this is not clear from this preliminary study.

In addition to T-lymphocytes, macrophages were identified within SCLC sections using an antibody that reacts to human CD68 (Fig. 6.5). CD68+ macrophages were present (grade 2 or greater) in both the peritumoral stroma and within the tumour cells mass in 10/10 SCLC sections at. However, macrophages were seen more commonly within the stroma than infiltrating the tumour cell islets; 8/10 SCLC patients had greater numbers of CD68+ cells within the tumour stroma. Predictably, the number of macrophages varied between patients in a similar fashion to the number of CD45+ cells.

CD20+ B-cells were also sought within SCLC tumour sections. Despite adequate staining of the positive control a paucity of CD20+ staining in SCLC sections was observed (Fig. 6.6). CD20+ B-cells were observed in small numbers (no greater than grade 2) in only 2/10 tumour sections from SCLC patients and were predominantly confined to the tumour stroma. The presence of B-cells did not appear to correlate with the degree of CD45+ infiltrate.

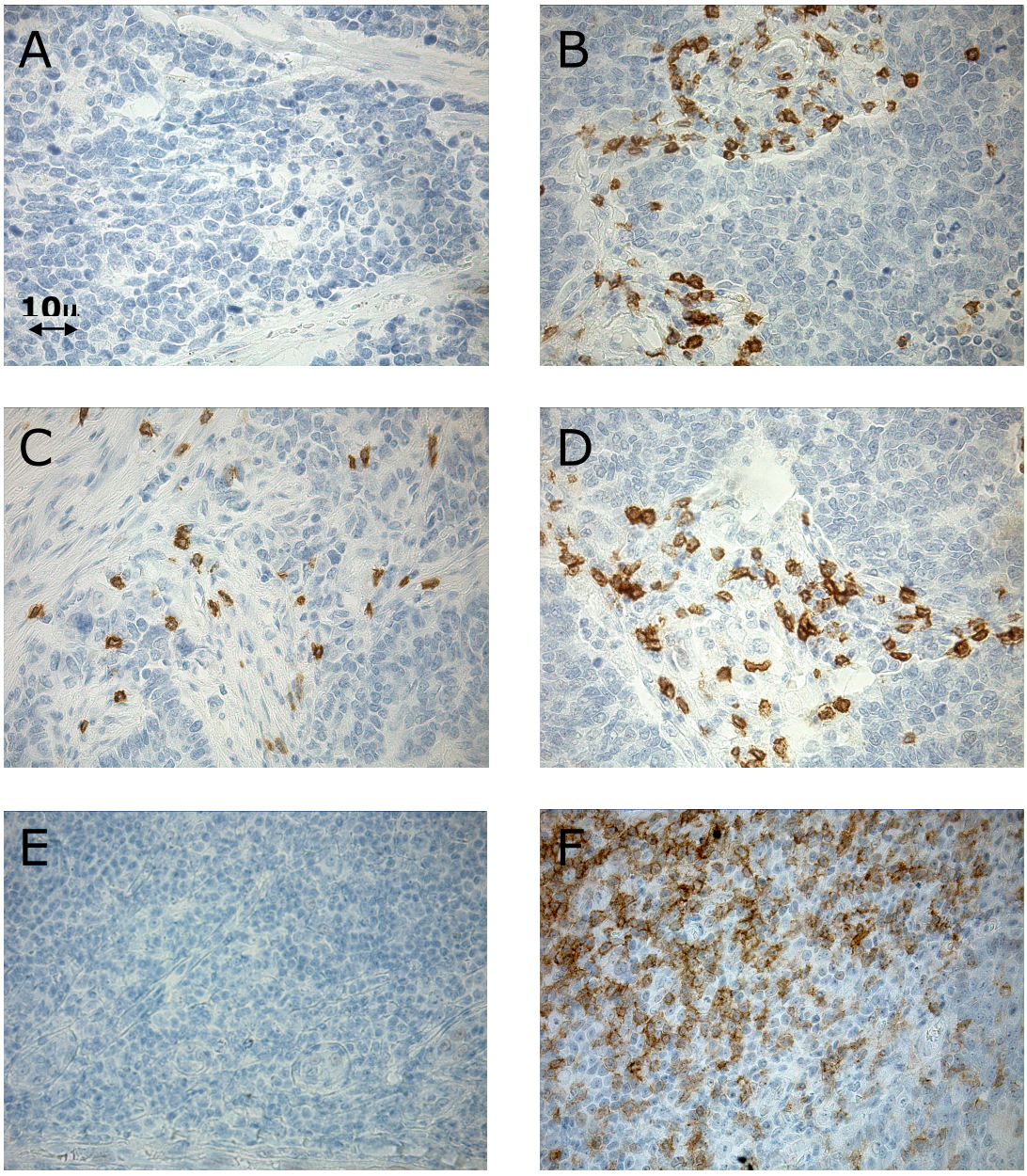
The abundance of CD3+ T-cells and CD68+ macrophages observed in this preliminary study suggests that these cell types comprise a significant component of the CD45+ infiltrate in SCLC sections. Similar findings have been described in other solid tumours (350-352). Interestingly in these studies significant variations in total mononuclear cell (CD45+) infiltrate were not observed. However, the data represented here suggests that tumour infiltration by CD45+ mononuclear cells (comprised of both T-cells and macrophages) varies considerably between SCLC patients suggesting significant differences in local tumour immune responses.

Figure 6.2: SCLC Sections Are Infiltrated By CD3+ T-Lymphocyte



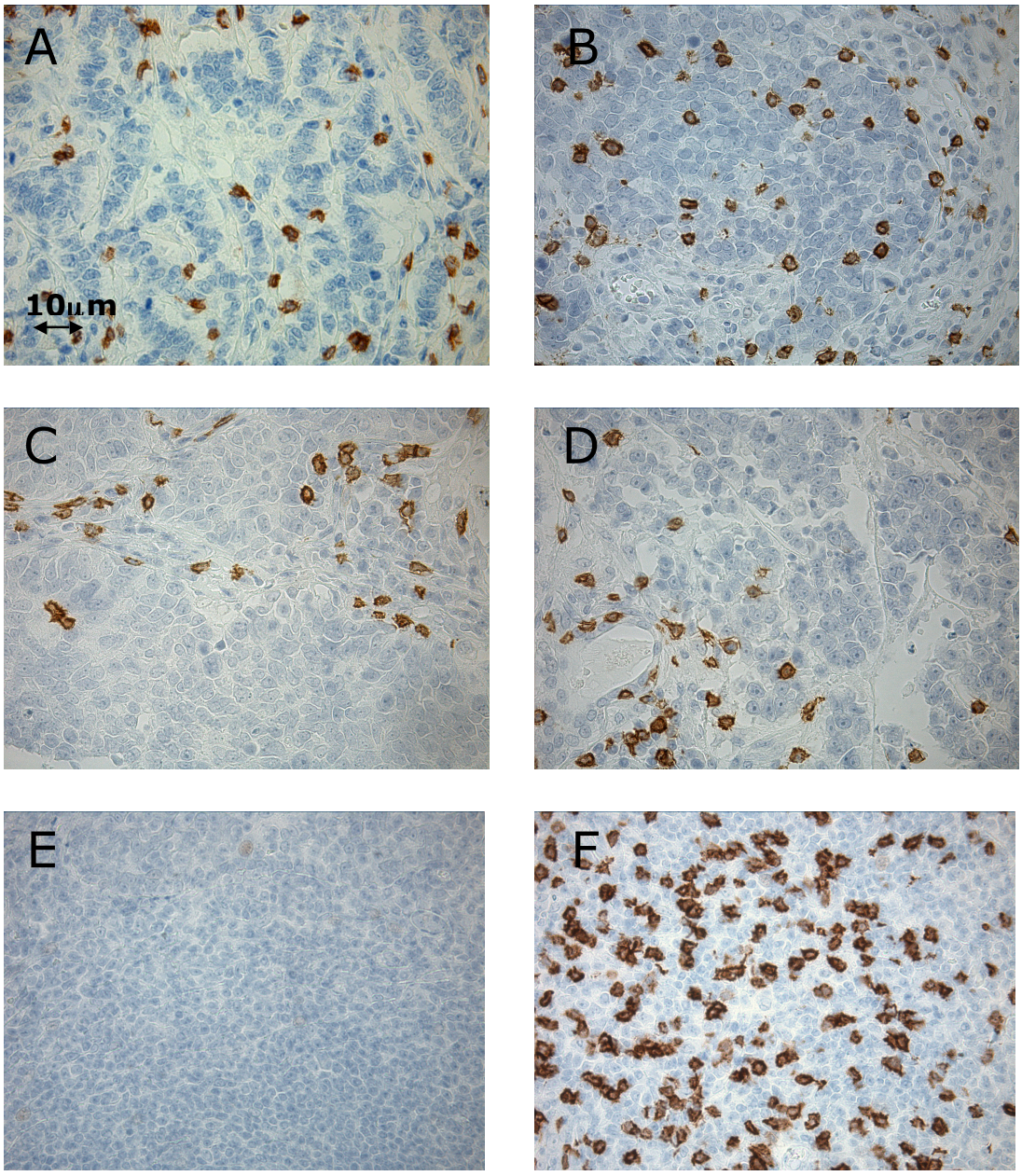
Formalin-fixed, paraffin-embedded tissue sections were probed with mouse anti-human CD3 antibody, followed by secondary rabbit anti-mouse HRP and DAB substrate. (A-D) Representative pictures (400x) of CD3 positive cells within tumour sections from 4 different SCLC patients. (E) CD3 negative control (formalin-fixed, paraffin-embedded glioblastoma section). (F) CD3 positive control (formalin-fixed, paraffin-embedded tonsil section).

Figure 6.3: SCLC Sections Are Infiltrated By CD4+ T-Lymphocytes.



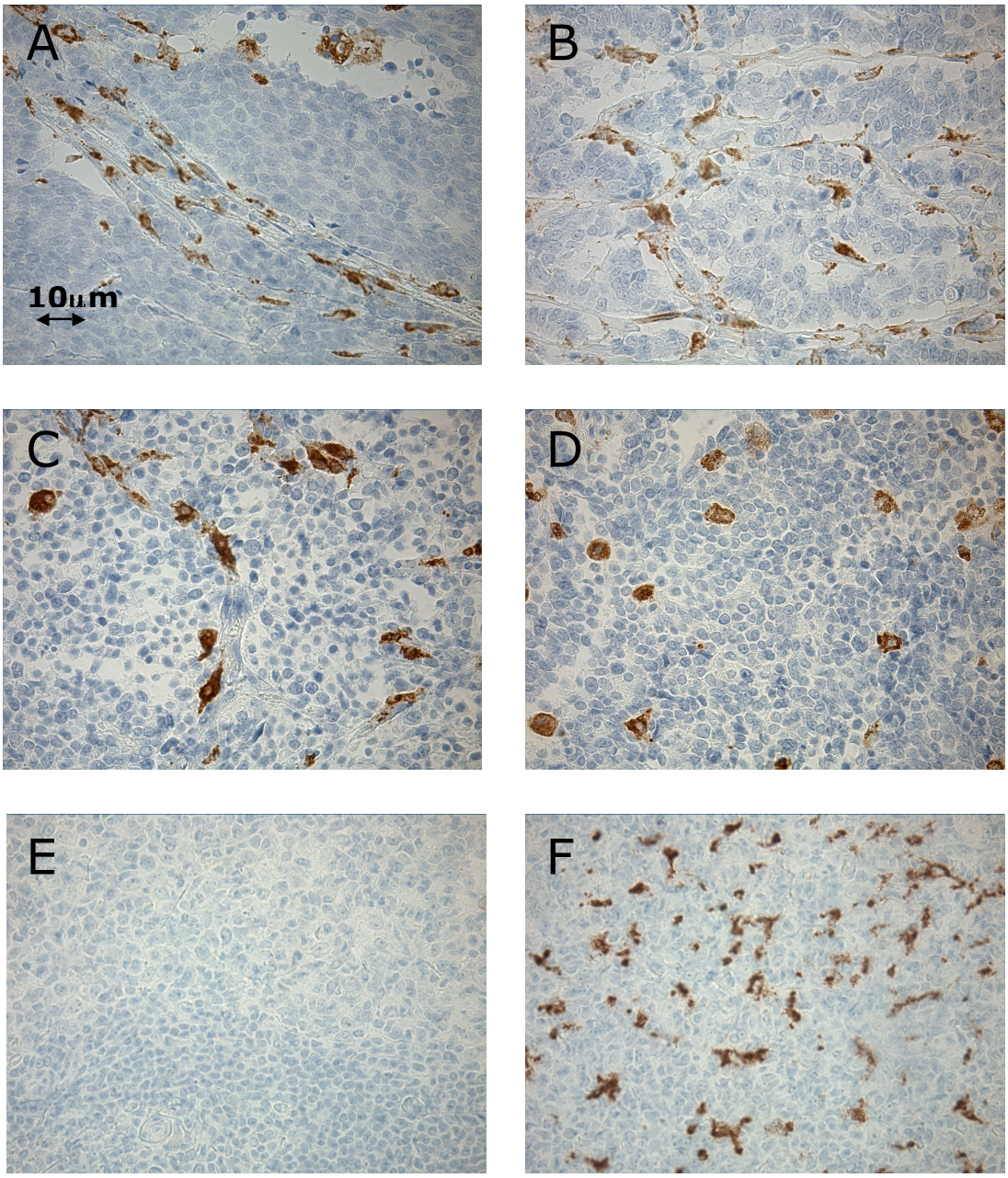
Formalin-fixed, paraffin-embedded tissue sections were probed with mouse anti-human CD4 antibody, followed by secondary rabbit anti-mouse HRP and DAB substrate. (A-D) Representative pictures (400x) of CD4 positive cells within tumour sections from 4 different SCLC patients. (E) CD4 negative control (formalin-fixed, paraffin-embedded glioblastoma section). (F) CD4 positive control (formalin-fixed, paraffin-embedded tonsil section).

Figure 6.4: SCLC Sections Are Infiltrated By CD8+ T-Lymphocytes.



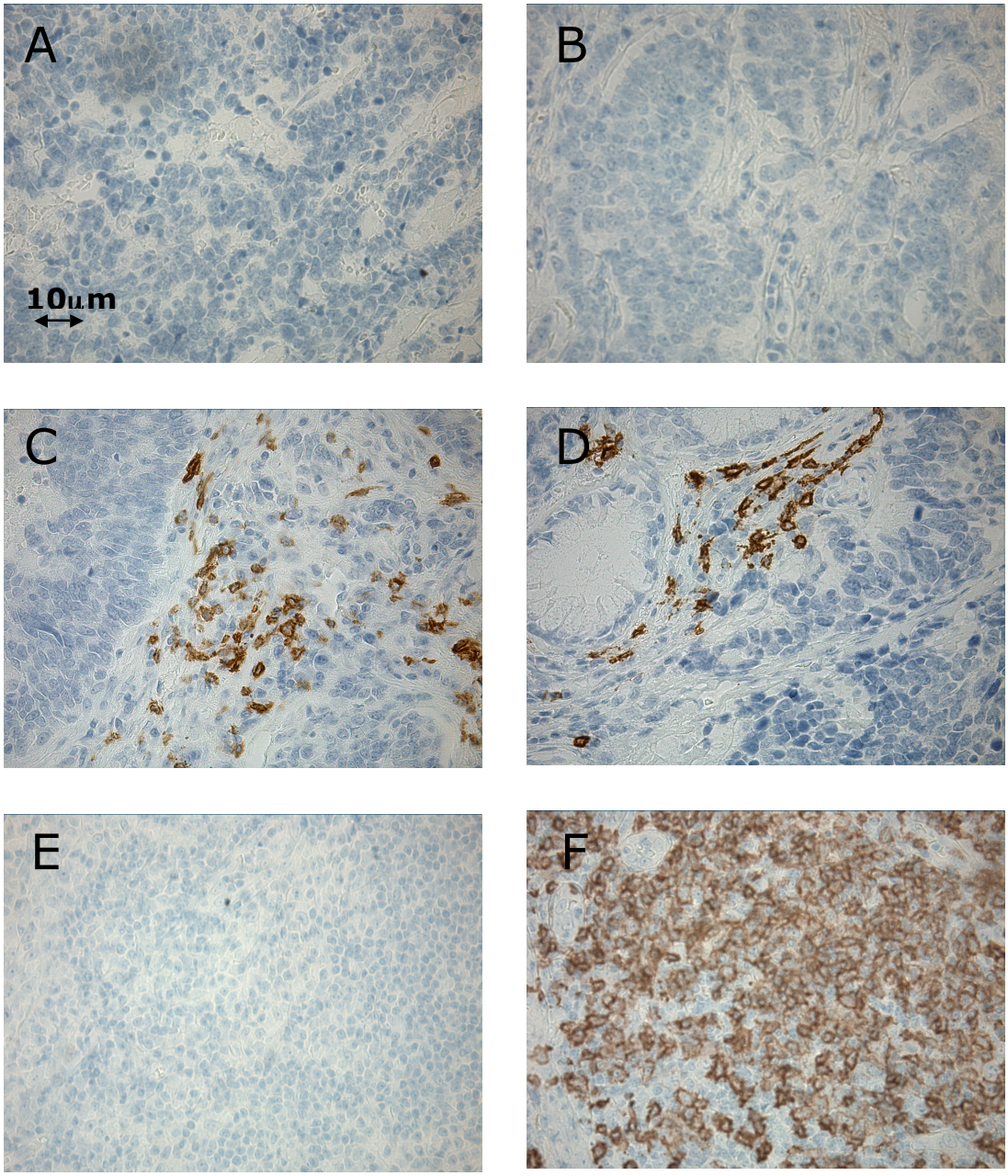
Formalin-fixed, paraffin-embedded tissue sections were probed with mouse anti-human CD8 antibody, followed by secondary rabbit anti-mouse HRP and DAB substrate. (A-D) Representative pictures (400x) of CD8 positive cells within tumour sections from 4 different SCLC patients. (E) CD8 negative control (formalin-fixed, paraffin-embedded glioblastoma section). (F) CD8 positive control (formalin-fixed, paraffin-embedded tonsil section).

Figure 6.5: SCLC Sections Are Infiltrated By CD68+ Macrophages.



Formalin-fixed, paraffin-embedded tissue sections were probed with mouse anti-human CD68 antibody, followed by secondary rabbit anti-mouse HRP and DAB substrate. (A-D) Representative pictures (400x) of CD68 positive cells within tumour sections from 4 different SCLC patients. (E) CD68 negative control (formalin-fixed, paraffin-embedded glioblastoma section). (F) CD68 positive control (formalin-fixed, paraffin-embedded tonsil section).

Figure 6.6: SCLC Sections Are Sparsely Infiltrated By CD20+ B-Lymphocytes.



Formalin-fixed, paraffin-embedded tissue sections were probed with mouse anti-human CD20 antibody, followed by secondary rabbit anti-mouse HRP and DAB substrate. (A-D) representative pictures (400x) of tumour sections from 4 different SCLC patients probed with anti-CD20 antibody. (E) CD20 negative control (formalin-fixed, paraffin-embedded glioblastoma section). (F) CD20 positive control (formalin-fixed, paraffin-embedded tonsil section).

6.2.2 The Presence Of A CD45-Positive Mononuclear Immune Cell Infiltrate Is Associated With Improved Survival In SCLC.

Prior research has indicated the importance of the immune system in controlling cancer growth and spread. In addition the local tumour immune cell infiltrate, including macrophages and lymphocytes has been shown to predict patient survival and response to treatment in a variety of solid tumours (181,350-352). SCLC patients display evidence of tumour specific immunity, the presence of which may improve patient outcome (353). Data here indicates the presence of CD45+ mononuclear cells in surgically resected SCLC tumour samples. A considerable variability in the amount of CD45+ cellular infiltrate between these cases is also observed. This infiltrate consists of macrophages and lymphocytes, both cell types that could affect local tumour growth and thus patient prognosis. Therefore, it was hypothesised that the amount of CD45+ infiltrate could predict patient survival in SCLC.

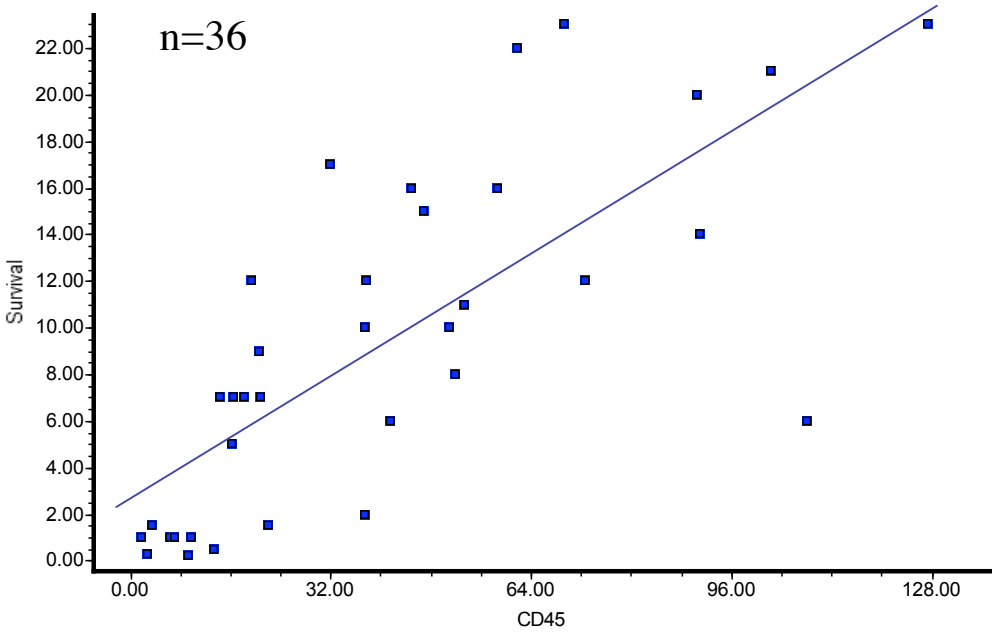
A retrospective analysis of 40 SCLC cases identified consecutively between the years 2000 and 2001 from the pathology archive at Lothian University NHS Trust was performed. In addition to the 10 resected SCLC cases described above, a further 30 SCLC cases diagnosed by either CT guided core biopsy of a lung lesion or bronchoscopic biopsy of an endobronchial tumour were identified. Fine needle aspirate specimens of lung lesions and biopsy material from other tumour sites including lymph nodes were not included. The histological diagnosis of SCLC was reconfirmed by Dr W. Wallace (consultant pathologist) in all cases prior to inclusion in the study. SCLC tumour sections were then probed with a mouse anti-human CD45 monoclonal antibody (Clone 565 Novacastra) and immunohistochemically stained. The average number of CD45+ cells/high power field was determined for each SCLC tumour sample; CD45+ cells were counted by two independent observers using light microscopy from at least 6 randomly selected high power fields (400x)/tumour sample. Fields were not counted if they did not contain tumour cells. In addition, information regarding demographics (age and sex), tumour stage, treatment, and survival (up to 24 months) was collated from patient records for each SCLC case.

The mean age at diagnosis for the 40 SCLC cases identified was 64.4 years. There was a predominance of males, with 26 out of 40 (65%) cases being of male sex. Smoking information was incomplete from patient records. Tumour stage information was available in all cases. 25 out of 40 (62.5%) patients had extensive disease as assessed by the clinical oncology and multi-disciplinary team. Median survival was 9.5 months and 4 out of 40 patients survived more than 2 years. Median survival for those patients with limited disease (LD) stage was 14 months and extensive disease (ED) stage was 7 months. The majority of patients received chemotherapy (29 out of 40) and 7 out of 15 LD stage patients also received radiotherapy to the mediastinum and cranium. Performance status (PS) was only recorded in 7 out of 40 patients and only 3 out of 40 patients had a serum LDH level measured. Thus, the study population was comparable in demographics and disease characteristics to patients with SCLC in the UK, although the data was incomplete regarding all known prognostic markers (4).

Initially it was determined whether the average number of CD45+ cells/high power field correlated with SCLC survival in months from diagnosis. Using a non-parametric test a significant correlation between average number of CD45+ cells/high power field and survival (up to 24 months) was found (Spearman $r = 0.8105$, $p<0.0001$) (Fig. 6.7). The median value for the average number of CD45+ cells/high power tumour field was 37.6 (range 1.9 to 127.4). This median value was used to divide the study population into two equal groups for further analysis; CD45 'low' (average number of CD45+ cells/high power field less than 37.6) and CD45 'high' (average number of CD45+ cells/high power field equal to or greater than 37.6). The univariate Kaplan–Meier method was used to determine the prognostic impact of the average number of CD45+ cells/high power field on survival in SCLC. Figure 6.8 shows survival curves for both groups. Median survival in the CD45 'low' group was 1.8 months compared with 16 months in the CD45 'high' group. Using a log rank test, a significant difference in survival between the two groups ($p< 0.0001$) was observed. In addition, a significant difference in survival curves for extensive (ED) and limited (LD) stage ($p<0.05$) was observed in keeping with other published data (81). No difference in survival was found for age ($p=0.1477$) or sex ($p=0.2$). Importantly, no association was observed between CD45+ infiltrate (low/high) and

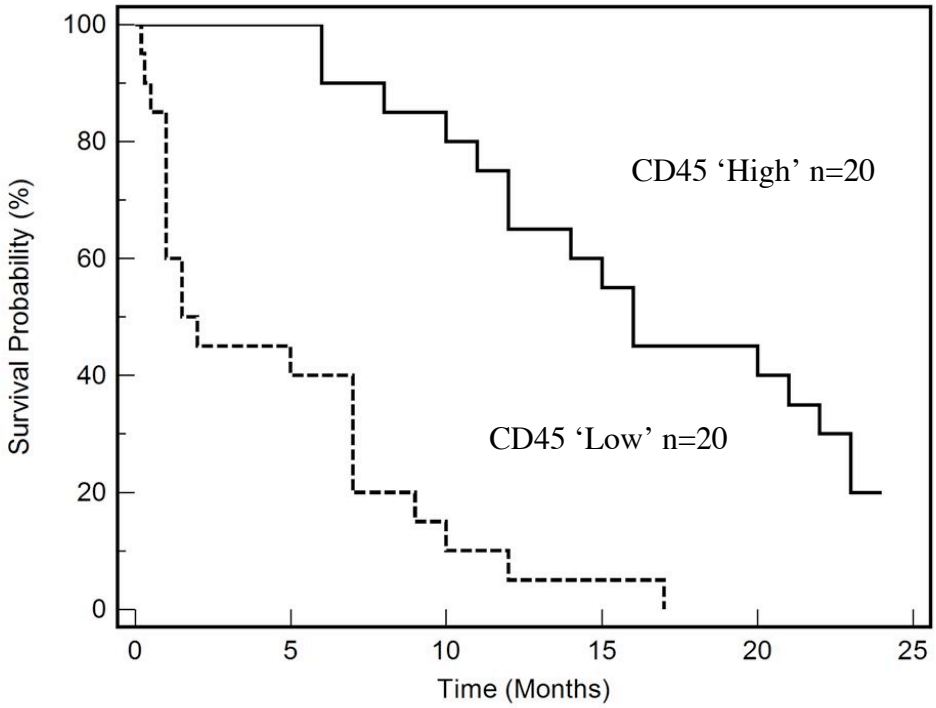
tumour stage (LD/ED) (Fisher's exact test; two tailed; p=0.1908). Furthermore, multivariate analysis (Cox proportional-hazards model) of age (</equal to 65 or >65), sex (male/female), stage (LD/ED) and CD45+ infiltrate (low/high) indicated that CD45 'high' immune cell infiltrate in tumour sections significantly and independently correlated with survival in SCLC (p<0.0001). Unfortunately due to the lack of data, it was not possible to determine whether the degree of CD45+ infiltrate was associated with patient health as indicated by performance status. However, this data suggests that average number of CD45+ cells/high power tumour is an independent prognostic factor for SCLC.

Figure 6.7: X-Y Scatter Plot Showing Correlation Between Average Number Of CD45+ Cells/High Power Tumour Field And Survival In SCLC.



Formalin-fixed, paraffin-embedded tumour sections from 40 SCLC cases were probed with mouse anti-human CD45 antibody, followed by secondary rabbit anti-mouse HRP and DAB substrate. The average number of CD45 positive cells/high power (400x) field for each SCLC case was determined by counting using light microscopy. Survival from diagnosis for each case was determined up to 24 months. 4 cases survived greater than 24 months and were excluded from analysis. Scatter graph shows average number of CD45 positive cells/field (CD45) on the X axis with survival in months (survival) on the Y axis. There is a significant correlation between average number of CD45+ cells/high power field and survival (Spearman r = 0.8105, p<0.0001).

Figure 6.8: Kaplan-Meier Survival Curves For 40 SCLC Cases Separated Into Equal CD45 'High' And CD45 'Low' Groups.



Formalin-fixed, paraffin-embedded tumour sections from 40 SCLC cases were probed with mouse anti-human CD45 antibody, followed by secondary rabbit anti-mouse HRP and DAB substrate. The average number of CD45 positive cells for each SCLC case was determined by counting the number of CD45 positive cells in at least 6 high power fields (400x) using light microscopy. Survival from diagnosis for each case was determined up to 24 months. Using a median cut-off (37.6 CD45+ cells/field) the SCLC cases were divided into equal groups; CD45 'Low' (<37.6 CD45+ cells/field) and CD45 'High' (equal to or > 37.6 CD45+ cells/field). The graph shows survival probability against time to death in months for the two groups plotted using the Kaplan-Meier method. A significant difference in survival between the two groups was observed ($p < 0.0001$).

5.3 Discussion.

It is widely accepted that tumour development occurs due to the accumulation of genetic alterations in normal tissue cells allowing uncontrolled growth and subsequent malignant transformation (357). However, for these cancer cells to survive a variety of changes need to occur in the surrounding normal tissue to create a permissive tumour microenvironment (164,166,180). This, in many aspects, reflects a chronic inflammatory response and is actively promoted by the developing tumour (164). The components of the tumour microenvironment have been studied and a variety of non-cancer cell types have been identified including endothelial cells forming new blood vessels, activated fibroblasts and immune cells. These cells interact with extracellular matrix within the tumour stroma and transformed cells, facilitating cancer survival, growth and spread. Understanding this complex host reaction to the tumour is critical to the development of new anti-cancer therapies.

Of the non-cancer cells in the tumour microenvironment, the most extensively studied has been the immune cell infiltrate in solid malignancies, including breast, colon, ovarian and non-small cell lung cancer (358). These studies have provided valuable information about the local immune reaction to such tumours and the role of inflammation in cancer development. In contrast, the local immune cell infiltrate in SCLC has not been extensively studied with previous research focusing on systemic immune defects in SCLC patients. Thus, the initial aim of the work described in this chapter was to define the immune cell content of the SCLC microenvironment, using resected tumour sections probed with monoclonal antibodies against mononuclear immune cells (CD45), T-lymphocytes (CD3, CD4 and CD8), B-lymphocytes (CD20) and macrophages (CD68). The results presented here indicate the presence of a CD45+ mononuclear immune cell infiltrate in the human SCLC microenvironment. This immune cell infiltrate consists of T-lymphocytes (both CD4+ and CD8+) and macrophages (CD68+), although there is a paucity of B-lymphocytes (CD20+). These observations are in direct agreement with a study of surgically resected SCLC tumours reported in 2000, which demonstrated a predominance of T-lymphocytes and macrophages infiltrating cancer cells (190). Interestingly, a much earlier investigation in SCLC suggested that there was a paucity of local immune cell infiltrate (359). The data presented here clearly demonstrates the presence of an

immune cell infiltrate in SCLC tumour sections. This may reflect the use of resected SCLC tumours, which allow a more careful and exhaustive analysis of immune cell infiltrate or the use of monoclonal antibodies to specifically detect macrophages and lymphocytes. Unfortunately, surgical resection is rare, thus this type of clinical material is sparse and may not reflect 'typical' SCLC. Further studies should be conducted on endobronchial or CT guided biopsy material.

The data shown here indicates that the quantity and distribution of T-cell subtypes within the SCLC microenvironment differs. CD8+ T-cells were observed in greater numbers than CD4+ T-cells. Furthermore, CD4+ T-cells were found predominantly in the tumour stroma, in contrast to CD8+ T-cells, which were more prominent in the tumour mass/islets. This has frequently been observed in other cancers and is in contrast to non-malignant inflammatory reactions were an excess of CD4+ T-cells is observed (360). A paucity of B-lymphocytes was also observed in all SCLC tumour sections examined. B-cells are uncommonly found in other solid malignancies although a plasma cell infiltrate has been observed in cervical and breast cancer (361,362). The role of these cells is uncertain and the majority of antibody-producing B-cells are assumed to reside in tumour draining lymph nodes. The distribution of CD68+ macrophages in the microenvironment of SCLC is also similar to that observed in other solid malignancies (363). These findings suggest that the observation of a mononuclear immune cell infiltrate within the SCLC microenvironment represents a specialised host response to cancer cells rather than a non-specific inflammatory reaction. Unfortunately, these data do not indicate the role of these cells in SCLC growth, spread and response to treatment.

Studies in other malignancies have attempted to determine the contribution of the local tumour immune cell infiltrate to cancer pathogenesis by correlating observations with patient outcome. In human ovarian and prostate cancer the presence of tumour infiltrating T-lymphocytes (TIL) has been shown to predict a favourable patient prognosis (352,364). It has been postulated that improved prognosis reflects control of cancer growth and spread through T-cell mediated cancer cell lysis (358). Studies have also investigated the role of tumour-associated macrophages (TAM). In breast cancer, a high TAM density has been clearly correlated with reduced disease free survival (365). In contrast, a high density of

peritumoural macrophage infiltration has been strongly correlated with reduced lymph node metastases and improved survival in colon cancer (366). Currently, there is limited published data on the role of the immune cell component of the tumour microenvironment in SCLC growth or spread. Older studies of immune prognostic factors in SCLC have typically focused on the defects in peripheral immunity (e.g. lymphocyte proliferation). At best these demonstrate poorer survival in patients with impaired systemic immunity that is difficult to dissociate from tumour burden (189,356). The only investigation directly examining the prognostic significance of tumour infiltrating immune cells in SCLC was performed on n=56 SCLC cases that were treated surgically (190). The results from this study indicate that small tumour size and improved patient survival correlate with high numbers of tumour infiltrating lymphocytes and macrophages (190). Unfortunately this study was performed on an unusual cohort of SCLC cases (being surgically treated) and there is no description of patient characteristics (190). However, these results suggest that the local immune cell infiltrate in SCLC may play a crucial role in control of cancer growth.

The initial investigation of surgically resected SCLC tumour sections reported in this chapter indicates a marked variability in the degree of CD45+ infiltrate between cases. This observation was therefore extended to include another 30 ‘typical’ SCLC cases identified from the pathology archive at Lothian University NHS trust. Interestingly, it was found that the amount of mononuclear immune cell infiltrate (number of CD45+ cells per high power field) correlated strongly with patient survival. In addition, the degree of CD45+ cell infiltrate was not associated with other well-described prognostic markers including patient age, sex or SCLC stage. Crucially, using a univariate Kaplan-Meier analysis and a multivariate Cox proportional-hazards analysis, high numbers (>37.6) of CD45+ cells per tumour field were shown to independently predict a favourable patient outcome. These results suggest that the local immune cell infiltrate in SCLC represents a host anti-tumour response, which may prolong disease free survival after treatment. Unfortunately, the significance of this observation remains unclear for several reasons which merit further discussion.

Firstly, this is a relatively small study (n=40) and includes 10 patients who had surgical resection of their lung tumours for diagnostic purposes and may therefore

not truly represent a 'typical' SCLC population. Despite this, age, sex, stage and oncology treatment was similar to other published SCLC data. Extension of the study to include larger numbers would address this. Secondly, information on performance status was lacking from this study due to inaccurate patient records. Performance status (PS) is rated on a 0-4 scale and gives an overall assessment of patient functional ability and health (367). It is well defined as a prognostic indicator in SCLC (81). Clearly, correlation of CD45+ cell numbers with PS is important as it could indicate whether local immune cell infiltrate was reduced non-specifically in those patients who are less well (higher PS) and more likely to die quickly from SCLC cancer. Thirdly, staging data in SCLC is less comprehensive than in other tumours that rely on the TMN system. Thus, although it is simple to determine limited and extensive disease stages from retrospective analysis of case notes disease burden varies considerably. For example, it is possible to have extensive disease with a small peripheral lung tumour and a solitary liver metastasis and limited disease with extensive mediastinal lymph node involvement. Therefore correlating immune cell infiltrate with SCLC stage does not represent the volume or loco-regional spread of cancer. A prospective study with records of PS and TMN staging would address these two concerns. Finally, the data reported in this chapter did not focus on the role of specific immune cell types in SCLC survival. This is of crucial importance, as the identification of different immune cells that contribute positively or negatively to SCLC prognosis could direct future immunotherapy development. The data reported in 2000 on surgically treated SCLC indicates that the role of tumour infiltrating CD8+ T-cells and macrophages should be examined (190). This could be extended to include regulatory T-cells, which have been shown in other tumours to correlate with poor survival (368-370). It is predicted that a predominance of regulatory T-cells may be observed in the microenvironment of SCLC cases with poor local immune response (i.e. reduced CD45+ infiltrate) suggesting a mechanism for SCLC immune suppression.

In conclusion, the data represented in this chapter provides further insight into the immune cell component of the SCLC microenvironment. Future studies should prospectively recruit SCLC patients, include immunohistochemical analysis of immune cell phenotype, tumour cell apoptosis, proliferation and angiogenesis and

correlate observations with disease-free survival, to provide a comprehensive analysis of the role of tumour infiltrating immune cells in SCLC pathogenesis. The results shown here indicate that this type of analysis may be performed on routinely acquired endobronchial and CT guided biopsy material increasing the clinical applicability of such research.

CHAPTER 7: Small Cell Lung Cancer Cells Suppress Cell-Mediated Immune Responses *In Vitro*.

7.1 Introduction.

The host immune system is an attractive target for the development of novel anti-cancer therapy. This is supported by the presence of immune cells in solid cancers that can be expanded to selectively eliminate tumour cells and the demonstration of tumour-associated antigens that can induce specific anti-tumour immune responses (182,185,360,371). Unfortunately, immunotherapy has met with limited success in clinical trials, in part because, despite recognition by the immune system, tumours can evade immune responses (184). Thus, the mechanisms by which cancer cells can suppress or subvert immune cell functions have been of recent interest.

The presence of a tumour specific immune response in SCLC has been suggested by case reports of SCLC complicated by neurological paraneoplastic syndromes, in which serum antibodies are detected that bind to surface proteins on both SCLC cells and neurons (36,186,353,354). These patients show an improved prognosis and a small proportion have been reported to show spontaneous tumour regression (186). Thus, it is possible that the presence of antibodies to SCLC cell antigens and spontaneous tumour regression indicates an effective anti-tumour immune response. However this is not observed in the majority of patients (186). In addition, SCLC patients frequently display signs of immuno-compromise suggesting that SCLC cells may adversely influence the behaviour of the immune system allowing unregulated tumour growth.

Early studies in SCLC patients have demonstrated several important defects in peripheral cell-mediated immune responses. SCLC patients have been shown to display the least skin delayed-type hypersensitivity (DTH) reactions of all lung tumour types (356). Defects in peripheral blood lymphocytes (PBL) numbers (high CD4/CD8 ratio) from patients with SCLC have been observed (372). PBLs from SCLC patients have been shown to display reduced proliferative responses and secretion of IL-2 and macrophage-activating factor in response to phytohaemagglutinin (PHA) than lymphocytes from healthy volunteers (187). Furthermore low IL-2 secretion by PBLs has been demonstrated to predict poor

survival in SCLC (188,189). Interestingly in one study IL-2 secretion was shown to return to normal when the tumour load was reduced (188). This data suggests that SCLC can alter immune cell function dramatically with effects detectable distant from the tumour site.

Defects in the local immune response to SCLC have also been demonstrated. Histological analysis of lung cancer tumour sections has revealed a paucity of inflammatory infiltrate in SCLC compared to other lung tumours (359). Subsequently, it has been shown that alveolar macrophages from bronchoalveolar lavage (BAL) specimens of SCLC patients poorly stimulate peripheral blood lymphocytes compared with healthy volunteers (373). In addition, alveolar macrophages from SCLC patients show reduced phagocytosis, reduced production of cytokines (TNF-α, IL-1 and IL-6), and reduced expression of major histocompatibility complex (MHC) class II antigen, ICAM-1 and CD83 (374). Using selectively cultured lymphocytes (using IL-2) and cancer cells from lung cancer specimens, it has been demonstrated that whilst lymphocytes from NSCLC patients were able to efficiently lyse autologous cancer cells those isolated from SCLC specimens were ineffective (375). Furthermore, data presented in chapter 6 of this thesis indicate that the local immune cell infiltrate in tumour sections varies between SCLC cases and correlates with survival. Taken together, these results suggest that specific defects are present in the cellular immune response of SCLC patients, which may in part be mediated by interaction of SCLC cells with immune cells in the local tumour microenvironment.

It has been shown that MHC class I antigens are expressed at very low levels on SCLC cells and in SCLC tumour sections (376). The loss of expression has been attributed to a defect in transporters associated with antigen presentation (TAP) alleles (377). MHC class I is required for tumour antigen presentation by SCLC and subsequent cytotoxic T-lymphoctye-mediated tumour cell lysis (378). Thus, down regulation of MHC class I may represent an important mechanism for evasion of immunosurveillance and may be selected for early in tumour development. MHC class I expression can be induced in SCLC cell lines *in vitro* by transfection with the interferon gamma (IFN-γ) gene, thus promoting antigen presentation to cytotoxic T-cells (379). Unfortunately a phase III clinical trial of recombinant IFN-γ in 179

chemo-responsive SCLC patients showed no survival benefit over best supportive care (380). The failure of IFN-γ to produce any clinical effect may indicate the presence of other immunosuppressive or -subversive mechanisms. It has been shown that SCLC cells can produce soluble factors, which may mediate immunosuppression (381,382). Serum extracted from patients with SCLC has been shown to suppress *in vitro* antibody production and the ability of T-lymphocytes to form rosettes with sheep erythrocytes (381). In addition, a protein component of the supernatants from SCLC cell lines has been shown to suppress PBL proliferative responses to PHA (382).

It is clear that before effective immunotherapy can be developed for SCLC further understanding of the mechanisms of immune suppression is required. Thus, an *in vitro* co-culture of peripheral blood mononuclear cells from healthy donors and human SCLC cell lines was established to determine the mechanisms by which SCLC cells could alter immune cell function.

7.2 Results.

7.2.1 H69 And H345 SCLC Cells Suppress Proliferation Of A Mixed Leukocyte Reaction.

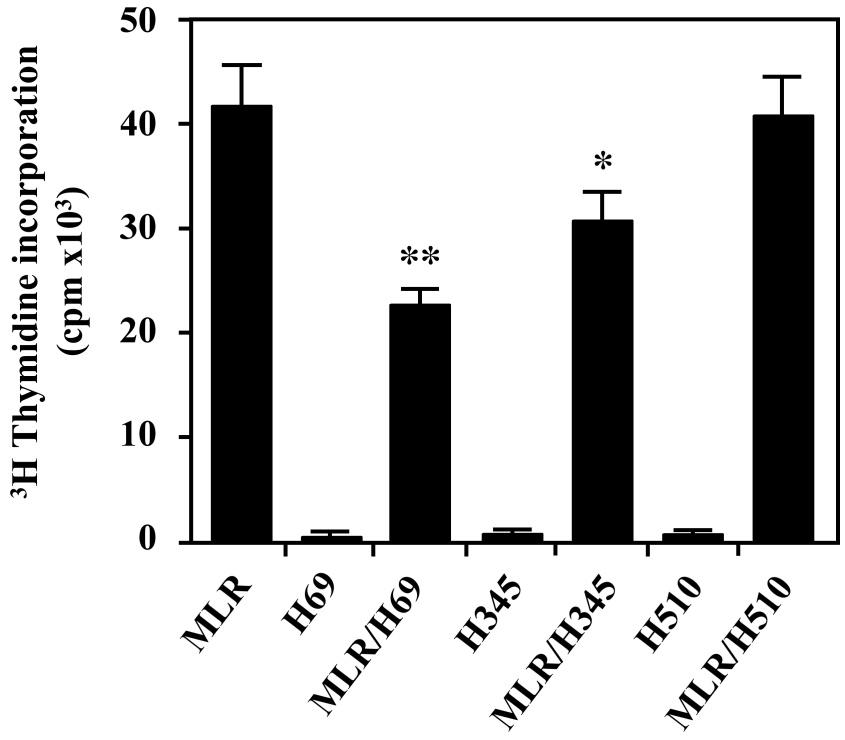
Prior research has demonstrated suppression of peripheral blood lymphocyte responses and delayed-type hypersensitivity in SCLC cases that predict patient survival, indicating that defects in cell-mediated immunity may be important in SCLC pathogenesis (187-189,356,372). The mixed leukocyte reaction is a widely used *in vitro* assay for functional studies of cellular immunity (383). It allows the activation of responder cells to alloantigens presented by stimulator cells to be measured by uptake of ^{3}H-thymidine, which is incorporated into newly synthesised DNA (383). Thus, this assay was used to determine whether the local interaction of SCLC cells with immune cells could suppress cell-mediated immune responses.

Peripheral blood mononuclear cells (PBMCs) were prepared from the blood of healthy human donors by layering over a polysaccharide gradient and subsequent centrifugation as described in chapter 2. Mixed leukocyte reactions (MLRs) were established by combining equal numbers of PBMCs from two separate donors (5 x 10^4 cells/donor) with Con A (5μg/ml) in a 96 well plate. To determine whether SCLC cells could suppress this cell-mediated immune response, cell lines derived from human SCLC tumours (H69, H345 and H510) were treated with mitomycin C (50μg/ml) and co-cultured with the MLR at a 1:1 ratio (1 x 10^5 SCLC cells: 1 x 10^5 mixed leukocytes). Proliferation of responder cells was determined at 72 hours by uptake of ^{3}H-thymidine.

As expected, MLRs stimulated with Con A (5μg/ml) actively incorporated ^{3}H-thymidine at 72 hours (42709 +/- 4173 cpm; mean of n=7 independent experiments +/- SEM) (Fig. 7.1). Importantly, SCLC cell lines treated with mitomycin C (50μg/ml) did not significantly uptake ^{3}H-thymidine (Fig. 7.1). However, co-culture of mitomycin C treated H69 and H345 SCLC cells resulted in a significant reduction in MLR ^{3}H-thymidine uptake (22260 +/- 1259 cpm, $p< 0.01$ and 30042 +/- 2570 cpm, $p<0.05$ respectively; mean of n=7 independent experiments +/- SEM) (Fig. 7.1). Interestingly, H510 SCLC cells did not significantly suppress MLR uptake of ^{3}H-thymidine (41495 +/- 4031 cpm, $p=0.837$; mean of n=7 independent experiments

+/- SEM) (Fig. 7.1). This data indicates that these observed effects are not due non-specific effects of co-culture such as toxic inhibition by mitomycin C or use of nutrients by SCLC cells. Instead, the results suggest that specific SCLC cell lines can suppress cell-mediated immune responses.

Figure 7.1: H69 And H345 SCLC Cell Lines Suppress ^{3}H-Thymidine Uptake By A Mixed Leukocyte Reaction.



Mixed leukocyte reactions were established by combining peripheral blood mononuclear cells from two separate healthy donors (5 x10^{4} cells/donor, 1x10^{5} cells in total) in 96 well plates with Con A (5μg/ml). Mixed leukocyte reactions were cultured alone (MLR) or with 1 x10^{5} mitomycin C treated SCLC cells (H69, H345 or H510) and activation of responder cells determined at 72 hours by uptake of ^{3}H-thymidine. The graph represents mean ^{3}H-thymidine uptake (counts per minute; cpm) for n=7 independent experiments +/- SEM. * indicates $p<0.05$ and ** $p<0.01$.

7.2.2 H69 and H345 SCLC Cell Lines Suppress Proliferation of Human CD4+ T-Cells.

The data presented above indicate that SCLC cell lines can suppress cell-mediated immunity *in vitro*. The mixed leukocyte reaction is a functional assay but involves different cell types including antigen presenting cells and lymphocytes. In order to investigate the mechanisms by which SCLC cells suppress cell-mediated immune responses it was necessary to examine the effects on specific immune cells types. The important effector cells for generating an anti-tumour response in SCLC are not known. However, research in other tumours indicates an important role for T-cells.

T-lymphocytes are broadly categorised into two groups based upon the surface expression of CD4 and CD8 (181). The CD4+ T-cell subset contains both the helper T-cells which co-ordinate immune responses and enable generation of effective cell-mediated and humoral immunity and regulatory CD4+ cells which can down-regulate immune responses (384). CD8+ T-cells mediate MHC class I restricted cytotoxicity and have been shown to have an important role in the immune response to many solid tumours (385). Prior research has also indicated a central role for CD4+ T-cells in cancer immunity. Tumour specific CD4+ T-cells that recognise tumour antigens have been demonstrated and can migrate to tumour sites (386). CD4+ T-cells have been demonstrated to be important for tumour rejection. Vaccination of mice with irradiated tumour cells prior to live tumour cell inoculation, results in markedly reduced/absent tumour growth, i.e. tumour rejection (387). Importantly, in these experiments CD8-/- knockout mice can still reject tumours in contrast to CD4-/- knockout mice that fail to do so (387). CD4+ T-cells may also act as effector cells early in anti-tumour immunity, a mechanism dependent on IFN-γ, which may be particularly important in low MHC class I expressing tumours (e.g. SCLC) (388). In contrast, promotion of CD4+CD25+ regulatory T-cells (Tregs) may represent a key mechanism by which solid tumours can evade effective immune responses (181,389). Given the importance of CD4+ T-cells in cell-mediated anti-tumour immunity, the effect of SCLC cell lines on CD4+ T-cell activation was investigated.

Human CD4+ T-cells were purified from healthy blood donor PBMCs using a magnetic bead negative selection technique as described in chapter 2. This routinely produced CD4+ T-cell purities (assessed by flow cytometry) in excess of 94%. To investigate the effect of SCLC cells on CD4+ T-cell proliferation, co-culture experiments were established. In 96 well plates, CD4+ T-cells (2 x 10^5 cells/well) activated with immobilised anti-CD3 (5μg/ml) and soluble anti-CD28 (1μg/ml) were cultured alone or in combination with equal numbers of mitomycin C treated (50μg/ml) SCLC cells (H69, H345 or H510 lines). CD4+ T-cell proliferation was assessed after 72 hours by uptake of ^{3}H-thymidine. As expected, anti-CD3/CD28 stimulation of CD4+ T-cells produced a marked uptake of ^{3}H-thymidine at 72 hours (122380 +/- 6708 cpm; mean n=12 experiments +/- SEM). However, CD4+ T-cells activated with anti-CD3/CD28 in co-culture with H69 SCLC cells showed significantly less ^{3}H-thymidine uptake (89556 +/- 4403 cpm; mean n=12 experiments +/- SEM $p<0.01$) (Fig. 7.2 a and 7.2 b). This occurred despite inactivation of the H69 SCLC cells as indicated by low ^{3}H-thymidine uptake at 72 hours. Co-culture of CD4+ T-cells with H345 SCLC cells also caused a trend towards suppression of T-cell proliferation as indicated by reduced ^{3}H-thymidine uptake at 72 hours although the difference between the means was not significant (123985 +/- 8393 compared with 97677 +/- 10560; mean of n=9 experiments +/- SEM, p=0.0689) (Fig. 7.2 b). H510 SCLC cells had no significant effect on CD4+ T-cell proliferation in response to anti-CD3/CD28 (Fig. 7.2 b).

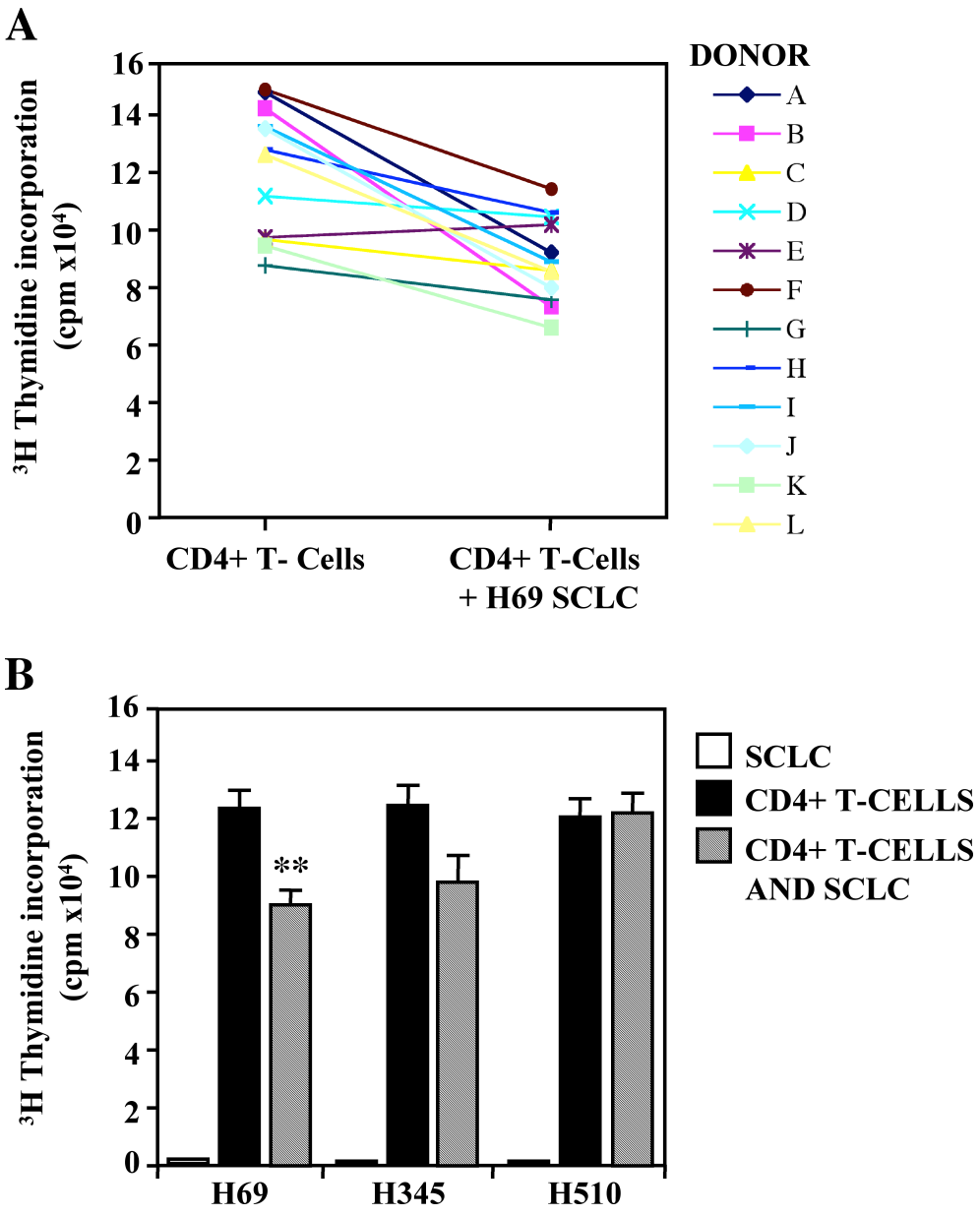
It is apparent from analysis of 10 resected SCLC tumours that the ratio of SCLC cells to CD4+ T-cells is frequently greater than 1:1 (see chapter 6). Therefore, in order to represent the tumour microenvironment more accurately, CD4+ T-cells were co-cultured with greater numbers of SCLC cells. In 96 well plates, 1 x 10^5 human CD4+ T-cells activated with anti-CD3/CD28 were cultured alone or with 1, 2 or 4 x 10^5 mitomycin C inactivated H69 SCLC cells. T-cell proliferation was determined by ^{3}H-thymidine uptake at 72 hours. As previously described CD4+ T-cells stimulated with anti-CD3/CD28 alone showed active uptake of ^{3}H-thymidine (131279 +/- 8114; mean cpm +/-SEM n=6 experiments) (Fig. 7.3a). Co-culture with 1 x 10^5 H69 SCLC cells did not significantly suppress CD4+ T-cell proliferation (111297 +/- 1378, p = 0.057). However, CD4+ T-cells co-cultured with 2 and 4 x10^5 H69 SCLC cells/well

showed significant suppression of ^{3}H-thymidine uptake compared to CD4+ T-cells alone (95378 +/- 6016, $p < 0.01$ and 61612 +/- 8675, $p < 0.001$ respectively; mean cpm +/- SEM n=6 experiments) (Fig. 7.3 a).

In the initial experiments described, H345 and H510 SCLC cell lines did not significantly affect CD4+ T-cell activation. To investigate whether greater numbers of these SCLC cell lines could suppress CD4+ T-cell activation, the experiments were repeated with either $4x10^{5}$ H345 or H510 cells/well. It was observed that co-culture with $4 x10^{5}$ H345 cells significantly suppressed CD4+ T-cell ^{3}H-thymidine uptake compared with CD4+ T-cells alone (90053 +/- 11401 c.f. 126372 +/- 8524, $p < 0.05$; mean +/- SEM n=4 experiments) (Fig. 7.3 b). However co-culture with H510 cells had no-significant effect on ^{3}H-thymidine uptake by CD4+ T-cells.

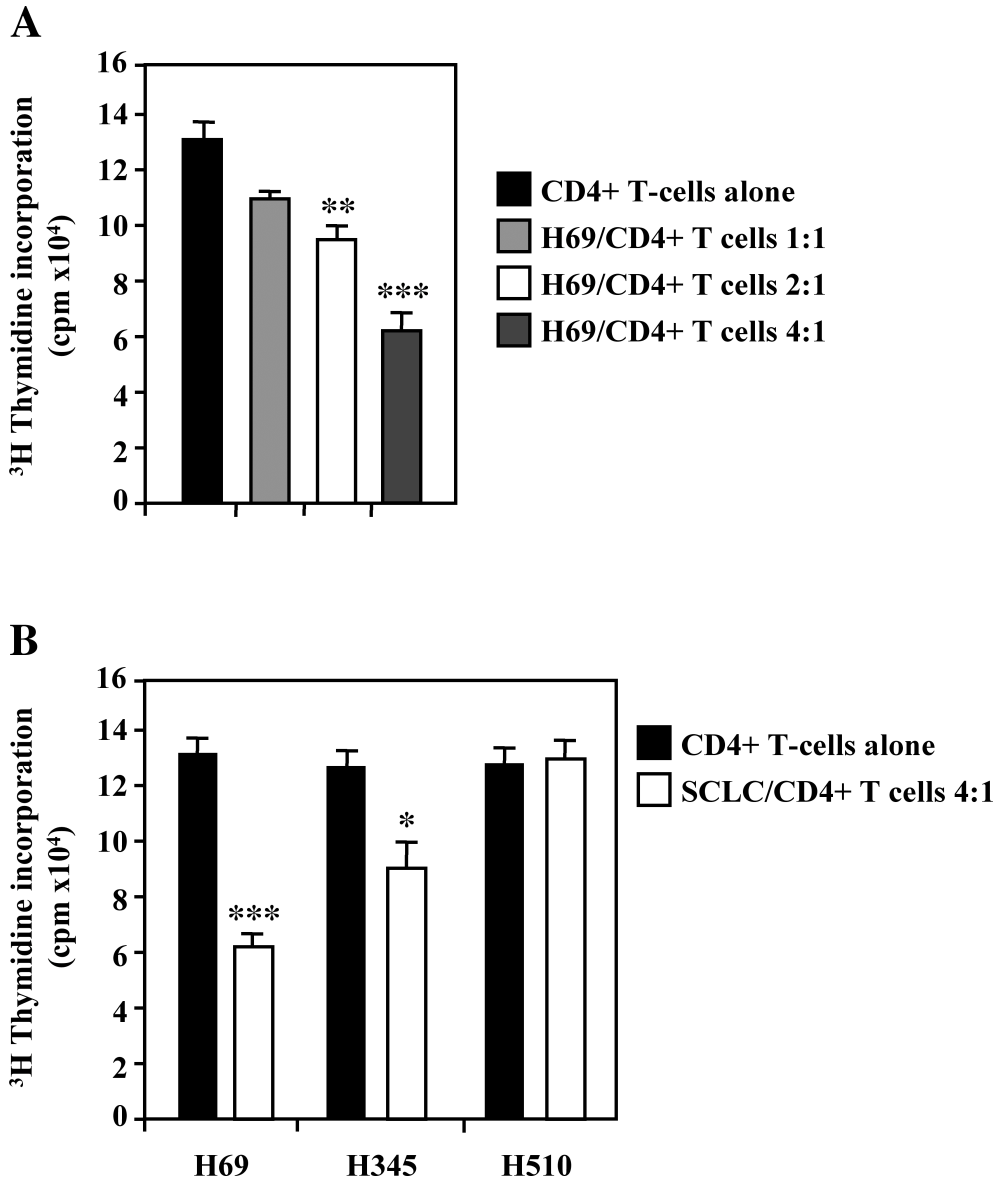
Taken together this data indicates that specific cell lines derived from human SCLC patients (i.e. H69 and H345) can suppress polyclonal T-cell receptor (TCR)-mediated proliferation of human CD4+ T-cells *in vitro*. This could represent an important mechanism by which SCLC cells can evade effective anti-tumour immune responses *in vivo*, as CD4+ T-cells co-ordinate many key aspects of tumour immunity (181). In addition, the failure of some cell lines (H510) to affect T-cell activation suggests that previously observed differences in cell-mediated immune responses between patients may reflect factors specific to the SCLC tumour rather than the host.

Figure 7.2: H69 SCLC Cell Lines Suppress CD4+ T-cell Proliferation.



CD4+ T-cells were purified from healthy donor peripheral blood mononuclear cells by negative selection and cultured in 96 well plates (2 x 10^5 cells/well) alone or with mitomycin C treated H69, H345 or H510 SCLC cells (2 x 10^5 cells/well). The CD4+ T-cells were stimulated with immobilised anti-CD3 and soluble anti-CD28 and uptake of ^{3}H-thymidine at 72 hours measured as a marker of proliferation. (A) Line graph shows uptake of ^{3}H-thymidine (counts per minute; cpm) by anti-CD3/CD28 stimulated CD4+ T-cells from 12 individual donors cultured alone (CD4+ T-cells) or with H69 SCLC cells (CD4+ T-cells + H69 SCLC). (B) Bar graph shows mean uptake of ^{3}H-thymidine +/- SEM by SCLC cells and anti-CD3/CD28 stimulated CD4+ T-cells cultured alone (CD4+ T-cells) or with SCLC cells (H69 n=12, H345 n=9, H510 n=6). ** indicates significant difference in mean ^{3}H-thymidine uptake (cpm) between CD4+T-cells cultured alone and with SCLC cells $p<0.01$.

Figure 7.3: Increasing The Ratio Of SCLC Cells To CD4+ T-cells In Co-culture Increases Suppression Of T-cell Proliferation.



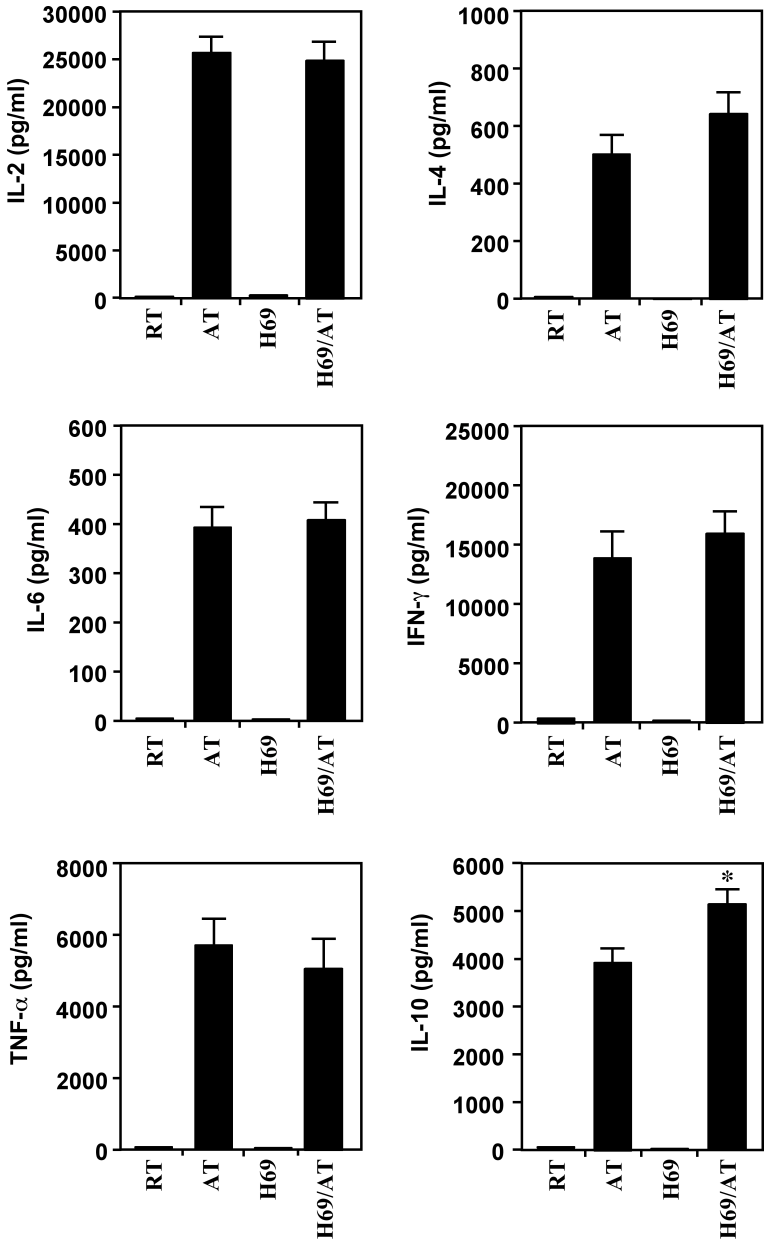
CD4+ T-cells were purified from healthy donor peripheral blood mononuclear cells by negative selection and cultured in 96 well plates (1 x 10^5 cells/well) alone or with mitomycin C treated H69, H345 or H510 SCLC cells. The CD4+ T-cells were stimulated with immobilised anti-CD3 and soluble anti-CD28 and uptake of ^{3}H-thymidine at 72 hours measured as a marker of activation. (A) Graph shows mean uptake of ^{3}H-thymidine (counts per minute; cpm) +/- SEM by CD4+ T-cells cultured alone or with H69 SCLC cells (1, 2 or 4 x 10^5 cells/well) (n=6 experiments). (B) Graph shows mean uptake of ^{3}H-thymidine (cpm) +/- SEM by CD4+ T-cells cultured alone or with 4 x10^5 SCLC cells lines. (n=6 H69, n=4 H345 and n=4 H510). Asterisks indicate significant difference in mean ^{3}H-thymidine uptake (cpm) between CD4+T-cells cultured alone and with SCLC cells. * $p < 0.05$, ** $p < 0.01$ and *** $p < 0.001$.

7.2.3 H69 SCLC Cell Lines Increase IL-10 Secretion By Activated CD4+ T-Cells.

Previous published data has indicated that suppression of CD4+ T-cell proliferation can be accompanied by inhibition of cytokine production (390). In particular, down-regulation of interleukin-2 (IL-2) secretion can promote the development of T-cell anergy preventing responses to further stimulation through the TCR (391). In contrast, tumour-infiltrating lymphocytes isolated from human renal cell carcinoma have been shown to produce IL-2 but do not proliferate in response to CD3 and co-stimulatory signals (392). Therefore, experiments were performed to determine whether SCLC cell suppression of activated CD4+ T-cells proliferation was accompanied by changes in cytokine release.

1 $x10^5$ CD4+ T-cells, prepared from human PBMCs were activated in 96 well plates with anti-CD3/CD28 and cultured alone or with 4 $x10^5$ mitomycin C treated H69 SCLC cells. Unstimulated CD4+ T-cells or mitomycin C treated H69 SCLC cells were cultured alone as controls. After 72 hours supernatants were removed from the cultures and the concentrations of IL-2, IL-4, IL-6, IL-10, IFN-γ and TNF-α were measured using a cytometric bead array. Cellular proliferation was assessed in all conditions by uptake of ^{3}H-thymidine. As predicted, resting CD4+ T-cells and H69 SCLC cells did not proliferate or produce significant amounts of any of the cytokines measured (Fig. 7.4). Activated CD4+ T-cells cultured alone produced significant amounts of all the cytokines measured (Fig. 7.4). Interestingly, despite showing suppressed proliferation, the supernatants from activated CD4+ T-cells co-cultured with H69 SCLC cells contained similar concentrations of IL-2 compared to activated CD4+ T-cells alone. Furthermore, co-culture of H69 SCLC cells with activated CD4+ T-cells did not significantly affect supernatant concentrations of IL-4, IL-6, IFN-γ or TNF-α (Fig. 7.4). This indicates that SCLC cells do not induce a shift to a TH1 or TH2 phenotpye in activated CD4+ T-cells *in vitro*. However, activated CD4+ T-cells co-cultured with H69 SCLC cells produced significantly greater amounts of IL-10 compared with activated CD4+ T-cells cultured alone (5182 +/- 146 vs. 3986 +/- 163 $p < 0.05$; mean concentration (pg/ml) n=5 experiments +/- SEM).

Figure 7.4: SCLC Cells Increase IL-10 Release By Activated CD4+ T-cells.



CD4+ T-cells, activated with anti-CD3/CD28, were cultured alone ($1x10^5$ cells/well) or with mitomycin C treated H69 SCLC cells ($4x10^5$ cells/well) in 96 well plates. Resting CD4+ T-cells and mitomycin C H69 SCLC cells were used as controls. Supernatants were collected after 72 hours and the concentrations of IL-2, IL-4, IL-6, IL-10 IFN-γ and TNF-α were measured using a cytometric bead array. Graphs show mean concentration (pg/ml) of indicated cytokine +/- SEM collected from resting CD4+ T-cells (RT), activated CD4+ T-cells (AT), H69 SCLC cells (H69) and activated CD4+ T-cells co-cultured with H69 SCLC cells (H69/AT) (n=5 experiments). * indicates significant difference in mean IL-10 concentration between AT and H69/AT $p < 0.05$.

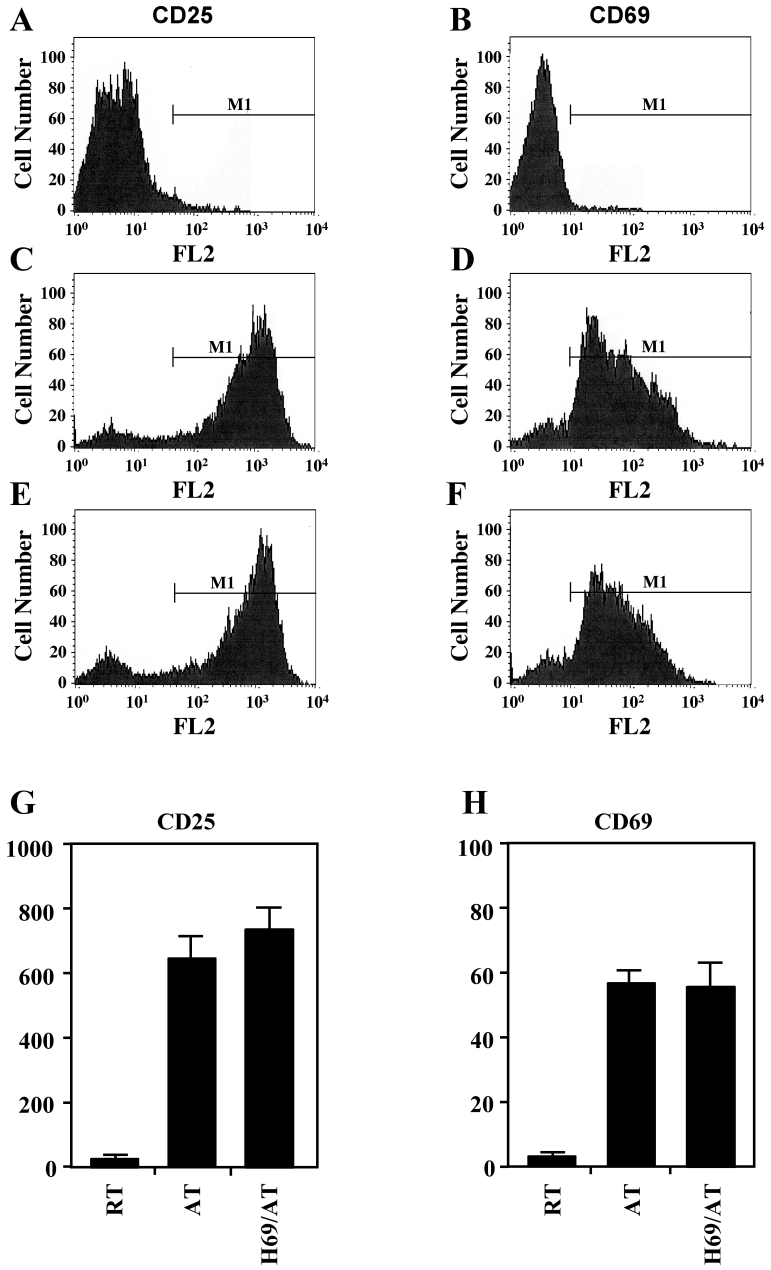
7.2.4 H69 SCLC Cells Do Not Alter CD4+ T-cell Surface Expression of Activation Markers CD25 or CD69.

CD25 is a 55kDa transmembrane protein that functions as the α-chain of the IL-2 receptor (IL-2R) (393). CD69 is a 60kDa transmembrane protein that is involved in early lymphocyte activation and can affect cellular Ca2+ influx and cytokine production (394). Activation of naïve CD4+ T-cells results in increased surface expression of CD25 and CD69. Furthermore, expression of these markers has been shown to correlate with ^{3}H-thymidine uptake (395). Thus, it was investigated whether SCLC cells could alter activated CD4+ T-cell expression of CD25 and CD69.

Human CD4+ T-cells (0.5 x 10^{6} cells/well) were activated with anti-CD3/CD28 and cultured alone or with mitomycin C treated H69 SCLC cells (2 x 10^{6} cells/well) in 24 well plates. Suppression of proliferation was confirmed by uptake of ^{3}H-thymidine. Resting CD4+ T-cells (0.5 x 10^{6} cells/well) were cultured as controls. After 72 hours, surface expression of CD25 or CD69 was analysed on CD4+ T-cells using flow cytometry (Fig. 7.5). It was found that activation of CD4+ T-cells with anti-CD3/CD28 markedly increased expression of both CD25 and CD69. Interestingly, co-culture with H69 SCLC cells did not significantly alter expression of CD25 or CD69 on activated CD4+ T-cells despite suppression of ^{3}H-thymidine uptake.

Taken together this data indicates that H69 and H345 but not H510 SCLC cell lines can suppress activated CD4+ T-cell proliferation *in vitro*. This is not caused by a down-regulation in IL-2 secretion or expression of IL-2R (CD25) but is accompanied by an increase in IL-10 secretion.

Figure 7.5: SCLC Cells Do Not Suppress Surface Expression Of CD25/CD69 On Activated CD4+ T-cells.



CD4+ T-cells, activated with anti-CD3/CD28, were cultured alone ($0.5x10^6$ cells/well) or with mitomycin C treated H69 SCLC cells ($1x10^6$ cells/well) in 24 well plates. Inactivated/resting CD4+ T-cells were cultured as controls. After 72 hours surface expression of CD25 or CD69 was determined on CD4+ T-cells by flow cytometry. (A-F) Representative histograms of FL-2 fluorescence intensity (surface expression of CD25 (A,C,E) or CD69 (B,D,F,)) on resting CD4+ T-cells (A,B), activated CD4+ T-cells (C,D) and activated CD4+ T-cells co-cultured with H69 SCLC cells (E,F). (G, H) Graphs showing average geo-mean FL-2 fluorescence intensity (surface expression of CD25 or CD69) within M1 marker on resting CD4+ T-cells (RT), activated CD4+ T-cells (AT) and activated CD4+ T-cells co-cultured with H69 SCLC cells (H69/AT) (n=5 experiments +/- SEM).

7.2.5 A Soluble Factor Secreted By SCLC Cells Mediates Suppression Of CD4+ T-cell Proliferation.

Prior research has suggested that a component of the media from SCLC cells can suppress lymphocyte proliferation in response to PHA (382). It is clear from data described above that H69 and H345 SCLC cell lines can suppress both MLR and CD4+ T-lymphocyte proliferation in co-culture. This could occur either through the secretion of immunosuppressive factors or direct SCLC cell-lymphocyte interaction. To investigate whether cell-cell contact was required for the observed suppression of CD4+ T-cell proliferation, SCLC cells were cultured in transwells (0.4 μm pores), which prevent direct surface contact with the lymphocytes but allow activity of soluble immunosuppressive factors.

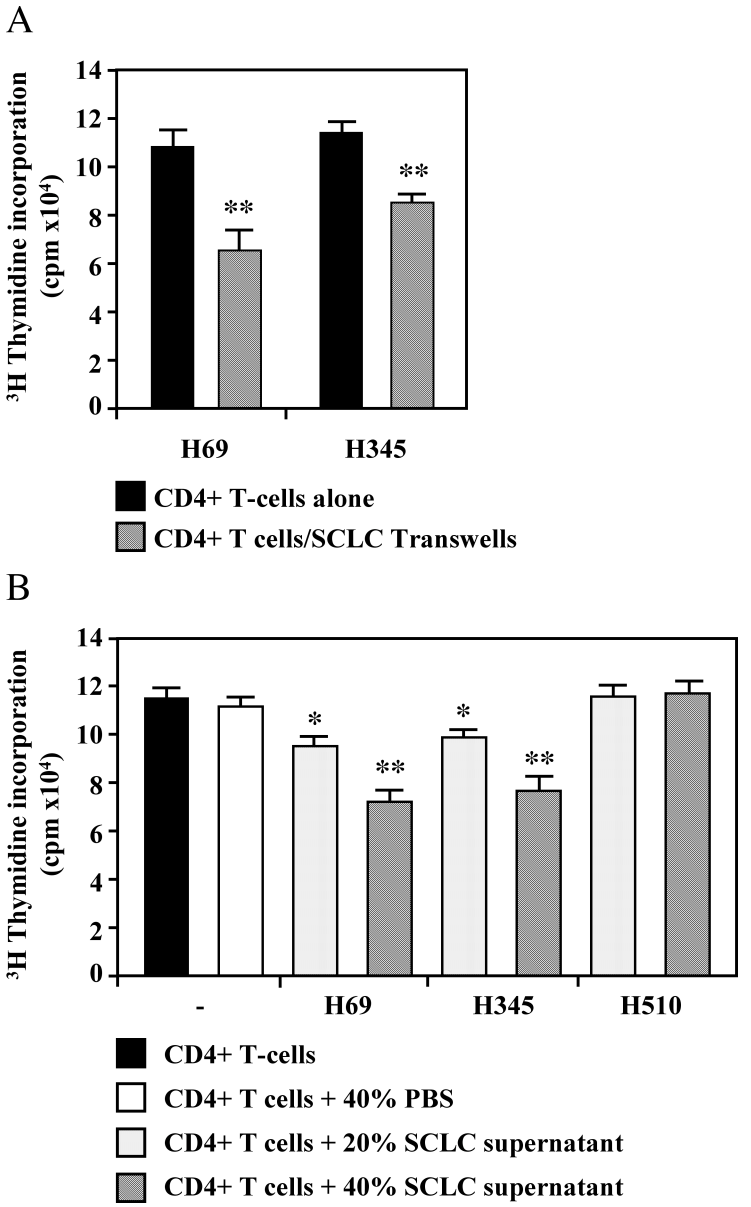
Human CD4+ T-cells (0.5 x 10^6 cells/well), activated with anti-CD3/CD28, were cultured in 24 well plates alone or with transwells containing SCLC cells (2 x 10^6 cells/well). After 72 hours transwells were removed and CD4+ T-cell proliferation was assessed by uptake of ^{3}H-thymidine. As previously observed, CD4+ T-cells proliferated significantly in response to anti-CD3/CD28 (109172 +/- 7015 cpm; mean ^{3}H-thymidine uptake +/- SEM n=7 experiments). However, co-culture with H69 SCLC cells in transwells significantly suppressed CD4+ T-cell proliferation (62278 +/- 8633 cpm; mean ^{3}H-thymidine uptake +/- SEM, n=7 experiments, $p < 0.01$) (Fig. 7.6a). In addition, CD4+ T-cells proliferation was significantly suppressed by co-culture with H345 SCLC cells in transwells (113546 +/- 5956 cpm vs. 86493 +/- 6785 cpm respectively; mean ^{3}H-thymidine uptake +/- SEM, n=4 experiments, $p < 0.05$) (Fig. 7.6a). This suggests that SCLC suppression of CD4+ T-cell proliferation is not dependent on direct cell-cell contact. However it does not exclude the possibility of cellular interactions between SCLC cells and lymphocytes mediated by soluble factors.

To determine whether SCLC cells constitutively produced a soluble factor that could suppress CD4+ T-cell proliferation, media from SCLC cells in tissue culture was used. SCLC cells were cultured in IMDM (10% FCS) at a starting density of 0.5 x 10^6 cells/ml in 24 well plates. After 72 hours supernatants were removed from the SCLC cells and diluted 1:5 (20%) or 2:5 (40%) with IMDM (plus 10% FCS). CD4+

T-cells in 96 well plates ($1x10^5$ cells/well), were activated with anti-CD3/CD28 and cultured with diluted SCLC supernatants or with 40% PBS (diluted in IMDM plus 10% FCS) as a control. After 72 hours CD4+ T-cell proliferation was measured by uptake of ^{3}H-thymidine. It was found that activated CD4+ T-cells showed significant uptake of ^{3}H-thymidine after 72 hours and the replacement of 40% of the culture medium with PBS did not significantly affect proliferation (116292 +/- 4602 cpm vs. 110631 +/- 2470 cpm respectively; mean ^{3}H-thymidine uptake (cpm) +/- SEM n=3 experiments p=0.306) (Fig. 7.6 b). However, addition of H69 and H345 SCLC supernatant caused significant suppression of activated CD4+ T-cell proliferation (Fig. 7.6 b). In addition the suppressive effect of 40% SCLC cell supernatant was greater than 20% (20% H69 supernatant: 94158 +/-1856 cpm vs. 40% H69 supernatant: 71895 +/- 2027 cpm; mean uptake of ^{3}H-thymidine (cpm) +/- SEM, n=3 experiments, $p < 0.05$). As expected, neither concentration of H510 supernatant suppressed CD4+ T-cell ^{3}H-thymidine uptake (Fig. 7.6b).

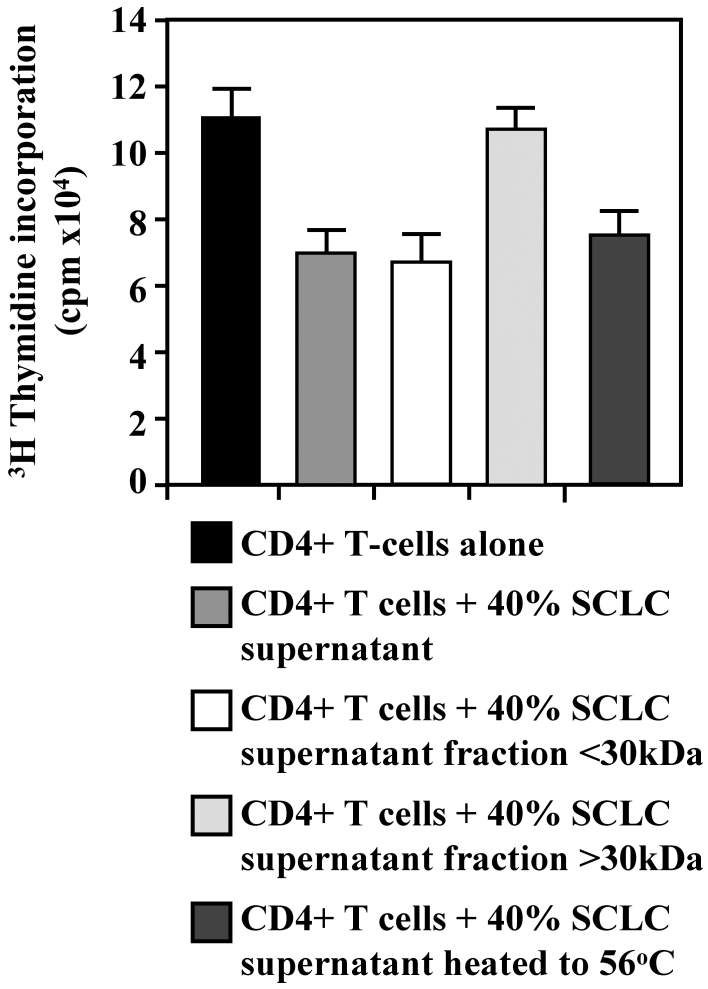
This data indicates that SCLC cells can produce a soluble factor in tissue culture, which suppresses CD4+ T-cell proliferation in a dose-dependent manner. To further investigate the nature of this factor H69 SCLC supernatants were separated into two fractions by molecular weight (i.e. less or greater than 30kDa) using micro-spin columns as described in chapter 2. SCLC supernatants were also heated to 56^oc for 10 minutes. Suppression of activated CD4+ T-cell proliferation was compared for supernatants prepared as indicated. It was found that the low molecular weight fraction (< 30kDa) of SCLC supernatants produced similar suppression of CD4+ T-cell proliferation to untreated supernatants (65742 +/- 9746 vs. 69870 +/- 8167 p=0.762; mean ^{3}H-thymidine uptake (cpm) +/- SEM, n=3 experiments) (Fig. 7.7). However the fraction containing soluble factors of molecular weight greater than 30kDa did not significantly suppress CD4+ T-cell proliferation (Fig. 7.7). In addition heat inactivated SCLC supernatants suppressed CD4+ T-cell proliferation similarly to untreated supernatants (73462 +/- 8215 vs. 69870 +/- 8167 p=0.772; mean ^{3}H-thymidine uptake (cpm) +/- SEM, n=3 experiments) (Fig. 7.7). This data suggests that SCLC cells produce a soluble factor that can suppress CD4+ T-cell proliferation, which is heat stable and of a molecular weight less than 30kDa.

Figure 7.6: SCLC Produce A Soluble Factor Which Suppresses CD4+ T-cell Proliferation.



(A) Human CD4+ T-cells ($0.5x10^6$ cells/well) were activated with anti-CD3/CD28 and cultured alone or with transwells (0.4 μm pore size) containing SCLC cells ($2x10^6$ cells/well). After 72 hours CD4+ T-cell proliferation was assessed by uptake of ^{3}H-thymidine. Bar graph shows mean uptake of ^{3}H-thymidine (counts per minute; cpm) +/- SEM by CD4+ T-cells (n=5 experiments). (B) H69, H345 and H510 SCLC cells (0.5×10^6 cells/ml) were cultured in IMDM (10% FCS) for 72 hours and supernatants removed. CD4+ T-cells (1×10^5 cell/well) were activated with anti-CD3/CD28 and cultured in 96 well plates with IMDM (10% FCS), IMDM (10% FCS) plus 40% PBS or IMDM (10% FCS) plus either 20% or 40% SCLC cell supernatant as indicated. After 72 hours T-cell proliferation was assessed by uptake of ^{3}H-thymidine. Bar graph shows mean uptake of ^{3}H-thymidine (cpm) +/- SEM by activated CD4+ T-cells (n=3 experiments). Asterisks indicate significant difference in mean ^{3}H-thymidine uptake (cpm) between CD4+T-cells cultured alone or with SCLC supernatant. * $p < 0.05$, ** $p < 0.01$.

Figure 7.7: The Soluble Factor Produced by H69 SCLC Cells That Suppresses CD4+ T-cell Proliferation Is < 30kDa and Thermostable.



H69 SCLC cells (0.5 x 10^6 cells/ml) were cultured in IMDM (10% FCS) for 72 hours, and supernatants removed. Supernatants were further treated by either separation into fractions containing soluble factors < 30kDa or > 30kDa or by heating to 56^{o}c for 10 minutes. CD4+ T-cells (1 x10^5 cell/well) were activated with anti-CD3/CD28 and cultured in 96 well plates. 40% SCLC cell supernatant treated as indicated was added to wells in triplicate. After 72 hours T-cell proliferation was assessed by uptake of ^{3}H-thymidine. Bar graph shows mean uptake of ^{3}H-thymidine (cpm) +/- SEM by activated CD4+ T-cells (n=3 experiments).

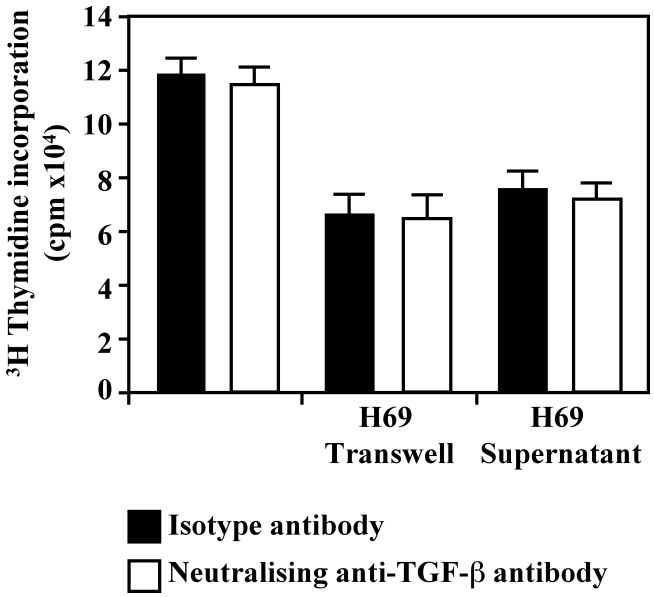
7.2.6 Suppression of Human CD4+ T-Cells Proliferation By H69 SCLC Cells Is Not Reversed By A TGF-β Neutralising Antibody.

The data above indicates that SCLC cells can suppress CD4+ T-cell proliferation via a soluble factor, which is less than 30kDa in molecular weight. Other solid tumours have been shown to produce a variety of soluble factors that can suppress cell-mediated immune responses (396). These include cytokines (e.g. IL-10, TGF-β), prostaglandins, enzymes, and lectins (396). It has been demonstrated in this chapter, using a cytometric bead array, that SCLC cell lines do not secrete IL-10 (Fig. 7.4). However, co-culture of SCLC cells with CD4+ T-cells activated through the T-cell receptor (TCR) increased IL-10 in supernatants (Fig. 7.4). IL-10 is a potent immunosuppressive cytokine that can be produced by thymus derived and peripherally generated CD4+CD25+ Tregs (397,398). Tregs do not proliferate in response to mitogenic stimuli and suppress activation of effector T-cells (398). Prior research has demonstrated that solid tumours can promote the generation of CD4+CD25+ Tregs from CD4+CD25- T-cells independent of the thymus (399). Furthermore, it has been shown that the suppressive cytokine TGF-β can induce CD4+CD25+Foxp3+ Tregs from naïve CD4+CD25- T-cells *in vitro* (400). TGF-β plays a key role in tumour pathogenesis and its expression is observed in a variety of human tumours (401). It has three isoforms in mammals (TGF-β 1-3) and the mature protein forms soluble dimers with a molecular weight of approximately 25kDa (402). Thus, it was hypothesised that SCLC cells could suppress CD4+ T-cell activation and promote IL-10 production through the secretion of TGF-β.

Initial experiments confirmed the presence of TGF-β1 in supernatants from H69 SCLC cells using an ELISA method (77.4 +/- 5.8 pg/ml; mean TGF-β1 concentration from n=3 experiments +/- SEM). The concentration of TGF-β1 in IMDM (10% FCS) was below the detection level of the ELISA (<31.25 pg/ml). To determine whether the suppression of CD4+ T-cell proliferation by SCLC cells was mediated by TGF-β, a neutralising antibody was used. As previously described, the ability of pan-isotype specific anti-TGF-β antibody to neutralise TGF-β1 activity *in vitro* was confirmed using stimulated CD4+ T-cells (see chapter 2) (403,404). Subsequently, T-cell culture media (IMDM with 10% FCS) or H69 SCLC

supernatants were pre-incubated with anti-TGF-β antibody or isotype control (10μg/ml) for 2 hours at 37°C. CD4+ T-cells were resuspended in these media, and cultured alone or with H69 SCLC cells in transwells in the presence of anti-CD3/CD28. The proliferation of CD4+ T-cells was determined after 72 hours by uptake of ^{3}H-thymidine. It was observed that neither the addition of isotype nor neutralising anti-TGF-β antibody had any effect on the proliferation of CD4+ T-cells in response to anti-CD3/CD28. Furthermore, anti-TGF-β antibody did not block the suppression of CD4+ T-cell proliferation mediated by H69 SCLC cells or H69 SCLC supernatant (Fig. 7.8). This data suggests that although SCLC cells can secrete TGF-β the effect on CD4+ T-cell proliferation is not mediated by this cytokine.

Figure 7.8: Suppression of Human CD4+ T-Cells Proliferation By SCLC Cells Is Not Mediated By TGF-β.



H69 SCLC cells (0.5 x 10^{6} cells/ml) were cultured in IMDM (10% FCS) for 72 hours, supernatants removed and diluted to 40% with IMDM (10% FCS). Anti-TGF-β (■) or isotype control antibody (□) (both 10μg/ml) were added to T-cell culture media (IMDM 10% FCS) or SCLC supernatants and incubated for 2 hours at 37°C. Human CD4+ T-cells were resuspended in these media (1x10^{6} cells/ml) as indicated and cultured alone or with H69 SCLC cells (2x10^{6} cells/well) in transwells in the presence of anti-CD3/CD28. After 72 hours, CD4+ T-cell proliferation was assessed by uptake of ^{3}H-thymidine. Bar graph shows mean uptake of ^{3}H-thymidine (counts per minute; cpm) +/- SEM by CD4+ T-cells (n=4 experiments).

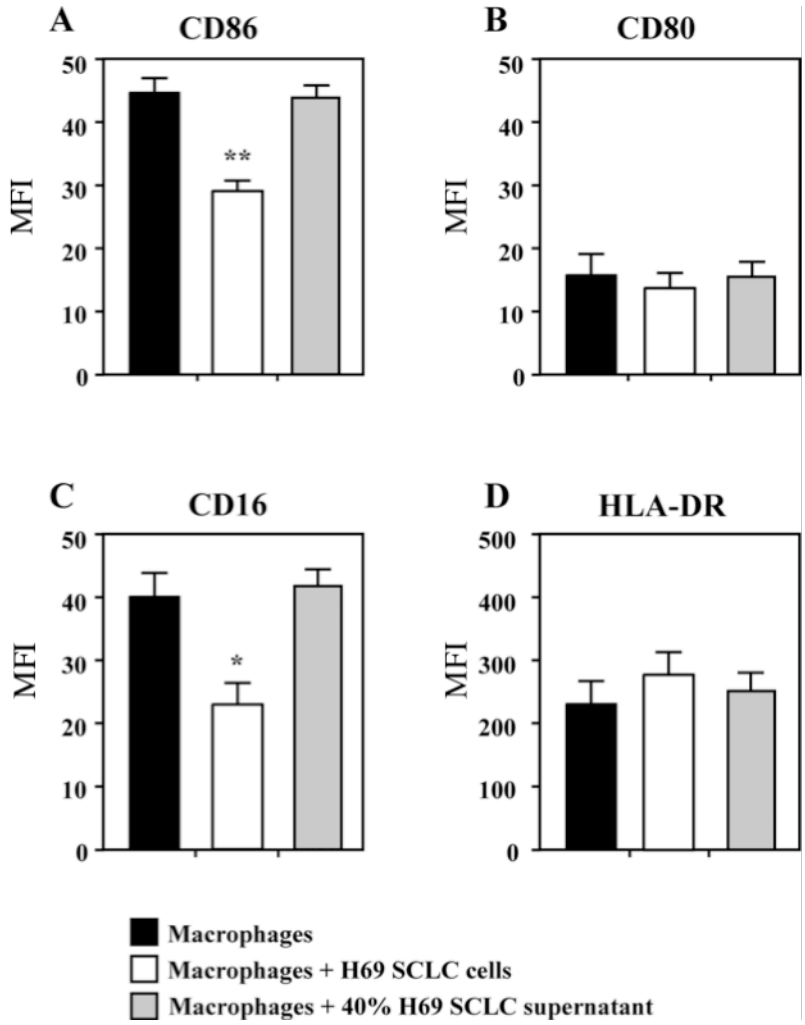
7.2.7 SCLC Cells Suppress Macrophage Surface Expression Of CD86 and CD16.

It has been demonstrated that CD4+ lymphocytes form part of the local immune cell infiltrate in SCLC (see chapter 6). Macrophages are also important and constitute a significant proportion of the leukocyte infiltrate observed in SCLC tumour sections. The macrophage has been shown to play a key role in tumour immunity and growth (183,363). Research in other solid malignancies has indicated that tumour associated macrophages (TAMs) have a complex relationship with cancer cells. Activated macrophages are multi-functional, capable of antigen presentation, regulation of inflammation and immunity, cytotoxicity, phagocytosis, tissue remodelling and angiogenesis (183,363). The two poles of the activated macrophage spectrum are classically activated (M1) macrophages, characterized by IFN-γ production and alternatively activated (M2) macrophages, triggered by anti-inflammatory cytokines e.g. IL-10 (183,363). In the context of effective anti-tumour immunity macrophages may be skewed towards the M1 phenotype acting as antigen presenting cells (APCs) and be directly tumoricidal (183,363). However, if macrophages are skewed towards an M2 phenotype they may contribute to tumour progression by inducing tolerance to tumour-associated antigens and promoting a tumour stroma rich in new blood vessels and extracellular matrix (183,363). Despite its obvious importance, the interaction of SCLC cells with macrophages has not been studied. The following data were obtained by Jonny Rodriguez (BSc Honours student) under direct supervision.

Macrophages were matured *in vitro* from adherent human peripheral blood mononuclear cells as described in chapter 2. To determine the effect of SCLC cells on macrophage phenotype, adherent human peripheral blood mononuclear cells were cultured in 6-well plates with H69 SCLC cells (1×10^6 cells/well), with H69 SCLC cell supernatant (diluted to 40% with normal culture media) or in standard culture media. After 7 days, adherent cells were removed from the wells and surface expression of CD80, CD86, CD16 or HLA-DR was determined on mature macrophages (CD11b/CD14 positive) using 3-colour flow cytometry. It was found that surface expression of CD86 and CD16 was significantly reduced on macrophages matured with H69 SCLC cells compared to macrophages matured in

standard culture media (Fig 7.9 a and c). However no significant difference was observed in the surface expression of CD80 or HLA-DR on macrophages matured in standard culture media or with H69 SCLC cells (Fig 7.9 b and d). These effects on CD86 and CD16 expression occurred without alterations in macrophage viability. Average macrophage viability after 7 days by trypan-blue exclusion was 87.4 +/- 3.7% for standard culture media compared with 83.5 +/-7.7% for culture with H69 SCLC cells (mean percentage viability +/- SEM; n=5 experiments). Interestingly, macrophages matured with H69 SCLC supernatants showed similar surface expression of CD86, CD80, CD16 and HLA-DR compared to macrophages matured in standard media. These results suggest that H69 SCLC cells can specifically suppress CD86 and CD16 expression on macrophages matured from monocytes. Furthermore, this effect appears to require an interaction between SCLC cells and macrophages rather than being mediated by a soluble factor constitutively produced by SCLC cells in culture.

Figure 7.9: Macrophages Matured From Monocytes With H69 SCLC Cells Show Reduced Surface Expression Of CD86 and CD16.



Adherent human peripheral blood mononuclear cells were cultured in 6-well plates with H69 SCLC cells (1 x 10^6 cells/well), with H69 SCLC cell supernatant (diluted 2:5 (40%) with normal culture media) or in standard culture media as indicated. After 7 days adherent cells were removed from the wells and surface expression of CD80, CD86, CD16 or HLA-DR was determined on mature macrophages (CD11b/CD14 positive) using 3-colour flow cytometry. **(**A-D) Graphs show on Y axis average geo-mean FL-3 fluorescence intensity (MFI) for surface expression of CD80, CD86, CD16 or HLA-DR on macrophages matured in standard culture media (black bars), with H69 SCLC cells (white bars) or with H69 SCLC supernatants (grey bars) (average of n=5 experiments +/- SEM). Asterisks indicate significant difference in average geo-mean FL-3 fluorescence intensity between monocytes matured in standard culture media or with H69 SCLC cells (* indicates $p < 0.05$, ** indicates $p < 0.01$).

7.2.8 Suppression Of MLR Proliferation By H69 SCLC Cells Is Reversed By The Bombesin Antagonist RC-3095.

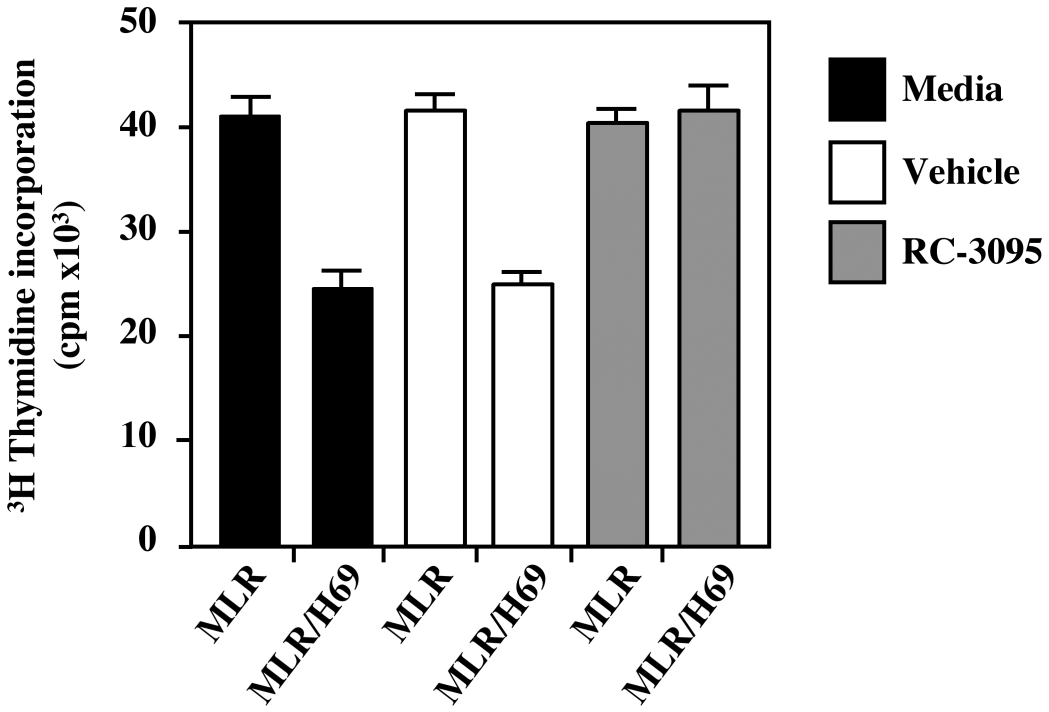
It has previously been demonstrated that SCLC cells secrete a variety of neuroendocrine growth factors that form essential autocrine growth loops allowing escape from anchorage-dependent control of cell proliferation (92,141). Interestingly, neuropeptides have also been shown to affect immune cell function regulating both antigen presenting cell capability and lymphocyte proliferation. In particular, bombesin, a 14 amino acid peptide isolated from frog skin, has been shown to suppress IL-2 dependent proliferation of murine lymphocytes (CTLL-2 cells) (405). Immunoreactivity for bombesin-like peptides, gastrin releasing peptide (GRP) and neuromedin B (NMB), has been demonstrated in SCLC cell lines (406). GRP and NMB have also been shown to suppress proliferation of murine lymphocytes derived from axillary nodes, spleen and thymus in response to Con A (407). Furthermore, bombesin-like peptides have been shown to inhibit dendritic cell maturation (decreased CD40, CD80 and CD86 expression) and IL-12 production, which could be prevented in part by a bombesin antagonist (408). Thus, it is possible that the observed effects of SCLC cell lines on CD4+ T-cells and macrophages described in this chapter could be mediated by bombesin-like neuropeptides.

To investigate this, a specific bombesin antagonist, RC-3095, was used. RC-3095 is a pseudononapeptide with chemical formula (D-Tpi6, Leu13 (CH2-NH)-Leu14)bombesin (6-14), which has been shown *in vitro* to compete with bombesin for binding to SCLC cells and to inhibit GRP-induced amylase release from rat pancreatic cells (409). Mixed leukocyte reactions (MLR) were activated with Con A and cultured alone or with transwells (0.4μM pore size) containing H69 SCLC cells. To cultures, either RC-3095 (1μM final concentration) or DMSO (vehicle, 0.1% final concentration) was added. Activation of responder cells in the MLR was determined after 72 hours by incorporation of ^{3}H-thymidine.

As expected, it was observed that MLRs stimulated with Con A (5μg/ml) actively incorporated ^{3}H-thymidine (40945 +/- 2045 cpm; mean of n=4 independent experiments +/- SEM) (Fig. 7.10). Co-culture of H69 SCLC cell lines in transwells resulted in a significant reduction in MLR ^{3}H-thymidine uptake despite prevention of

SCLC-immune cell contact (24950 +/- 1914 cpm, $p < 0.05$; mean of n=4 experiments +/- SEM). This suggests that the inhibitory effect of SCLC cells on MLR activation was mediated by a soluble factor. The addition of 0.1% DMSO (vehicle) had no effect on the proliferation of a MLR and did not prevent H69 SCLC cells from suppressing MLR activation (41472 +/- 1915 cpm and 24795 +/- 1415 cpm respectively; mean of n=4 experiments +/- SEM). Importantly, the addition of 1μM RC-3095 did not significantly affect MLR proliferation but did prevent the suppression of MLR activation by H69 SCLC cells (40042 +/- 1864 cpm and 41696 +/- 2415 cpm respectively, $p=0.6702$; mean of n=4 experiments +/- SEM). These data suggest that antagonism of bombesin-like peptides prevents SCLC cells from suppressing cell-mediated immunity. It remains to be elucidated whether this is as a result of an effect on SCLC cells, which use these neuropeptides as growth factors, or through the blockade of bombesin-like peptide receptors on immune cells.

Figure 7.10: The Bombesin Receptor Antagonist RC-3095 Reverses MLR Suppression By H69 SCLC Cell Line.



Mixed leukocyte reactions (MLR) were established by combining peripheral blood mononuclear cells from two separate healthy donors ($0.5x10^6$ cells/well) in 24 well plates with Concanavalin A (5mg/ml). MLR were cultured alone or with transwells (0.4μm pore size) containing H69 SCLC cells ($2x10^6$ cells/well) (designated MLR/H69). The bombesin antagonist RC-3095 (1μM final concentration) or 0.1% DMSO (vehicle) was added to cultures as indicated. Activation of responder cells was determined at 72 hours by uptake of ^{3}H-thymidine. The graph represents mean ^{3}H-thymidine uptake (counts per minute; cpm) for n=4 independent experiments +/- SEM.

7.3 Discussion.

It has been clearly demonstrated in this chapter that H69 and H345 human SCLC cells can suppress the proliferation of a mixed leukocyte reaction (MLR) derived from healthy human blood donors. H510 SCLC cells do not inhibit mixed leukocyte proliferation, suggesting that specific SCLC cell lines can suppress cell-mediated immune responses. To investigate the mechanisms underpinning this observation the effect of SCLC cells on CD4+ T-cell proliferation and macrophage maturation was observed. It was found that H69 and H345 SCLC cells suppress CD4+ T-cell proliferation and that the effect is maximal at greater SCLC cell numbers. CD4+ T-cells co-cultured with SCLC cells show increased IL-10 production but no change in IL-2 secretion or expression of the IL-2 receptor α chain (CD25). In addition H69 SCLC cells suppress CD16 and co-stimulatory molecule (CD86) expression by macrophages matured from monocytes. Interestingly, SCLC cells produce these effects on CD4+ T-cells and macrophages via separate mechanisms. A soluble factor, which is not TGF-β, produced by SCLC cells can suppress CD4+ T-cell proliferation but direct cell interaction is required for the effect on macrophage surface marker expression. Furthermore, preliminary data suggests that bombesin-like peptides may play an important role in SCLC cell suppression of MLR activation. Taken together these data indicate a complex interaction between SCLC cells and mononuclear immune cells that results in suppression of cell-mediated immunity.

In 1973, Brugarolas and Takita demonstrated that, in comparison to squamous cell lung cancer, patients with SCLC showed a poorer response to delayed hypersensitivity (DTH) skin testing (410). This correlated with *in vitro* assessments of lymphocyte function from a small cohort (n=21) of SCLC patients. Following this observation, it was shown that an anergic response to a DTH skin reaction predicted poor prognosis in patients with SCLC (356). To study this further, Masuno *et al* (1986) isolated peripheral blood lymphocytes from SCLC and NSCLC patients and assessed proliferative responses to PHA and IL-2 (187). They demonstrated that the proliferation of lymphocytes from SCLC patients was significantly reduced in comparison to lymphocytes from patients with NSCLC (187). In 1991, it was confirmed that SCLC cells could suppress peripheral blood lymphocyte proliferation

in response to *in vitro* mitogenic stimulation (382). In addition, it has been demonstrated that peripheral blood leukocytes from SCLC patients show suppressed IL-2 secretion in response to mitogen stimulation compared to healthy donors (188). Importantly, the impairment of cytokine production improved upon reduction of the SCLC tumour burden (188). Taken together, this suggests that SCLC can suppress cell-mediated immune responses and that this may be important in the pathogenesis of the cancer.

The mixed leukocyte reaction has been widely used as an *in vitro* model for studying cell-mediated immunity with T-lymphocytes proliferating in response to signals presented by antigen-presenting cells (383). It has been clearly demonstrated in this chapter that H69 and H345 cell lines can inhibit ^{3}H-thymidine incorporation by human MLRs. H510 SCLC cells did not inhibit a MLR, indicating that this observation was not due to a non-specific effect of cell co-culture e.g. nutrient use. Instead these results support the previously published data that SCLC cells can suppress cell-mediated immune reactions. Importantly, each cell line was prepared from separate human tumours and therefore these data also suggest that the previously observed differences in cellular immune responses in SCLC patients may result from tumour-derived factors rather than host-dependent responses. The results described in chapter 6 indicate that the tumour immune cell infiltrate in SCLC is a prognostic factor and therefore the ability of SCLC cells to locally suppress cell-mediated immunity may be an important pathogenic feature and therapeutic target.

The mechanisms of cell-mediated immune suppression by SCLC cells were investigated. Initial experiments focused on the proliferative responses of CD4+ T-cells in co-culture with SCLC cells. The results described in this chapter indicate that SCLC cell lines can suppress human CD4+ T-cell proliferation in response to T-cell receptor-mediated activation. This suppressive effect was not observed with H510 SCLC cells even at higher tumour:lymphocyte cell ratios again confirming that it was not an effect of co-culture. Although prior research has demonstrated that SCLC cells can suppress proliferative responses of peripheral blood lymphocytes in response to mitogens, the effect on specific T-cell subsets have not been investigated. Crucially, CD4+ T-cells act as central co-ordinators of cell-mediated immunity (386). Furthermore, *in vivo* experiments have indicated that depletion of CD4+ T-

cells reduces effective anti-tumour immunity despite adequate CD8+ T-cell numbers and subversion of CD4+ T-cell function is important in tumour immune-evasion (386-389). Thus, suppression of CD4+ T-cell activation could represent a central mechanism by which SCLC cells evade or subvert cell-mediated immunity.

The cytokine IL-2 is an important stimulus to CD4+ T-cell proliferation and is released in response to activation (391). Thus, it is possible that SCLC cells could suppress CD4+ proliferation through reduced IL-2 secretion, as has been observed in other tumours (411,412). However, the data shown here indicates that SCLC cells do not alter IL-2 release or CD25 (IL2Rα) expression by CD4+ T-cells suggesting that suppression of proliferation is not mediated via alterations in IL-2. A similar observation has been published in tumour-derived lymphocytes from renal carcinoma, which show reduced proliferation in response to mitogenic stimulation but no alteration in IL-2 release (392). Further analysis of IL-2 receptor downstream signalling (e.g. STAT5 or Akt) in CD4+ T-cells co-cultured with SCLC cells is required to confirm that IL-2 signalling is active.

Although there was no alteration in IL-2 release, it was observed that IL-10 was increased in supernatants from CD4+ T-cells co-cultured with SCLC cells. Importantly, SCLC cells did not produce IL-10 when cultured alone indicating that this was a specific result of SCLC/CD4+ T-cell interaction. IL-10 can function as an immuno-inhibitory cytokine, suppressing TH-1 pro-inflammatory cytokine synthesis and antigen-presenting cell function (413). Importantly, prior studies have demonstrated that tumour-infiltrating lymphocytes are enriched in a 'regulatory' CD4+CD25+ population, which can secrete IL-10 and suppress activation of CD4+CD25- responder cells (414). Thus, SCLC cells could inhibit cell-mediated immune responses by enriching a population of IL-10 producing CD4+ T-lymphocytes. Further experiments are required to determine whether neutralisation of IL-10 in co-cultures can reverse suppression of CD4+ T-cell proliferation. In addition it is of interest to determine whether CD4+ T-cells co-cultured with SCLC cells or those identified in the tumour microenvironment have a regulatory phenotype (i.e. can suppress naïve CD4+ T-cell proliferation).

The data presented regarding CD4+ T-cells suggests that the suppressive effects of SCLC cells on cellular immunity are mediated primarily through direct inhibition of lymphocyte proliferation. However, effects on antigen-presenting cell function cannot be excluded and may explain some of the observed suppression of MLR activation. Tumour-associated macrophages have been shown in chapter 6 to constitute a significant proportion of the infiltrating immune cells and may play a significant role in controlling or promoting tumour growth. No prior data exists on the phenotype of SCLC-associated macrophages or whether SCLC cells can affect macrophage function. Therefore the *in vitro* effect of SCLC cells on macrophages was determined. Initial experiments investigated changes in expression of surface markers of macrophage phenotype in the presence of SCLC cells. The data in this chapter indicates that macrophages matured from peripheral blood monocytes in the presence of H69 SCLC cells down-regulate CD16 and CD86. CD16, the receptor for the Fc portion of IgG, is important in antibody-mediated cell cytotoxicity and CD86 is an important co-stimulatory molecule for T-cell activation (415). Therefore down-regulation of these surface molecules may inhibit the anti-tumour function of macrophages and prevent activation of T-cells within the tumour microenvironment. Further analysis of the functional relevance of these findings is required using *in vitro* cytotoxicity and co-stimulation experiments. In addition analysis of macrophage surface marker expression in SCLC tumour sections correlated to tumour stage and survival would provide an indication of *in vivo* relevance.

The observation that SCLC cells can suppress specific aspects of cell-mediated immunity is important, but to design rational therapies to boost anti-tumour immunity the mediators of this immune suppression require to be defined. The results shown here indicate that SCLC cells produce a soluble factor that is responsible for suppressing CD4+ T-cell proliferation as indicated by transwell and conditioned media experiments. This concurs with a previously published description of a soluble factor produced by SCLC cells *in vitro* that suppresses lymphocyte proliferation (382). However, the data shown in this chapter indicates that the soluble factor(s) responsible for suppression of CD4+ T-cell proliferation is less than 30kDa in molecular weight. The factor described by Ikeda *et al* in 1991 was shown to have a molecular weight of 98-102kDa (382). The results presented in this chapter are

more compatible with a previous description by Manke *et al* (1986) of a 10kDa factor in SCLC patient serum that suppresses T-lymphocyte rosette formation (381). This suggests that SCLC cells may produce more than one soluble immunosuppressive molecule. In addition, SCLC cells appear to suppress CD16 and CD86 expression on macrophages through a mechanism that is not mediated by a soluble factor secreted *in vitro*. These results indicate that SCLC cells may possess several mechanisms for suppressing cell-mediated immunity.

Due to time constraints and the complex nature of SCLC-immune cell interaction, attempts to identify a mediator of immunosupression were focused on the soluble factor(s) secreted by SCLC cells *in vitro*. TGF-β has previously been described as important soluble immunosuppressive factor produced by tumour cells and has a molecular weight less than 30kDa (402). Unfortunately, the data shown here indicates that TGF-β is unlikely to be responsible for the suppression of lymphocyte proliferation by SCLC cells. This is not unexpected, as prior data suggests that TGF-β has only weak anti-proliferative effects on CD4+ T-cells in the presence of co-stimulation (anti-CD28) (416). However, TGF-β has been shown to increase IL-10 secretion by maximally stimulated CD4+ T-cells (416). Thus, the experiments presented in figure 7.8 should be repeated without co-stimulation in the presence of TGF-β neutralising antibody. Furthermore, the effect of anti-TGF-β on IL-10 release should be determined.

Preliminary results presented in this chapter suggest a role for bombesin-like neuropeptides in SCLC suppression of cell-mediated immunity. SCLC cells have been shown to produce a wide range of neuropeptides that form autocrine growth loops, promoting anchorage independent survival and tumorigenesis (141). Interestingly, bombesin-like neuropeptides have also been shown to suppress lymphocyte proliferation and dendritic cell antigen presenting function (407,408). Importantly, the addition of a bombesin antagonist (RC-3095) was shown here to reverse SCLC cell suppression of MLR proliferation. Although this observation is encouraging, these results have several possible explanations. Firstly, bombesin secreted by SCLC cells may suppress lymphocyte proliferation through a novel pathway, which is effectively antagonised by RC-3095. Secondly, RC-3095 may

prevent bombesin from suppressing dendritic cell function. Lastly, bombesin antagonism may inhibit SCLC cell proliferation through blockade of an autocrine loop, thus reducing the number of cells present to secrete another immunosuppressive factor. Further experiments should be performed to address these issues, specifically culture of CD4+ T-cells in SCLC media with and without RC-3095. In addition, the concentration of bombesin-like peptides secreted by each SCLC cell line should be assayed and correlated with suppression of T-cell proliferation. It would also be of interest to determine the effect of recombinant bombesin-like peptides on CD4+ T-cell proliferation and IL-10 production. In this way a definitive role for neuropeptides in SCLC immune evasion would be described. This is of critical importance, not only for understanding SCLC biology, but also for the design and clinical trial of novel peptide antagonists.

In conclusion, this chapter confirms prior data that SCLC cells can suppress cell-mediated immune responses in vitro. Furthermore, the results here show that this occurs through effects on both CD4+ T-cells and macrophages, although the mechanisms of immune suppression appear to be different for each cell type. Suppression of lymphocyte proliferation is mediated by a soluble factor as described by other investigators and this factor may be a bombesin-like neuropeptide. However, further work is required to define the exact role of bombesin and to demonstrate its significance *in vivo* through the study of patient tumour sections and animal models. Ultimately, it is anticipated that understanding the complex interactions between SCLC and the cellular components of the immune system will proffer new therapeutic targets to optimise host clearance of tumour cells and improve patient survival.

CHAPTER 8: Conclusions and Future Directions.

The work presented in this thesis indicates a complex interaction between SCLC cells and components of the surrounding tumour microenvironment. Furthermore, it explores several important mechanisms involved in this interaction, which may prove to be novel therapeutic targets. The significant conclusions will be discussed in the following sections and future experiments will be highlighted.

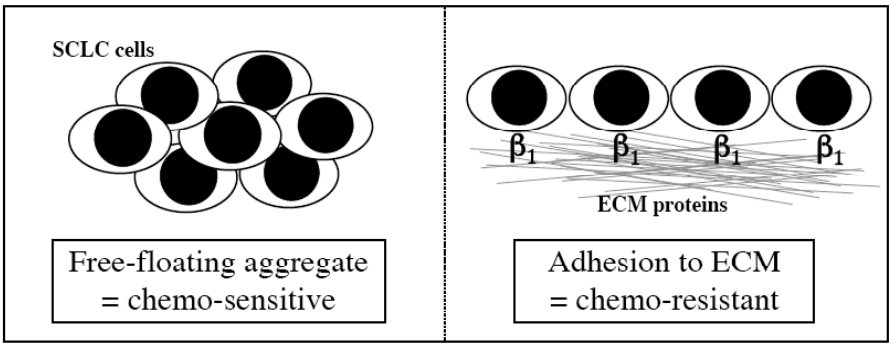
8.1 ECM-mediated chemo-resistance in SCLC cells.

The data presented in chapter 3 demonstrate that ECM proteins, identified in the tumour microenvironment of SCLC cases, protect SCLC cells *in vitro* from chemo- and radiotherapy induced cell cycle arrest and subsequent apoptosis. Thus, it seems likely that interaction with ECM in the tumour stroma may allow a proportion of SCLC cells to survive initial treatment resulting in tumour relapse. Furthermore, it is shown here that ECM does not prevent the formation of DNA double-strand breaks by genotoxic agents, allowing SCLC cells to survive with genetic damage. This could potentially result in the accumulation of mutations in key cell survival pathways (e.g. c-Kit, p53 or Rb) promoting more aggressive SCLC growth and acquired chemo-resistance. Therefore, blocking interactions between SCLC cells and ECM in the surrounding stroma may improve disease-free survival and reduce the development of multi-drug resistance in relapsed tumour after initial chemotherapy. To design rational strategies a clear understanding of the mechanisms involved in this interaction is required.

ECM-mediated drug resistance has been demonstrated in variety of other tumours including breast cancer cell lines and haematological malignancies (201,231,232,417). Several mechanisms have been proposed for how ECM may protect cancer cells from chemotherapy, including alterations in drug penetration, changes in drug targets and altered cell survival signalling (200). The data described in chapter 3 clearly demonstrates that ECM-mediated protection of SCLC cells from chemo- and radiotherapy induced cell cycle arrest and apoptosis occurs via cell surface β1 integrins and that blockade of β1 integrins with monoclonal antibodies can inhibit ECM-mediated effects. The central role of β1 integrins in chemo-

resistance has been demonstrated in other tumours including liver, haematological and breast (201,417,418). In addition, the data in chapter 3 confirms that ECM does not affect the activity of the chemotherapeutic agent etoposide and Robert Rintoul has previously shown that ECM proteins do not modulate topoisomerase II levels or activity (167). Thus, the data here, and that of others, demonstrate that integrin-ECM interaction is an important mechanism of drug resistance in cancer (Fig. 8.1).

Figure 8.1: ECM protects SCLC cells via β1 integrins.



Simple schematic demonstrating SCLC cells in suspension and adhered to ECM in the tumour microenvironment via β1 integrins (β1). Non-adherent cells survive and proliferate through autocrine growth loops. The data in chapter 3 shows that adhesion to ECM promotes chemo-resistance thus allowing SCLC cells to survive initial therapy. The result is recurrence or persistence of tumour, which may have acquired further multi-drug resistance. It is predicted that interrupting this interaction may improve response to therapy and disease free survival.

The results presented in chapter 3 suggest that inhibition of β1 integrin-ECM interaction may be a novel strategy for preventing initial chemo-resistance in SCLC cells and other tumours. However, further experiments are required to address the role of ECM and integrins in SCLC growth, survival and metastasis *in vivo*. It has been previously indicated that SCLC is a rapidly growing, highly metastatic tumour (44). Therefore it seems paradoxical that SCLC cells may use integrin-mediated adhesion to ECM proteins as a survival mechanism. In support of this, prior research has indicated that over-expression of α3 integrin subunits in SCLC cell lines reduces anchorage-independent growth in soft agar (419). It is proposed, that reduced α3

integrin expression allows tumour cell growth without requirement for adhesion to ECM, a process important in metastasis (419). In addition, tissue expression of matrix metalloproteinase (MMPs), a family of proteolytic enzymes that degrade ECM and facilitate tumour invasion, has been demonstrated in SCLC cases and shown to correlate with poor survival (138,420). On the basis that MMPs permit cellular migration and metastasis, and since pre-clinical models suggested that MMP inhibitors are able to inhibit tumour growth and dissemination, a phase III trial of the MMP inhibitor, marimastat was conducted in SCLC (163). Unfortunately, no survival advantage was demonstrated over placebo and, in fact, marimastat reduced quality of life (163). This may reflect the fact that this trial was conducted in patients with advanced SCLC, in whom widespread metastasis had already taken place (163). Thus MMP inhibitors could not be expected to reverse this metastatic process, although they may reduce ECM degradation and turnover in the tumour microenvironment, promoting SCLC resistance to apoptosis.

It appears likely that SCLC cells show varying degrees of adhesion to ECM during tumour growth. In fact, cellular adhesion to basement membrane must vary in different phases of 'normal' cellular behaviour. For example, during mitosis, cells are seen to become detached from underlying matrix so that cellular division can occur satisfactorily. In addition, for active migration to occur, it has been argued that an optimum degree of adhesion between cell and matrix must exist (421). It is predicted that these changes in cell adhesion are mediated by alterations in β1 integrin affinity through 'inside-out' signalling mechanisms. Therefore, when SCLC cells display high-affinity integrins they will be strongly adhered to ECM, with a survival advantage in the face of chemotherapy. When integrin affinity is reduced, cells will be less strongly adhered, more mobile with a greater propensity to metastasize, but more susceptible to chemotherapy-induced apoptosis. Chemotherapy would thus selectively spare those cells most adherent and most protected. This may help to explain why clinical recurrence of SCLC is often at the same sites as the initial disease, where there would be the highest likelihood of a subpopulation of cells with strong cell-ECM contacts. Therefore, understanding the effects of β1 integrin blockade on SCLC metastatic spread is crucial before adopting this as a therapeutic approach.

To further complicate this issue, it is clear from prior studies that β1 integrins play a central role in many important processes including tissue repair, haematopoiesis, inflammation and immunity (422). The complex effects of therapeutic β1 integrin blockade can be appreciated by considering the non-tumour cells in the SCLC stroma, namely fibroblasts, leukocytes and endothelial cells (blood vessels). Each of these different cell types expresses β1 integrins, which have a central role in their cellular function (summarised in Figure 8.2). β1 integrins have been shown to be important in leukocyte trafficking to sites of inflammation, T-lymphocyte activation, maintaining fibroblast viability, promoting matrix assembly, endothelial cell survival and angiogenesis (423-426). Therefore, although blocking β1 integrin function could improve cancer treatment by reducing chemo-resistance in SCLC cells, it could also prevent an adequate anti-tumour immune response and promote tumour angiogenesis facilitating growth and metastasis. Taken together these arguments suggest that non-specific inhibition of β1 integrins may have unwanted effects on SCLC growth and spread that limit the effectiveness of this strategy.

To address these concerns it is clear that further studies of β1 integrin blocking strategies are required in pre-clinical models. Prior studies have confirmed that human SCLC cells can be implanted (xenograft) in the flank of nude mice and will form small tumours (168). Furthermore, it has been demonstrated that tumour growth is enhanced by the addition of ECM proteins (Matrigel™, fibronectin or laminin) at the time of implantation (168). Using this model, β1 integrins blocking antibodies or isotype controls can be administered to mice either at implantation or following early tumour development and the effect on tumour growth, local invasion and metastatic spread determined. In addition, analysis of tumour sections would allow assessment of the effects of β1 integrin inhibition on tumour cell apoptosis (tunnel staining) and proliferation (Ki67) and on angiogenesis (micro-vessel counts) within the tumour stroma. The administration of chemotherapy +/- β1 integrin blockade could also be studied with this model to confirm the *in vivo* applicability of the *in vitro* data presented in chapter 3. Furthermore, analysis of SCLC cells surviving chemotherapy in this system would allow recognition of novel acquired drug resistance mechanisms. Unfortunately, the effects of β1 integrin blockade on the anti-tumour

immune response are difficult to study with present models and await the development of a murine SCLC cell line.

Figure 8.2: The multiple cellular functions of β1 integrins.

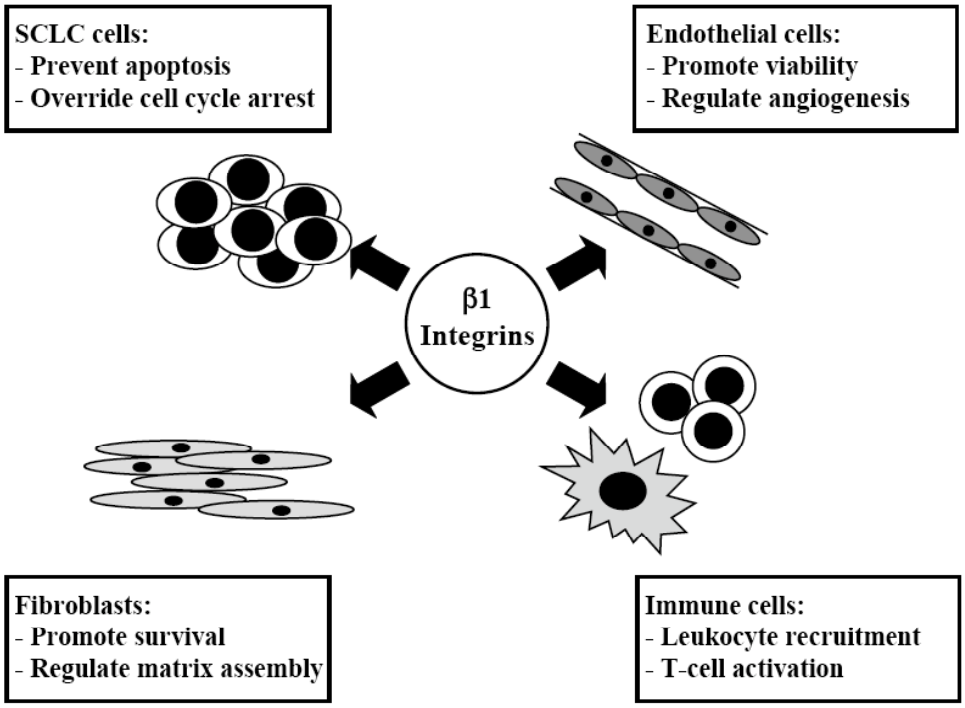


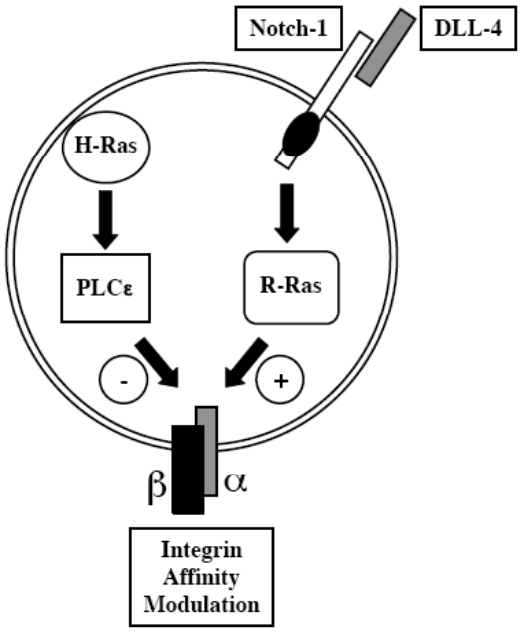
Diagram demonstrating the complex functions of β1 integrins on cells frequently observed within the tumour microenvironment. In this thesis, β1 integrins have been shown to protect SCLC cells from cytotoxic therapies. In addition, β1 integrins play a crucial role in fibroblast survival and ECM assembly. Therefore, integrin blockade may promote the effectiveness of chemotherapy by reducing cancer cell-ECM interaction. However, β1 integrins are also important for leukocyte recruitment/activation and angiogenesis. Thus non-specific integrin blocking strategies may prevent effective anti-tumour immunity and promote metastatic tumour spread.

8.2 Integrin affinity modulators.

It is clear that β1 integrins have multiple important physiological functions and thus non-specific blockade may be an unattractive option. The development of specific integrin inhibitors requires an in depth understanding of the 'inside-out' intracellular pathways that modulate integrin affinity in cancer cells. The data presented in chapters 4 and 5 define two new cell signalling pathways that modulate integrin activation status. These are summarised in figure 8.3. In chapter 4 the mechanisms of

integrin suppression by H-Ras were investigated. These results demonstrate that H-Ras suppresses integrin activation by two cell signalling pathways, one involving ERK and the other dependent on a recently described phospholipase, PLCε. This data explains prior observed discrepancies in H-Ras-mediated suppression and describes a new 'physiological' role for PLCε. In chapter 5, the effect of Notch signalling on integrin activation was investigated. This data indicates that intracellular Notch-1 can activate β1 integrins in an R-Ras dependent manner, thus defining a new Notch signalling pathway and a novel R-Ras activator.

Figure 8.3: Integrin affinity modulation by PLCε and Notch.



A simple diagram demonstrating H-Ras and Notch-1 signalling events modulating integrin affinity within a single cell. The data in chapter 4 demonstrates that H-Ras can suppress β1 integrin affinity (-) through a new PLCε-dependent pathway. The data in chapter 5 shows that activation of Notch-1 by Delta-like ligand-4 (DLL-4) can activate β1 integrins (+) through an R-Ras dependent pathway.

Although these results contribute significantly to the understanding of integrin biology the exact role of these pathways in SCLC remain to be elucidated. SCLC cell lines have been shown to infrequently display mutations in H-Ras suggesting that this pathway may not be important in carcinogenesis of this tumour (427).

Furthermore, over-expression of H-Ras in SCLC cells may promote a NSCLC cell phenotype (428). However, pharmacological interruption of Ras signalling in SCLC cell lines with simvastatin has been shown to reduce *in vivo* tumour growth and increase chemo-sensitivity (429). Unfortunately, the role of integrin-mediated ECM adhesion in this observation was not investigated (429). This suggests that modulation of H-Ras signalling in SCLC cells may have multiple effects possibly due to the presence of several cell-signalling pathways downstream of H-Ras. Further research is required to determine whether H-Ras activation, specifically through PLCε, can suppress SCLC cell integrin affinity and reduce ECM-mediated chemo-resistance.

The role of Notch signalling in SCLC remains complex. Prior data has indicated that Notch-1 and -2 over-expression in SCLC cells promotes an adherent cell phenotype in SCLC cell lines with no native Notch protein expression (314). Furthermore it has been shown that Notch-1 signalling restricts neuroendocrine differentiation in lung development and SCLC cells (314,430). Therefore, it has been suggested that activation of Notch in SCLC cells may act as a tumour suppressor pathway. The data presented in this thesis demonstrates that some SCLC cell lines express Notch signalling components, although Notch-2 appears to be pre-dominant. Interestingly, the Notch ligand Jagged-1 is shown in chapter 5 to up-regulate Hes-1 expression and to protect H69 SCLC cells from etoposide-induced apoptosis, but not to promote cell adhesion to ECM proteins. This indicates that Notch-2 activation does not modulate integrin affinity. This was confirmed using the CHO(α-β)py assay. Furthermore, this data suggests an as yet undefined cell-signalling pathway by which Notch-2 promotes chemo-resistance in SCLC cells. Thus, activation of different Notch receptor subtypes appears to have differing effects on SCLC cells making the development of targeted therapies more challenging. It is clear that further work is needed to define the precise role of Notch both in SCLC pathogenesis and in cell fate decisions in early lung cancer development.

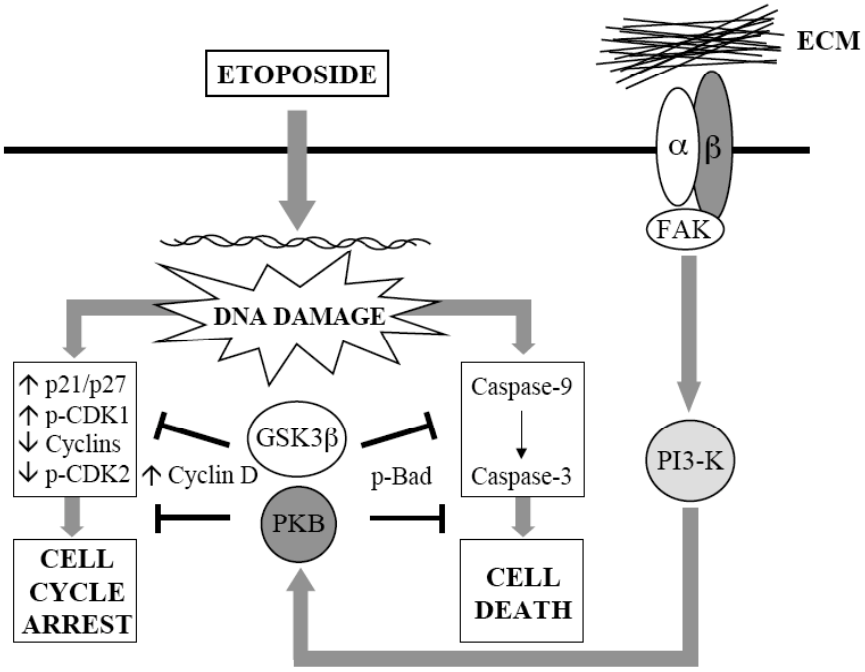
It is apparent that a rationale strategy targeting integrin activation in SCLC cells is not going to be available in the immediate future. Initial experiments should address whether β1 integrin blockade with monoclonal antibodies alter SCLC growth,

metastasis and chemo-resistance in xenograft models as described in section 8.1. If this proves to be an acceptable strategy for promoting tumour response to chemotherapy then further research should focus on the identification of cell signalling cascades specific to SCLC cells that promote integrin activation and the development of small molecule inhibitors of these pathways. The CHO(α-β)py system described in chapters 4 and 5 could be utilised to screen potential integrin modulators. However, it seems likely that identifying the downstream targets of activated integrins that promote survival in cancer cells will produce more readily available therapeutic options.

8.3 Integrin-mediated survival mechanisms in SCLC.

A clear understanding of the specific mechanisms in SCLC cells that mediate β1 integrin protection against the pro-apoptotic effect of DNA damaging drugs is required to develop novel therapeutic targets in the circumvention of multi-drug resistance. The data in chapter 3 indicates that ECM proteins via β1 integrins protect SCLC cells against the pro-apoptotic effects of etoposide and ionizing radiation through tyrosine kinase-mediated PI3-kinase activation. Robert Rintoul demonstrated that adhesion of SCLC cells to ECM stimulated PI3-kinase activity with subsequent phosphorylation of downstream protein kinase B (PKB) and glycogen synthase kinase-3β (GSK3β). These effects were reproduced by β1 integrin stimulating antibodies and sodium orthovanadate. Importantly, it is demonstrated in chapter 3 that adhesion of SCLC cells to ECM prevents etoposide-induced activation of the caspase cascade and that chemical and genetic inhibitors of PI3-kinase signalling block these chemo-protective effects (Fig. 8.4). Furthermore, it is shown that etoposide and ionizing radiation lead to G2/M cell cycle arrest in SCLC cells and that β1 integrin/PI3-kinase activation promotes progression through the G2/M checkpoint. This occurs through alteration in expression of key cell cycle regulators including $p21^{Cip1/WAF1}$, $p27^{Kip1}$, CDK and cyclins. Thus, these data define a new mechanism by which ECM can protect SCLC cells from chemotherapy-induced cell cycle arrest and subsequent apoptosis (Fig. 8.4).

Figure 8.4: The mechanisms of β1 integrin-mediated chemo-protection in SCLC.



In SCLC cells, etoposide or radiation -induced DNA damage causes cell cycle arrest at the G2/M checkpoint through increased expression of $p21^{Cip1/WAF1}$, $p27^{Kip1}$ and phosphorylated CDK 1 (p-CDK1) and decreased expression of phosphorylated CDK 2 (p-CDK2) and cyclins A, D and E. Etoposide-induced DNA damage also causes cleavage of caspase-9, initiating the caspase cascade resulting in SCLC apoptosis. Activation of β1 integrins by extracellular matrix (ECM), activates phosphoinositide-3-OH kinase (PI3-K), and its downstream targets protein kinase B (PKB) and glycogen synthase kinase 3β (GSK3β), blocking DNA damage-induced effects on key cell cycle regulators and caspase cleavage, thus preventing cell cycle arrest and subsequent apoptosis.

The importance of the PI3-kinase pathway as a mechanism for cell cycle control and survival is supported by work in other cancers and untransformed cell lines. Prior studies have shown that both PI3-kinase and PKB suppress anoikis and promote chemoresistance (431). The introduction of a constitutively active form of PKB has been demonstrated to confer resistance to anoikis in mammary epithelial cells; the same construct expressed in non-small cell lung cancer (NSCLC) cells also resulted in increased chemo-resistance to mitoxantrone and cisplatin (432). It has been shown that PKB is constitutively activated in NSCLC and confers resistance to both radiation- and chemotherapy-induced apoptosis (433). PI3-kinase activation has been shown to be sufficient to induce G1 transit in fibroblasts and to increase cyclin D1

stability through PKB-dependent phosphorylation of GSK3β (434–436). In addition, PI3-kinase has been shown to down-regulate expression and function of $p27^{Kip1}$ (240). Therefore, targeted inhibition of PI3-kinase could form an important adjunct to standard cytotoxic anticancer therapy.

Future experiments should address the role of PI3-kinase in SCLC growth and chemo-resistance *in vivo* using well-established pre-clinical models. For example, SCLC cells could be implanted in the flank of nude mice, allowed to develop into palpable tumours and then followed by the systemic administration of a chemical PI3-kinase inhibitor (e.g. LY294002). These experiments would allow investigation of the effects of PI3-kinase manipulation on SCLC cell apoptosis, proliferation and growth in the context of an established tumour microenvironment. Crucially, the addition of chemo- or radiotherapy to these studies would demonstrate the potential of PI3-kinase inhibition as an adjunct to standard anticancer therapy and would indicate the predicted side-effect profile. In addition to these experiments it is important to identify the specific PI3-kinase isoforms active in SCLC, either through cell-line or human tumour sample analysis, so that novel 'cancer-specific' inhibitors of this pathway can be developed.

8.4 The interaction of SCLC with immune cells.

Immune cells comprise a significant proportion of the cellular component of the tumour microenvironment. This local host immune response has been shown to control tumour growth and even eradicate malignant cells. Thus, utilising the immune system as a targeted anticancer therapy is very attractive. However, the 'inflammatory' reaction around tumours has a dual-function and can often support cancer cell growth. Furthermore, tumour cells can suppress immune cell function to prevent an effective anti-cancer immune response. Understanding the mechanisms regulating tumour-immune cell interaction is key to the design of effective cancer vaccines and may uncover novel therapeutic targets.

The immune cell infiltrate in SCLC has not been extensively studied. The data presented in chapter 6 shows that, SCLC tumour samples are infiltrated by CD45+ mononuclear immune cells including T-lymphocytes and macrophages. This infiltrate is similar in cellular composition to that of other cancers. Interestingly, the

study described here of 40 SCLC tumour sections found a marked difference in the amount of CD45+ cells between patients, which correlated with improved patient survival independently of other prognostic indicators. Although this is a small preliminary study, it suggests that the local leukocyte infiltrate in SCLC may represent a specific anti-tumour immune response. This appears to be inadequate to control established tumour growth but may kill residual cancer cells present after chemotherapy thus preventing or increasing the time to patient relapse.

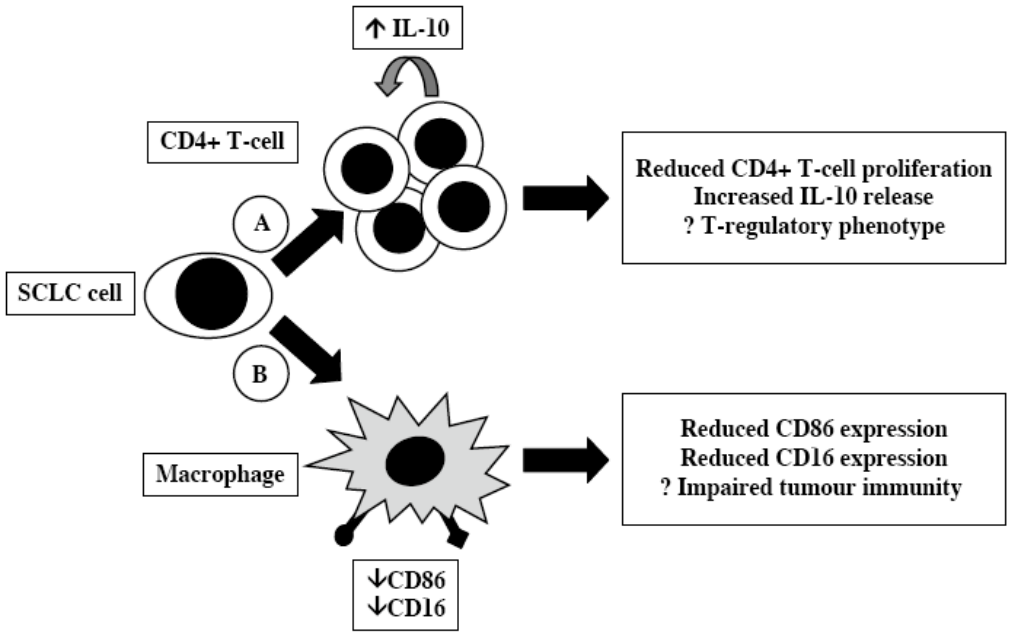
Prior clinical studies in SCLC have demonstrated the presence of defects in cell-mediated immune responses that improve on reduction in tumour burden (187,188,356,382). This taken together with the stark differences in leukocyte infiltration observed between patients, suggests that SCLC cells may produce local immunosuppressive factors, which can prevent an adequate immune response. The *in vitro* co-culture experiments described in chapter 7 were performed to investigate the mechanisms of immunosuppression by SCLC cells. It is shown that SCLC cells can suppress activation of a mixed-leukocyte reaction, CD4+ T-cell proliferation and macrophage surface expression of co-stimulatory molecules (Fig. 8.5). Furthermore, it is demonstrated that some of these effects are mediated by a low molecular weight, heat-stable, soluble factor constitutively produced by SCLC cells which increases IL-10 release by CD4+ T-cells. Preliminary data suggests that this factor may be the neuropeptide bombesin/GRP although further confirmation of this is required. These observations suggest some important questions that should be the focus of future experiments and will be discussed below.

8.4.1 Why do CD45+ infiltrating leucocytes predict patient prognosis in SCLC?

It is hypothesised that the presence of CD45+ cells in SCLC tumour sections represents a specific anti-tumour immune response. Thus CD45+ infiltration should predict a longer time to relapse from tumour recurrence and be accompanied by an increase in SCLC cell death. Future studies should aim to collect SCLC tumour samples prospectively and stain these using immunohistochemistry for the presence of CD45 (leucocytes), Ki67 (proliferation), TUNEL (apoptosis) and CD34 (angiogenesis). These markers should then be correlated with established patient

prognostic indicators (e.g. PS, age, sex), tumour stage (LD, ED, TMN), overall survival time and time to relapse. Primarily, these experiments should determine the role of CD45 as an independent marker of patient prognosis and provide direct *in vivo* evidence of a mechanism by which tumour leukocytes can affect SCLC growth.

Figure 8.5: The interaction of SCLC cells with CD4+ T-cells and macrophages.



Schematic showing the observed effects of SCLC cells on human CD4+ T-cells and macrophages. SCLC cells suppress CD4+ T-cell proliferation and macrophage surface expression of CD86 and CD16 *in vitro*. Furthermore, IL-10 release by activated CD4+ T-cells is increased by co-culture with SCLC cells. These effects on CD4+ T-cells and macrophages appear to be mediated by different mechanisms: (A) a soluble factor secreted by SCLC cells into culture medium; (B) a process requiring cell-cell interaction. Defining these mechanisms is key to improving the host immune response to SCLC.

8.4.2 Do tumour-infiltrating CD4+ T-cells predict patient prognosis?

Assessment of the specific immune cell types infiltrating SCLC tumours may predict patient prognosis more accurately than assessment of total leukocyte infiltrate. Lymphocyte-mediated immune functions appear to be important in SCLC prognosis (356,372). Furthermore, the data in chapter 7 suggests that SCLC cells can suppress CD4+ proliferation and increase IL-10 release *in vitro*. CD4+ T-cells co-ordinate

many immune functions and have been shown to promote tumour rejection *in vivo* (387). Therefore, the presence of CD4+ T-cells within the tumour microenvironment may correlate accurately with improved patient prognosis. Future experiments should aim to identify CD4+ T-cells within SCLC tumour sections collected prospectively and correlate number and distribution with patient survival and tumour stage. In addition, studies should be performed to investigate the phenotype of CD4+ T-cells with particular reference to IL-10 producing T-regulatory cells. It is predicted that in contrast to T-helper cells, T-regulatory cells would correlate with reduced total leukocyte infiltrate and poorer patient prognosis. These investigations would provide evidence for the *in vivo* role of CD4+ T-cells in SCLC indicating the importance of these cells as targets for anticancer therapy.

8.4.3 Why do patients have differences in leucocyte infiltration?

The results presented in chapter 7 show that soluble factors produced by SCLC cells *in vitro* can suppress the function of immune cells derived from healthy volunteers. It is hypothesised that *in vivo* production of immuno-inhibitory factors by SCLC cells suppress local immune cell function (e.g. CD4+ T-cells), which prevents an adequate host immune response. Therefore, differences in the production of these factors in the tumour microenvironment could underpin the observed differences in leukocyte infiltrate and thus patient survival. Future experiments should initially focus on whether SCLC cells can induce T-regulatory cells *in vitro* using co-culture experiments. Secondly the role of neuropeptides in SCLC-mediated suppression of CD4+ T-cell proliferation should be determined as described in chapter 7. If these experiments show that bombesin/GRP is responsible for the suppressive effects then a study of bombesin/GRP expression in SCLC tumour samples should be undertaken and correlated with immune cell infiltrate and patient survival. This could then be followed by phase I/II trials of specific bombesin inhibitors. In the absence of a role for bombesin, then the tumour microenvironment could be investigated for expression of other immunosuppressive factors using immunohistochemistry (e.g. TNF ligands) or DNA microarrays. The results of these exploratory studies could then be used to guide future *in vitro* mechanistic research. It is predicted that these

experiments will define central mechanisms by which SCLC cells alter host immune responses.

Particular focus has been given here to key experiments that will answer specific questions about the applicability of potential strategies for disrupting ECM-mediated chemo-resistance in SCLC. In addition, translational studies have been outlined to determine important immunosuppressive mechanisms of SCLC. It is hoped that the conclusions drawn from data presented in this thesis form the basis for such research into the microenvironment interactions of SCLC with the subsequent development of novel treatments in the future.

REFERENCES:

(1) Ferlay J, Autier P, Boniol M, Heanue M, Colombet M, Boyle P. Estimates of the cancer incidence and mortality in Europe in 2006 Ann Oncol. 2007;18:581-92.

(2) Franceschi S, Bidoli E. The epidemiology of lung cancer. Ann Oncol. 1999;10:S3-6.

(3) Ginsberg MS, Grewal RK, Heelan RT. Lung cancer. Radiol Clin North Am. 2007;45:21-43.

(4) Harkness EF, Brewster DH, Kerr KM, Fergusson RJ, MacFarlane GJ. Changing trends in incidence of lung cancer by histologic type in Scotland. Int J Cancer. 2002;102:179-83

(5) Janssen-Heijnen ML, Coebergh JW. The changing epidemiology of lung cancer in Europe. Lung Cancer. 2003;41:245-58.

(6) Ettinger DS. Overview and state of the art in the management of lung cancer. Oncology (Williston Park). 2004;18:3-9.

(7) Ohe Y. Chemoradiotherapy for lung cancer: current status and perspectives. Int J Clin Oncol 2004;9:435-443

(8) Smythe WR. Treatment of stage I non-small cell lung carcinoma. Chest 2003;123:181-7

(9) Molina JR, Yang P, Cassivi SD, Schild SE, Adjei AA. Non-small cell lung cancer: epidemiology, risk factors, treatment, and survivorship. Mayo Clin Proc. 2008;83:584-94.

(10) Sandler A. Extensive small-cell lung cancer: a treatment overview. Oncology (Williston Park). 2000;14:49-55.

(11) El Maalouf G, Rodier JM, Faivre S, Raymond E. Could we expect to improve survival in small cell lung cancer? Lung Cancer. 2007;57:30-4.

(12) Govindan R, Page N, Morgensztern D, Read W, Tierney R, Vlahiotis A, Spitznagel EL, Piccirillo J. Changing epidemiology of small-cell lung cancer in the United States over the last 30 years: Analysis of the Surveillance, Epidemiologic, and End Results database. J Clin Oncol 2006;24:4539–44.

(13) Westlake S, Cooper N. Cancer incidence and mortality: trends in the United Kingdom and constituent countries, 1993 to 2004. Health Stat Q. 2008;38:33-46.

(14) Jemal A, Siegel R, Ward E, Murray T, Xu J, Thun MJ. Cancer statistics, 2007. CA Cancer J Clin. 2007;57:43-66.

(15) Govindan R, Page N, Morgensztern D, Read W, Tierney R, Vlahiotis A, Spitznagel EL, Piccirillo J. Changing epidemiology of small-cell lung cancer in the United States over the last 30 years: analysis of the surveillance, epidemiologic, and end results database. J Clin Oncol. 2006;24:4539-44.

(16) Office for National Statistics, Cancer Statistics registrations: Registrations of cancer diagnosed in 2004, England. Series MB1 no.33. 2005, National Statistics: London.

(17) Quinn M, Babb P, Brock A, Kirby L, Jones J. Cancer Trends in England & Wales 1950-1999. SMPS No. 66: TSO, 2001

(18) Radzikowska E, Gaz P, Roszkowski K. Lung cancer in women: age, smoking, histology, performance status, stage, initial treatment and survival. Population-based study of 20 561 cases. Ann Oncol. 2002;13:1087-93.

(19) The US National Cancer Institute. Surveillance Epidemiology and End Results (SEER) data base, 1973-2004, http://seer.cancer.gov/ 2007.

(20) Doll R, Hill AB. Smoking and carcinoma of the lung; preliminary report. Br Med J. 1950;2:739-48.

(21) Crispo A, Brennan P, Jöckel KH, Schaffrath-Rosario A, Wichmann HE, Nyberg F, Simonato L, Merletti F, Forastiere F, Boffetta P, Darby S. The cumulative risk of lung cancer among current, ex- and never-smokers in European men. Br J Cancer. 2004;91:1280-6.

(22) Doll R, Peto R. Cigarette smoking and bronchial carcinoma: dose and time relationships among regular smokers and lifelong non-smokers. J Epidemiol Community Health. 1978;32:303-13.

(23) Toh CK, Gao F, Lim WT, Leong SS, Fong KW, Yap SP, Hsu AA, Eng P, Koong HN, Thirugnanam A, Tan EH. Differences between small-cell lung cancer and non-small-cell lung cancer among tobacco smokers. Lung Cancer. 2007;56:161-6.

(24) De Stefani E, Boffetta P, Ronco AL, Brennan P, Correa P, Deneo-Pellegrini H, Gutiérrez LP, Mendilaharsu M. Squamous and small cell carcinomas of the lung: similarities and differences concerning the role of tobacco smoking. Lung Cancer. 2005;47:1-8.

(25) Alberg AJ, Samet JM. Epidemiology of lung cancer. Chest. 2003;123:21-49.

(26) Shibuya K, Inoue M, Lopez AD. Statistical modeling and projections of lung cancer mortality in 4 industrialized countries. Int J Cancer. 2005;117:476-85.

(27) Karim-Kos HE, de Vries E, Soerjomataram I, Lemmens V, Siesling S, Coebergh JW. Recent trends of cancer in Europe: A combined approach of incidence, survival and mortality for 17 cancer sites since the 1990s. Eur J Cancer. 2008;44:1345-89.

(28) Chute CG, Greenberg ER, Baron J, Korson R, Baker J, Yates J. Presenting conditions of 1539 population-based lung cancer patients by cell type and stage in New Hampshire and Vermont. Cancer 1985;56:2107–11.

(29) Gustafsson BI, Kidd M, Chan A, Malfertheiner MV, Modlin IM. Bronchopulmonary neuroendocrine tumors. Cancer. 2008;113:5-21.

(30) Dearing MP, Steinberg SM, Phelps R, Anderson MJ, Mulshine JL, Ihde DC, Johnson BE. Outcome of patients with small-cell lung cancer: effect of changes in staging procedures and imaging technology on prognostic factors over 14 years. J Clin Oncol. 1990;8:1042-9.

(31) Murren JR, Turrisi AT, Pass HI. Small cell lung cancer. In: DeVita VTJ, Hellman S, Rosenberg SA. Cancer: principles and practice of oncology. 7th ed. Philadelphia, PA: Lippincott, Williams & Wilkins, 2005;810–843.

(32) Marchioli CC, Graziano SL. Paraneoplastic syndromes associated with small cell lung cancer. Chest Surg Clin N Am. 1997;7:65-80.

(33) List AF, Hainsworth JD, Davis BW, Hande KR, Greco FA, Johnson DH. The syndrome of inappropriate secretion of antidiuretic hormone (SIADH) in small-cell lung cancer. J Clin Oncol. 1986;4:1191-8.

(34) Campling BG, Sarda IR, Baer KA, Pang SC, Baker HM, Lofters WS, Flynn TG. Secretion of atrial natriuretic peptide and vasopressin by small cell lung cancer. Cancer 1995;75:2442–51.

(35) Shepherd FA, Laskey J, Evans WK, Goss PE, Johansen E, Khamsi F. Cushing's syndrome associated with ectopic corticotropin production and small-cell lung cancer. J Clin Oncol. 1992;10:21-7.

(36) Elrington GM, Murray NM, Spiro SG, Newsom-Davis J. Neurological paraneoplastic syndromes in patients with small cell lung cancer. A prospective survey of 150 patients. J Neurol Neurosurg Psychiatry. 1991;54:764-7.

(37) O'Neill JH, Murray NM, Newsom-Davis J. The Lambert-Eaton myasthenic syndrome. A review of 50 cases. Brain. 1988;111:577-96.

(38) Motomura M, Lang B, Johnston I, Palace J, Vincent A, Newsom-Davis J. Incidence of serum anti-P/O-type and anti-N-type calcium channel autoantibodies in the Lambert-Eaton myasthenic syndrome. J Neurol Sci. 1997;147:35-42.

(39) Quoix E, Fraser R, Wolkove N, Finkelstein H, Kreisman H. Small cell lung cancer presenting as a solitary pulmonary nodule. Cancer. 1990;66:577-582.

(40) Quinn D, Gianlupi A, Broste S. The changing radiographic presentation of bronchogenic carcinoma with reference to cell types. Chest 1996;110:1474-79.

(41) Rivera MP, Detterbeck F, Mehta AC. Diagnosis of lung cancer: the guidelines. Chest. 2003;123:129-36.

(42) Travis WD, Colby TV, Corrin B, Shimosato Y, Brambilla E. Histological Typing of Lung and Pleural Tumours. 3rd ed. Berlin, Germany: Springer-Verlag; 1999. World Health Organization International Histological Classification of Tumours.

(43) Guinee DG Jr, Fishback NF, Koss MN, Abbondanzo SL, Travis WD. The spectrum of immunohistochemical staining of small-cell lung carcinoma in specimens from transbronchial and open-lung biopsies. Am J Clin Pathol 1994;102:406-414.

(44) Argiris A, Murren JR. Staging and clinical prognostic factors for small-cell lung cancer. Cancer J 2001;7:437-47.

(45) Micke P, Faldum A, Metz T, Beeh KM, Bittinger F, Hengstler JG, Buhl R. Staging small cell lung cancer: Veterans Administration Lung Study Group

versus International Association for the Study of Lung Cancer--what limits limited disease? Lung Cancer. 2002;37:271-6.

(46) Shepherd FA, Crowley J, Van Houtte P, Postmus PE, Carney D, Chansky K, Shaikh Z, Goldstraw P. The International Association for the Study of Lung Cancer lung cancer staging project: proposals regarding the clinical staging of small cell lung cancer in the forthcoming (seventh) edition of the tumor, node, metastasis classification for lung cancer. J Thorac Oncol. 2007;2:1067-77.

(47) Anraku M, Waddell TK. Surgery for small-cell lung cancer. Semin Thorac Cardiovasc Surg. 2006;18:211–16.

(48) Carmichael J, Mitchell JB, DeGraff WG, Gamson J, Gazdar AF, Johnson BE, Glatstein E, Minna JD. Chemosensitivity testing of human lung cancer cell lines using the MTT assay. Br J Cancer. 1988;57:540-7.

(49) Green R, Humphrey E, Close H, Patno ME. Alkylating agents in bronchogenic carcinoma. Am J Med 1969;46:516–25.

(50) Argiris A, Murren JR. Advances in chemotherapy for small cell lung cancer: single-agent activity of newer agents. Cancer J. 2001;7:228–35.

(51) Bunn P, Cohen M, Ihde DC. Advances in small cell bronchogenic carcinoma. Cancer Treat Rep 1977;61:333-42.

(52) Mascaux C, Paesmans M, Berghmans T. A systematic review of the role of etoposide and cisplatin in the chemotherapy of small cell lung cancer with methodology assessment and meta-analysis. Lung Cancer. 2000;30:23–36.

(53) Roth BJ, Johnson DH, Einhorn LH, Schacter LP, Cherng NC, Cohen HJ, Crawford J, Randolph JA, Goodlow JL, Broun GO, Omura GA, Greco FA. Randomized Study of Cyclophosphamide, Doxorubicin, and Vincristine Versus Etoposide and Cisplatin Versus Alternation of These Two Regimens in Extensive Small-Cell Lung Cancer: A Phase III Trial of the Southeastern Cancer Study Group. J Clin Oncol 1992;10:282–91.

(54) Skarlos DV, Samantas E, Kosmidis P, Fountzilas G, Angelidou M, Palamidas P, Mylonakis N, Provata A, Papadakis E, Klouvas G. Randomized comparison of etoposide-cisplatin vs. etoposide-carboplatin and irradiation in

small-cell lung cancer. A Hellenic Co-operative Oncology Group study. Ann Oncol. 1994;5:601-7.

(55) Sundstrøm S, Bremnes RM, Kaasa S, Aasebø U, Hatlevoll R, Dahle R, Boye N, Wang M, Vigander T, Vilsvik J, Skovlund E, Hannisdal E, Aamdal S. Cisplatin and etoposide regimen is superior to cyclophosphamide, epirubicin, and vincristine regimen in small-cell lung cancer: results from a randomized phase III trial with 5 years' follow-up. J Clin Oncol. 2002;20:4665-72.

(56) Mavroudis D, Papadakis E, Veslemes M, Tsiafaki X, Stavrakakis J, Kouroussis C, Kakolyris S, Bania E, Jordanoglou J, Agelidou M, Vlachonicolis J, Georgoulias V. A multicenter randomized clinical trial comparing paclitaxel-cisplatin-etoposide versus cisplatin-etoposide as first-line treatment in patients with small-cell lung cancer. Ann Oncol. 2001;12:463-70.

(57) Tiseo M, Ardizzoni A. Current status of second-line and novel therapies for snall cell lung cancer. J Thorac Oncol. 2007;2:764-72

(58) Wolf M. Dose intensive chemotherapy in small cell lung cancer. Lung Cancer. 2001;33:125-35.

(59) Tjan-Heijnen VC, Wagener DJ, Postmus PE. An analysis of chemotherapy dose and dose-intensity in small-cell lung cancer: lessons to be drawn. Ann Oncol. 2002;13:1519-30.

(60) Bozcuk H, Artac M, Ozdogan M, Savas B. Does maintenance/consolidation chemotherapy have a role in the management of small cell lung cancer (SCLC)? A metaanalysis of the published controlled trials. Cancer. 2005;104:2650-7.

(61) Thatcher N, Qian W, Clark PI, Hopwood P, Sambrook RJ, Owens R, Stephens RJ, Girling DJ. Ifosfamide, carboplatin, and etoposide with midcycle vincristine versus standard chemotherapy in patients with small-cell lung cancer and good performance status: clinical and quality-of-life results of the British Medical Research Council multicenter randomized LU21 trial. J Clin Oncol. 2005;23:8371-9.

(62) Crossin KL, Carney DH. Microtubule stabilization by taxol inhibits initiation of DNA synthesis by thrombin and by epidermal growth factor. Cell. 1981;27:341-50.

(63) Kirschling RJ, Grill JP, Marks RS, Kugler JW, Gerstner JB, Kuross SA, Michalak JC, Windschitl HE, Krewer KD, Jett JR. Paclitaxel and G-CSF in previously untreated patients with extensive stage small-cell lung cancer: a phase II study of the North Central Cancer Treatment Group. Am J Clin Oncol. 1999;22:517-22.

(64) Niell HB, Herndon JE 2nd, Miller AA, Watson DM, Sandler AB, Kelly K, Marks RS, Perry MC, Ansari RH, Otterson G, Ellerton J, Vokes EE, Green MR; Cancer and Leukemia Group. Randomized phase III intergroup trial of etoposide and cisplatin with or without paclitaxel and granulocyte colony-stimulating factor in patients with extensive-stage small-cell lung cancer: Cancer and Leukemia Group B Trial 9732. J Clin Oncol. 2005;23:3752-9.

(65) Hertel LW, Boder GB, Kroin JS, Rinzel SM, Poore GA, Todd GC, Grindey GB. Evaluation of the antitumor activity of gemcitabine (2',2'-difluoro-2'-deoxycytidine). Cancer Res. 1990;50:4417-22.

(66) Hesketh PJ, Chansky K, Israel V, Grapski RT, Mekhail TM, Spiridonidis CH, Mills GM, Kelly K, Crowley JJ, Gandara DR. Phase II study of gemcitabine and cisplatin in patients with previously untreated extensive stage small cell lung cancer: Southwest Oncology Group Study 9718. J Thorac Oncol. 2007;2:440-4.

(67) Sugimoto Y, Tsukahara S, Oh-hara T, Isoe T, Tsuruo T. Decreased expression of DNA topoisomerase I in camptothecin-resistant tumor cell lines as determined by a monoclonal antibody. Cancer Res. 1990;50:6925-30.

(68) Noda K, Nishiwaki Y, Kawahara M, Negoro S, Sugiura T, Yokoyama A, Fukuoka M, Mori K, Watanabe K, Tamura T, Yamamoto S, Saijo N; Japan Clinical Oncology Group. Irinotecan plus cisplatin compared with etoposide plus cisplatin for extensive small cell lung cancer. N Engl J Med. 2002;346:85-91.

(69) Hanna N, Bunn PA Jr, Langer C, Einhorn L, Guthrie T Jr, Beck T, Ansari R, Ellis P, Byrne M, Morrison M, Hariharan S, Wang B, Sandler A.

Randomized phase III trial comparing irinotecan/cisplatin with etoposide/cisplatin in patients with previously untreated extensive-stage disease small-cell lung cancer. J Clin Oncol. 2006;24:2038-43.

(70) von Pawel J, Schiller JH, Shepherd FA, Fields SZ, Kleisbauer JP, Chrysson NG, Stewart DJ, Clark PI, Palmer MC, Depierre A, Carmichael J, Krebs JB, Ross G, Lane SR, Gralla R. Topotecan versus cyclophosphamide, doxorubicin, and vincristine for the treatment of recurrent small-cell lung cancer. J Clin Oncol. 1999;17:658-67.

(71) Carmichael J, Degraff WG, Gamson J, Russo D, Gazdar AF, Levitt ML, Minna JD, Mitchell JB. Radiation sensitivity of human lung cancer cell lines. Eur J Cancer Clin Oncol. 1989;25:527-34.

(72) Warde P, Payne D. Does thoracic irradiation improve survival and local control in limited-stage small-cell carcinoma of the lung? A meta-analysis. J Clin Oncol. 1992;6:890-5

(73) Pignon JP, Arriagada R, Ihde DC. A meta-analysis of thoracic radiotherapy for small-cell lung cancer. N Engl J Med. 1992;23:1618-24.

(74) Simon GR, Turrisi A; American College of Chest Physicians. Management of small cell lung cancer: ACCP evidence-based clinical practice guidelines (2nd edition). Chest. 2007;132:324-39.

(75) Pijls-Johannesma M, De Ruysscher D, Vansteenkiste J, Kester A, Rutten I, Lambin P. Timing of chest radiotherapy in patients with limited stage small cell lung cancer: a systematic review and meta-analysis of randomised controlled trials. Cancer Treat Rev. 2007;33:461-73.

(76) Choi NC, Herndon JE II, Rosenman J. Phase I study to determine the maximum-tolerated dose of radiation in standard daily and hyperfractionated-accelerated twice-daily radiation schedules with concurrent chemotherapy for limited-stage small-cell lung cancer. J Clin Oncol. 1998;16:3528-36.

(77) Bogart JA, Herndon JE II, Lyss AP. 70 Gy thoracic radiotherapy is feasible concurrent with chemotherapy for limited-stage small-cell lung cancer: Analysis of Cancer and Leukemia Group B study 39808. Int J Radiat Oncol Biol Phys. 2004;59:460-8.

(78) Turrisi AT III, Kim K, Blum R. Twice-daily compared with once-daily thoracic radiotherapy in limited small-cell lung cancer treated concurrently with cisplatin and etoposide. N Engl J Med. 1999;340:265-71.

(79) Seute T, Leffers P, Wilmink JT, ten Velde GP, Twijnstra A. Response of asymptomatic brain metastases from small-cell lung cancer to systemic first-line chemotherapy. J Clin Oncol. 2006;24:2079-83.

(80) Aupérin A, Arriagada R, Pignon JP, Le Péchoux C, Gregor A, Stephens RJ, Kristjansen PE, Johnson BE, Ueoka H, Wagner H, Aisner J. Prophylactic cranial irradiation for patients with small-cell lung cancer in complete remission. Prophylactic Cranial Irradiation Overview Collaborative Group. N Engl J Med. 1999;341:476-84.

(81) Bremnes RM, Sundstrom S, Aasebø U, Kaasa S, Hatlevoll R, Aamdal S; Norweigian Lung Cancer Study Group. The value of prognostic factors in small cell lung cancer: results from a randomised multicenter study with minimum 5-year follow-up. Lung Cancer. 2003;39:303-13.

(82) Sato M, Shames DS, Gazdar AF, Minna JD. A translational view of the molecular pathogenesis of lung cancer. J Thorac Oncol. 2007;2:327-43.

(83) Brambilla E, Lantuejoul S, Sturm N. Divergent differentiation in neuroendocrine lung tumors. Semin Diagn Pathol. 2000;17:138-48.

(84) North WG. Gene regulation of vasopressin and vasopressin receptors in cancer. Exp Physiol. 2000;85:27-40.

(85) Anbazhagan R, Tihan T, Bornman DM, Johnston JC, Saltz JH, Weigering A, Piantadosi S, Gabrielson E. Classification of small cell lung cancer and pulmonary carcinoid by gene expression profiles. Cancer Res. 1999;59:5119-22.

(86) Hibi K, Takahashi T, Yamakawa K, Ueda R, Sekido Y, Ariyoshi Y, Suyama M, Takagi H, Nakamura Y, Takahashi T. Three distinct regions involved in 3p deletion in human lung cancer. Oncogene. 1992;7:445-9.

(87) Kok K, Naylor SL, Buys CH. Deletions of the short arm of chromosome 3 in solid tumors and the search for suppressor genes. Adv Cancer Res. 1997;71:27-92.

(88) Sozzi G, Veronese ML, Negrini M, Baffa R, Cotticelli MG, Inoue H, Tornielli S, Pilotti S, De Gregorio L, Pastorino U, Pierotti MA, Ohta M, Huebner K, Croce CM. The FHIT gene 3p14.2 is abnormal in lung cancer. Cell. 1996;85:17-26.

(89) Miura I, Graziano SL, Cheng JQ, Doyle LA, Testa JR. Chromosome alterations in human small cell lung cancer: frequent involvement of 5q. Cancer Res. 1992;52:1322-8.

(90) D'Amico D, Carbone D, Mitsudomi T, Nau M, Fedorko J, Russell E, Johnson B, Buchhagen D, Bodner S, Phelps R. High frequency of somatically acquired p53 mutations in small-cell lung cancer cell lines and tumors. Oncogene. 1992;7:339-46.

(91) Harbour JW, Lai SL, Whang-Peng J, Gazdar AF, Minna JD, Kaye FJ. Abnormalities in structure and expression of the human retinoblastoma gene in SCLC. Science. 1988;241:353-7.

(92) Hodkinson PS, Mackinnon A, Sethi T. Targeting growth factors in lung cancer. Chest. 2008;133:1209-16.

(93) Langdon S, Sethi T, Ritchie A, Muir M, Smyth J, Rozengurt E. Broad spectrum neuropeptide antagonists inhibit the growth of small cell lung cancer *in vivo*. Cancer Res. 1992;52:4554-7.

(94) Wittau N, Grosse R, Kalkbrenner F, Gohla A, Schultz G, Gudermann T. The galanin receptor type 2 initiates multiple signaling pathways in small cell lung cancer cells by coupling to G(q), G(i) and G(12) proteins. Oncogene. 2000;19:4199-209.

(95) Waters CM, MacKinnon AC, Cummings J, Tufail-Hanif U, Jodrell D, Haslett C, Sethi T. Increased gastrin-releasing peptide (GRP) receptor expression in tumour cells confers sensitivity to [Arg6,D-Trp7,9,NmePhe8]-substance P (6-11)-induced growth inhibition. Br J Cancer. 2003;88:1808-16.

(96) Chaudhry A, Carrasquillo JA, Avis IL, Shuke N, Reynolds JC, Bartholomew R, Larson SM, Cuttitta F, Johnson BE, Mulshine JL. Phase I and imaging trial of a monoclonal antibody directed against gastrin-releasing peptide in patients with lung cancer. Clin Cancer Res. 1999;5:3385-93.

(97) Fischer B, Marinov M, Arcaro A. Targeting receptor tyrosine kinase signalling in small cell lung cancer (SCLC): what have we learned so far? Cancer Treat Rev. 2007;33:391-406.

(98) Micke P, Basrai M, Faldum A, Bittinger F, Rönnstrand L, Blaukat A, Beeh KM, Oesch F, Fischer B, Buhl R, Hengstler JG. Clin Cancer Res. Characterization of c-kit expression in small cell lung cancer: prognostic and therapeutic implications. 2003;9:188-94.

(99) Krystal GW, Honsawek S, Litz J, Buchdunger E. The selective tyrosine kinase inhibitor STI571 inhibits small cell lung cancer growth. Clin Cancer Res. 2000;6:3319-26.

(100) Yu H, Spitz MR, Mistry J, Gu J, Hong WK, Wu X. Plasma levels of insulin-like growth factor-I and lung cancer risk: a case-control analysis. J Natl Cancer Inst. 1999;91:151-6.

(101) Nakanishi Y, Mulshine JL, Kasprzyk PG, Natale RB, Maneckjee R, Avis I, Treston AM, Gazdar AF, Minna JD, Cuttitta F. Insulin-like growth factor-I can mediate autocrine proliferation of human small cell lung cancer cell lines *in vitro*. J Clin Invest. 1988;82:354-9.

(102) Grandori C, Cowley SM, James LP, Eisenman RN. The Myc/Max/Mad network and the transcriptional control of cell behavior. Annu Rev Cell Dev Biol. 2000;16:653-99.

(103) Takahashi T, Obata Y, Sekido Y, Hida T, Ueda R, Watanabe H, Ariyoshi Y, Sugiura T, Takahashi T. Expression and amplification of myc gene family in small cell lung cancer and its relation to biological characteristics. Cancer Res. 1989;49:2683-8.

(104) Funa K, Steinholtz L, Nou E, Bergh J. Increased expression of N-myc in human small cell lung cancer biopsies predicts lack of response to chemotherapy and poor prognosis. Am J Clin Pathol. 1987;88:216-20.

(105) Dosaka-Akita H, Akie K, Hiroumi H, Kinoshita I, Kawakami Y, Murakami A. Inhibition of proliferation by L-myc antisense DNA for the translational initiation site in human small cell lung cancer. Cancer Res. 1995;55:1559-64.

(106) Adachi J, Ookawa K, Shiseki M, Okazaki T, Tsuchida S, Morishita K, Yokota J. Induction of apoptosis but not G1 arrest by expression of the wild-

type p53 gene in small cell lung carcinoma. Cell Growth Differ. 1996;7:879-86.

(107) Peoc'h M, Brambilla E, Moro D, Gazzeri S, Brambilla C. Respective roles of the products of the MDR1 and p53 genes in drug resistance of bronchial cancers. Bull Cancer. 1994;81:98-104.

(108) Cory S. Regulation of lymphocyte survival by the bcl-2 gene family. Annu Rev Immunol. 1995;13:513-43.

(109) Jiang SX, Sato Y, Kuwao S, Kameya T. Expression of bcl-2 oncogene protein is prevalent in small cell lung carcinomas. Pathol. 1995;177:135-8.

(110) Ikegaki N, Katsumata M, Minna J, Tsujimoto Y. Expression of bcl-2 in small cell lung carcinoma cells. Cancer Res. 1994;54:6-8.

(111) Sartorius UA, Krammer PH. Upregulation of Bcl-2 is involved in the mediation of chemotherapy resistance in human small cell lung cancer cell lines. Int J Cancer. 2002;97:584-92.

(112) Rodier F, Campisi J, Bhaumik D. Two faces of p53: aging and tumor suppression. Nucleic Acids Res. 2007;35:7475-84.

(113) Mitsiades CS, Mitsiades N, Koutsilieris M. The Akt pathway: molecular targets for anti-cancer drug development. Curr Cancer Drug Targets. 2004;4: 235-56.

(114) Kennedy SG, Wagner AJ, Conzen SD, Jordán J, Bellacosa A, Tsichlis PN, Hay N. The PI 3-kinase/Akt signaling pathway delivers an anti-apoptotic signal. Genes Dev. 1997;11:701-13.

(115) Kulik G, Weber MJ. Akt-dependent and -independent survival signaling pathways utilized by insulin-like growth factor I. Mol Cell Biol. 1998;18:6711-8.

(116) Feng LX, Ravindranath N, Dym M. Stem cell factor/c-kit up-regulates cyclin D3 and promotes cell cycle progression via the phosphoinositide 3-kinase/p70 S6 kinase pathway in spermatogonia. J Biol Chem. 2000;275:25572-6.

(117) Moore SM, Rintoul RC, Walker TR, Chilvers ER, Haslett C, Sethi T. The presence of a constitutively active phosphoinositide 3-kinase in small cell

lung cancer cells mediates anchorage-independent proliferation via a protein kinase B and p70s6k-dependent pathway. Cancer Res. 1998;58:5239-47.

(118) Sonneveld P. Multidrug resistance in haematological malignancies. J Intern Med. 2000;247:521-34.

(119) Hsia TC, Lin CC, Wang JJ, Ho ST, Kao A. Relationship between chemotherapy response of small cell lung cancer and P-glycoprotein or multidrug resistance-related protein expression. Lung. 2002;180:173-9.

(120) Sohn JW, Lee SY, Lee SJ, Kim EJ, Cha SI, Kim CH, Lee JT, Jung TH, Park JY. MDR1 polymorphisms predict the response to etoposide-cisplatin combination chemotherapy in small cell lung cancer. Jpn J Clin Oncol. 2006;36:137-41.

(121) Campling BG, Young LC, Baer KA, Lam YM, Deeley RG, Cole SP, Gerlach JH. Expression of the MRP and MDR1 multidrug resistance genes in small cell lung cancer. Clin Cancer Res. 1997;3:115-22.

(122) McClendon AK, Osheroff N. DNA topoisomerase II, genotoxicity, and cancer. Mutat Res. 2007;623:83-97.

(123) Andoh T, Nishizawa M, Hida T, Ariyoshi Y, Takahashi T, Ueda R. Reduced expression of DNA topoisomerase II confers resistance to etoposide (VP-16) in small cell lung cancer cell lines established from a refractory tumor of a patient and by in vitro selection. Oncol Res. 1996;8:229-38.

(124) Folkman J. Angiogenesis: an organizing principle for drug discovery? Nat Rev Drug Discov. 2007;6:273-286.

(125) Ferrara N. VEGF and the quest for tumour angiogenesis factors. Nat Rev Cancer. 2002;2:795-803.

(126) Hasegawa Y, Takanashi S, Okudera K, Kumagai M, Hayashi A, Morimoto T, Okumura K. Vascular endothelial growth factor level as a prognostic determinant of small cell lung cancer in Japanese patients. Intern Med. 2005;44:26-34.

(127) Lucchi M, Mussi A, Fontanini G, Faviana P, Ribechini A, Angeletti CA. Small cell lung carcinoma (SCLC): the angiogenic phenomenon. Eur J Cardiothorac Surg. 2002;21:1105-10.

(128) Litz J, Sakuntala Warshamana-Greene G, Sulanke G, Lipson KE, Krystal GW. The multi-targeted kinase inhibitor SU5416 inhibits small cell lung cancer growth and angiogenesis, in part by blocking Kit-mediated VEGF expression. Lung Cancer. 2004;46:283-91.

(129) Ueno K, Inoue Y, Kawaguchi T, Hosoe S, Kawahara M. Increased serum levels of basic fibroblast growth factor in lung cancer patients: relevance to response of therapy and prognosis. Lung Cancer. 2001;31:213-9.

(130) Rygaard K, Nakamura T, Spang-Thomsen M. Expression of the proto-oncogenes c-met and c-kit and their ligands, hepatocyte growth factor/scatter factor and stem cell factor, in SCLC cell lines and xenografts. Br J Cancer. 1993;67:37-46.

(131) Maulik G, Kijima T, Ma PC, Ghosh SK, Lin J, Shapiro GI, Schaefer E, Tibaldi E, Johnson BE, Salgia R. Modulation of the c-Met/hepatocyte growth factor pathway in small cell lung cancer. Clin Cancer Res. 2002;8:620-7.

(132) Maulik G, Madhiwala P, Brooks S, Ma PC, Kijima T, Tibaldi EV, Schaefer E, Parmar K, Salgia R. Activated c-Met signals through PI3K with dramatic effects on cytoskeletal functions in small cell lung cancer. J Cell Mol Med. 2002;6:539-53.

(133) Stella MC, Comoglio PM. HGF: a multifunctional growth factor controlling cell scattering. Int J Biochem Cell Biol. 1999;31:1357-62.

(134) Damstrup L, Rude Voldborg B, Spang-Thomsen M, Brünner N, Skovgaard Poulsen H. In vitro invasion of small-cell lung cancer cell lines correlates with expression of epidermal growth factor receptor. Br J Cancer. 1998;78:631-40.

(135) Gamou S, Shimosato Y, Merlino GT, Shimizu N. Methylation status of epidermal growth factor receptor gene in lung carcinoma cells. Jpn J Cancer Res. 1988;79:989-95.

(136) Patel O, Shulkes A, Baldwin GS. Gastrin-releasing peptide and cancer. Biochim Biophys Acta. 2006;1766:23-41.

(137) Bonomi P. Matrix metalloproteinases and matrix metalloproteinase inhibitors in lung cancer. Semin Oncol. 2002;29:78-86.

(138) Michael M, Babic B, Khokha R, Tsao M, Ho J, Pintilie M, Leco K, Chamberlain D, Shepherd FA. Expression and prognostic significance of metalloproteinases and their tissue inhibitors in patients with small-cell lung cancer. J Clin Oncol. 1999:17:1802-8.

(139) Zucker S, Cao J, Chen WT. Critical appraisal of the use of matrix metalloproteinase inhibitors in cancer treatment. Oncogene. 2000;19:6642-50.

(140) Hartmann TN, Burger M, Burger JA. The role of adhesion molecules and chemokine receptor CXCR4 (CD184) in small cell lung cancer. J Biol Regul Homeost Agents. 2004;18:126-30.

(141) Cuttitta F, Carney DN, Mulshine J, Moody TW, Fedorko J, Fischler A, Minna JD. Bombesin-like peptides can function as autocrine growth factors in human small-cell lung cancer. Nature. 1985;316:823-6.

(142) Kelley MJ, Linnoila RI, Avis IL, Georgiadis MS, Cuttitta F, Mulshine JL, Johnson BE. Antitumor activity of a monoclonal antibody directed against gastrin-releasing peptide in patients with small cell lung cancer. Chest. 1997;112:256-61.

(143) Jensen R, Jones SW, Folkers K, Gardner JD. A synthetic peptide that is a bombesin receptor antagonist. Nature 1984;309:61-63.

(144) Woll PJ, Rozengurt E. Two classes of antagonist interact with receptors for the mitogenic neuropeptides bombesin, bradykinin, and vasopressin. Growth Factors 1988;1:75-83.

(145) Sethi T, Langdon S, Smythe J, Rozengurt E. Growth of small cell lung cancer cells: stimulation by multiple neuropeptides and inhibition by broad spectrum neuropeptides antagonists in vitro and in vivo. Cancer Res. 1992;52:27375-425.

(146) Clive S, Webb DJ, MacLellan A, Young A, Byrne B, Robson L, Smyth JF, Jodrell DI. Forearm blood flow and local responses to peptide vasodilators: a novel pharmacodynamic measure in the phase I trial of antagonist G, a neuropeptide growth factor antagonist. Clin Cancer Res. 2001;10:3071-8.

(147) Heinrich MC, Griffith DJ, Druker BJ, Wait CL, Ott KA, Zigler AJ. Inhibition of c-kit receptor tyrosine kinase activity by STI 571, a selective tyrosine kinase inhibitor. Blood. 2000;96:925-32.

(148) Krug LM, Crapanzano JP, Azzoli CG, Miller VA, Rizvi N, Gomez J, Kris MG, Pizzo B, Tyson L, Dunne M, Heelan RT. Imatinib mesylate lacks activity in small cell lung carcinoma expressing c-kit protein: a phase II clinical trial. Cancer. 2005;103:2128-31.

(149) Spigel DR, Hainsworth JD, Simons L, Meng C, Burris HA 3rd, Yardley DA, Grapski R, Schreeder M, Mallidi PV, Greco FA. Irinotecan, carboplatin, and imatinib in untreated extensive-stage small-cell lung cancer: a phase II trial of the Minnie Pearl Cancer Research Network. J Thorac Oncol. 2007;2:854-61.

(150) Bates D. ZD-6474. AstraZeneca. Curr Opin Investig Drugs. 2003;4:1468-72.

(151) Yano S, Muguruma H, Matsumori Y, Goto H, Nakataki E, Edakuni N, Tomimoto H, Kakiuchi S, Yamamoto A, Uehara H, Ryan A, Sone S. Antitumor vascular strategy for controlling experimental metastatic spread of human small-cell lung cancer cells with ZD6474 in natural killer cell-depleted severe combined immunodeficient mice. Clin Cancer Res. 2005;11:8789-98.

(152) Arnold AM, Seymour L, Smylie M, Ding K, Ung Y, Findlay B, Lee CW, Djurfeldt M, Whitehead M, Ellis P, Goss G, Chan A, Meharchand J, Alam Y, Gregg R, Butts C, Langmuir P, Shepherd F. Phase II study of vandetanib or placebo in small-cell lung cancer patients after complete or partial response to induction chemotherapy with or without radiation therapy: National Cancer Institute of Canada Clinical Trials Group Study BR.20. J Clin Oncol. 2007;25:4278-84.

(153) Rudin CM, Salgia R, Wang X, Hodgson LD, Masters GA, Green M, Vokes EE. Randomized phase II Study of carboplatin and etoposide with or without the bcl-2 antisense oligonucleotide oblimersen for extensive-stage small-cell lung cancer: CALGB 30103. J Clin Oncol. 2008;26:870-6.

(154) Stauffer SR. Small molecule inhibition of the Bcl-X(L)-BH3 protein-protein interaction: proof-of-concept of an in vivo chemopotentiator ABT-737. Curr Top Med Chem. 2007;7:961-5.

(155) Hann CL, Daniel VC, Sugar EA, Dobromilskaya I, Murphy SC, Cope L, Lin X, Hierman JS, Wilburn DL, Watkins DN, Rudin CM. Therapeutic efficacy of ABT-737, a selective inhibitor of BCL-2, in small cell lung cancer. Cancer Res. 2008;68:2321-8.

(156) Hidalgo M, Rowinsky EK. The rapamycin-sensitive signal transduction pathway as a target for cancer therapy. Oncogene. 2000;19:6680-6.

(157) Pandya KJ, Dahlberg S, Hidalgo M, Cohen RB, Lee MW, Schiller JH, Johnson DH. A randomized, phase II trial of two dose levels of temsirolimus (CCI-779) in patients with extensive-stage small-cell lung cancer who have responding or stable disease after induction chemotherapy: a trial of the Eastern Cooperative Oncology Group (E1500). J Thorac Oncol. 2007;2:1036-41.

(158) Chen HX, Gore-Langton RE, Cheson BD. Clinical trials referral resource: Current clinical trials of the anti-VEGF monoclonal antibody bevacizumab. Oncology (Williston Park). 2001;15:1023-6.

(159) D'Amato RJ, Loughnan MS, Flynn E, Folkman J. Thalidomide is an inhibitor of angiogenesis. Proc Natl Acad Sci U S A. 1994;91:4082-5.

(160) Dowlati A, Subbiah S, Cooney M, Rutherford K, Mekhail T, Fu P, Chapman R, Ness A, Cortas T, Saltzman J, Levitan N, Warren G. Phase II trial of thalidomide as maintenance therapy for extensive stage small cell lung cancer after response to chemotherapy. Lung Cancer. 2007;56:377-81.

(161) Pujol JL, Breton JL, Gervais R, Tanguy ML, Quoix E, David P, Janicot H, Westeel V, Gameroff S, Genève J, Maraninchi D. Phase III double-blind, placebo-controlled study of thalidomide in extensive-disease small-cell lung cancer after response to chemotherapy: an intergroup study FNCLCC cleo04 IFCT 00-01.J Clin Oncol. 2007;25:3945-51.

(162) Li X, Liu X, Wang J, Wang Z, Jiang W, Reed E, Zhang Y, Liu Y, Li QQ. Effects of thalidomide on the expression of angiogenesis growth factors in human A549 lung adenocarcinoma cells. Int J Mol Med. 2003;11:785-90.

(163) Shepherd FA, Giaccone G, Seymour L, Debruyne C, Bezjak A, Hirsh V, Smylie M, Rubin S, Martins H, Lamont A, Krzakowski M, Sadura A, Zee B. Prospective, randomized, double-blind, placebo-controlled trial of marimastat

after response to first-line chemotherapy in patients with small-cell lung cancer: a trial of the National Cancer Institute of Canada-Clinical Trials Group and the European Organization for Research and Treatment of Cancer. J Clin Oncol. 2002;20:4434-9.

(164) Balkwill F, Mantovani A. Inflammation and cancer: back to Virchow?, Lancet. 2001;357:539-45.

(165) Paget S. The distribution of secondary growths in cancer of the breast. Lancet. 1889;1:571-73.

(166) Mueller MM. Inflammation in epithelial skin tumours: old stories and new ideas. Eur J Cancer. 2006;42:735-44.

(167) Sethi T, Rintoul RC, Moore SM, MacKinnon AC, Salter D, Choo C, Chilvers ER, Dransfield I, Donnelly SC, Strieter R, Haslett C. Extracellular matrix proteins protect small cell lung cancer cells against apoptosis: a mechanism for small cell lung cancer growth and drug resistance in vivo. Nat Med. 1999;5:662-8.

(168) Fridman R, Giaccone G, Kanemoto T, Martin GR, Gazdar AF, Mulshine JL. Reconstituted basement membrane (matrigel) and laminin can enhance the tumorigenicity and the drug resistance of small cell lung cancer cell lines. Proc Natl Acad Sci U S A. 1990;87:6698-702.

(169) Kiaris H, Chatzistamou I, Kalofoutis Ch, Koutselini H, Piperi Ch, Kalofoutis A. Tumour-stroma interactions in carcinogenesis: basic aspects and perspectives. Mol Cell Biochem. 2004;261:117-22.

(170) De Wever O, Mareel M. Role of myofibroblasts at the invasion front. Biol Chem. 2002;383:55-67.

(171) Micke P, Ostman A. Tumour-stroma interaction: cancer-associated fibroblasts as novel targets in anti-cancer therapy? Lung Cancer. 2004;45:163-75.

(172) Camps JL, Chang SM, Hsu TC, Freeman MR, Hong SJ, Zhau HE, von Eschenbach AC, Chung LW. Fibroblast-mediated acceleration of human epithelial tumor growth in vivo. Proc Natl Acad Sci USA. 1990;87:75–9.

(173) Barcellos-Hoff MH, Ravani SA. Irradiated mammary gland stroma promotes the expression of tumorigenic potential by unirradiated epithelial cells. Cancer Res. 2000;60:1254–60.

(174) Picard O, Rolland Y, Poupon MF. Fibroblast-dependent tumorigenicity of cells in nude mice: implication for implantation of metastases. Cancer Res 1986;46:3290–4.

(175) Damstrup L, Rygaard K, Spang-Thomsen M, Skovgaard Poulsen H. Expression of transforming growth factor beta (TGF beta) receptors and expression of TGF beta 1, TGF beta 2 and TGF beta 3 in human small cell lung cancer cell lines. Br J Cancer. 1993;67:1015-21.

(176) Fischer JR, Darjes H, Lahm H, Schindel M, Drings P, Krammer PH. Constitutive secretion of bioactive transforming growth factor beta 1 by small cell lung cancer cell lines. Eur J Cancer. 1994;30:2125-9.

(177) Eickelberg O, Köhler E, Reichenberger F, Bertschin S, Woodtli T, Erne P, Perruchoud AP, Roth M. Extracellular matrix deposition by primary human lung fibroblasts in response to TGF-beta1 and TGF-beta3. Am J Physiol. 1999;276:814-24.

(178) Rozengurt E, Sinnett-Smith J. Bombesin stimulation of DNA synthesis and cell division in cultures of Swiss 3T3 cells. Proc Natl Acad Sci U S A. 1983;80:2936-40.

(179) Mastroianni A, Invernizzi L, Tagliabue E, Fassina G, Albini A, Ménard S, Colnaghi MI. Alteration of laminin production in small-cell lung carcinoma: possible correlation with the absence of the basement membrane. Tumour Biol. 1993;14:279-87.

(180) Zitvogel L, Tesniere A, Kroemer G. Cancer despite immunosurveillance: immunoselection and immunosubversion. Nat Rev Immunol. 2006;6:715-27.

(181) Yu P, Fu YX. Tumor-infiltrating T lymphocytes: friends or foes? Lab Invest. 2006 Mar;86(3):231-45.

(182) Renkvist N, Castelli C, Robbins PF, Parmiani G. A listing of human tumor antigens recognized by T cells. Cancer Immunol. Immunother. 2001;50:3–15.

(183) Allavena P, Sica A, Solinas G, Porta C, Mantovani A. The inflammatory microenvironment in tumor progression: the role of tumor-associated macrophages. Crit Rev Oncol Hematol. 2008;66:1-9.

(184) Pawelec G. Immunotherapy and immunoselection -- tumour escape as the final hurdle. FEBS Lett. 2004;567:63-6.

(185) Graus F, Dalmou J, Reñé R, Tora M, Malats N, Verschuuren JJ, Cardenal F, Viñolas N, Garcia del Muro J, Vadell C, Mason WP, Rosell R, Posner JB, Real FX. Anti-Hu antibodies in patients with small-cell lung cancer: association with complete response to therapy and improved survival. J Clin Oncol. 1997;15:2866-72.

(186) Darnell RB, DeAngelis LM. Regression of small-cell lung carcinoma in patients with paraneoplastic neuronal antibodies. Lancet. 1993;341:21-2.

(187) Masuno T, Ikeda T, Yokota S, Komuta K, Ogura T, Kishimoto S. Immunoregulatory T-lymphocyte functions in patients with small cell lung cancer. Cancer Res. 1986;46:4195-9.

(188) Fischer JR, Schindel M, Stein N, Lahm H, Gallati H, Krammer PH, Drings P. Selective suppression of cytokine secretion in patients with small-cell lung cancer. Ann Oncol. 1995;6:921-6.

(189) Fischer JR, Schindel M, Bülzebruck H, Lahm H, Krammer PH, Drings P. Decrease of interleukin-2 secretion is a new independent prognostic factor associated with poor survival in patients with small-cell lung cancer. Ann Oncol. 1997;8:457-61.

(190) Eerola AK, Soini Y, Pääkkö P. A high number of tumor-infiltrating lymphocytes are associated with a small tumor size, low tumor stage, and a favorable prognosis in operated small cell lung carcinoma. Clin Cancer Res. 2000;6:1875-81.

(191) Krug LM. Vaccine therapy for small cell lung cancer. Semin Oncol. 2004;31:112-6.

(192) Fenczik CA, Sethi T, Ramos JW, Hughes PE, Ginsberg MH. Complementation of dominant suppression implicates CD98 in integrin activation. Nature. 1997;390:81-5.

(193) Schroeter EH, Kisslinger JA, Kopan R. Notch-1 signalling requires ligand-induced proteolytic release of intracellular domain. Nature. 1998;393:382-6.

(194) Aster JC, Xu L, Karnell FG, Patriub V, Pui JC, Pear WS. Essential roles for ankyrin repeat and transactivation domains in induction of T-cell leukemia by notch1. Mol Cell Biol. 2000;20:7505-15.

(195) Kuroda K, Han H, Tani S, Tanigaki K, Tun T, Furukawa T, Taniguchi Y, Kurooka H, Hamada Y, Toyokuni S, Honjo T. Regulation of marginal zone B cell development by MINT, a suppressor of Notch/RBP-J signaling pathway. Immunity. 2003;18:301-12.

(196) Watson JV, Chambers SH, Smith PJ. A pragmatic approach to the analysis of DNA histograms with a definable G1 peak. Cytometry. 1987;8(1):1-8.

(197) Kelley GG, Kaproth-Joslin KA, Reks SE, Smrcka AV, Wojcikiewicz RJ. G-protein-coupled receptor agonists activate endogenous phospholipase Cepsilon and phospholipase Cbeta3 in a temporally distinct manner. J Biol Chem. 2006;281:2639-48.

(198) de Rooij J, Bos JL. Minimal Ras-binding domain of Raf1 can be used as an activation-specific probe for Ras. Oncogene. 1997;14:623-5.

(199) Liddington RC, Ginsberg MH. Integrin activation takes shape. J Cell Biol. 2002;158:833-9.

(200) Elliott T, Sethi T. Integrins and extracellular matrix: a novel mechanism of multidrug resistance. Expert Rev Anticancer Ther. 2002;2:449-59.

(201) Aoudjit F, Vuori K. Integrin signaling inhibits paclitaxel-induced apoptosis in breast cancer cells. Oncogene. 2001;20:4995-5004.

(202) Uhm JH, Dooley NP, Kyritsis AP, Rao JS, Gladson CL. Vitronectin, a glioma-derived extracellular matrix protein, protects tumor cells from apoptotic death. Clin Cancer Res. 1999;5:1587-94.

(203) Kouniavsky G, Khaikin M, Zvibel I, Zippel D, Brill S, Halpern Z, Papa M. Stromal extracellular matrix reduces chemotherapy-induced apoptosis in colon cancer cell lines. Clin Exp Metastasis. 2002;19:55-60.

(204) Kastan MB, Bartek J. Cell-cycle checkpoints and cancer. Nature. 2004;432:316-23.

(205) Gregorc V, Ludovini V, Pistola L, Darwish S, Floriani I, Bellezza G, Sidoni A, Cavaliere A, Scheibel M, De Angelis V, Bucciarelli E, Tonato M. Relevance of p53, bcl-2 and Rb expression on resistance to cisplatin-based chemotherapy in advanced non-small cell lung cancer. Lung Cancer. 2003;39:41-8.

(206) Hui R, Finney GL, Carroll JS, Lee CS, Musgrove EA, Sutherland RL. Constitutive overexpression of cyclin D1 but not cyclin E confers acute resistance to antiestrogens in T-47D breast cancer cells. Cancer Res. 2002;62:6916-23.

(207) Danen EH, Yamada KM. Fibronectin, integrins, and growth control. J Cell Physiol. 2001;189:1-13.

(208) Guadagno TM, Ohtsubo M, Roberts JM, Assoian RK. A link between cyclin A expression and adhesion-dependent cell cycle progression. Science. 1993;262:1572-5.

(209) Fang F, Orend G, Watanabe N, Hunter T, Ruoslahti E. Dependence of cyclin E-CDK2 kinase activity on cell anchorage. Science. 1996;271:499-502.

(210) Massague J. G1 cell-cycle control and cancer. Nature. 2004;432:298-306.

(211) Boonstra J. Progression through the G1-phase of the on-going cell cycle. J Cell Biochem. 2003;90:244-52.

(212) Woo RA, Poon RY. Cyclin-dependent kinases and S phase control in mammalian cells. Cell Cycle. 2003;2:316-24.

(213) Zhu X, Ohtsubo M, Bohmer RM, Roberts JM, Assoian RK. Adhesion-dependent cell cycle progression linked to the expression of cyclin D1, activation of cyclin E-cdk2, and phosphorylation of the retinoblastoma protein. J Cell Biol. 1996;133:391-403.

(214) Krystal GW, Sulanke G, Litz J. Inhibition of phosphatidylinositol 3-kinase-Akt signaling blocks growth, promotes apoptosis, and enhances sensitivity of small cell lung cancer cells to chemotherapy. Mol Cancer Ther. 2002;1:913-22.

(215) Downward J. PI3-kinase, Akt and cell survival. Semin Cell Dev Biol. 2004;15:177-82.

(216) Xia H, Nho RS, Kahm J, Kleidon J, Henke CA. Focal adhesion kinase is upstream of phosphatidylinositol 3-kinase/Akt in regulating fibroblast survival in response to contraction of type I collagen matrices via a beta 1 integrin viability signaling pathway. J Biol Chem. 2004;279:33024-34.

(217) Diehl JA, Cheng M, Roussel MF, Sherr CJ. Glycogen synthase kinase-3beta regulates cyclin D1 proteolysis and subcellular localization. Genes Dev. 1998;12:3499-511.

(218) Troussard AA, Tan C, Yoganathan TN, Dedhar S. Cell-extracellular matrix interactions stimulate the AP-1 transcription factor in an integrin-linked kinase- and glycogen synthase kinase 3-dependent manner. Mol Cell Biol. 1999;19:7420-7.

(219) Buss H, Dorrie A, Schmitz ML, Frank R, Livingstone M, Resch K, Kracht M. Phosphorylation of serine 468 by GSK-3beta negatively regulates basal p65 NF-kappaB activity. Biol Chem. 2004;279:49571-4.

(220) Ginsberg MH, Partridge A, Shattil SJ. Integrin regulation. Curr Opin Cell Biol. 2005;17:509-16.

(221) Khwaja A, Rodriguez-Viciana P, Wennstrom S, Warne PH, Downward J. Matrix adhesion and Ras transformation both activate a phosphoinositide 3-OH kinase and protein kinase B/Akt cellular survival pathway. EMBO J. 1997;16:2783-93.

(222) Mitsiades CS, Mitsiades N, Koutsilieris M. The Akt pathway: molecular targets for anti-cancer drug development. Curr Cancer Drug Targets. 2004;4:235-56.

(223) Gharbi SI, Zvelebil MJ, Shuttleworth SJ, Hancox T, Saghir N, Timms JF, Waterfield MD. Exploring the specificity of the PI3K family inhibitor LY294002. Biochem J. 2007;404:15-21.

(224) Kaufmann SH. Induction of endonucleolytic DNA cleavage in human acute myelogenous leukemia cells by etoposide, camptothecin, and other cytotoxic anticancer drugs: a cautionary note. Cancer Res. 1989;49:5870-8.

(225) Kaufmann SH. Cell death induced by topoisomerase-targeted drugs: more questions than answers. Biochim Biophys Acta. 1998;1400:195-211.

(226) Olive PL. Detection of DNA damage in individual cells by analysis of histone H2AX phosphorylation. Methods Cell Biol. 2004;75:355-73.

(227) Stein WD, Bates SE, Fojo T. Intractable cancers: the many faces of multi-drug resistance and the many targets it presents for therapeutic attack. Curr Drug Targets. 2004;5:333-46.

(228) Norbury CJ, Hickson ID. Cellular responses to DNA damage. Annu Rev Pharmacol Toxicol. 2001;41:367-401.

(229) Hannun YA. Apoptosis and the dilemma of cancer chemotherapy. Blood. 1997;89:1845-53.

(230) Ruoslahti E, Reed JC. Anchorage dependence, integrins, and apoptosis. Cell. 1994;77:477-8.

(231) Hazlehurst LA, Damiano JS, Buyuksal I, Pledger WJ, Dalton WS. Adhesion to fibronectin via beta1 integrins regulates p27kip1 levels and contributes to cell adhesion mediated drug resistance (CAM-DR). Oncogene. 2000;19:4319-27.

(232) Hazlehurst LA, Valkov N, Wisner L, Storey JA, Boulware D, Sullivan DM, Dalton WS. Reduction in drug-induced DNA double-strand breaks associated with beta1 integrin-mediated adhesion correlates with drug resistance in U937 cells. Blood. 2001;98:1897-903.

(233) Hoyt DG, Rusnak JM, Mannix RJ, Modzelewski RA, Johnson CS, Lazo JS. Integrin activation suppresses etoposide-induced DNA strand breakage in cultured murine tumor-derived endothelial cells. Cancer Res. 1996;56:4146-9.

(234) Su JM, Gui L, Zhou YP, Zha XL. Expression of focal adhesion kinase and alpha5 and beta1 integrins in carcinomas and its clinical significance. World J Gastroenterol. 2002;8:613-8.

(235) Kang S, Bader AG, Vogt PK. Phosphatidylinositol 3-kinase mutations identified in human cancer are oncogenic. Proc Natl Acad Sci USA. 2005;102:802-7.

(236) Phillips-Mason PJ, Raben DM, Baldassare JJ. Phosphatidylinositol 3-kinase activity regulates alpha -thrombin-stimulated G1 progression by its effect on

cyclin D1 expression and cyclin-dependent kinase 4 activity. J Biol Chem. 2000;275:18046-53.

(237) Page K, Li J, Wang Y, Kartha S, Pestell R, Hershenson MB. Regulation of cyclin D(1) expression and DNA synthesis by phosphatidylinositol 3-kinase in airway smooth muscle cells. Am J Respir Cell Mol Biol. 2000;23:436-43.

(238) Tong W, Pollard JW. Genetic evidence for the interactions of cyclin D1 and p27 (Kip1) in mice. Mol Cell Biol. 2001;21:1319-28.

(239) Resnitzky D. Ectopic expression of cyclin D1 but not cyclin E induces anchorage-independent cell cycle progression. Mol Cell Biol. 1997;17:5640-7.

(240) Cappellini A, Tabellini G, Zweyer M, Bortul R, Tazzari PL, Billi AM, Fala F, Cocco L, Martelli AM. The phosphoinositide 3-kinase/Akt pathway regulates cell cycle progression of HL60 human leukemia cells through cytoplasmic relocalization of the cyclin-dependent kinase inhibitor p27(Kip1) and control of cyclin D1 expression. Leukemia. 2003;17:2157-67.

(241) Smith PJ, Wiltshire M, Chin SF, Rabbitts P, Soues S. Cell cycle checkpoint evasion and protracted cell cycle arrest in X-irradiated small-cell lung carcinoma cells. Int J Radiat Biol. 1999;75:1137-47

(242) Hughes PE, Renshaw MW, Pfaff M, Forsyth J, Keivens VM, Schwartz MA, Ginsberg MH. Suppression of integrin activation: a novel function of a Ras/Raf-initiated MAP kinase pathway. Cell. 1997;88:521-30

(243) Sethi T, Ginsberg MH, Downward J, Hughes PE. The small GTP-binding protein R-Ras can influence integrin activation by antagonizing a Ras/Raf-initiated integrin suppression pathway. Mol Biol Cell. 1999;10:1799-809.

(244) Hughes PE, Oertli B, Hansen M, Chou FL, Willumsen BM, Ginsberg MH. Suppression of integrin activation by activated Ras or Raf does not correlate with bulk activation of ERK MAP kinase. Mol Biol Cell. 2002;13:2256-65.

(245) Hansen M, Rusyn EV, Hughes PE, Ginsberg MH, Cox AD, Willumsen BM. R-Ras C-terminal sequences are sufficient to confer R-Ras specificity to H-Ras. Oncogene. 2002;21:4448-61.

(246) Chou FL, Hill JM, Hsieh JC, Pouyssegur J, Brunet A, Glading A, Uberall F, Ramos JW, Werner MH, Ginsberg MH. PEA-15 binding to ERK1/2 MAPKs

is required for its modulation of integrin activation. J Biol Chem. 2003;278:52587-97.

(247) White MA, Nicolette C, Minden A, Polverino A, Van A, Karin M, Wigler MH. Multiple Ras functions can contribute to mammalian cell transformation. Cell. 1995;80:533-41.

(248) Rodriguez-Viciana P, Warne PH, Khwaja A, Marte BM, Pappin D, Das P, Waterfield MD, Ridley A, Downward J. Role of phosphoinositide 3-OH kinase in cell transformation and control of the actin cytoskeleton by Ras. Cell. 1997;89;457-67.

(249) Diaz-Meco MT, Lozano J, Municio MM, Berra E, Frutos S, Sanz L, Moscat J. Evidence for the in vitro and in vivo interaction of Ras with protein kinase C zeta. J Biol Chem. 1994;269:31706-10

(250) Han L, Colicelli J. A human protein selected for interference with Ras function interacts directly with Ras and competes with Raf1. Mol Cell Biol. 1995;15:1318-23

(251) Kuriyama M, Harada N, Kuroda S, Yamamoto T, Nakafuku M, Iwamatsu A, Yamamoto D, Prasad R, Croce C, Canaani E, Kaibuchi K. dentification of AF-6 and canoe as putative targets for Ras. J Biol Chem.1996;271:607-10

(252) Leblanc V, Tocque B, Delumeau I. Ras-GAP controls Rho-mediated cytoskeletal reorganization through its SH3 domain. Mol Cell Biol. 1998;18:5567-78

(253) Kelley GG, Reks SE, Ondrako JM, Smrcka AV. Phospholipase C(epsilon): a novel Ras effector. EMBO J. 2001;20:743-54

(254) Song C, Hu CD, Masago M, Kariya K, Yamawaki-Kataoka Y, Shibatohge M, Wu D, Satoh T, Kataoka T. Regulation of a novel human phospholipase C, PLCepsilon, through membrane targeting by Ras. J Biol Chem. 2001;276:2752-57

(255) Lopez I, Mak EC, Ding J, Hamm HE, Lomasney JW. A novel bifunctional phospholipase c that is regulated by Galpha 12 and stimulates the Ras/mitogen-activated protein kinase pathway. J Biol Chem. 2001;276:2758-65.

(256) Berridge MJ, Irvine RF. Inositol phosphates and cell signalling. Nature. 1989;341:197-205.

(257) Majerus PW, Ross TS, Cunningham TW, Caldwell KK, Jefferson AB, Bansal VS. Recent insights in phosphatidylinositol signaling. Cell. 1990;63:459-65.

(258) Rhee SG. Regulation of phosphoinositide-specific phospholipase C. Annu Rev Biochem. 2001;70:281-312.

(259) Wing MR, Houston D, Kelley GG, Der CJ, Siderovski DP, Harden TK. Activation of phospholipase C-epsilon by heterotrimeric G protein betagamma-subunits. J Biol Chem. 2001;276:48257-61.

(260) Jin TG, Satoh T, Liao Y, Song C, Gao X, Kariya K, Hu CD, Kataoka T. Role of the CDC25 homology domain of phospholipase Cepsilon in amplification of Rap1-dependent signaling. J Biol Chem. 2001;276:30301-7.

(261) Vossmeyer D, Hofmann W, Löster K, Reutter W, Danker K. Phospholipase Cgamma binds alpha1beta1 integrin and modulates alpha1beta1 integrin-specific adhesion. J Biol Chem. 2002;277:4636-43.

(262) Quinton TM, Kim S, Dangelmaier C, Dorsam RT, Jin J, Daniel JL, Kunapuli SP. Protein kinase C- and calcium-regulated pathways independently synergize with Gi pathways in agonist-induced fibrinogen receptor activation. Biochem J. 2002;368:535-43.

(263) Lad Y, McHugh B, Hodkinson PS, Mackinnon AC, Haslett C, Ginsberg MH, Sethi T. Phospholipase C epsilon suppresses integrin activation. J Biol Chem. 2006;281:29501-12.

(264) Song C, Satoh T, Edamatsu H, Wu D, Tadano M, Gao X, Kataoka T. Differential roles of Ras and Rap1 in growth factor-dependent activation of phospholipase C epsilon. Oncogene. 2002;21:8105-13.

(265) de Bruyn KM, Zwartkruis FJ, de Rooij J, Akkerman JW, Bos JL. The small GTPase Rap1 is activated by turbulence and is involved in integrin [alpha]IIb[beta]3-mediated cell adhesion in human megakaryocytes. J Biol Chem. 2003;278:22412-7.

(266) Rebstein PJ, Cardelli J, Weeks G, Spiegelman GB. Mutational analysis of the role of Rap1 in regulating cytoskeletal function in Dictyostelium. Exp Cell Res. 1997;231:276-83.

(267) Brinkmann T, Daumke O, Herbrand U, Kühlmann D, Stege P, Ahmadian MR, Wittinghofer A. Rap-specific GTPase activating protein follows an alternative mechanism. J Biol Chem. 2002;277:12525-31.

(268) Hynes RO. Integrins: versatility, modulation, and signaling in cell adhesion. Cell. 1992;69:11-25.

(269) Webb CP, Van Aelst L, Wigler MH, Woude GF. Signaling pathways in Ras-mediated tumorigenicity and metastasis. Proc Natl Acad Sci U S A. 1998;95:8773-8.

(270) Zhang XF, Settleman J, Kyriakis JM, Takeuchi-Suzuki E, Elledge SJ, Marshall MS, Bruder JT, Rapp UR, Avruch J. Normal and oncogenic p21ras proteins bind to the amino-terminal regulatory domain of c-Raf-1. Nature. 1993;364:308-13.

(271) Zhang Z, Vuori K, Wang H, Reed JC, Ruoslahti E. Integrin activation by R-ras. Cell. 1996;85:61-9.

(272) Horwitz A, Duggan K, Buck C, Beckerle MC, Burridge K. Interaction of plasma membrane fibronectin receptor with talin--a transmembrane linkage. Nature. 1986;320:531-3.

(273) Liu S, Calderwood DA, Ginsberg MH. Integrin cytoplasmic domain-binding proteins. J Cell Sci. 2000;113:3563-71.

(274) Janmey PA. Phosphoinositides and calcium as regulators of cellular actin assembly and disassembly. Annu Rev Physiol. 1994;56:169-91.

(275) Di Paolo G, Pellegrini L, Letinic K, Cestra G, Zoncu R, Voronov S, Chang S, Guo J, Wenk MR, De Camilli P. Recruitment and regulation of phosphatidylinositol phosphate kinase type 1 gamma by the FERM domain of talin. Nature. 2002;420:85-9.

(276) Calderwood DA, Zent R, Grant R, Rees DJ, Hynes RO, Ginsberg MH. The Talin head domain binds to integrin beta subunit cytoplasmic tails and regulates integrin activation. J Biol Chem. 1999;274:28071-4.

(277) Tadokoro S, Shattil SJ, Eto K, Tai V, Liddington RC, de Pereda JM, Ginsberg MH, Calderwood DA. Talin binding to integrin beta tails: a final common step in integrin activation. Science. 2003;302:103-6.

(278) Ling K, Doughman RL, Firestone AJ, Bunce MW, Anderson RA. Type I gamma phosphatidylinositol phosphate kinase targets and regulates focal adhesions. Nature. 2002;420:89-93.

(279) Martel V, Racaud-Sultan C, Dupe S, Marie C, Paulhe F, Galmiche A, Block MR, Albiges-Rizo C. Conformation, localization, and integrin binding of talin depend on its interaction with phosphoinositides. J Biol Chem. 2001;276:21217-27.

(280) Ulkü AS, Schäfer R, Der CJ. Essential role of Raf in Ras transformation and deregulation of matrix metalloproteinase expression in ovarian epithelial cells. Mol Cancer Res. 2003;1:1077-88.

(281) Sorli SC, Bunney TD, Sugden PH, Paterson HF, Katan M. Signaling properties and expression in normal and tumor tissues of two phospholipase C epsilon splice variants. Oncogene. 2005;24:90-100.

(282) Bai Y, Edamatsu H, Maeda S, Saito H, Suzuki N, Satoh T, Kataoka T. Crucial role of phospholipase Cepsilon in chemical carcinogen-induced skin tumor development. Cancer Res. 2004;64:8808-10.

(283) Campbell SL, Khosravi-Far R, Rossman KL, Clark GJ, Der CJ. Increasing complexity of Ras signaling. Oncogene. 1998;17:1395-413.

(284) Malumbres M, Pellicer A. RAS pathways to cell cycle control and cell transformation. Front Biosci. 1998;3:887-912.

(285) Artavanis-Tsakonas S, Matsuno K, Fortini ME. Notch signaling. Science. 1995;268:225-32.

(286) de Celis JF, Garcia-Bellido A, Bray SJ. Activation and function of Notch at the dorsal-ventral boundary of the wing imaginal disc. Development. 1996;122:359-69.

(287) Roehl H, Bosenberg M, Blelloch R, Kimble J. Roles of the RAM and ANK domains in signaling by the C. elegans GLP-1 receptor. Embo J. 1996;15:7002-12.

(288) Conlon RA, Reaume AG, Rossant J. Notch1 is required for the coordinate segmentation of somites. Development. 1995;121:1533-45.

(289) Liu ZJ, Shirakawa T, Li Y, Soma A, Oka M, Dotto GP, Fairman RM, Velazquez OC, Herlyn M. Regulation of Notch1 and Dll4 by vascular

endothelial growth factor in arterial endothelial cells: implications for modulating arteriogenesis and angiogenesis. Mol Cell Biol. 2003;23:14-25.

(290) Beatus P, Lendahl U. Notch and neurogenesis. J Neurosci Res. 1998;54:125-36.

(291) Maillard I, Adler SH, Pear WS. Notch and the immune system. Immunity. 2003;19:781-91.

(292) Radtke F, Raj K. The role of Notch in tumorigenesis: oncogene or tumour suppressor? Nat Rev Cancer. 2003;3:756-67.

(293) Wharton KA, Johansen KM, Xu T, Artavanis-Tsakonas S. Nucleotide sequence from the neurogenic locus notch implies a gene product that shares homology with proteins containing EGF-like repeats. Cell. 1985;43:567-81.

(294) Lindsell CE, Boulter J, diSibio G, Gossler A, Weinmaster G. Expression patterns of Jagged, Delta1, Notch1, Notch2, and Notch3 genes identify ligand-receptor pairs that may function in neural development. Mol Cell Neurosci. 1996;8:14-27.

(295) Stump G, Durrer A, Klein AL, Lutolf S, Suter U, Taylor V. Notch1 and its ligands Delta-like and Jagged are expressed and active in distinct cell populations in the postnatal mouse brain. Mech Dev. 2002;114:153-9.

(296) Kopan R, Schroeter EH, Weintraub H, Nye JS. Signal transduction by activated mNotch: importance of proteolytic processing and its regulation by the extracellular domain. Proc Natl Acad Sci U S A. 1996;93:1683-8.

(297) Mumm JS, Schroeter EH, Saxena MT, Griesemer A, Tian X, Pan DJ, Ray WJ, Kopan R. A ligand-induced extracellular cleavage regulates gamma-secretase-like proteolytic activation of Notch1. Mol Cell. 2000;5:197-206.

(298) Jarriault S, Brou C, Logeat F, Schroeter EH, Kopan R, Israel A. Signalling downstream of activated mammalian Notch. Nature. 1995;377:355-8.

(299) Kopan R, Nye JS, Weintraub H. The intracellular domain of mouse Notch: a constitutively activated repressor of myogenesis directed at the basic helix-loop-helix region of MyoD. Development. 1994;120:2385-96.

(300) Iso T, Kedes L, Hamamori Y. HES and HERP families: multiple effectors of the Notch signaling pathway. J Cell Physiol. 2003;194:237-55.

(301) Kidd S, Lieber T, Young MW. Ligand-induced cleavage and regulation of nuclear entry of Notch in Drosophila melanogaster embryos. Genes Dev. 1998;12:3728-40.

(302) Ramain P, Khechumian K, Seugnet L, Arbogast N, Ackermann C, Heitzler P. Novel Notch alleles reveal a Deltex-dependent pathway repressing neural fate. Curr Biol. 2001;11:1729-38.

(303) Shawber C, Nofziger D, Hsieh JJ, Lindsell C, Bogler O, Hayward D, Weinmaster G. Notch signaling inhibits muscle cell differentiation through a CBF1-independent pathway. Development. 1996;122:3765-73.

(304) Bush G, diSibio G, Miyamoto A, Denault JB, Leduc R, Weinmaster G. Ligand-induced signaling in the absence of furin processing of Notch1. Dev Biol. 2001;229:494-502.

(305) Clegg DO, Wingerd KL, Hikita ST, Tolhurst EC. Integrins in the development, function and dysfunction of the nervous system. Front Biosci. 2003;8:723-50.

(306) Darribere T, Skalski M, Cousin HL, Gaultier A, Montmory C, Alfandari D. Integrins: regulators of embryogenesis. Biol Cell. 2000;92:5-25.

(307) Hynes RO. A reevaluation of integrins as regulators of angiogenesis. Nat Med. 2002;8:918-21.

(308) Nagato M, Heike T, Kato T, Yamanaka Y, Yoshimoto M, Shimazaki T, Okano H, Nakahata T. Prospective characterization of neural stem cells by flow cytometry analysis using a combination of surface markers. J Neurosci Res. 2005;80:456-66.

(309) Tate MC, Garcia AJ, Keselowsky BG, Schumm MA, Archer DR, LaPlaca MC. Specific beta1 integrins mediate adhesion, migration, and differentiation of neural progenitors derived from the embryonic striatum. Mol Cell Neurosci. 2004;27:22-31.

(310) Campos LS, Decker L, Taylor V, Skarnes W. Notch, epidermal growth factor receptor, and beta1-integrin pathways are coordinated in neural stem cells. J Biol Chem. 2006;281:5300-9.

(311) Leong KG, Hu X, Li L, Noseda M, Larrivée B, Hull C, Hood L, Wong F, Karsan A. Activated Notch4 inhibits angiogenesis: role of beta 1-integrin activation. Mol Cell Biol. 2002;22:2830-41.

(312) Julich D, Geisler R, Holley SA. Integrinalpha5 and delta/notch signaling have complementary spatiotemporal requirements during zebrafish somitogenesis. Dev Cell. 2005;8:575-86.

(313) Chong SW, Jiang YJ. Off limits--integrins holding boundaries in somitogenesis. Trends Cell Biol. 2005;15:453-7.

(314) Sriuranpong V, Borges MW, Ravi RK, Arnold DR, Nelkin BD, Baylin SB, Ball DW. Notch signaling induces cell cycle arrest in small cell lung cancer cells. Cancer Res. 2001;61:3200-5.

(315) Formstecher E, Ramos JW, Fauquet M, Calderwood DA, Hsieh JC, Canton B, Nguyen XT, Barnier JV, Camonis J, Ginsberg MH, Chneiweiss H. PEA-15 mediates cytoplasmic sequestration of ERK MAP kinase. Dev Cell. 2001;1:239-50.

(316) Eagar TN, Tang Q, Wolfe M, He Y, Pear WS, Bluestone JA. Notch 1 signaling regulates peripheral T cell activation. Immunity. 2004;20:407-15.

(317) De Strooper B, Annaert W, Cupers P, Saftig P, Craessaerts K, Mumm JS, Schroeter EH, Schrijvers V, Wolfe MS, Ray WJ, Goate A, Kopan R. A presenilin-1-dependent gamma-secretase-like protease mediates release of Notch intracellular domain. Nature. 1999;398:518-22.

(318) Zecchini V, Brennan K, Martinez-Arias A. An activity of Notch regulates JNK signalling and affects dorsal closure in Drosophila. Curr Biol. 1999;9:460-9.

(319) Fortini ME, Artavanis-Tsakonas S. The suppressor of hairless protein participates in notch receptor signaling. Cell. 1994;79:273-82.

(320) Kato H, Taniguchi Y, Kurooka H, Minoguchi S, Sakai T, Nomura-Okazaki S, Tamura K, Honjo T. Involvement of RBP-J in biological functions of mouse Notch1 and its derivatives. Development. 1997;124:4133-41.

(321) Kurooka H, Kuroda K, Honjo T. Roles of the ankyrin repeats and C-terminal region of the mouse notch1 intracellular region. Nucleic Acids Res. 1998;26:5448-55.

(322) Martinez Arias A, Zecchini V, Brennan K. CSL-independent Notch signalling: a checkpoint in cell fate decisions during development? Curr Opin Genet Dev. 2002;12:524-33.

(323) Lubman OY, Korolev SV, Kopan R. Anchoring notch genetics and biochemistry; structural analysis of the ankyrin domain sheds light on existing data. Mol Cell. 2004;13:619-26.

(324) Ramos JW, Kojima TK, Hughes PE, Fenczik CA, Ginsberg MH. The death effector domain of PEA-15 is involved in its regulation of integrin activation. J Biol Chem. 1998;273:33897-900.

(325) Yin Z, Gabriele E, Leprini A, Perris R, Colombatti A. Differential cation regulation of the alpha 5 beta 1 integrin-mediated adhesion of leukemic cells to the central cell-binding domain of fibronectin. Cell Growth Differ. 1997;8:1339-47.

(326) Lam LT, Ronchini C, Norton J, Capobianco AJ, Bresnick EH. Suppression of erythroid but not megakaryocytic differentiation of human K562 erythroleukemic cells by notch-1. J Biol Chem. 2000;275:19676-84.

(327) Varnum-Finney B, Wu L, Yu M, Brashem-Stein C, Staats S, Flowers D, Griffin JD, Bernstein ID. Immobilization of Notch ligand, Delta-1, is required for induction of notch signaling. J Cell Sci. 2000;113:4313-8.

(328) Nijjar SS, Wallace L, Crosby HA, Hubscher SG, Strain AJ. Altered Notch ligand expression in human liver disease: further evidence for a role of the Notch signaling pathway in hepatic neovascularization and biliary ductular defects. Am J Pathol. 2002;160:1695-703.

(329) Krebs LT, Xue Y, Norton CR, Shutter JR, Maguire M, Sundberg JP, Gallahan D, Closson V, Kitajewski J, Callahan R, Smith GH, Stark KL, Gridley T. Notch signaling is essential for vascular morphogenesis in mice. Genes Dev. 2000;14:1343-52.

(330) Komatsu M, Ruoslahti E. R-Ras is a global regulator of vascular regeneration that suppresses intimal hyperplasia and tumor angiogenesis. Nat Med. 2005;11:1346-50.

(331) Sundaram MV. Vulval development: the battle between Ras and Notch. Curr Biol. 2004;14:311-3.

(332) Nagaraj R, Banerjee U. The little R cell that could. Int J Dev Biol. 2004;48:755-60.

(333) zur Lage P, Jarman AP. Antagonism of EGFR and notch signalling in the reiterative recruitment of Drosophila adult chordotonal sense organ precursors. Development. 1999;126:3149-57.

(334) Hasson P, Egoz N, Winkler C, Volohonsky G, Jia S, Dinur T, Volk T, Courey AJ, Paroush Z. EGFR signaling attenuates Groucho-dependent repression to antagonize Notch transcriptional output. Nat Genet. 2005;37:101-5.

(335) Culi J, Martin-Blanco E, Modolell J. The EGF receptor and N signalling pathways act antagonistically in Drosophila mesothorax bristle patterning. Development. 2001;128:299-308.

(336) Berset T, Hoier EF, Battu G, Canevascini S, Hajnal A. Notch inhibition of RAS signaling through MAP kinase phosphatase LIP-1 during C. elegans vulval development. Science. 2001;291:1055-8.

(337) Alberola-Ila J, Hernandez-Hoyos G. The Ras/MAPK cascade and the control of positive selection. Immunol Rev. 2003;191:79-96.

(338) Sundaram MV. The love-hate relationship between Ras and Notch. Genes Dev. 2005;19:1825-39.

(339) Ehrhardt A, Ehrhardt GR, Guo X, Schrader JW. Ras and relatives--job sharing and networking keep an old family together. Exp Hematol. 2002;30:1089-106.

(340) Oertli B, Han J, Marte BM, Sethi T, Downward J, Ginsberg M, Hughes PE. The effector loop and prenylation site of R-Ras are involved in the regulation of integrin function. Oncogene. 2000;19:4961-9.

(341) Furuhjelm J, Peranen J. The C-terminal end of R-Ras contains a focal adhesion targeting signal. J Cell Sci. 2003;116:3729-38.

(342) Nobes CD, Hall A. Rho GTPases control polarity, protrusion, and adhesion during cell movement. J Cell Biol. 1999;144:1235-44.

(343) Endo Y, Osumi N, Wakamatsu Y. Bimodal functions of Notch-mediated signaling are involved in neural crest formation during avian ectoderm development. Development. 2002;129:863-73.

(344) Langdon T, Hayward P, Brennan K, Wirtz-Peitz F, Sanders P, Zecchini V, Friday A, Balayo T, Martinez Arias A. Notch receptor encodes two structurally separable functions in Drosophila: A genetic analysis. Dev Dyn. 2006;235:998-1013.

(345) Gutierrez A, Look AT. NOTCH and PI3K-AKT pathways intertwined. Cancer Cell. 2007;12:411-3.

(346) Jang MS, Miao H, Carlesso N, Shelly L, Zlobin A, Darack N, Qin JZ, Nickoloff BJ, Miele L. Notch-1 regulates cell death independently of differentiation in murine erythroleukemia cells through multiple apoptosis and cell cycle pathways. J Cell Physiol. 2004;199:418-33.

(347) Parr C, Watkins G, Jiang WG. The possible correlation of Notch-1 and Notch-2 with clinical outcome and tumour clinicopathological parameters in human breast cancer. Int J Mol Med. 2004;14:779-86.

(348) Danen EH. Integrins: regulators of tissue function and cancer progression. Curr Pharm Des. 2005;11:881-91.

(349) Ellyard JI, Simson L, Parish CR. Th2-mediated anti-tumour immunity: friend or foe? Tissue Antigens. 2007;70:1-11.

(350) Taylor RC, Patel A, Panageas KS, Busam KJ, Brady MS. Tumor-infiltrating lymphocytes predict sentinel lymph node positivity in patients with cutaneous melanoma. J Clin Oncol. 2007;25:869-75.

(351) Iwamoto M, Shinohara H, Miyamoto A, Okuzawa M, Mabuchi H, Nohara T, Gon G, Toyoda M, Tanigawa N. Prognostic value of tumor-infiltrating dendritic cells expressing CD83 in human breast carcinomas. Int J Cancer. 2003;104:92-7.

(352) Sato E, Olson SH, Ahn J, Bundy B, Nishikawa H, Qian F, Jungbluth AA, Frosina D, Gnjatic S, Ambrosone C, Kepner J, Odunsi T, Ritter G, Lele S, Chen YT, Ohtani H, Old LJ, Odunsi K. Intraepithelial CD8+ tumor-infiltrating lymphocytes and a high CD8+/regulatory T cell ratio are associated with favorable prognosis in ovarian cancer. Proc Natl Acad Sci U S A. 2005;102:18538-43.

(353) Graus F, Keime-Guibert F, Reñe R, Benyahia B, Ribalta T, Ascaso C, Escaramis G, Delattre JY. Anti-Hu-associated paraneoplastic encephalomyelitis: analysis of 200 patients. Brain. 2001;124:1138-48.

(354) Manley GT, Smitt PS, Dalmau J, Posner JB. Hu antigens: reactivity with Hu antibodies, tumor expression, and major immunogenic sites. Ann Neurol. 1995;38:102-10.

(355) Giaccone G, Debruyne C, Felip E, Chapman PB, Grant SC, Millward M, Thiberville L, D'addario G, Coens C, Rome LS, Zatloukal P, Masso O, Legrand C. Phase III study of adjuvant vaccination with Bec2/bacille Calmette-Guerin in responding patients with limited-disease small-cell lung cancer. J Clin Oncol. 2005;23:6854-64.

(356) Johnston-Early A, Cohen MH, Fossieck BE Jr, Harwood S, Ihde DC, Bunn PA Jr, Matthews MJ, Minna JD, Makuch R. Delayed hypersensitivity skin testing as a prognostic indicator in patients with small cell lung cancer. Cancer. 1983;52:1395-400.

(357) Yokota J, Kohno T. Molecular footprints of human lung cancer progression. Cancer Sci. 2004;95:197-204.

(358) Talmadge JE, Donkor M, Scholar E. Inflammatory cell infiltration of tumors: Jekyll or Hyde. Cancer Metastasis Rev. 2007;26:373-400.

(359) Ioachim HL, Dorsett BH, Paluch E. The immune response at the tumor site in lung carcinoma. Cancer. 1976;38:2296-2309.

(360) Whiteside TL. Tumor Infiltrating Lymphocytes as antitumor effector cells. Biotherapy. 1992;5:47-61.

(361) O'Brien PM, Tsirimonaki E, Coomber DW, Millan DW, Davis JA, Campo MS. Immunoglobulin genes expressed by B-lymphocytes infiltrating cervical carcinomas show evidence of antigen-driven selection. Cancer Immunol Immunother. 2001;50:523-32.

(362) Coronella JA, Spier C, Welch M, Trevor KT, Stopeck AT, Villar H, Hersh EM. Antigen-driven oligoclonal expansion of tumor-infiltrating B cells in infiltrating ductal carcinoma of the breast. J Immunol. 2002;169:1829-36.

(363) Mantovani A, Bottazzi B, Colotta F, Sozzani S, Ruco L. The origin and function of tumor-associated macrophages. Immunol Today. 1992;13:265-70.

(364) Kärjä V, Aaltomaa S, Lipponen P, Isotalo T, Talja M, Mokka R. Tumour-infiltrating lymphocytes: A prognostic factor of PSA-free survival in patients with local prostate carcinoma treated by radical prostatectomy. Anticancer Res. 2005;25:4435-8.

(365) Tsutsui S, Yasuda K, Suzuki K, Tahara K, Higashi H, Era S. Macrophage infiltration and its prognostic implications in breast cancer: the relationship with VEGF expression and microvessel density. Oncol Rep. 2005;14:425-31.

(366) Funada Y, Noguchi T, Kikuchi R, Takeno S, Uchida Y, Gabbert HE. Prognostic significance of CD8+ T cell and macrophage peritumoral infiltration in colorectal cancer. Oncol Rep. 2003;10:309-13.

(367) Oken MM, Creech RH, Tormey DC, Horton J, Davis TE, McFadden ET, Carbone PP. Toxicity And Response Criteria Of The Eastern Cooperative Oncology Group. Am J Clin Oncol. 1982;5:649-655.

(368) Wolf D, Wolf AM, Rumpold H, Fiegl H, Zeimet AG, Muller-Holzner E, Deibl M, Gastl G, Gunsilius E, Marth C. The expression of the regulatory T cell-specific forkhead box transcription factor FoxP3 is associated with poor prognosis in ovarian cancer. Clin Cancer Res. 2005;11:8326-31.

(369) Kono K, Kawaida H, Takahashi A, Sugai H, Mimura K, Miyagawa N, Omata H, Fujii H. CD4(+)CD25high regulatory T cells increase with tumor stage in patients with gastric and esophageal cancers. Cancer Immunol Immunother. 2006;55:1064-71.

(370) Bates GJ, Fox SB, Han C, Leek RD, Garcia JF, Harris AL, Banham AH. Quantification of regulatory T cells enables the identification of high-risk breast cancer patients and those at risk of late relapse. J Clin Oncol. 2006;24:5373-80.

(371) Weidmann E, Whiteside TL, Giorda R, Herberman RB, Trucco M. The T-cell receptor V beta gene usage in tumor-infiltrating lymphocytes and blood of patients with hepatocellular carcinoma. Cancer Res. 1992;52:5913-20.

(372) Nakamura H, Saji H, Ogata A, Hosaka M, Hagiwara M, Kawasaki N, Konaka C, Kato H. Immunologic parameters as significant prognostic factors in lung cancer. Lung Cancer. 2002;37:161-9.

(373) Weissman DN, deShazo RD, Banks DE, Baser Y. Immunomodulation by bronchial lavage cells in normal individuals and patients with bronchogenic carcinoma. Am J Med Sci. 1986;292:187-92.

(374) Pouniotis DS, Plebanski M, Apostolopoulos V, McDonald CF. Alveolar macrophage function is altered in patients with lung cancer. Clin Exp Immunol. 2006;143:363-72.

(375) Kurnick JT, Kradin RL, Blumberg R, Schneeberger EE, Boyle LA. Functional characterization of T lymphocytes propagated from human lung carcinomas. Clin Immunol Immunopathol. 1986;38:367-80.

(376) Doyle A, Martin WJ, Funa K, Gazdar A, Carney D, Martin SE, Linnoila I, Cuttitta F, Mulshine J, Bunn P. Markedly decreased expression of class I histocompatibility antigens, protein, and mRNA in human small-cell lung cancer. J Exp Med. 1985;161:1135-51.

(377) Chen HL, Gabrilovich D, Tampé R, Girgis KR, Nadaf S, Carbone DP. A functionally defective allele of TAP1 results in loss of MHC class I antigen presentation in a human lung cancer. Nat Genet. 1996;13:210-3.

(378) Möller P, Hämmerling GJ. The role of surface HLA-A,B,C molecules in tumour immunity. Cancer Surv. 1992;13:101-27.

(379) Traversari C, Meazza R, Coppolecchia M, Basso S, Verrecchia A, van der Bruggen P, Ardizzoni A, Gaggero A, Ferrini S. IFN-gamma gene transfer restores HLA-class I expression and MAGE-3 antigen presentation to CTL in HLA-deficient small cell lung cancer. Gene Ther. 1997;4:1029-35.

(380) van Zandwijk N, Groen HJ, Postmus PE, Burghouts JT, ten Velde GP, Ardizzoni A, Smith IE, Baas P, Sahmoud T, Kirkpatrick A, Dalesio O, Giaccone G. Role of recombinant interferon-gamma maintenance in responding patients with small cell lung cancer. A randomised phase III study of the EORTC Lung Cancer Cooperative Group. Eur J Cancer. 1997;33:1759-66.

(381) Manke HG, Aulenbacher P, Rüster S, Drings P. Inhibition of antibody synthesis and expression of T-cell membrane markers by serum factors of patients with small cell carcinoma of the lung. Anticancer Res. 1986;6:869-73.

(382) Ikeda T, Masuno T, Ogura T, Watanabe M, Shirasaka T, Hara H, Tanio Y, Kawase I, Kishimoto S. Characterization and purification of an immunosuppressive factor produced by a small cell lung cancer cell line. Jpn J Cancer Res. 1991;82:332-8.

(383) Bishara A, Malka R, Brautbar C, Barak V, Cohen I, Kedar E. Cytokine production in human mixed leukocyte reactions performed in serum-free media. J Immunol Methods. 1998;215:187-90.

(384) Zhu J, Paul WE. CD4 T cells: fates, functions, and faults. Blood. 2008;112:1557-69.

(385) Appay V, Douek DC, Price DA. CD8+ T cell efficacy in vaccination and disease. Nat Med. 2008;14:623-8.

(386) Pardoll DM, Topalian SL. The role of CD4+ T cell responses in antitumor immunity. Curr Opin Immunol. 1998;10:588-94.

(387) Hung K, Hayashi R, Lafond-Walker A, Lowenstein C, Pardoll D, Levitsky H. The central role of CD4(+) T cells in the antitumor immune response. J Exp Med. 1998;188:2357-68.

(388) Beatty G, Paterson Y. IFN-gamma-dependent inhibition of tumor angiogenesis by tumor-infiltrating CD4+ T cells requires tumor responsiveness to IFN-gamma. J Immunol. 2001;166:2276-82.

(389) Curiel TJ. Tregs and rethinking cancer immunotherapy. J Clin Invest. 2007;117:1167-74.

(390) Taga K, Tosato G. IL-10 inhibits human T cell proliferation and IL-2 production. J Immunol. 1992;148:1143-8.

(391) Beverly B, Kang SM, Lenardo MJ, Schwartz RH. Reversal of in vitro T cell clonal anergy by IL-2 stimulation. Int Immunol. 1992;4:661-71.

(392) Alexander JP, Kudoh S, Melsop KA, Hamilton TA, Edinger MG, Tubbs RR, Sica D, Tuason L, Klein E, Bukowski RM. T-cells infiltrating renal cell carcinoma display a poor proliferative response even though they can

produce interleukin 2 and express interleukin 2 receptors. Cancer Res. 1993;53:1380-7.

(393) Stauber DJ, Debler EW, Horton PA, Smith KA, Wilson IA. Crystal structure of the IL-2 signaling complex: paradigm for a heterotrimeric cytokine receptor. Proc Natl Acad Sci U S A. 2006;103:2788-93.

(394) Sancho D, Santis AG, Alonso-Lebrero JL, Viedma F, Tejedor R, Sánchez-Madrid F. Functional analysis of ligand-binding and signal transduction domains of CD69 and CD23 C-type lectin leukocyte receptors. J Immunol. 2000;165:3868-75.

(395) Caruso A, Licenziati S, Corulli M, Canaris AD, De Francesco MA, Fiorentini S, Peroni L, Fallacara F, Dima F, Balsari A, Turano A. Flow cytometric analysis of activation markers on stimulated T cells and their correlation with cell proliferation. Cytometry. 1997;27:71-6.

(396) Gajewski TF, Meng Y, Blank C, Brown I, Kacha A, Kline J, Harlin H. Immune resistance orchestrated by the tumor microenvironment. Immunol Rev. 2006;213:131-45.

(397) Levings MK, Bacchetta R, Schulz U, Roncarolo MG. The role of IL-10 and TGF-beta in the differentiation and effector function of T regulatory cells. Int Arch Allergy Immunol. 2002;129:263-76.

(398) Stephens LA, Mottet C, Mason D, Powrie F. Human CD4(+)CD25(+) thymocytes and peripheral T cells have immune suppressive activity in vitro. Eur J Immunol. 2001;31:1247-54.

(399) Valzasina B, Piconese S, Guiducci C, Colombo MP. Tumor-induced expansion of regulatory T cells by conversion of CD4+CD25- lymphocytes is thymus and proliferation independent. Cancer Res. 2006;66:4488-95.

(400) Liu VC, Wong LY, Jang T, Shah AH, Park I, Yang X, Zhang Q, Lonning S, Teicher BA, Lee C. Tumor evasion of the immune system by converting CD4+CD25- T cells into CD4+CD25+ T regulatory cells: role of tumor-derived TGF-beta. J Immunol. 2007;178:2883-92.

(401) Wahl SM, Wen J, Moutsopoulos N. TGF-beta: a mobile purveyor of immune privilege. Immunol Rev. 2006;213:213-27.

(402) Khalil N. TGF-beta: from latent to active. Microbes Infect. 1999;1:1255-63.

(403) Tsang ML, Zhou L, Zheng BL, Wenker J, Fransen G, Humphrey J, Smith JM, O'Connor-McCourt M, Lucas R, Weatherbee JA. Characterization of recombinant soluble human transforming growth factor-beta receptor type II (rhTGF-beta sRII). Cytokine. 1995;7:389-97.

(404) Ahuja SS, Paliogianni F, Yamada H, Balow JE, Boumpas DT. Effect of transforming growth factor-beta on early and late activation events in human T cells. J Immunol. 1993;150:3109-18.

(405) Fink R, Ehrhardt R, Dancygier H. Bombesin and its analogues inhibit interleukin-2-induced proliferation of CTLL-2 cells. Regul Pept. 1988;23:323-30.

(406) Yang HK, Scott FM, Trepel JB, Battey JF, Johnson BE, Kelley MJ. Correlation of expression of bombesin-like peptides and receptors with growth inhibition by an anti-bombesin antibody in small-cell lung cancer cell lines. Lung Cancer. 1998;21:165-75.

(407) Del Rio M, Hernanz A, de la Fuente M. Bombesin, gastrin-releasing peptide, and neuromedin C modulate murine lymphocyte proliferation through adherent accessory cells and activate protein kinase C. Peptides. 1994;15:15-22.

(408) Makarenkova VP, Shurin GV, Tourkova IL, Balkir L, Pirtskhalaishvili G, Perez L, Gerein V, Siegfried JM, Shurin MR. Lung cancer-derived bombesin-like peptides down-regulate the generation and function of human dendritic cells. J Neuroimmunol. 2003;145:55-67.

(409) Radulovic S, Cai RZ, Serfozo P, Groot K, Redding TW, Pinski J, Schally AV. Biological effects and receptor binding affinities of new pseudononapeptide bombesin/GRP receptor antagonists with N-terminal D-Trp or D-Tpi. Int J Pept Protein Res. 1991;38:593-600.

(410) Brugarolas A, Takita H. Immunologic status in lung cancer. Chest. 1973;64:427-30.

(411) Rubbert A, Manger B, Lang N, Kalden JR, Platzer E. Functional characterization of tumor-infiltrating lymphocytes, lymph-node lymphocytes and peripheral-blood lymphocytes from patients with breast cancer. Int J Cancer. 1991;49:25-31.

(412) Guilloux Y, Viret C, Gervois N, Le Dréan E, Pandolfino MC, Diez E, Jotereau F. Defective lymphokine production by most CD8+ and CD4+ tumor-specific T cell clones derived from human melanoma-infiltrating lymphocytes in response to autologous tumor cells in vitro. Eur J Immunol. 1994;24:1966-73.

(413) Katsikis PD, Cohen SB, Londei M, Feldmann M. Are CD4+ Th1 cells pro-inflammatory or anti-inflammatory? The ratio of IL-10 to IFN-gamma or IL-2 determines their function. Int Immunol. 1995;7:1287-94.

(414) Ichihara F, Kono K, Takahashi A, Kawaida H, Sugai H, Fujii H. Increased populations of regulatory T cells in peripheral blood and tumor-infiltrating lymphocytes in patients with gastric and esophageal cancers. Clin Cancer Res. 2003;9:4404-8.

(415) Mantovani A, Sozzani S, Locati M, Allavena P, Sica A. Macrophage polarization: tumor-associated macrophages as a paradigm for polarized M2 mononuclear phagocytes. Trends Immunol. 2002;23:549-55.

(416) Sung JL, Lin JT, Gorham JD. CD28 co-stimulation regulates the effect of transforming growth factor-beta1 on the proliferation of naïve CD4+ T cells. Int Immunopharmacol. 2003;3:233-45.

(417) Damiano JS, Hazlehurst LA, Dalton WS. Cell adhesion-mediated drug resistance (CAM-DR) protects the K562 chronic myelogenous leukemia cell line from apoptosis induced by BCR/ABL inhibition, cytotoxic drugs, and gamma-irradiation. Leukemia. 2001;15:1232-9.

(418) Zhang H, Ozaki I, Mizuta T, Matsuhashi S, Yoshimura T, Hisatomi A, Tadano J, Sakai T, Yamamoto K. Beta 1-integrin protects hepatoma cells from chemotherapy induced apoptosis via a mitogen-activated protein kinase dependent pathway. Cancer. 2002;95:896-906.

(419) Barr LF, Campbell SE, Bochner BS, Dang CV. Association of the decreased expression of alpha3beta1 integrin with the altered cell: environmental interactions and enhanced soft agar cloning ability of c-myc-overexpressing small cell lung cancer cells. Cancer Res. 1998;58:5537-45.

(420) Ylisirnio S, Hoyhtya M, Turpeenniemi-Hujanen T. Serum matrix metalloproteinases -2, -9 and tissue inhibitors of metalloproteinases -1, -2 in

lung cancer--TIMP-1 as a prognostic marker. Anticancer Res. 2000;20:1311-6.

(421) Lauffenburger DA, Horwitz AF. Cell migration: a physically integrated molecular process. Cell. 1996;84:359-69.

(422) Brakebusch C, Fassler R. beta 1 integrin function in vivo: adhesion, migration and more. Cancer Metastasis Rev. 2005;24:403-11.

(423) Sixt M, Bauer M, Lammermann T, Fassler R. Beta1 integrins: zip codes and signaling relay for blood cells. Curr Opin Cell Biol. 2006;18:482-90.

(424) Tian B, Lessan K, Kahm J, Kleidon J, Henke C. beta 1 integrin regulates fibroblast viability during collagen matrix contraction through a phosphatidylinositol 3-kinase/Akt/protein kinase B signaling pathway. J Biol Chem. 2002;277:24667-75.

(425) Mettouchi A, Meneguzzi G. Distinct roles of beta1 integrins during angiogenesis. Eur J Cell Biol. 2006;85:243-7.

(426) Luscinskas FW, Lawler J. Integrins as dynamic regulators of vascular function. Faseb J. 1994;8:929-38.

(427) Kashii T, Mizushima Y, Monno S, Nakagawa K, Kobayashi M. Gene analysis of K-, H-ras, p53, and retinoblastoma susceptibility genes in human lung cancer cell lines by the polymerase chain reaction/single-strand conformation polymorphism method. J Cancer Res Clin Oncol. 1994;120:143-8.

(428) Risse-Hackl G, Adamkiewicz J, Wimmel A, Schuermann M. Transition from SCLC to NSCLC phenotype is accompanied by an increased TRE-binding activity and recruitment of specific AP-1 proteins. Oncogene. 1998;16:3057-68.

(429) Khanzada UK, Pardo OE, Meier C, Downward J, Seckl MJ, Arcaro A. Potent inhibition of small-cell lung cancer cell growth by simvastatin reveals selective functions of Ras isoforms in growth factor signalling. Oncogene. 2006;25:877-87.

(430) Shan L, Aster JC, Sklar J, Sunday ME. Notch-1 regulates pulmonary neuroendocrine cell differentiation in cell lines and in transgenic mice. Am J Physiol Lung Cell Mol Physiol. 2007;292:500-9.

(431) Schmidt M, Hovelmann S, Beckers TL. A novel form of constitutively active farnesylated Akt1 prevents mammary epithelial cells from anoikis and suppresses chemotherapy-induced apoptosis. Br J Cancer. 2002;87:924-32.

(432) Hovelmann S, Beckers TL, Schmidt M. Molecular alterations in apoptotic pathways after PKB/Akt-mediated chemoresistance in NCI H460 cells. Br J Cancer. 2004;90:2370-7.

(433) Brognard J, Clark AS, Ni Y, Dennis PA. Akt/protein kinase B is constitutively active in non-small cell lung cancer cells and promotes cellular survival and resistance to chemotherapy and radiation. Cancer Res. 2001;61:3986-97.

(434) Phillips-Mason PJ, Raben DM, Baldassare JJ. Phosphatidylinositol 3-kinase activity regulates alpha -thrombin-stimulated G1 progression by its effect on cyclin D1 expression and cyclin-dependent kinase 4 activity. J Biol Chem. 2000;275:18046-53.

(435) Diehl JA, Cheng M, Roussel MF, Sherr CJ. Glycogen synthase kinase-3beta regulates cyclin D1 proteolysis and subcellular localization. Genes Dev. 1998;12:3499-511.

(436) Page K, Li J, Wang Y, Kartha S, Pestell RG, Hershenson MB. Regulation of cyclin D(1) expression and DNA synthesis by phosphatidylinositol 3-kinase in airway smooth muscle cells. Am J Respir Cell Mol Biol. 2000;23:436-43.

APPENDIX: Published Papers.